THE UNIVERSITY OF CALGARY

Calmodulin Interactions with Peptides, Hormones, Drugs and Metal Ions

by

Hui Ouyang

A DISSERTATION

SUBMITTED TO THE FACULTY OF GRADUATE STUDIES IN PARTIAL FULFILLMENT OF THE REQUIREMENTS FOR THE DEGREE OF DOCTOR OF PHILOSOPHY

DEPARTMENT OF BIOLOGICAL SCIENCES

CALGARY, ALBERTA

April, 2000

Abstract

Calmodulin (CaM), the ubiquitous Ca^{2+}-regulatory protein, binds four Ca^{2+} ions in response to increases in the intracellular Ca^{2+} level. Subsequently Ca^{2+}-CaM recognizes target proteins through its exposed Met-rich hydrophobic surfaces. However, calcium ions and target proteins are not the only "ligands" that bind to CaM. In this work, I have examined the interactions of CaM with different metal ions, hormones, drugs, and peptides. CaM binds a host of other metal ions based on their similarity in ionic radius with Ca^{2+}. These metal ions bind to CaM in a different fashion. For example, unlike Ca^{2+}, Mg^{2+} has a higher affinity for the N-terminal domain than the C-terminal domain of the protein, which could have a physiological significance in resting cells. Binding of the neurohormone melatonin and its structural analogs also was studied. My results show that the interactions between these molecules and CaM are very weak, and are unlikely to play a role *in vivo*. In contrast to melatonin and its analogs, the anticancer platinum drugs, cisplatin and carboplatin, bind CaM covalently through its Met sidechains. These drugs can reduce CaM's peptide-binding ability, which suggests that such interactions might be involved in the severe side effects of these drugs. The binding of melittin, a bee venom peptide, has also been studied as a "model" CaM-binding peptide. Melittin is different from other typical CaM-binding peptides because it possesses a single Trp residue close to the C-terminus. Melittin has been found to bind CaM in a different orientation

compared to other CaM-binding peptides, which could be the result of the unusual location of the Trp residue. The LLP-1 segments from the cytoplasmic domain of HIV-1 transmembrane glycoprotein were also found to interact with CaM in an unconventional way. My data indicate that the LLP-1 peptides form a more extended complex with CaM compared to normal CaM-binding peptides derived from typical target proteins. In addition, this dissertation also describes my attempts at purifying the M-domain from *E. coli* ffh protein, which, like CaM, recognizes peptides in a sequence-independent manner. Homology modeling indicates that most Met residues in the M-domain are located in the peptide binding site, which implies that, as in CaM, they play important roles in the peptide recognition event.

Acknowledgement

First of all, I would like to thank my supervisor, Dr. Hans J. Vogel, for providing proper guidance, inspiring ideas, continuous encouragement, and tireless efforts to correct my English. The knowledge, experience, and skills I have developed under his supervision are priceless.

Next, I would like to thank those who have helped me with particular aspects of my work, including Dr. T. Yuan for performing proton and cadmium-113 NMR experiments on the melittin projects; Dr. D. D. McIntyre for chemical synthesis of isotope-labeled cisplatin and methionine; Mr. A. M. Weljie for homology modeling of the M-domain; Dr. J. H. Wang for a gift of calcineurin; Dr. G. Lajoie and Dr. J. Chen (University of Waterloo) for performing electrospray mass spectroscopy; and Dr. R. C. Montelaro (University of Pittsburgh) for the gifts of LLP-1 peptides; and Dr. H. Yoshino for performing small angle X-ray scattering spectroscopy.

I am indebted to Dr. D. L. Severson, Dr. R. J. French, and Dr. B. M. Phipps for being on my supervisory committee and for their helpful suggestions and comments. I would like to thank Dr. S. R. W. Chen for participating my thesis defense, and Dr. L. Burtnick (University of British Columbia) for being my external examiner. I wish to acknowledge the generous financial support from the Alberta Heritage Foundation for Medical Research (AHFMR).

I would also like to thank the members of Dr. Vogel's laboratory. I thank Dr. M. Zhang, Dr. J. M. Aramini, and Dr. T. Yuan whom introduced me

to NMR spectroscopy; Dr. D. D. McIntyre for maintaining the NMR spectrometers; Mrs. K. Bagh for keeping the laboratory so well organized. Special thanks to Richard Brokx, Teresa Clarke, Aalim Weljie, Craig Shepherd, David Schibli, Pheobe Franco for fruitful discussions and friendship, and for proofreading this dissertation.

Last, but certainly not least, I would like to thank my wife and my parents for their continuous support and encouragement. I couldn't have done this without them.

To My Lovely Wife ...

Table of Contents

List of Tables

List of Figures

Abbreviations

1(2,3)D	one-(two, three)dimensional
ATP	adenosine triphosphate
BSA	bovine serum albumin
CaM	calmodulin
CaMKI	calmodulin-dependent protein kinase I
CD	circular dichroism
cNOS	constitutive nitric oxide synthase
cTnC	cardiac muscle troponin C
DTT	dithiothreitol
E. coli	Escherichia coli
EDTA	ethylenediaminetetra-acetic acid
EPR	electron paramagnetic resonance
ER	endoplasmic reticulum
HIV	human immunodeficiency virus
HMQC	heteronuclear multiple quantum coherence
IP_3	inositol 1,4,5-triphosphate
IP_3R	inositol 1,4,5-triphosphate receptor
IPTG	isopropyl-β-d-thiogalactopyranoside
LB	Luria-Bertani (broth/agar)
LLP	lentivirus lytic peptide
LMTA	low melting temperature agarose
MBP	maltose-binding protein
MLCK	myosin light chain kinase
MOPS	3-(N-morpholino)propanesulfonic acid
MT	mitochondria
NMR	nuclear magnetic resonance
NO	nitric oxide
PAGE	polyacrylamide gel electrophoresis

PCR	polymerase chain reaction
PDE	3':5'-cyclic nucleotide phosphodiesterase 1A2
PMSF	phenylmethylsulfonyl fluoride
PNPP	*p*-nitrophenyl phosphate
R_1	spin-lattice relaxation rate
RYR	ryanodine receptor
SR	sarcoplasmic reticulum
SRP	signal recognition particle
sTnC	skeletal muscle troponin C
T_1	spin-lattice relaxation time
TEMPOL	4-hydroxyl-2,2,6,6-tetramethylpiperidinyl-1-oxy
TFE	2,2,2-trifluroethanol
Tris	tris(hydroxymethyl)aminomethane

Chapter 1

Introduction

Calcium Homeostasis and Signaling

Unlike other abundant light elements, such as H, C, N, O, P, S, K, and Mg, which were utilized by biological systems at the very beginning of life, calcium action was developed later in evolution. It is believed that early in evolution, calcium (Ca^{2+}) was rejected from cells because it acts as an ionic crosslinking agent, leading to precipitation of intracellular metabolites. The intracellular Ca^{2+} concentration of a primitive prokaryote was kept at a low level, 10^{-5} M, compared to 10^{-3} M outside the cell (Williams 1997, 1998). Calcium acted merely as a protective external cross-linking agent and was only utilized externally in outer cell walls and membranes. Bacteria comfortably survive considerable variations in external Ca^{2+} concentration. Although the intracellular Ca^{2+} level of bacteria is low, it appears to be variable under different conditions (Norris *et al.* 1996, Williams 1996). Moreover, it is known that mitochondria, which are probably derived from bacteria, can stand an internal Ca^{2+} concentration high enough to cause precipitation of calcium salts (Williams 1996). Therefore, even though prokaryotes have export mechanisms to keep the cytoplasmic Ca^{2+} level low, intracellular Ca^{2+} homeostasis is not strictly required. A few recent studies

suggest that some prokaryotes can use the extracellular/intracellular Ca^{2+} gradient in message systems (Onek & Smith 1992, Smith 1995, Norris *et al.* 1996), however, the use of Ca^{2+} is not very extensive because a prokaryote must multiply rapidly rather than constantly adjust itself to environmental stimuli.

The evolution of cellular organization toward that of the eukaryote involved major structural changes. One such change was the development of intracellular compartments which made it possible for localized activities that increased efficiency in the use of materials and energy. The complexity of the organization needed more complicated communication systems. Many inorganic and organic communicating pathways have been developed in eukaryotes, especially in multicellular organisms. In eukaryotic cells, Ca^{2+} is pumped out and cytoplasmic Ca^{2+} is now down to 10^{-7} M (Williams 1997). The intracellular Ca^{2+} level is strictly controlled in nonstimulated cells, which enables Ca^{2+} to serve as a signaling ion that communicates between the environment and the cytoplasm. At this evolutionary stage, Ca^{2+} became not just a potential poison but a homeostatic agent for the cytoplasm and a trigger for many intracellular activities.

It is well recognized today that Ca^{2+} is a ubiquitous secondary messenger that is responsible for triggering a wide variety of cellular processes. Ca^{2+} plays important roles in fertilization, cell cycle control, muscle contraction, exocytosis, energy metabolism, chemotaxis, synaptic plasticity and cell death (Clapham 1992, Berridge 1997, Nicotera & Orrenius 1998).

Because of the importance of Ca^{2+} signaling, Ca^{2+} concentration is tightly regulated in both extracellular and intracellular fluids in higher organisms. The vast majority of Ca^{2+} in animals (more than 99%) is immobilized in the bones and teeth as hydroxyapatite [$Ca_{10}(PO_4)_6(OH)_2$] in human beings. These Ca^{2+} deposits help to control extracellular Ca^{2+} at a fixed level (around 1 - 2 mM) (Carafoli 1987, Williams 1998a). Extracellular Ca^{2+} derives its importance from its relationship with intracellular Ca^{2+}, which fulfills its major tasks. The maintenance of the extracellular Ca^{2+} level (10^{-3} M compared to 10^{-7} M in the intracellular milieu) in a narrow range ensures a large Ca^{2+} gradient across the cell membrane. This Ca^{2+} gradient results in a strong electrochemical force on Ca^{2+} which is very suitable for its role as an intracellular regulator, since even a minor change in the permeability of plasma membrane to Ca^{2+} will result in significant fluctuations in its cytosolic concentration (Carafoli 1987).

The cytosolic Ca^{2+} concentration is also under rigid homeostatic control. The intracellular Ca^{2+} is maintained at a very low level because prolonged elevation of Ca^{2+} concentration cause irreversible cellular damage as occurs during cardiac or cerebral ischaemia (Trump & Berezesky 1995). Moreover, the low cytosolic Ca^{2+} level also facilitates the Ca^{2+} gradient across the plasma membrane which is convenient for Ca^{2+} signaling as mentioned above. The cytosolic Ca^{2+} level is maintained by an extensive array of Ca^{2+} pumps and exchangers which rapidly sequester Ca^{2+} or remove it from the cytoplasm. Eukaryotic cells possess Ca^{2+} pumps (ATPases) in the plasma membrane, in

endo(sarco)-plasmic reticulum (Carafoli 1987, 1994), as well as in Golgi vesicles (Virk *et al.* 1985) and lysosomes (Klemper 1985). Ca^{2+} pumps can transport Ca^{2+} from the cytoplasm to extracellular fluids or to intracellular Ca^{2+} stores, e.g. to the sarcoplasmic reticulum in muscle cells (Figure 1.1). These Ca^{2+}-ATPases vary in structures and kinetic properties to satisfy different requirements of cells during the function cycle.

Ca^{2+} can enter the cytoplasm from two sources, namely extracellular fluids and intracellular Ca^{2+} stores. There are a variety of Ca^{2+} channels on the cytoplasm membrane, such as the voltage-operated channels and receptor-operated channels, which allow Ca^{2+} to enter from the outside. Ca^{2+} can also be released from Ca^{2+} stores, usually from endo(sarco)plasmic reticulum[1] (Figure 1.1). Which of these sources is used is somewhat cell-specific; however, in most cells, it is the internal stores that provide most of the Ca^{2+} for signaling (Berridge 1997). There are two main types of intracellular Ca^{2+}-channels, ryanodine receptor (RYR) family and inositol 1,4,5-triphosphate receptor (IP_3R) family (Carafoli 1987). The operation of these channels is controlled by the binding of the signaling molecules, such as IP_3. One of the most important features of these Ca^{2+} channels is their sensitivity to Ca^{2+}. Ca^{2+} has a biphasic

[1] Mitochondria can also accumulate large amounts of Ca^{2+} as mentioned earlier. Mitochondria take up Ca^{2+} by an electrophoretic route and release it with a calcium-sodium exchanger. The inner member of some mitochondria also allows calcium-proton exchange. Recent research suggests that the accumulation of Ca^{2+} in mitochondria is important for the functions of dehydrogenases in the matrix; and the regulation of cytosolic Ca^{2+} is unlikely to be the major function of mitochondria Ca^{2+} (for a review, see Carafoli 1994).

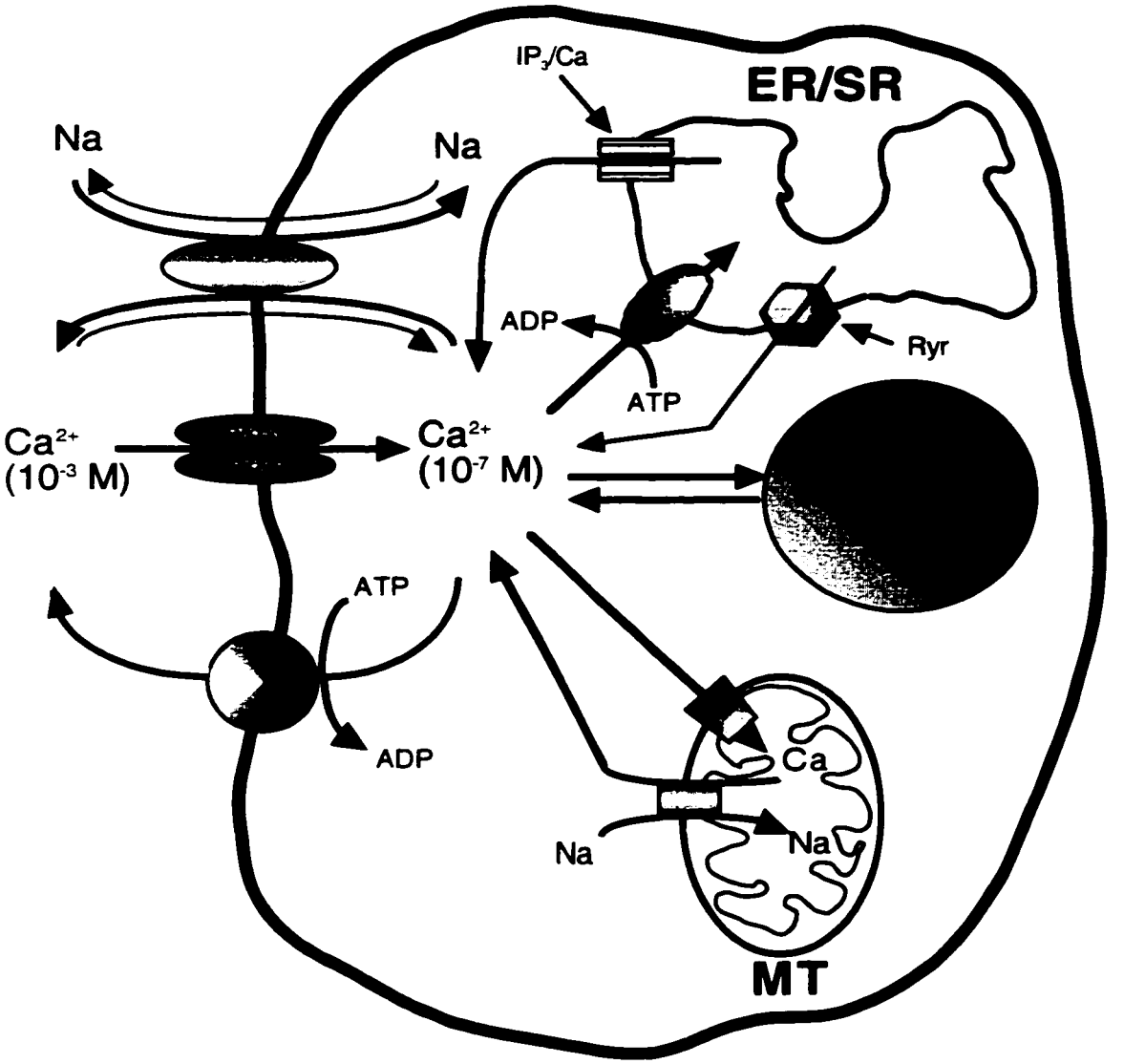

Figure 1.1 Schematic diagram of calcium transport systems in a eukaryotic cell. Three systems are known in plasma membranes: an ATPase, a sodium-calcium exchanger, and calcium channels of several kinds. The systems in the nuclear envelope are poorly understood; independent regulation of nuclear calcium has been suggested (Badminton et al, 1998). Ca^{2+} uptake and release of mitochondria are unlikely an important part of their function (see the footnote of text). There are a few systems on endo(sarco)plasmic reticulum: an ATPase for Ca^{2+} uptake, and intracellular channels for Ca^{2+} release which are normally under dual regulation (see text for details).

effect on RYRs and IP_3Rs: it initially exerts a positive feedback effect by enhancing the opening of the channels as its concentration is increased, displaying the phenomenon of Ca^{2+}-induced Ca^{2+} release (CICR). However, as soon as the concentration reaches a certain level, the feedback switches from positive to negative and Ca^{2+} then inhibits the channels (Bezprozvanny & Ehrlich 1995). The positive feedback enables rapid Ca^{2+} concentration increases in the cytoplasm which means a quick Ca^{2+} signal; on the other hand, the negative feedback ensures that Ca^{2+} is not overloaded into the cytoplasm, avoiding the potential cytotoxicity of this ion.

The positive feedback also provides one of the mechanisms for coordinating individual receptors which makes Ca^{2+} release regenerative. The receptors can communicate with each other using Ca^{2+} as a messenger (Bootman & Berridge, 1995). A specific region within the cell usually functions as an initiation site which first releases Ca^{2+}; Ca^{2+} then diffuses outwards to neighboring receptors causing the opening of these channels, thereby setting up a Ca^{2+} wave (Jaffe 1993, Berridge 1997). A cellular Ca^{2+} signal is thus produced by coordinating release of Ca^{2+} from all the receptors. The regenerative process is potentially dangerous because of the possibility of random triggering of a single channel. To avoid this possibility, mechanisms for these intracellular receptors have been developed to regulate the excitability in resting cells. For example, the excitability of IP_3Rs is regulated by the generation of IP_3 by cell surface receptors which is only triggered by agonists. The binding of IP_3 to IP_3Rs dramatically increases their sensitivity

to the action of Ca^{2+}. Thus, IP_3Rs are under dual regulation of IP_3 and Ca^{2+} (Berridge 1997, Dawson 1997). Evidence also suggests that RYRs may be under similar dual regulatory mechanisms (Lee 1994, Galione & White 1994).

In summary, Ca^{2+} signaling functions against the strictly controlled Ca^{2+} homeostasis. In resting cells, the cytosolic Ca^{2+} concentration is maintained at a very low level by Ca^{2+} pumps and exchangers. When the cell is excited by hormones, nerve impulses, or other stimuli, the cytosolic Ca^{2+} concentration rapidly rises to 10^{-6} M by entering from the outside or release from internal Ca^{2+} stores. The rise of the intracellular Ca^{2+} level results in a wide variety of cellular activities, including muscle contraction, production of nitric oxides, oxidative phosphorylation, protein phosphorylation, DNA replication, cell proliferation, and so on. However, the increase of Ca^{2+} concentration *per se* cannot have so many functions; all these cellular events are mediated by a variety of Ca^{2+}-binding proteins.

Calcium-Binding Proteins and Calmodulin

"Ca^{2+}-binding proteins" refers to a large family of proteins. Some of them are listed in Table 1.1. These Ca^{2+}-binding proteins include soluble proteins and transmembrane proteins with all kinds of functions, which are in accordance with the wide range of cellular effects of Ca^{2+} (a large number of Ca^{2+}-binding proteins are extracellular proteins which are not relevant to intracellular Ca^{2+} signals, and thus they won't be discussed here).Many Ca^{2+}-binding membrane proteins are Ca^{2+}-sensitive transporters for Ca^{2+} or other

Table 1.1 Examples of Ca^{2+}-binding proteins[1]

Protein[2]	Protein Function[3]
Calmodulin	Ubiquitous modulator of many cellular components
Protein kinase C	Ubiquitous protein kinases
Calcineurin	Phosphatase
Calretinin	Activator of guanylyl cyclase
IP_3-specific PLC	Generator of IP_3 and diacylglycerol
Phospholipase A_2	Generator of arachidonic acid
Troponin C	Modulator of muscle contraction
Caldesmon	Regulator of muscle contraction
α-Actinin	Actin-bundling protein
Gelsolin	Actin-severing protein
IP_3 receptor	Effector of intracellular Ca^{2+} release
Ryanodine receptor	Effector of intracellular Ca^{2+} release
Ca^{2+}-ATPase	Ca^{2+} pump across the membrane
Na^+/Ca^{2+} exchanger	Exchange of Na^+ and Ca^{2+} across the membrane
Annexins	Associated with membranes; endo- and exocytosis
S-100	Associated with many filamentous structures
Parvalbumin	Ca^{2+} buffer
Calbindin	Ca^{2+} buffer
Calsequestrin	Ca^{2+} buffer

[1] For reviews, see Clapham 1995, Williams 1996, 1998b.

[2] Some proteins are representing a family of proteins which has many family members. For example, annexin is a family of more than ten proteins.

[3] Some proteins may have a large number of different functions which may not be summarized completely in this table. The exact cellular functions of some proteins, like many members of the annexin and S-100 families, have yet to be elucidated.

molecules, like IP_3Rs and RYRs. The soluble proteins can be divided into three groups according to the effects of Ca^{2+} on them. First, there are Ca^{2+}-buffering proteins. Calsequestrin is one such protein in the endoplasmic reticulum with a high Ca^{2+}-binding capacity and no other known function (Clapham 1995, Wang *et al.* 1998). The second group of Ca^{2+}-binding proteins consists of Ca^{2+}-activated proteins. For example, calpain is a Ca^{2+}-binding cysteine protease in the cell nucleus, and its activity is absolutely dependent on Ca^{2+} (Gilchrist *et al.* 1994). The last group of Ca^{2+}-binding proteins are Ca^{2+}-regulatory messenger proteins which serve as Ca^{2+} "decoders" to pass the Ca^{2+} signal to downstream proteins and enzymes. Calmodulin (CaM) is no doubt the most versatile and ubiquitous Ca^{2+}-binding messenger protein which can rapidly respond to fluctuations of cytosolic Ca^{2+} concentration. Upon binding of four Ca^{2+} ions, CaM undergoes a major conformational change which enables it to recognize and activate a wide variety of proteins and enzymes. CaM modulates many essential processes, including DNA replication, gene transcription, muscle contraction, nitric oxide synthesis, protein phosphorylation and dephosphorylation, and other signal transduction pathways (Vogel 1994, Crivici & Ikura 1995, Vogel & Zhang 1995, Ikura 1996, Carifoli *et al.* 1997, Agell *et al.* 1998).

Structure of CaM

CaM is a small acidic protein, with 148 residues and a molecular weight of 16.7 kDa. CaM is highly conserved in all eukaryotic cells. CaM can

bind four Ca^{2+} ions; and Ca^{2+}-CaM can further bind target proteins and enzymes. Thus, CaM has three forms in cells, namely apo-CaM, Ca^{2+}-CaM and CaM-substrate complexes.

Ca^{2+}-CaM The structure of Ca^{2+}-CaM was first determined by X-ray crystallography. The crystal structure of bovine Ca^{2+}-CaM revealed that this protein has a dumbbell shaped appearance (Babu *et al.* 1985, Babu *et al.* 1988, Barbato *et al.* 1992). The protein contains two domains which are linked by a long, solvent-exposed central helix. Each domain has a globular shape and binds two Ca^{2+} ions in two adjacent loops that form a small antiparallel β-sheet (Figure 1.2B).

In the X-ray structure, there are seven α-helices in Ca^{2+}-CaM comprising residues 5 to 9, 29 to 38, 45 to 55, 65 to 92, 102 to 111, 118 to 128, 138 to 147. Overall, 66% of the protein residues are in an α-helical conformation. The most striking feature of the protein molecule is its long central-linking α-helix. At 2.2 Å resolution, there appears to be a kink in the central region of the helix, around residue 79 to 81. The presence of this distortion may reflect the high flexibility of the helix (Chattopadhyaya *et al.* 1992), a property that is indeed supported by nuclear magnetic resonance (NMR) studies (Ikura *et al.* 1991, Spera *et al.* 1991, Barbato *et al.* 1992). In fact, this long central α-helix should be considered as two connected short α-helices. This flexibility of the central α-helix is important for substrate

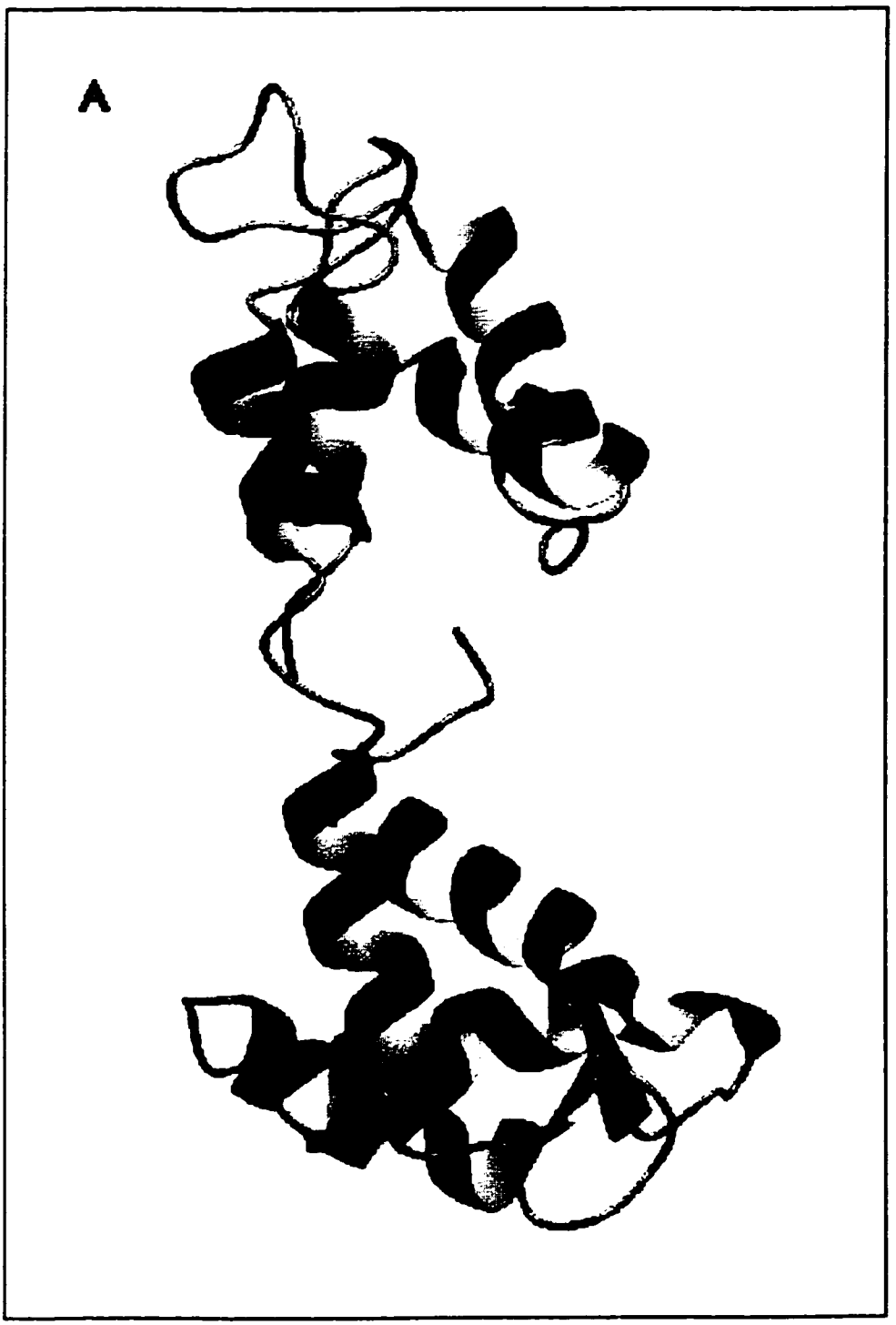
A

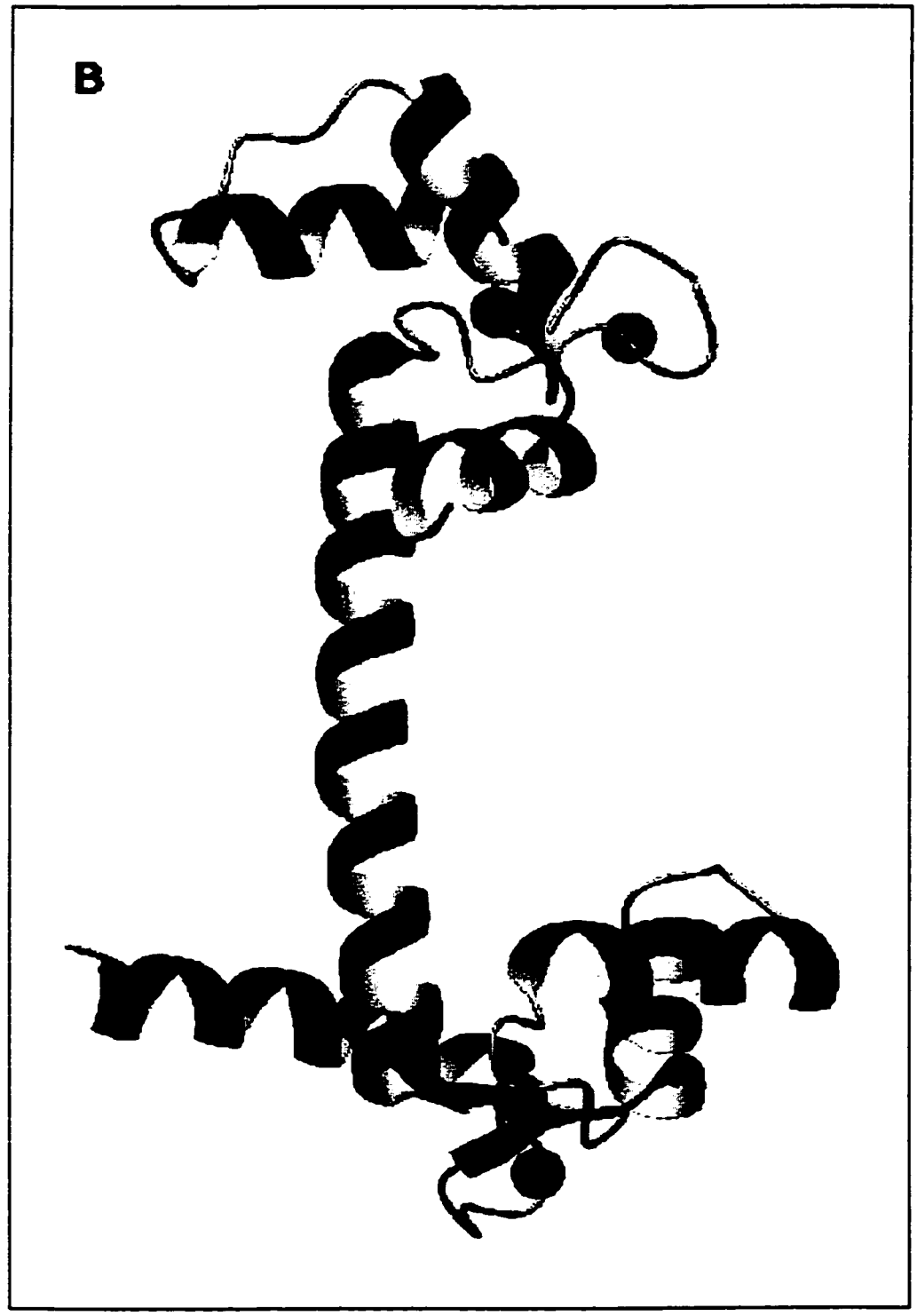
B

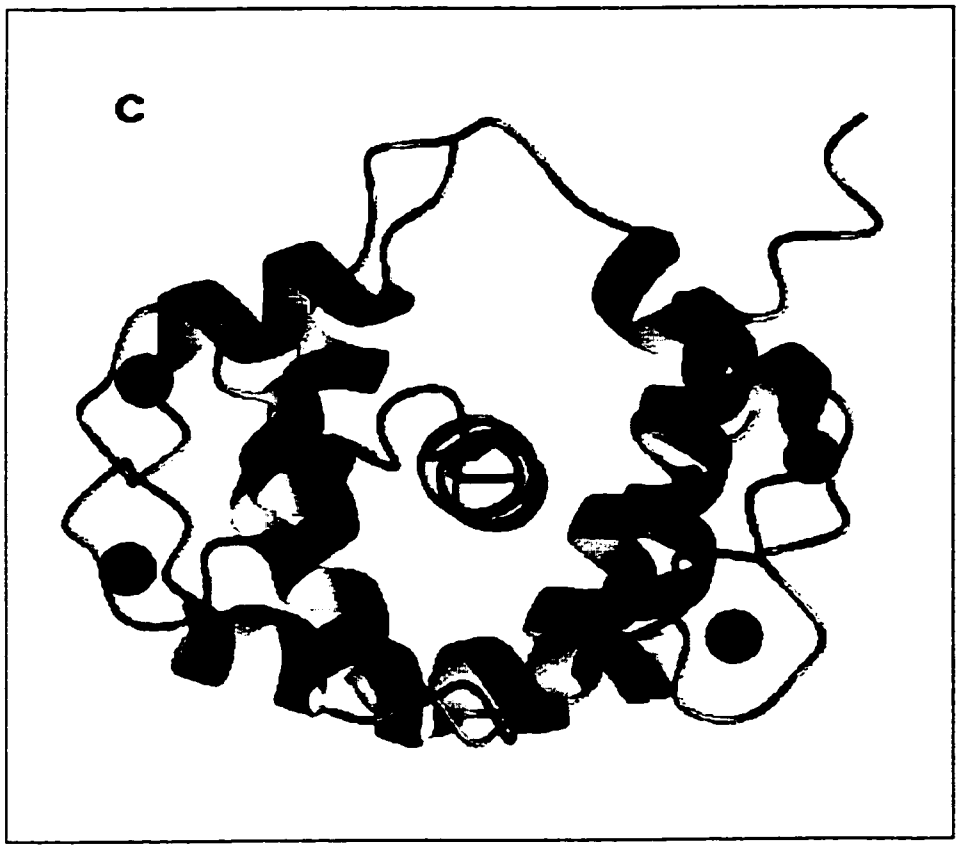

Figure 1.2 Structure of CaM. (A) apo-CaM; (B) Ca^{2+}-CaM; (C) Ca^{2+}-CaM complexed with a MLCK peptide.

recognition since it enables CaM to adjust the distance between the two domains and adopt the proper orientation when CaM interacts with various target proteins. Limited proteolysis studies showed that CaM could be readily cleaved in the middle of the central α-helix by trypsin, releasing two independent domains that contain two Ca^{2+}-binding sites each (Drabikowski *et al.* 1982, Andersson *et al.* 1983b, Vogel *et al.* 1983, Thurlin *et al.* 1984). These two proteolytic fragments and the intact protein show great structural similarity as revealed by previous proton NMR experiments (Linse *et al.* 1991), suggesting that the two halves of CaM are independently folded . The Ca^{2+}-binding constants of the two tryptic fragments are also similar to the intact protein; and the C-terminal domain of CaM has a higher affinity for Ca^{2+} than the N-terminal domain (Andersson *et al.* 1983, Linse *et al.* 1991). CaM binds Ca^{2+} ions in a stepwise manner: two Ca^{2+} ions bind first to the C-terminal domain (sites III and IV) cooperatively, followed by the next two Ca^{2+} ions binding to the N-terminal sites (sites I and II) also in a cooperative fashion. The positive cooperativity of the four Ca^{2+}-binding sites is one of the crucial features for CaM. The binding of Ca^{2+} ions is necessary for the activities of CaM as we shall see later, and this positive cooperativity enables CaM to function effectively as an on/off switch over the narrow range of Ca^{2+} concentrations that distinguishes the resting and stimulated cells (10^{-7} M to 10^{-6} M).

Recently, we found some evidence suggesting that the central α-helix might also provide communication between the two lobes of CaM on Ca^{2+}-

binding. We measured the surface exposure of Met sidechains in CaM upon binding Ca^{2+} (Yuan *et al.* 1999a). The binding of two Ca^{2+} ions to the C-terminal domain results in a minor conformational change in the N-terminal domain. The Met sidechains in the N-lobe, which is still in its apo form, become more exposed to solvent, a feature resembling Ca^{2+}-CaM (see the following sections). Such a phenomenon was not observed in separated domains, which suggests that the central linker helix may play a role in transmitting Ca^{2+}-binding information from the C-lobe to the N-lobe in CaM. This result may reveal a previously unrecoginized function of the central α-helix of CaM. The long central α-helix is normally believed to just provide a flexible linker between the two globular domains (Putkey *et al.* 1988, VanBerkum *et al.* 1990, Persechini *et al.* 1993). However, the function of CaM is not only to bind substrates when it is saturated by Ca^{2+}, but to react rapidly to an increase of the intracellular Ca^{2+} level. CaM possesses high affinity Ca^{2+}-binding sites (see below), and more importantly, positive-cooperativity between these sites. Our result suggests the possibility of the inter-domain communication in CaM in the absence of a target protein or peptide. The binding of two Ca^{2+} ions into the C-terminal domain can cause slight conformational changes in the N-terminal domain (Yuan *et al.* 1999a). Such a conformational change may not be enough to fully activate CaM, but it may result in a "half-open" state in the N-terminal domain, which prepares the N-terminal domain for further Ca^{2+} and target binding.

Ca^{2+}-Binding Sites All four Ca^{2+}-binding sites in CaM have a characteristic helix-loop-helix structure which often is referred to as an "EF-hand" (Kawasaki & Kretsinger 1994), which was first described in the structrure of carp parvalbumin (Kretsinger & Nockolds 1973). The EF-hand is a very common and conserved Ca^{2+}-binding motif that has been found in many Ca^{2+}-binding proteins. This motif consists of an α-helix, a 12-residue loop around a Ca^{2+} ion, and a second α-helix (Figure 1.3A). The helix-loop-helix motifs usually occur in pairs of adjacent motifs from the same polypeptide chain. In CaM, each domain consists of two EF-hands, also referred to as a lobe. The two helices of the EF-hands form an angle of about 90° in Ca^{2+}-CaM. All four Ca^{2+} ions in CaM have a coordination number of seven, and the ligands are provided by the Ca^{2+}-binding loops. Five residues in these loops which provide the Ca^{2+} ligands are highly conserved in terms of both sequence and position (Marsden *et al.* 1990, Kawasaki & Kretsinger 1994). These five residues are always located at position 1, 3, 5, 7, 9, and 12 of the loop. The Ca^{2+} is coordinated by an oxygen atom of the side chains of residues 1, 3, and 5 while the residue at position 7 uses its backbone carbonyl oxygen as a ligand. The side chain of the 9th residue in Ca^{2+}-binding loops normally use a water molecule as a bridge to interact with Ca^{2+} ions. The last amino acid residue in the loop is always a Glu; and this Glu coordinates the Ca^{2+} ion with both oxygen atoms of its side chain, providing the sixth and seventh ligands of Ca^{2+}. These seven ligands form a pentagonal bipyramid shape whose axis is ligand 1-ligand 7 (Figure 1.3B). Other than those Ca^{2+} ligands, the Gly residues in

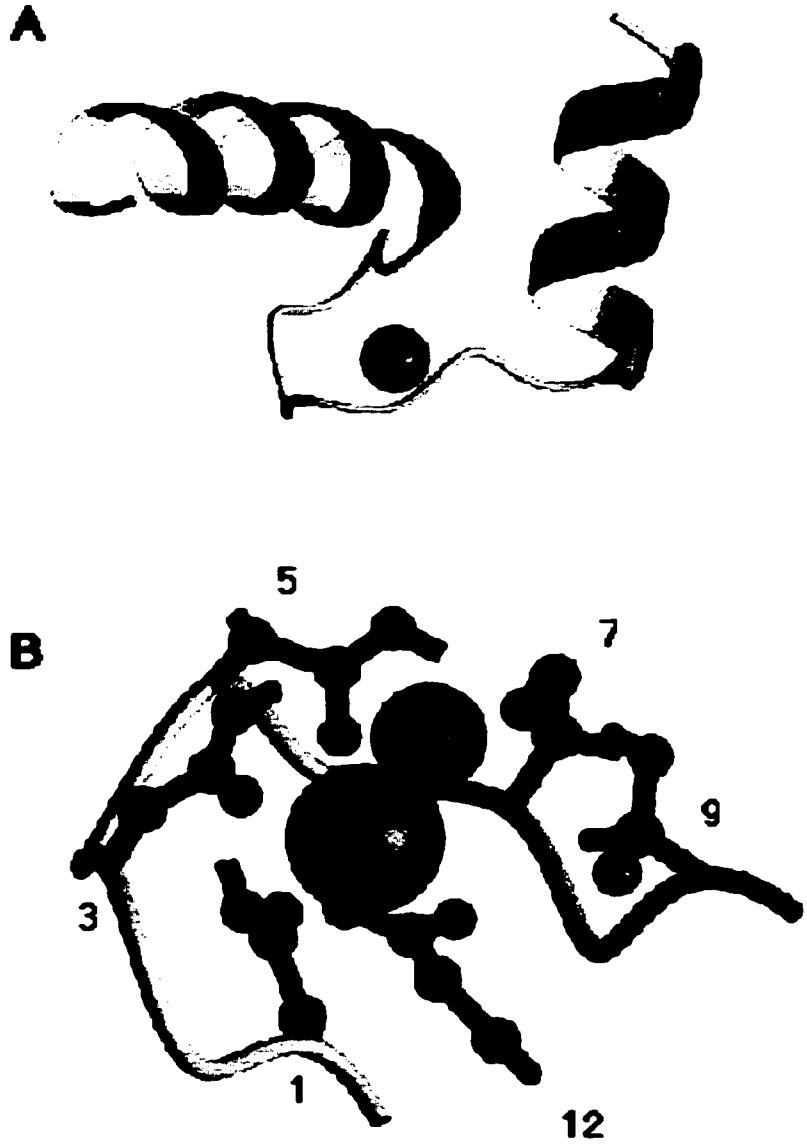

Figure 1.3 The structure of a Ca^{2+}-binding site in CaM. (A) The ribbon structure of the first EF-hand (residues 5 - 40) in CaM. (B) The first Ca^{2+}-binding loop in CaM. The side chains of the residues providing Ca^{2+} ligands are shown (residue 1 is Asp20). The residue at position 7 coordinate Ca^{2+} (the largest ball at the center) with its backbone carbonyl oxygen which is not shown in this figure. One of the Ca^{2+} ligands is H_2O whose oxygen atom is presented as a big ball beside Ca^{2+}.

Ca^{2+}-binding loops are also highly conserved. The positions 4 and 6 are always occupied by Gly (Table 3.2). These Gly residues provide the large flexibility which is necessary to the loop. There are a total of eleven Gly residues in CaM, eight of which are located in Ca^{2+}-binding loops (two in each Ca^{2+}-binding site), which makes Gly a very good reporting group for the loops during NMR experiments (see Chapter 3).

Calcium is a secondary messenger whose cytosolic concentration is around 10^{-7} M in resting cells. When the cell is excited, e. g. a muscle twitch, the cytoplasmic Ca^{2+} level rises to 10^{-6} M for a short period of time, perhaps a millisecond, before the cell returns to rest (Williams 1992). To pass the Ca^{2+} signal downstream, CaM has to switch on and off rapidly according to the intracellular Ca^{2+} level. On the one hand, a high Ca^{2+}-binding affinity is required to respond to the Ca^{2+} signal; on the other hand, CaM has to release Ca^{2+} fast after the cytosolic Ca^{2+} is back down to resting levels to avoid prolonged excitement of the cell. In fact, such a quick on/off switch of CaM is achieved by a fast, 10^{9} s^{-1}, diffusion-controlled Ca^{2+}-binding, and a fast, 10^{3} s^{-1}, release of Ca^{2+} with a dissociation constant close to 10^{-6} M (Williams 1992). The 10^{-6} M dissociation constant and cooperativity of Ca^{2+}-binding make CaM very sensitive to the cytosolic Ca^{2+} concentration fluctuation, which is suitable for its role in signal transduction pathways. Some other proteins, e.g. parvalbumin, have similar Ca^{2+}-binding affinities as CaM but much slower kinetics. It is believed that the major function of parvalbumin is to remove free Ca^{2+} in the cytosol much more rapidly than the outward Ca^{2+} pumps can

operate. Thus the pulse of free Ca^{2+} is shortened by parvalbumin buffering. This buffering is particularly important for cells requiring very fast relaxation. For example, there are large amounts of parvalbumin in fast muscle cells (Williams 1992).

Another concern about the Ca^{2+}-binding ability of CaM *in vivo* is its selectivity of Ca^{2+} over the closely related Mg^{2+} ion which has an intracellular concentration of 10^{-3} M, 10000 fold higher than Ca^{2+}. The reason for such ion selectivity is that the high coordination number of the Ca^{2+}-binding sites in CaM is not suitable for Mg^{2+}; and Mg^{2+} tends to bind water molecules very tightly which also greatly weakens its equilibrium binding with the protein side chains (Frausto de Silva & Williams 1991, Vogel 1996). More details about the metal ion binding properties of CaM will be discussed in Chapter 3.

Apo-CaM and Conformational Changes The structure of apo-CaM has also been determined by NMR (Kuboniwa *et al.* 1995, Zhang *et al.* 1995a). The overall structure of apo-CaM is very similar to that of Ca^{2+}-CaM, showing two well-folded domains with four helices in each domain (Figure 1.2A). Generally, apo-CaM is more flexible than Ca^{2+}-CaM. NMR studies showed that the helices in apo-CaM are less stable and uniformly shorter than that of Ca^{2+}-CaM, which gives apo-CaM a reduced overall helicity. In apo-CaM, the Ca^{2+}-binding loops (residues 20-31, 56-67, 93-104, and 129-140) are partially unstructured, while they are well defined in Ca^{2+}-CaM. The binding of Ca^{2+} to CaM not only restricts the movement of the Ca^{2+}-binding loops but induces

further conformational changes in the protein. As stated earlier, both apo-CaM and Ca^{2+}-CaM are α-helical proteins with four α-helices in each domain. However, the interhelical angles in these two forms of CaM are rather different. NMR studies indicated that the interhelical angles of EF-hand motifs in apo-CaM are 36°-44° larger than those in Ca^{2+}-CaM, which means that the two helices in each EF-hand are more antiparallel (Zhang *et al.* 1995a). These substantial conformational changes are caused by the binding of Ca^{2+} ions, which result in drastic changes of the protein surface. In contrast, the Ca^{2+}-buffering protein calbindin D_{9k} shows virtually no changes in interhelical angles of the EF-hands upon binding calcium (Skelton *et al.* 1994).

The surface properties of apo-CaM and Ca^{2+}-CaM are dramatically different. In Ca^{2+}-CaM, there is a large, solvent-exposed hydrophobic region in each domain. These crescent-shaped hydrophobic surfaces show 71% direct sequence homology (Zhang 1993); each of them is approximately 10.0 Å x 12.5 Å large and about 9.5 Å in depth. Each hydrophobic patch is surrounded by a polar rim which is rich in negatively charged residues (Babu *et al.* 1985, Babu *et al.* 1988). At the center of each surface, there is a deep hydrophobic cavity that can accommodate an aromatic or a long aliphatic side chain of the target proteins (Ikura *et al.* 1992, Meador *et al.* 1992, 1993). These deep hydrophobic cavities are completely absent in apo-CaM. The large hydrophobic patch on each domain essentially disappears in apo-CaM although there are still clusters of hydrophobic residues on the protein surface (Zhang *et al.* 1995a). Thus the large hydrophobic patch on the surface of Ca^{2+}-CaM is the major

conformational change induced by Ca^{2+}, which also forms the basis for the purification of CaM by affinity chromatography (also see Chapter 2).

Activation of CaM-Binding Enzymes The binding of Ca^{2+} enables CaM to interact with target proteins. As a versatile secondary messenger protein, CaM can recognize numerous downstream proteins and enzymes involved in many cellular activities, such as gene expression, cell proliferation, protein phosphorylation and dephosphorylation, muscle contraction, and so on (Figure 1.4). Many of these proteins bind to Ca^{2+}-CaM with high affinity (Kd ~ 1 nM). For the vast majority of these CaM-regulated proteins, Ca^{2+}-CaM is an absolute requirement for their functions; and the interactions between Ca^{2+}-CaM and target proteins can be reversed by reducing the Ca^{2+} concentration. However, there are a few proteins that can bind CaM *in vitro* in the absence of Ca^{2+}. For example, neuromodulin is an abundant protein in neuronal cells which has been found to interact with apo-CaM. The binding affinity in such cases are usually lower (around μM range), and hence a higher apo-CaM concentration is required for the interaction. More investigations have yet to be conducted to elucidate whether these types of interactions can occur under physiological conditions. The physiological functions of such interactions are also not clear yet. Some researchers have suggested that one function of neuromodulin could be to bind and concentrate CaM in growth cones of neuronal cells (Liu & Storm 1989, and references therein). While most target proteins will only bind to CaM after it has bound calcium, some Ca^{2+}-CaM

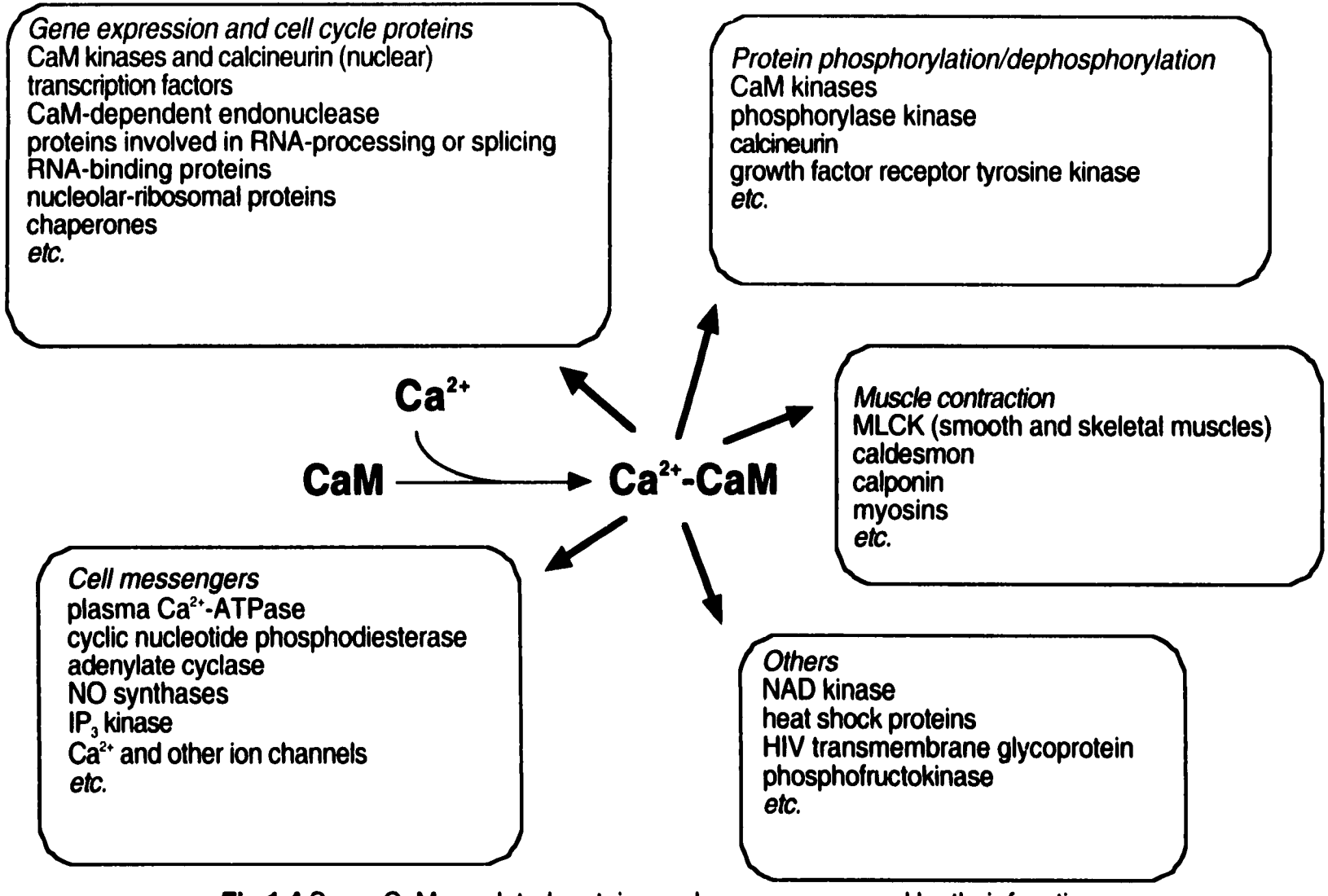

Fig 1.4 Some CaM-regulated proteins and enzymes grouped by their functions

activated target proteins can also bind to apo-CaM at physiological salt concentrations, such as cyclic nucleotide phosphodiesterase (PDE) and inducible nitric oxide sythase (Yuan *et al.* 1998, 1999b). The phosphadiesterase CaM-binding region has a β-turn structure when bound to apo-CaM. However when this complex binds calcium, the CaM undergoes a conformational change, and the bound phosphodiesterase peptide now becomes completely α-helical (Yuan *et al.* 1999b). This change in structure leads to the activation of the target protein.

One of the best characterized Ca^{2+}-regulated intracellular activities is muscle contraction. The role which Ca^{2+} and CaM play in smooth muscle contraction has been intensively studied. In response to an increase of the cytosolic Ca^{2+} level, CaM is saturated by Ca^{2+} ions which allows CaM to bind and activate myosin light chain kinase (MLCK). MLCK will phosphorylate the light chain subunit of myosin, which will then form a complex with actin and subsequently promote the actomyosin ATPase activity that accompanies contractility. The myosin light chain can then be dephosphorylated by myosin light chain phosphatase and the muscle relaxes (Allen & Walsh 1994, Walsh 1994). Evidently, MLCK is important in this process. The apoenzyme of MLCK is virtually inactive and only the $4Ca^{2+}$-CaM-MLCK complex[2] is fully

[2] In this dissertation, "Ca^{2+}-CaM" is normally used to represent the Ca^{2+}-saturated CaM. However, in some cases, the number of Ca^{2+} ion on CaM is important for discussion, where the number is added in front of "Ca^{2+}-CaM". Recently, there is some evidence suggesting that $2Ca^{2+}$-CaM can also bind MLCK, but cannot activate the enzyme. Only $4Ca^{2+}$-CaM-MLCK complex represents the fully active enzyme (Dr. M. Walsh, University of Calgary, personal communication).

functional. In apo-MLCK, the active site is blocked by another domain of the enzyme, a so-called "autoinhibitory" or "pseudosubstrate" domain. The sequence of the autoinhibitory domain resembles the amino acid sequence around the phosphorylation site on myosin light chain. In the apo-enzyme, the autoinhibitory domain is folded into the active site and blocks the access of myosin to MLCK. On the other hand, the autoinhibitory domain partially overlaps the CaM-binding domain in MLCK. The binding of $4Ca^{2+}$-CaM to the CaM-binding domain removes the autoinhibitory domain from the myosin-binding site on MLCK and the enzyme is hence activated. This autoinhibitory model is strongly supported by limited proteolysis studies. MLCK stays inactive and unaffected by Ca^{2+}-CaM if the CaM-binding domain has been cleaved and the removal of the autoinhibitory domain will result in a constitutively active enzyme (Allen & Walsh 1994).

CaM-Binding Domain/Peptide There are dozens of CaM-regulated proteins and enzymes whose CaM-binding sites have been mapped out (Rhoads & Friedberg 1997). The CaM-binding domains usually comprise a ~20 amino acid region in the protein. The amino acid sequences of some of the CaM-binding domains are aligned in Figure 1.5. Synthetic polypeptides derived from the CaM-binding domain of several proteins have been used to investigate the interaction between CaM and target proteins, since these peptides show similar binding affinity to CaM as intact proteins with dissociation constants in the high picomolar to low nanomolar range (O'Neil &

DeGrado 1990). The CaM-binding domains in substrate proteins do not share any obvious sequence homology. In fact, sequence-independent recognition is one of the striking features of the interaction between CaM and target enzymes. However, one common feature of these peptides is that they all contain many hydrophobic and positively charged residues; and that these peptides tend to form amphiphilic α-helices in solution (O'Neil & DeGrado 1990).

Several structures of the complexes of CaM and target peptides have been determined by NMR and X-ray crystallography (Ikura *et al.* 1992, Meador *et al.* 1992, 1993, Elshorst *et al.* 1999, Osawa *et al.* 1999). The NMR structure of the complex of Ca^{2+}-CaM-MLCK(peptide) is shown in Figure 1.2C. As we can see in the figure, the peptide adopts an α-helix conformation when it is bound to CaM, although the peptide itself is virtually unstructured in solution. The α-helix is amphiphilic which means one side is hydrophobic and the other is positively charged. The aforementioned hydrophobic patches on Ca^{2+}-CaM serve as the major interface between the protein and the peptide. The solvent-exposed hydrophobic patches on Ca^{2+}-CaM become fully buried in the complex (Yuan *et al.* 1999a). The positively charged residues on the peptide can also make electrostatic interactions with the negatively charged residues on the rim of the hydrophobic patches of CaM. The N-terminus and the C-terminus of Ca^{2+}-CaM are pulled closer to each other by binding of the α-helical substrate peptide, giving the complex a more globular shape (Figure 1.2C). The two ends of CaM move closer to make a surface region which is

	1								8						1314							
skMLCK	K	R	R	**W**	K	K	N	F	I	A	**V**	S	A	A	N	**R**	**F**	K	K	I	S	S
smMLCK	R	R	K	W	Q	K	T	G	H	A	V	R	A	I	G	R	L	S	S	S		
CaM Kinase I	A	K	S	K	W	K	Q	A	F	N	A	T	A	V	V	R	H	M	R	K	L	Q
CaM Kinase II	A	R	R	K	L	K	G	A	I	L	T	T	M	L	A	T	R	N	F	S		
Ca^{2+} pump	G	Q	R	L	W	F	R	G	L	N	R	I	Q	T	Q	I	R	V	N	A	F	R	S
PFkinase	F	M	N	N	W	E	V	Y	K	L	L	A	N	I	R	P	P	A	P	K	S	G	S
Spectrin	T	A	S	P	W	K	S	A	R	L	M	V	H	T	V	A	T	F	N	S	I	K	E
Calcineurin	R	K	E	V	I	R	W	K	R	A	I	G	K	M	A	R	V	S	F	V	L		
Caldesmon	R	A	E	F	L	N	K	S	A	Q	K	S	G	M	K	P	A	N					
Calspermin	A	R	R	K	L	K	A	A	V	K	A	V	V	A	S	S	R	L	G	S			
NO synthase	R	A	G	F	K	K	L	A	E	A	V	K	F	S	A	K	L	M	G	Q			
Phosphodiesterase	T	E	K	M	W	Q	R	L	K	G	I	L	R	C	L	V	K	Q	L				

Figure 1.5 Sequence alignment of some of the CaM-binding domains. The important residues in skMLCK peptide are highlighted. There is a noteble lack of sequence homology among these domains.

opposite to that of the central α-helix linker. This surface region may play a crucial role in activating some of the substrate enzymes. Some recent evidence showed that mutation of certain residues in this region can significantly lower CaM's ability to activate MLCK (Persechini *et al.* 1996, Dr. M. Walsh, personal communication).

In the skMLCK-CaM complex, the peptide binds to CaM in an antiparallel orientation with the N-terminal region predominantly interacting with the C-lobe of CaM. Two bulky hydrophobic residues, Trp at position 1 and Phe at position 14, anchor the peptide into the C- and N-

position 1 and Phe at position 14, anchor the peptide into the C- and N-terminal domains of CaM respectively; the hydrophobic residue at position 8 makes contacts with both domains; the basic residue at position 13 forms a salt bridge with a negatively charged side chain on CaM. Overall, the hydrophobic interactions play a major role in CaM-peptide recognition, while electrostatic interactions also make some contributions.

One intriguing question about the target-recognition of CaM is how CaM can interact with so many different peptides without sequence specificity? The answer may lie in the large hydrophobic patches on the protein surface. An interesting feature of these hydrophobic patches is that they are rich in Met residues. There are four Met residues in each domain of Ca^{2+}-CaM (another Met is in the central linker region) and all of them are part of the hydrophobic surfaces. The Met residues actually contribute as much as 46% of the total hydrophobic surface area in Ca^{2+}-CaM (Babu *et al.* 1988). The high content of Met in these surfaces is believed to be an important reason for the sequence-independent recognition because Met has some unique properties compared to other hydrophobic amino acids. Met has a flexible long unbranched side chain. The two S-C bonds are longer than C-C bonds, and the rotation around these bonds is virtually free in contrast to C-C bonds which have hindered rotation (Gellman 1991, Vogel 1994). Moreover, the sulfur atom in Met side chain is highly polarizable, which can contribute to the London dispersion forces and thus add to the stickiness of the hydrophobic surfaces in a complex (Gellman 1991, Zhang & Vogel 1994,

Weljie & Vogel 2000). Site-directed mutagenesis studies showed that the mutation of Met to Leu or Gln in the hydrophobic patch has drastic effects on CaM activity, even though such mutations do not cause any significant changes in the protein structure (Zhang *et al.* 1994a, Chin *et al.* 1997, Edwards *et al.* 1998). For example, M36L CaM is virtually incapable of activating cyclic nucleotide phosphodiesterase (Zhang *et al.* 1994a), while M124L has a significant effect on MLCK activation (Edwards *et al.* 1998), and M144V abolishes activation of nitric oxide synthase (Kondo *et al.* 1999). Hence, the Met residues on the surface of Ca^{2+}-CaM are important for target protein recognition, and different residues are crucial for different target enzymes.

Scope of This Dissertation

Normally, there are three forms of CaM to consider in a physiological setting: apo-CaM, Ca^{2+}-CaM, and Ca^{2+}-CaM-target protein complexes. Calcium and target proteins are the "natural" ligands of CaM. However, CaM is exposed to many other molecules in the complicated intracellular environment, which can also interact with CaM. Studies of these "unusual" CaM-ligand interactions will further our understanding of CaM and its role in signal transduction pathways. Most of the research projects included in this dissertation are dealing with such CaM-ligand interactions, and the "ligands" studied are other metal ions, hormones, drugs, or "unusual" peptides.

Although CaM is the major intracellular calcium signal receptor, it can also bind many other metal ions based on their similarity in ionic radius with

calcium. Chapter 3 describes the study of the binding of a host of metal ions to CaM using NMR and fluorescence spectroscopy.

It has been reported that the neurohormone melatonin can interact with the two large hydrophobic patches on the surface of CaM. Chapter 4 describes my attempts to verify such interactions. Structural homologues of melatonin, such as serotonin, tryptophan, and 4-hydroxytryptophan, were also included in this work.

In Chapter 5, the interaction of CaM with the anticancer platinum drugs, cisplatin and carboplatin, was studied. These drugs were shown to bind covalently to the Met residues of CaM. This interaction is unique among the CaM-ligand interactions studied in this dissertation, and may play a role in the side effects that accompany the administration of these drugs.

Studies on two different kinds of CaM-binding peptides, melittin and LLP-1 peptides from different HIV-1 isolates, are described in Chapter 6 and 7 respectively. These peptides are not derived from the "usual" intracellular CaM-target proteins. Melittin, a bee venom peptide, is often used as a "model" CaM-binding peptide due to its high affinity for CaM. Our studies have shown that it is actually quite different from the other CaM-binding peptide because of the rather "unusual" location of the anchor residue, Trp, in its sequence. LLP-1 peptides are derived from the cytoplasmic C-terminal segment from HIV transmembrane glycoprotein gp41. The CaM-LLP-1 interaction might play a key role in HIV pathogenesis.

Chapter 8 deals with another protein, the M-domain from the *ffh*

protein in *E. coli*. Since the M-domain is not covered in this introduction chapter, a detailed introduction section is provided in Chapter 8. Like CaM, the M-domain recognizes peptides in a sequence-independent manner; it is Met rich and hence it resembles the interactions between CaM and its target proteins. Chapter 8 describes an attempt of expression, purification, and homology modeling of the *E. coli* M-domain.

Finally, a summary of this dissertation is provided in Chapter 9, where more general conclusions and future directions are provided.

Chapter 2

Materials and Methods

The materials and experimental techniques described in this chapter were used throughout this dissertation. The first part of this chapter involves the preparation of CaM and its tryptic fragments, which were the subjects of several projects included in this dissertation. Since NMR was the major tool I employed in my research, a brief introduction of the theory and practice of biological NMR will be provided in the second part of this chapter. It is certainly not possible to discuss the complete theory of NMR in this dissertation, rather, a simple introduction of bio-NMR will be provided. Several other methods I frequently used will also be described in this chapter. I will address the theory and rationale behind the application of these methods in each section. The experimental conditions may vary for specific purposes, therefore, I will only provide general information in this chapter. More specific materials and methods that have been employed to investigate the particular questions addressed in the subsequent chapters will be described therein.

Materials and Protein Preparation

Expression and Purification of CaM from E. coli

CaM is expressed and purified from an *E. coli* strain harboring the

pCaM plasmid[1]. *E. coli* strain MM294 was used to express wild type CaM in my studies. The frozen *E. coli* strain (stored at -80°C) was activated by streaking to a fresh ampicillin LB plate 18-20 hours prior to the inoculation. A single colony was then picked and inoculated into 1 L LB media with 50 mg/L ampicillin. The cells were grown in a shaker at 30°C for 8-9 hours until the cell density measured by OD_{600} reached 1.0-1.3. The growth temperature was increased to 37°C, and 160 mg isopropyl-β-d-thiogalactopyranoside (IPTG) was added, and the protein expression was induced for another 4 hours before the cells were harvested by centrifugation (8000 rpm, 10 min). The cells were then washed with 50 mM Tris-HCl, pH 7.5 with 5 mM EDTA, 1 mM DTT, and 100 mM KCl. Normally, the cells were stored in a -20°C freezer overnight to facilitate cell wall breakage.

The CaM purification process was started by lysozyme treatment of the cells. The cells were thawed out and resuspended into 100 ml lysate buffer (50 mM Tris-HCl, pH 7.5 with 2 mM EDTA and 1 mM DTT). Lysozyme (24 mg) was dissolved in the same buffer (20 ml) and added into the cell suspension. The suspension was stirred in the cold room for 40 minutes before it was centrifuged (15000 rpm, 20 min) at 4 °C. The pellet was discarded and 2 M MgCl was added into the supernatant until its final concentration was 5

[1] The plasmid was a generous gift from Dr. T. Grundström (University of Umea, Sweden) several years ago. The pCaM vector is a so called "run-away" plasmid of which the copy number is thermal-dependent. The expression of CaM is under control of the LacZ promoter which is inducible by IPTG (see the preceding section). The *E. coli* strain MM294 was routinely used to produce mammalian CaM in our lab (Zhang 1993, David 1997, Yuan 1998).

mM. Then 120 µl of 10 mg/ml DNase I was added and the solution was stirred in the cold room for 40 minutes to reduce the viscosity of the solution. This solution was then loaded on a Phenyl-Sepharose (Pharmacia) column (30-40 ml) which was equilibrated with buffer E (50 mM Tris-HCl, pH 7.5, 5 mM EDTA, 1 mM DTT, and 100 mM KCl). The breakthrough of this column containing CaM was collected. The column was washed with 50 ml of buffer E and was combined with the eluent solution. The volume of the eluent was measured and 2 M $CaCl_2$ was added until the final concentration of Ca^{2+} reached 10 mM. This solution was subject to a second Phenyl-Sepharose column equilibrated with buffer A (50 mM Tris-HCl, pH 7.5, 1 mM $CaCl_2$, and 1 mM $MgCl_2$). The column was washed with buffer A extensively (overnight, at least 15 bed volumes) with a flow rate of 100 ml/h, then by buffer B (buffer A containing 0.5 M NaCl) and C (50 mM Tris-HCl, pH 7.5, with 50 mM NaCl). CaM was eluted by buffer D (50 mM Tris-HCl, pH 7.5, 50 mM NaCl, and 1 mM EDTA) and collected 4 ml per fraction. The fractions with OD_{280} over 0.2 were pooled and dialyzed against 50 mM NH_4HCO_3 extensively before the sample was lyophilized. The freeze-dried protein is ready for use. The protein appears as a single band on SDS-PAGE. The yield of this method for wild type CaM is normally 60 -80 mg per liter of culture.

Specific Isotope Labeling of CaM

It is often necessary to incorporate isotope-enriched (^{15}N or ^{13}C) amino acids, or amino acid analogs, into CaM to facilitate NMR experiments. In

order to achieve high incorporation rates, certain *E. coli* auxotrophic strains have been used. The auxotrophic strains were obtained from the *E. coli* Genomic Stock Center at Yale University. In my studies, strains DL41 and DL39G were used for incorporating isotope-labeled Met and Gly into CaM, respectively. The following section describes the preparation of Methyl-^{13}C-Met labeled CaM. Other specific isotope labeled CaM, like ^{15}N-Gly labeled CaM, can be obtained in a similar manner.

Preparation of methyl-^{13}C-Met labeled CaM The plasmid for expressing CaM in *E. coli*, pCaM, was purified from *E. coli* strain MM294 harboring this plasmid with the EasyPrep Plasmid Prep Kit (Pharmacia). Transformation of the competent cells of DL41 with pCaM was performed using standard $CaCl_2$ method (Sambrook 1989).

The cells were plated and a single colony was inoculated into 1 L LB media as usual (see the preceding section). The cells were grown at 30°C for 8-9 hours until the cell density measured by OD_{600} reached 1.0-1.3. The cells were spun down at room temperature and transferred into 800 ml MOPS media (room temperature). Another portion of MOPS media (200 ml) was prewarmed to 65 °C and added to the cell culture to make the final temperature of the media 37 °C. The MOPS media contains all the amino acids except the amino acid to be incorporated, in this case, Met. Methyl-^{13}C-Met (50 mg) and IPTG (160 mg) were added into the MOPS cell culture. The cells were grown at 37°C for another 4 hours before harvesting by

centrifugation. The purification of methyl-^{13}C-Met labeled CaM was accomplished in the same way as that of unlabeled CaM.

Normally, an incorporation rate of over 95% can be accomplished using this method as indicated by mass spectrometry (Dr. T. Yuan, personal communication). It should be pointed out that the incorporation pathways vary for different amino acids. High incorporation rates are very difficult to achieve for some amino acids, such as Asn, for example, due to complications from different cellular metabolic pathways.

Se-Met Labeling of CaM

Labeling of CaM with seleno-Met (Se-Met) was accomplished in very similar fashion to that of Methyl-^{13}C-Met. One difference was that the cells were grown at 37 °C in LB media for about an hour before they were spun down and transferred to MOPS media. This step was omitted in labeling CaM with isotope-labeled natural amino acids (see last section). The main purpose of this step was to increase the plasmid copies in the cell before it was transferred to a media containing unnatural amino acids. We have found that some amino acid analogs inhibit the multiplication of the plasmid which can result in very low yield. Such inhibition has not been observed in the case of Se-Met. However, this step was introduced as a precaution for incorporation of any unnatural amino acid.

The incorporation rate of Se-Met can be determined by amino acid analysis or by natural-abundance ^{1}H,^{13}C HMQC NMR experiments. The

amino acid analysis was carried out by Dr. D. McKay, Protein Sequencing Facility, Faculty of Medicine, University of Calgary. Table 2.1 shows the amino acid composition of Se-Met labeled CaM which indicates that the incorporation rate of Se-Met in CaM was above 80%. This result was also supported by NMR experiments. Figure 2.1 shows the spectrum of a natural-abundance $^{1}H,^{13}C$ HMQC experiment. Comparison of the intensities of the methyl groups of Met and Se-Met also reveals that the incorporation rate is about 80%. Generally, the incorporation rates of isotope-labeled natural amino acids are usually higher than that of unnatural amino acid analogs.

Table 2.1 Results of Amino Acid Analysis of Se-Met labeled CaM

A.A.	A.A. Composition[1]	A.A.	A.A. Composition[1]
Asp	23.106	**Met**	**1.546**[2]
Thr	11.292	Ile	14.376
Ser	3.929	Leu	9.666
Glu	28.237	Tyr	1.787
Pro	2.127	Phe	6.738
Gly	11.78	His	0.783
Ala	11.27	Lys	8.000
Val	6.943	Arg	5.296

[1] A.A. analysis data were converted to A.A. composition data normalized to Lys=8.000.

[2] Incorporation rate of Se-Met = (9.0-1.5)/9.0 = 83%.

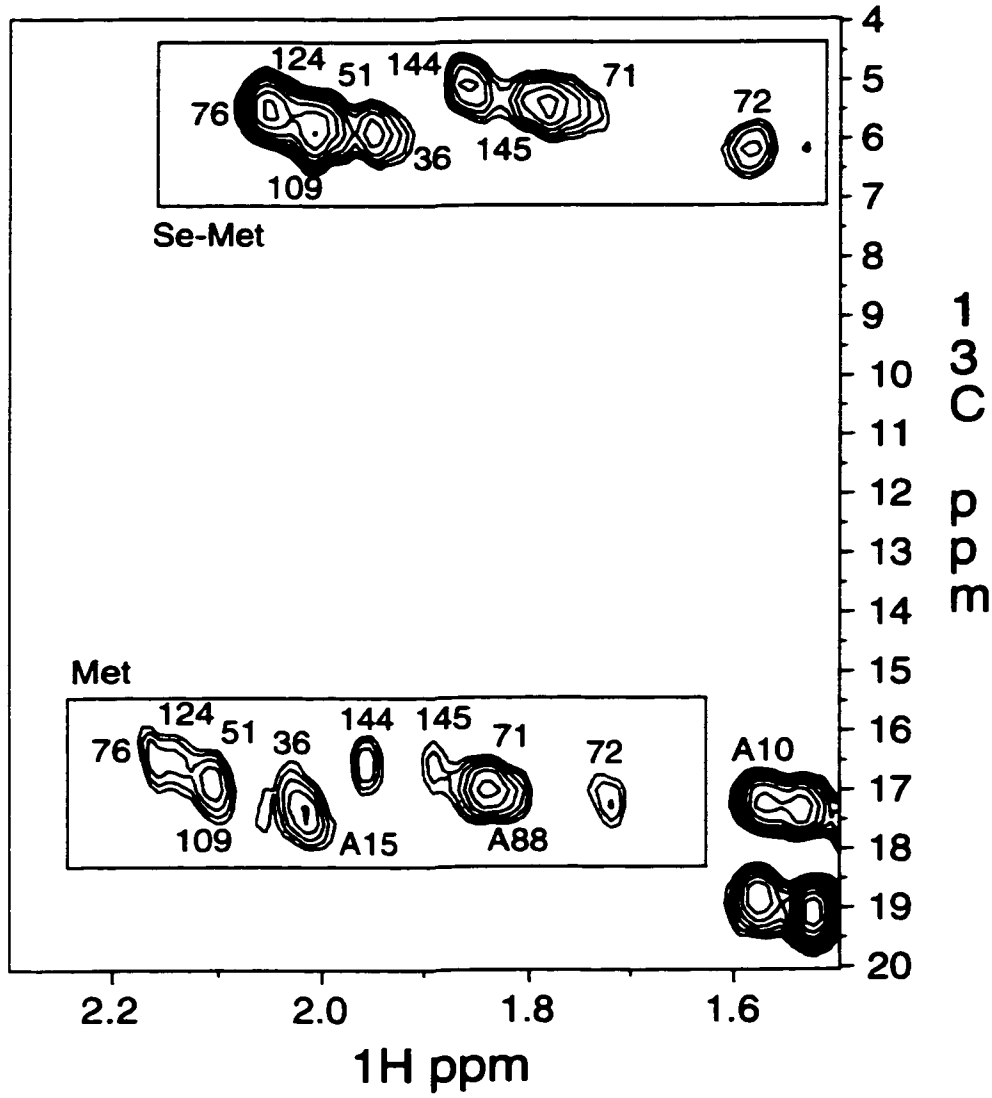

Figure 2.1 Natural abundance $^{1}H,^{13}C$ HMQC NMR spectrum of Se-Met labeled CaM. The resonances in the upper box are the methyl groups of Se-Met sidechains. The majority of the peaks in the bottom box are methyl groups of natural Met sidechains. The signals from Se-Met and Met are labeled by their residue number. Some resonances in this region are from Ala sidechains which are also labeled.

Preparation of Apo-CaM

Apo-CaM was prepared by passing the protein sample through a Chelex-100 (Bio-Rad) column. This procedure was usually performed only shortly before the NMR experiments because apo-CaM is less stable than Ca^{2+}-CaM and apo-CaM is not suitable for long-term storage. Typically, 15-20 ml Chelex-100 resin column (suspended in 50 mM NH_4HCO_3 buffer) was washed with 50 mM NH_4HCO_3 for two bed volumes. CaM (15-20 mg) dissolved in 1-2 ml of the same buffer was applied to the column and washed with 50 mM NH_4HCO_3 by gravity flow. The eluant was collected at 2 ml per fraction and the absorbance was checked at 280 nm. The fractions containing CaM were pooled and lyophilized. Absence of calcium was checked by collecting 1 D proton NMR spectra. These procedures can be repeated one more time if necessary.

Limited Proteolysis of CaM

As mentioned in the Chapter 1, Ca^{2+}-CaM can be cleaved by trypsin in the middle of the central α-helix. The N- and C-terminal domains of CaM are thus separated, and the fragments are named TR1C and TR2C, respectively. In fact, TR1C (1-75) can be overexpressed from a partial gene construct and purified from *E. coli* using the same procedure as for CaM. However, for some unkown reasons, the TR2C gene cannot be overexpressed well in *E. coli* and the TR2C fragment has to be obtained through limited proteolysis.

The preparation of the tryptic fragments of CaM started with the

cleavage by trypsin. Typically, 50 mg CaM was dissolved in 2 ml freshly made Buffer I (50mM NH_4HCO_3, 50 mM NaCl, pH7.9) with 8 mM $CaCl_2$. Trypsin (Sigma) stock solution was freshly prepared by dissolving 5 mg trypsin in 1 ml 1 mM HCl. The CaM solution was incubated with 0.5 mg trypsin (100 µl of the stock) at 37°C for 40 minutes. The reaction was stopped by adding 1 mg soybean trypsin inhibitor (200 µl from a stock solution of 5 mg inhibitor (Sigma) in 1 ml 1 mM HCl) into the reaction mixture. The digested protein solution was quickly applied to a Sephadex G-50 (Pharmacia) column (1.5x100 cm) equilibrated with Buffer I in order to separate the fragments from intact CaM. Elution of the fragments with Buffer I was followed with a UV spectrophotometer at 280 nm. The fractions containing the fragments were pooled and 2 M $CaCl_2$ was added into the solution until the final concentration was 5 mM.

This solution was then loaded onto a 30 ml Phenyl-Sepharose (Pharmacia) column which was pre-equilibrated with Buffer II (50 mM Tris-HCl, pH 7.5, 1 mM $CaCl_2$) to separate the two fragments. The column was washed with 30 ml of the same buffer. TR1C was eluted by Buffer III (2 mM Tris-HCl, pH 7.5, 1 mM $CaCl_2$). Since there are no Tyr residue in TR1C, the elution of TR1C was monitored by UV absorption at 258 nm for Phe residues. A typical TR1C UV spectrum is shown in Figure 2.2. TR2C was eluted by distilled H_2O (pH was adjusted to 7.5 by diluted NaOH) which can be followed by UV absorbance at 280 nm, because this fragment contains Tyr residues (Figure 2.2). Note that CaM is devoid of Trp residues.

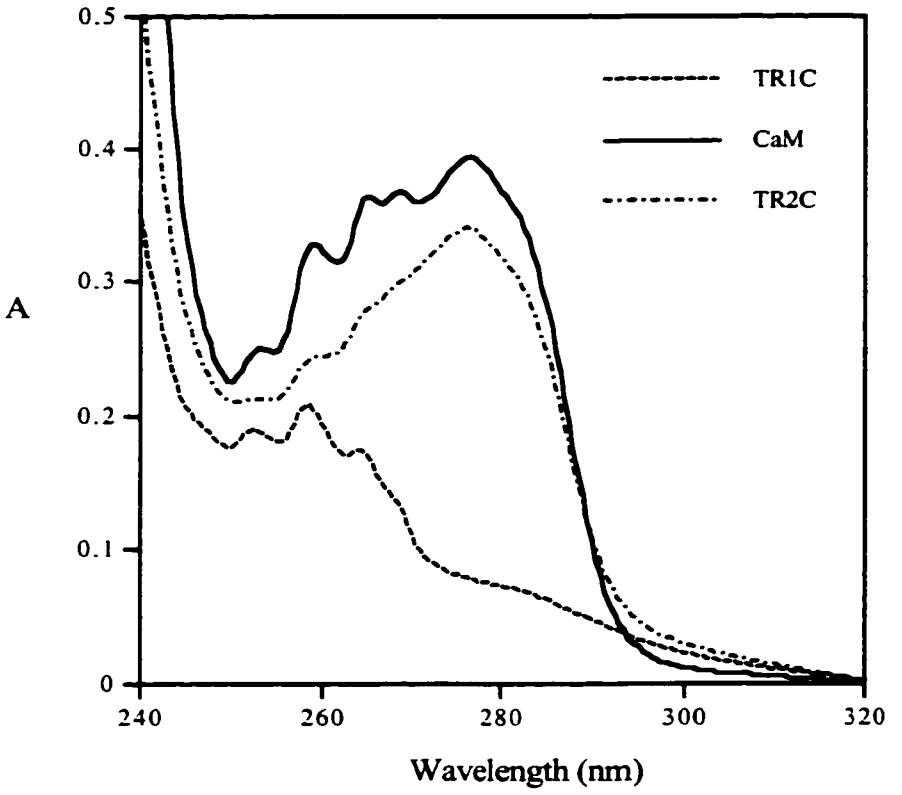

Figure 2.2 UV spectra of CaM and its tryptic fragments, TR1C and TR2C. Note the unusual absorption of TR1C.

Desalting of CaM and its Tryptic Fragments

The tryptic fragments of CaM are less stable than intact CaM, therefore, extensive dialysis should be avoided during the purification. The fractions of the fragments were pooled together and freeze dried right after they were eluted from the column. The fragments were then desalted by a gel filtration column. The column used in my studies was a prepacked 10 ml

PG10 column which is available from Bio-Rad. TR1C or TR2C was dissolved in 3 ml 50 mM NH_4HCO_3 and applied to the column which was equilibrated with the same buffer. The first 3 ml of the elution was discarded and the next 4 ml was collected and freeze dried. The sample was then stored in a -20°C freezer. CaM can also be desalted following the same procedure.

Frequently Used Methods

Nuclear Magnetic Resonance (NMR)

Most of the biological activities are carried out by proteins in cells. To understand the function of a protein requires a full understanding of its structure. NMR spectroscopy has evolved into an indispensable technique for biologists to study the biological systems at the molecular level since Saunders and colleagues acquired the first NMR spectrum of a protein, ribonuclease A, in 1957. Together, X-ray crystallography and NMR spectroscopy provide two major methods for scientists to reveal 3D structures of biological macromolecules. To date, there are hundreds of proteins in the protein data bank (PDB) whose structures have been solved by these two techniques. The elucidation of protein structures sheds light on the mechanism of their functions, conformational changes and ligand (substrate)-binding. With more and more structures being solved and deposited in the PDB, researchers are now able to predict the structures of related proteins whose structures are unknown, based on their amino acid sequence alone.

Both X-ray crystallography and NMR spectroscopy can provide us with the information about the 3D structure of a protein at an atomic level. The major advantage of NMR spectroscopy over X-ray crystallography is that researchers can study a protein in solution which is closer to its "natural" state than in a crystal. Since proteins are "breathing", the NMR structures can provide "real-time", dynamic images of the protein in solution, which reflects the actual state of the protein in a biological system. Moreover, NMR spectroscopy is more suitable for studying ligand-binding or protein-substrate interactions even if the interactions are relatively weak, because such complexes are normally more difficult to crystallize.

Like any other method, NMR spectroscopy has its own disadvantages. It can only handle smaller proteins since large proteins have longer correlation time which result in broader NMR signals. Protein NMR spectroscopy also requires highly concentrated samples. For example, above 1 mM protein concentration (about 15 mg in 500 μl for CaM) is desired for a good NMR sample of CaM. The demand of large quantities of sample proteins makes it necessary to establish a good expression and purification system for the protein of interest. The expression system used for CaM is a perfect example. The expression and purification procedures of CaM are simple and the yield is high. A yield of 60 - 80 mg pure protein per liter culture can be readily achieved for wild-type CaM. Although the yield of labeled CaM is lower than that, it is normally enough for a few NMR samples.

Basically, NMR spectroscopy can be used to characterize any nucleus with either an odd mass number or even atomic number that possesses the property of nuclear spin ($I \neq 0$). Isotopes of nuclei that possess a symmetrical distribution of charge have a nuclear spin of 1/2 which can be readily characterized by NMR spectroscopy because of their predictable properties. Many other nuclei, so called quadrupolar nuclei, have an asymmetrical distribution of charge with a nuclear spin >1/2. The quadrupolar nuclei have much more complicated NMR characteristics which result in very broad peaks that are hard to detect. However, recent development in NMR techniques indicated that quadrupolar nuclei can also serve as a very useful tool for investigating ligand-binding and conformational changes (Saponja & Vogel 1996, Aramini *et al.* 1997, Aramini & Vogel 1998).

The use of spin 1/2 nuclei ^{1}H, ^{13}C and ^{15}N dominates in the biological NMR field. ^{1}H is by far the most important nucleus in NMR for protein structure determination because of its high natural abundance and high sensitivity. The natural abundance of ^{1}H, normally referred to as "proton", is 99.985%. Such a high natural abundance is a big advantage in research since an isotope-enriched compound is not needed for proton NMR. The proton has the highest sensitivity among all the nuclei. Two other nuclei that are also extensively used in protein structure studies, ^{13}C and ^{15}N, have sensitivities which are only 0.176% and 0.00385% of that of ^{1}H, respectively. The majority of the other nuclei have similar sensitivities as ^{13}C and ^{15}N, or even lower. Only one nucleus, ^{19}F, has a sensitivity close to that of ^{1}H (83.4%). Unfortunately, ^{19}F

does not naturally occur in proteins. ^{19}F NMR can be a useful tool in structural biochemistry if ^{19}F-labeled amino acid analogs are incorporated into the protein (Danielson & Falke 1996, David 1997). A lot of 1D and 2D NMR techniques have been developed and extensively used solely for detecting ^{1}H signals. Many multi-dimensional heteronuclear NMR experiments also depend on correlations between proton and ^{13}C or ^{15}N to take advantage of the high sensitivity of the protons. Proton NMR is normally the first choice for NMR spectroscopists in protein structure research. The disadvantages of ^{1}H NMR are the interference of the water peak in the spectra and the overlap of resonances in a relatively narrow chemical shift range. Since most protein NMR experiments are carried out in solution, the signal from H_2O of the solution will result in a prominent peak which dominates the spectrum. This can be overcome by some NMR techniques such as presaturation. An alternative for H_2O is to use D_2O in NMR samples, which improves the spectral quality by minimizing the water peak. However, proton exchange could be a problem. Protons bound to a carbon atom do not exchange with protons in water. Therefore, using D_2O as solvent is safe if one is interested in studying protons bound to carbon atoms. If a proton is attached to a nitrogen atom, especially when it is on the protein surface, it can exchange and will not be visible in the ^{1}H NMR spectra if D_2O is used. Thus H_2O has to be used as solvent in this case and 10% D_2O is normally used to provide a lock signal.

Note that common biological nuclei such as ^{12}C or ^{16}O have $I = 0$ and therefore do not give an NMR signal. The two other nuclei that are extensively

used in protein NMR spectroscopy are ^{13}C and ^{15}N. Not only are the NMR sensitivities of these nuclei significantly lower than proton, but their natural abundances are much lower. The natural abundance of ^{13}C and ^{15}N are 1.108% and 0.37% respectively. Hence sometimes it is necessary to incorporate these isotopes in a 99% enriched form into the protein of interest in order to limit ^{13}C and ^{15}N NMR data acquisition time to a reasonable period of time.

Generally, a protein can be either uniformly or selectively labeled. Uniform isotope labeling can be achieved by growing the bacteria expressing the protein in a minimal medium with ^{13}C-labeled glucose as the only carbon source and/or ^{15}N-labeled NH_4Cl as the only nitrogen source. As a result, all carbon and/or nitrogen atoms in the protein will be ^{13}C and/or ^{15}N. Uniformly labeled protein is especially important in multi-dimensional NMR for total structure determination. Selective isotope labeling means specifically labeling one kind of group in the protein. For example, methyl-^{13}C-Met labeled protein refers to a protein with only the methyl group of the Met side chains labeled. Selective labeling can be achieved by culturing the bacteria in a media with isotope-labeled amino acids (which are usually commercially available) and all the other normal amino acids. Detailed procedures for preparing selectively labeled CaM were provided earlier in this chapter. Selectively isotope labeled proteins have the advantages of lower costs and simplified spectra. The ^{13}C or ^{15}N NMR spectra of a selectively labeled protein are normally much simpler because only resonances of the labeled groups can be observed in the spectra. They enable researchers to focus on the particular

groups of the protein and examine these closely.

When a nucleus is placed in a strong , static magnetic field (B_0), its spin (I) interacts with the magnetic field and creates an angular momentum. This angular momentum confers a magnetic moment on the nucleus and therefore a given energy in the magnetic field. A nucleus of spin I can have 2I+1 possible orientations in the magnetic field. For example, a spin 1/2 nucleus may have 2 orientations with respect to B_0, -1/2 (antiparallel) and 1/2 (parallel). The energy levels for these two orientations are different, and the energy difference is dependent on the strength of the magnetic field for a given set of nuclei. The distribution of parallel and antiparallel states is unequal (which can be defined by the Boltzmann expression) as a result of the energy difference. The nuclei can reorient by absorbing energy from a radiofrequency (rf) pulse which is applied during the NMR experiments. NMR spectroscopy detects this energy absorbance, and thus gives a signal in the spectrum. The frequency of the rf pulse that must be applied to a sample in order to observe different sets of nuclei are different. This frequency is called the Larmor frequency. However, the precise signal that each nucleus produces depends not only on Larmor frequency, but also on the local environment of the nucleus. It is this phenomenon that makes NMR a useful tool in structural biology. The local environments can be affected by through-bond or through-space interactions. This is why the same chemical group, for example, the methyl group of Met side chains, will give rise to distinct signals if it is located in different parts of a protein. Similarly, when a protein undergoes a

conformational change or experiences a ligand-binding process, the microenvironments around that specific region will be altered, which will further result in changes in the NMR spectra.

Circular Dichroism (CD) Spectropolarimetry

CD spectropolarimetry is a commonly used approach to examine the content of the secondary structure of a protein. CD arises from the differential absorption of circularly polarized light beams by the sample. Model polypeptides with different secondary structures display a different shape of CD spectra, especially in the far-UV range (185-255 nm). CaM is largely an α-helical protein, therefore the far-UV CD spectrum of CaM shows characteristic bands for α-helical conformation (Figure 2.3). The spectrum has two negative peaks around 208 nm and 222 nm, and a positive peak around 195 nm. An important application of CD in this work was to examine the binding of target peptides to CaM. Normally the peptide itself is not structured in solution, and thus it does not have CD absorption. When the peptide is bound to CaM, it adopts an α-helical conformation which will enhance the CD signals of CaM at 208 and 222 nm (Figure 2.3A). NMR and isotope edited FT-IR data have shown that there are only minimal changes in the secondary structure of the two lobes of CaM (Zhang *et al.* 1994a, Zhang *et al.* 1995a), hence the enhanced negative ellipticity arises from induction of α-helical structure in the bound peptide. It has also been found that near-UV

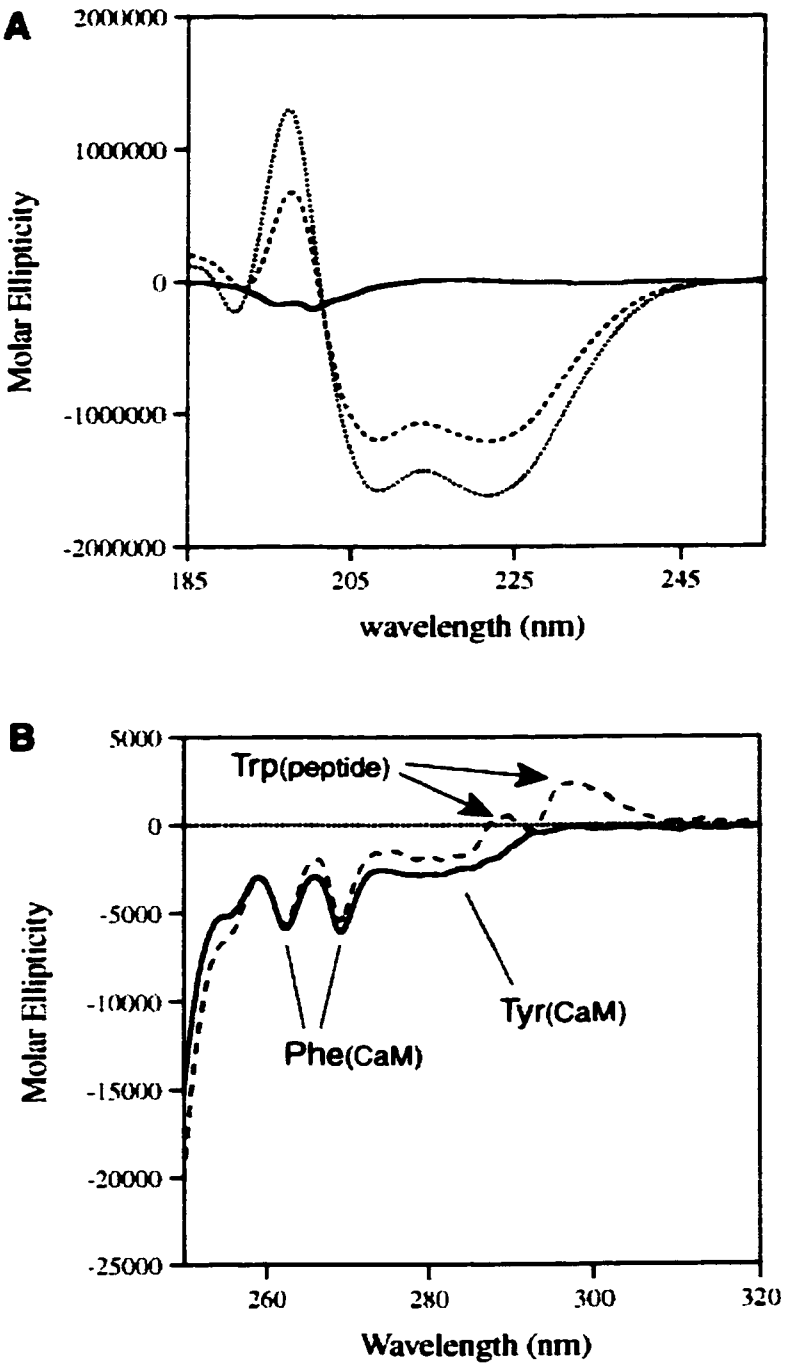

Figure 2.3 CD spectra of CaM. (A) Far-UV CD spectra of cNOS peptide (solid line), Ca^{2+}-CaM (dashed line), and CaM-cNOS complex (dotted line). (B) Near-UV CD spectrum of SIV-N peptide (dotted line), Ca^{2+}-CaM (solid line), and CaM-SIV-N complex (dashed line). Signals from aromatic residues are indicated. Note the Trp residue does not give rise to any signal in the free peptide, while it has two positive bands in the complex with CaM.

CD (250-310 nm) is useful to study the aromatic residues in CaM (Barth *et al.* 1998, Yuan *et al.* 1999b, Gomes *et al.* 2000). Tyr and Phe residues in CaM give rise to characteristic CD bands in the near-UV region (Figure 2.3B). This indicates that Tyr and Phe are held in a dissymetric environment in CaM. For a peptide with a Trp, it is possible to study its near UV CD spectrum when it becomes bound to CaM and enters the hydrophobic binding pocket (Figure 2.3B). In many cases, e.g. PDE, MLCK, PGD, CaM kinase I, and SIV peptide, a spectrum of two positive bands is obtained for the bound Trp (Yuan & Vogel 1998, Yuan *et al.* 1999b, Gomes *et al.* 2000). All CD experiments included in this dissertation were carried out at room temperature on a Jasco J-715 spectropolarimeter equipped with an Austin personal computer. Protein and peptide samples were prepared in 10 mM Tris-HCl buffer, pH7.4. For far-UV experiments, a 1 mm cell path length and 10 μM CaM concentration was used. Because the sensitivity of near-UV CD experiments is lower, a 10 mm cell path length and 40 μM protein concentrations were normally used.

Calcineurin Activity Assay

The activity of CaM can be measured by a calcineurin activity assay (calcineurin was a generous gift from Dr. J. Wang). Calcineurin is a CaM-dependent phosphatase. Since the activity of calcineurin is absolutely dependent on the binding of CaM, it can be used to measure the activity of CaM. *P*-nitrophenyl-phosphate (PNPP) was used as the substrate in this

assay, and the reaction was monitored by measuring the absorbance at 400 nm. The reaction buffer contained 20 mM Tris-HCl (pH 8.0), 100 mM NaCl, 6 mM $MgCl_2$, 18 μM $MnCl_2$, 1.5 mM $CaCl_2$, 0.45 mM DTT, and 0.1 mg/ml bovine serum albumin (BSA). The reaction was carried out in the cuvettes, and the formation of p-nitrophenolate was monitored at 400 nm for 30 minutes on a Varian Cary UV-visible spectrophotometer.

Fluorescence Spectroscopy

A fluorophore is a molecular group that can give rise to emission of radiation when it returns from an excited electronic state to the ground state. The fluorescence intensity and the wavelength of maximum emission are very sensitive to the environment of the fluorophore. Therefore, fluorescence spectroscopy can be used to monitor conformational change and substrate binding in proteins. Trp and Tyr sidechains are commonly studied fluorophores in proteins. Trp and Tyr side chains in a protein can be excited by a certain wavelength of UV light which corresponds to their absorption spectra; and emission at longer wavelength can be observed when these side chains relax. Many target peptides of CaM have Trp residues in their sequences (Figure 1.5), while there is no Trp in CaM. Hence, Trp fluorescence can be used to monitor the binding of Trp-containing peptides to CaM. The model peptide used in my studies was MLCK peptide, which corresponds to the CaM-binding domain of skeletal muscle MLCK. The protein and peptide concentrations were normally 10 μM each. The excitation wavelength used

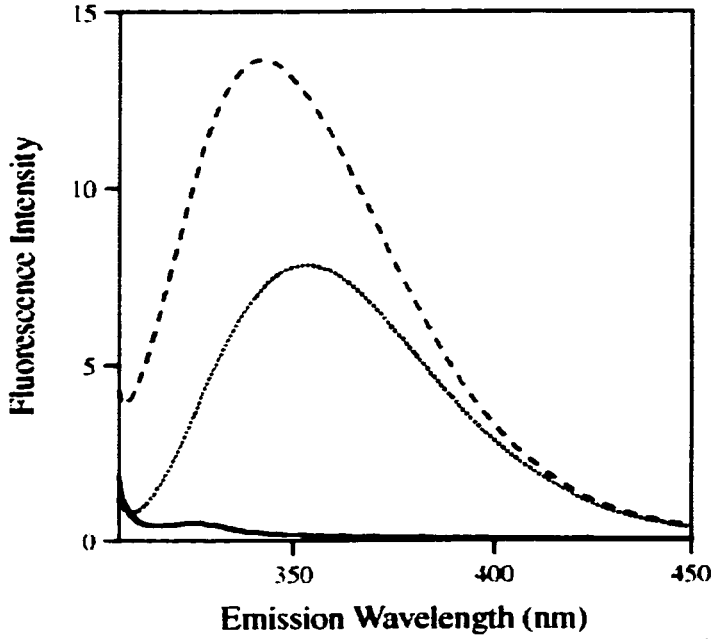

Figure 2.4 Trp fluorescence spectrum MLCK peptide (dotted line), CaM (solid line), and CaM-MLCK peptide complex (dashed line).

was 297 nm, which was enough to excite the Trp residue in the peptide while avoiding the excitation of the Tyr residues in CaM. The emission spectra were recorded in the range of 300-450 nm. When the peptide is bound to CaM, the Trp residue anchors into the hydrophobic cavity on the protein. When the fluorophore moves from a polar environment to a nonpolar one, its emission peak usually experiences a blue shift. In the case of the MLCK peptide, the emission peak shifts from 355 nm to 335 nm when the peptide binds to CaM. Simultaneously, the emission intensity also increases significantly, as shown in Figure 2.4.

Gel Band Shift Assay

The binding of target peptide to CaM can also be studied by non-denaturing urea polyacrylamide gel electrophoresis (PAGE). Urea gels contained 15% acrylamide, 4 M urea, 0.375 M Tris-HCl (pH 8.8), and 1 mM $CaCl_2$. The sample buffer contained 4 M urea, 100 mM Tris-HCl (pH 7.2), and 1 mM $CaCl_2$. Ca^{2+}-CaM is a very stable protein and can still bind substrate peptides in the presence of 4 M urea. The 4 M urea is included to prevent the formation of nonspecific interactions. However, experience in our laboratory has shown that the same results can be obtained in this experiment, whether the gel is made with or without 4 M urea. Typically, 30 μM CaM and 30 μM peptide were used and the binding of target peptide to CaM occurs under these conditions. CaM was incubated with the peptides for an hour at room temperature. An equal volume of 50% glycerol was added and 10 μl of the sample was applied to the urea gel. A constant voltage of 100 V was used to run the gel at room temperature.

The gel band shift assay provides a fast and easy method for studying the binding of substrate peptide to CaM. The complex of CaM and target peptide is less mobile on the gel, as shown in Figure 2.5.

Although the gel band shift assay is a quick and convenient way to investigate CaM-peptide binding, it is only effective for strong interactions. In Figure 2.5shows results for a few distinct CaM-binding peptides. cNOS and melittin peptide have been shown to bind to CaM with high affinity, therefore

the complexes of CaM with these two peptides were less mobile than free CaM. However, the complexes of CaM with the other peptides were not observed on this gel, although these peptides are also known CaM targets. In fact, the interaction between LLP1-E peptide and CaM has been detected by fluorescence spectroscopy and NMR experiments (see Chapter 7 for more details), as well as by mass spectrometry (Lajoie & Vogel, unpublished results). Such interactions are relatively weak (Kd ~100 μM), which cannot be detected with the gel band shift assay under our experimental conditions.

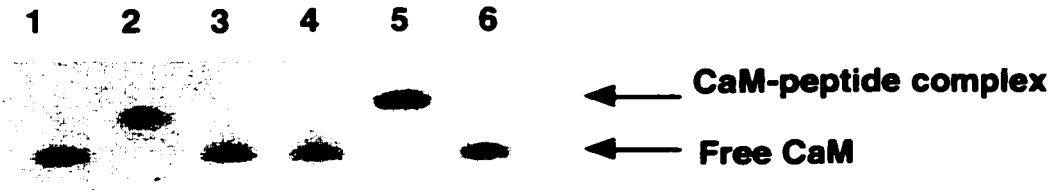

Figure 2.5 Nondenaturing native urea gel of CaM and equimolar CaM-peptide complexes. The samples are: 1, Ca^{2+}-CaM; 2, CaM with cNOS peptide; 3, CaM with LLP-1 peptide; 4, CaM with LLP-1E peptide; 5, CaM with melittin; and 6, CaM with TEF-IQ peptide.

Chapter 3

Metal Ion Binding to Calmodulin: NMR and Fluorescence Studies

Abstract

Calmodulin is an important second messenger protein which is involved in a large variety of cellular pathways. CaM is sensitive to fluctuations in the intracellular Ca^{2+} concentration and is activated by the binding of four Ca^{2+} ions. In spite of the important role it plays in signal transduction pathways, it shows a surprising lack of specificity in its binding of metal ions. Using ^{15}N-Gly biosynthetically-labeled calmodulin, we have studied the binding of different metal ions to calmodulin, including K^{+}, Na^{+}, Ca^{2+}, Mg^{2+}, Zn^{2+}, Cd^{2+}, Pb^{2+}+, Hg^{2+}+, Sr^{2+}, La^{2+}, and Lu^{3+}, by ^{1}H,^{15}N HMQC NMR experiments. The effects of these ions on the substrate-binding ability of calmodulin has also been studied by fluorescence spectroscopy of the single tryptophan residue in a 22-residue synthetic peptide encompassing the skeletal muscle myosin light chain kinase calmodulin-binding domain. Most of these metal ions can activate a calmodulin target enzyme to some extent, though they bind to calmodulin in a different manner. Mg^{2+}, which is of direct physiological interest, has a distinct site-preference for calmodulin, as it shows the highest affinity for site I in the N-terminal domain, while the C-terminal sites III and IV are the high affinity binding sites for Ca^{2+} (as well as for Cd^{2+}). At a high concentration of Mg^{2+} and a low concentration of Ca^{2+},

calmodulin can bind Mg^{2+} in its N-terminal lobe while the C-terminal domain is occupied by Ca^{2+}; this species could exist in resting cells in which the Mg^{2+} level significantly exceeds that of Ca^{2+}. Moreover, our data suggest that the toxicity of Pb^{2+}, which, like Sr^{2+}, binds with an equal and high affinity to all four sites, may be related to its capacity to tightly bind and improperly activate calmodulin.

Introduction

The calcium ion is an important intracellular messenger involved in signal transduction processes. Normally, the free Ca^{2+} level in most resting cells is around 10^{-7} M. The intracellular Ca^{2+} concentration can increase rapidly to 10^{-6} - 10^{-5} M when the cell is excited by hormones, nerve impulses, or other stimuli. The increase of the cytoplasmic Ca^{2+} level gives rise to changes in a wide range of biological events, including muscle contraction, production of nitric oxides, oxidative phosphorylation, protein phosphorylation, DNA replication, and cell proliferation. Many of the Ca^{2+} effects are mediated by a class of intracellular helix-loop-helix Ca^{2+}-binding proteins of which calmodulin (CaM) appears to be the most versatile and ubiquitous (Vogel 1994, Vogel & Zhang 1995, Ikura, 1996).

CaM is a highly conserved secondary messenger protein which has been found in almost every eukaryotic cell. More than thirty proteins and enzymes with various cellular functions have been found to be activated by CaM. The vast majority of these target enzymes are activated only by Ca^{2+}-saturated

CaM, although apo-CaM has also been found to interact with a few proteins. Ca^{2+}-CaM induces amphiphilic α-helices in the target enzymes via hydrophobic and ion-pair interactions (O'Neil & DeGrado 1990, Crivici & Ikura 1995, Vogel & Zhang, 1995). X-ray and NMR studies have shown that Ca^{2+}-CaM contains two lobes which are linked by a long α-helix in the crystal structure and by a flexible linker in solution (Babu *et al.* 1988, Barbato *et al.* 1992). Each lobe has two Ca^{2+}-binding sites which show typical helix-loop-helix structures often referred to as "EF-hands" (Kawasaki & Kretsinger 1994). There is a large hydrophobic patch on the surface of each domain of CaM which is essential for substrate binding. The binding of Ca^{2+} ions triggers the reorientation of the helices, resulting in the exposure of the hydrophobic surfaces on both domains, which enables the protein to recognize its substrates (Vogel 1994, Zhang *et al.* 1995a, Ikura 1996). Thus, the Ca^{2+}-binding process and the subsequent conformational changes are a key feature for the target enzyme activation mediated by CaM.

Ca^{2+} ions bind to apo-CaM in a step-wise manner: first, two Ca^{2+} ions bind to the C-terminal domain (sites III and IV) cooperatively; this is followed by the binding of the next two Ca^{2+} ions to the N-terminal domain (sites I and II), also in a cooperative fashion (Andersson *et al.* 1983, Ikura *et al.* 1983). Cooperativity of metal ion binding between the two lobes has been found in the presence of substrate proteins (Hiraoki & Vogel 1987, Vogel 1994). This positive cooperativity within four Ca^{2+}-binding sites allows CaM to function effectively as an on/off switch over the narrow range of Ca^{2+} concentration that

distinguishes resting and stimulated cells (10^{-7} and 10^{-6} M, respectively). Although Ca^{2+}-CaM plays many important roles in signal transduction pathways, Ca^{2+} does not seem to be the exclusive ion that can activate CaM. CaM displays a surprising ability to bind a wide variety of metal ions. More than ten different metal ions have been found to be able to substitute for Ca^{2+} in CaM. Most of these metal ions can enable CaM to activate one of its target enzymes, the CaM-dependent phosphodiesterase, to some extent (Chao *et al.* 1984). These authors also reported relative binding constants which were determined by competition dialysis equilibrium measurements (Chao *et al.* 1984). The capacity for these ions to substitute for Ca^{2+} is probably based on the similarity of their ionic radii with Ca^{2+} (0.99 Å). The presence of many other metal ions in the physiological environment suggests that CaM might be binding metal ions other than Ca^{2+} ions, especially in resting cells in which the Ca^{2+} concentration is particularly low. Thus, it is of importance to investigate the general metal ion binding properties of CaM. In this work, we have studied the binding of the metal ions, K^+, Na^+, Ca^{2+}, Mg^{2+}, Zn^{2+}, Cd^{2+}, Pb^{2+}, Hg^{2+}, Sr^{2+}, La^{2+}, and Lu^{3+} to CaM with NMR techniques (the ionic radii of these different metal ions are listed in Table 3.1). The effects of these ions on the substrate-binding ability of CaM have also been studied by fluorescence spectroscopy of the binding of the CaM-binding domain peptide derived from skeletal MLCK. This peptide contains a single Trp residue, while CaM is devoid of Trp, thus making it straightforward to study its binding by fluorescence spectroscopy. Our data show that many of these metal cations

Table 3.1 Ionic radius of various metal ions used in this work*

Cation	Ionic radius(Å)
Na^{+}	0.97
K^{+}	1.33
Mg^{2+}	0.66
Zn^{2+}	0.72
Cd^{2+}	0.97
Ca^{2+}	0.99
Hg^{2+}	1.10
Sr^{2+}	1.13
Pb^{2+}	1.20
La^{3+}	1.02
Lu^{3+}	0.85

*Taken from CRC Handbook.

can bind to CaM, but that they all bind in a different manner and they allow interaction of CaM with the MLCK peptide to some extent.

Materials and methods

Materials

$CaCl_2$, $MgCl_2$, $ZnCl_2$, $CdCl_2$, $Pb(NO_3)_2$, $HgCl_2$, NaCl, KCl, $SrCl_2$, $LuCl_3$, and $LaCl_3$ were obtained from Aldrich at the highest available quality. ^{15}N-glycine and D_2O (99.9%) were purchased from Cambridge Isotope

Laboratories. The MLCK peptide, a 22-residue peptide with sequence KRRWKKNFIAVSAANRFKKISS, was obtained from the Peptide Synthesis Facility at Queens University (Kingston, ON, Canada); it contains residues 577 to 598 of skeletal muscle MLCK, which constitutes its CaM-binding domain (Blumenthal *et al.* 1988). The *E. coli* strains, MM294 and Dl39G (a Gly auxotroph) were used as hosts to express nonlabeled, and ^{15}N-Gly labeled CaM respectively. CaM was expressed in *E. coli* and purified by hydrophobic affinity chromatography as previously described (Zhang *et al.* 1994b, also see Chapter 2). All the glassware and plastic tubes used were acid-washed to reduce metal ion contamination.

NMR Spectroscopy Experiments

Apo-CaM was prepared by passing a solution of CaM through a Chelex-100 column (Bio-Rad) equilibrated with 50 mM NH_4HCO_3 buffer, pH 8.0. Typically, NMR samples were prepared by dissolving 15 mg lyophilized apo-CaM in 500 µl 90% H_2O—10% D_2O, followed by the adjustment of the pH to 6.4. The samples also contain 0.1 M KCl to mimic physiological conditions except for the samples used for the titrations with K^+ and Na^+. The concentration of CaM was determined by optical absorbance using a $\Delta\mathcal{E}^{1\%}_{276/320}$ value of 1.8. The binding of the metal ions to CaM was studied by titrating the apo-CaM sample with the metal ions of interest. The titrations were monitored by ^{1}H,^{15}N HMQC NMR experiments. Microliter amounts of a stock solution of the metal ions (0.1 M to 3 M) were added to the desired

concentration at each titration point, while the pH was maintained at pH 6.4. If some protein precipitated during the titration, the sample was centrifuged at 14,000 rpm in a microcentrifuge and the supernatant was used for the next NMR experiment. All NMR spectra were recorded at 25 °C on a Bruker AMX-500 spectrometer. The $^{1}H,^{15}N$ HMQC data were recorded using the pulse sequence described by Sklenár and Bax (1987). The spectra were processed on a Silicon Graphics Indy R5000 computer using NMRpipe software. The assignments of the Gly residues of the apo- and calcium-forms of CaM were taken from Ohki *et al.* (1997) and Ikura *et al.* (1991) respectively.

Fluorescence Spectroscopy Experiments

Fluorescence spectroscopy experiments were performed on a Hitachi F-2000 Fluorescence spectrophotometer at room temperature. The concentration of the peptide was determined by optical absorbance using ε_{280}=5500 $cm^{-1}M^{-1}$. The sample buffer containing 10 mM Tris-Cl (pH 7.4), 0.1 M KCl was passed through a Chelex-100 column (Bio-Rad) to remove divalent and trivalent cations. Apo-CaM (10 μM) and MLCK peptide (10 μM) were incubated in the sample buffer with or without 2 mM $CaCl_2$ (or $MgCl_2$, $ZnCl_2$, $CdCl_2$, $Pb(NO_3)_2$, $HgCl_2$, $SrCl_2$, $LuCl_3$, $LaCl_3$) at room temperature for at least 60 minutes before the spectra were recorded. The samples were spun at 14,000 rpm on a bench top centrifuge if protein precipitation was observed. The samples were excited at 295 nm and the emission spectra were recorded in the range 310 - 450 nm. The excitation and emission slit widths were 1

nm, and the emission spectra scanning was done at 60 nm/min with an 1-cm path length cuvette.

Results

There are in total, eleven Gly residues in CaM. Table 3.2 shows that all four Ca^{2+}-binding loops of CaM have two Gly residues at homologous positions; these are highly conserved through all EF-hand Ca^{2+}-binding motifs (Kawasaki and Kretsinger 1994). Two additional Gly residues (G40 and G113) are located in homologous positions in the loops that connect the two helix-loop-helix structures in each lobe of CaM. The final G33 residue is located close to the first calcium binding loop. Thus, the Gly residues were chosen as convenient reporter groups to monitor the binding of metal ions to the four Ca^{2+}-binding loops of CaM. Figure 3.1 shows NMR spectra of the titration of ^{15}N-Gly labeled apo-CaM with Ca^{2+} ions. Obvious changes were observed when the first two equivalents of Ca^{2+} were added to CaM, and these changes were limited to the C-terminal domain of the protein. As can be seen

Table 3.2 Primary structures of the four Ca^{2+}-binding loops of CaM

site I	20	D	K	D	**G**	D	**G**	T	I	T	T	K	E	31
site II	56	D	A	D	**G**	N	**G**	T	I	D	F	P	E	67
site III	93	D	K	D	**G**	N	**G**	Y	I	S	A	A	E	104
site IV	129	N	I	D	**G**	D	**G**	Q	V	N	Y	E	E	139

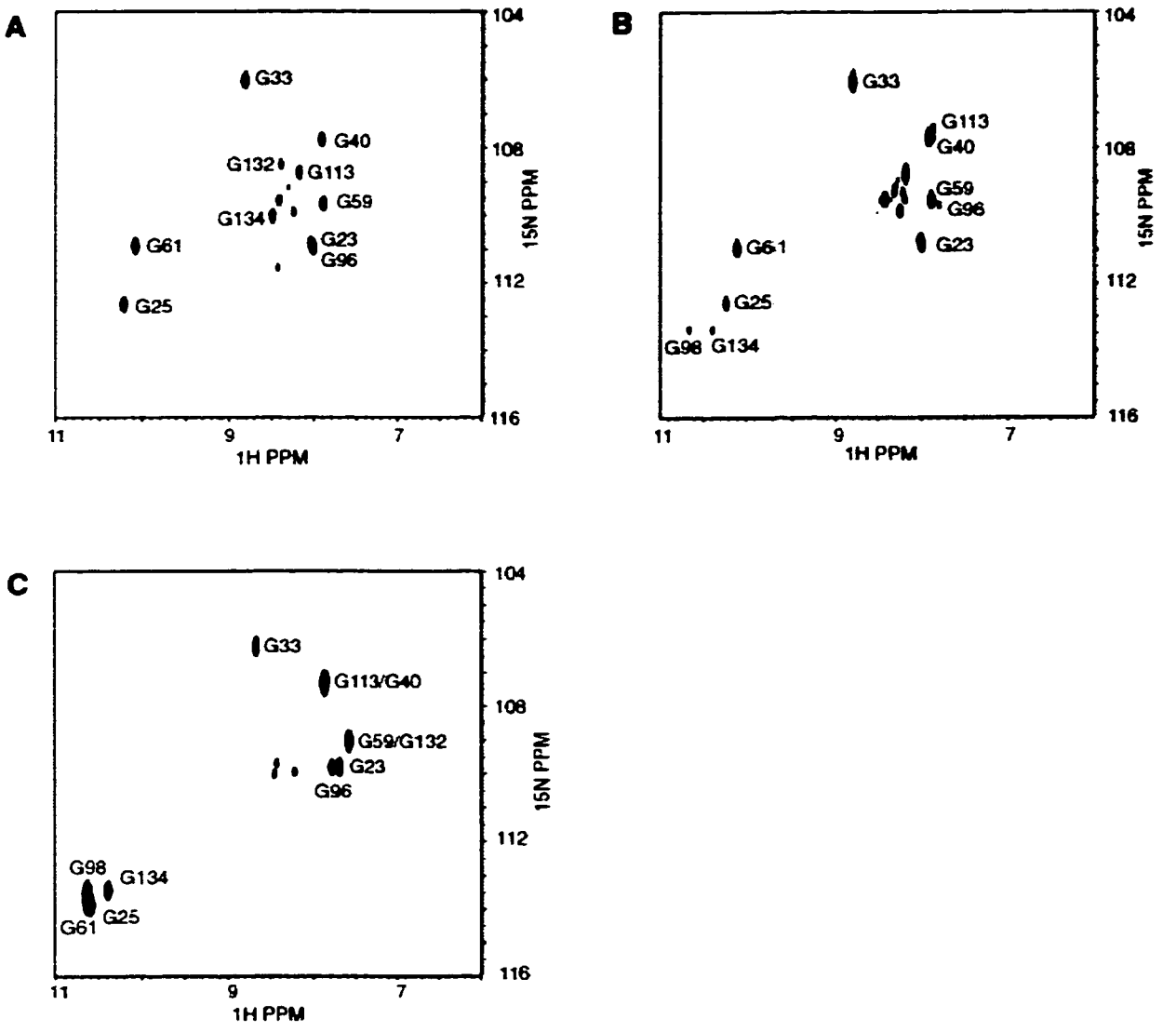

Figure 3.1 2D $^{1}H,^{15}N$ HMQC spectra of the titration of CaM (1.47 mM, pH 6.4) with (A) 0 equivalent, (B) 2 equivalents, and (C) 4 equivalents of $CaCl_2$.

in Panel 3.1B, the intensity of peaks G132 and G134 (site IV) decreased (as measured from the number of peak contours) as the Ca^{2+} concentration increased, and new peaks emerge at the known positions of G132 and G134 in the Ca^{2+}-saturated CaM spectrum. G98 (site III), which is not observed in the apo-CaM spectrum, also appeared at its known position for Ca^{2+}-CaM. G96 (site III) disappeared gradually and a new peak emerged at the correct position corresponding to G96 in Ca^{2+}-CaM, which demonstrated a typical slow-exchange that was also observed for peak G113, the Gly residue in the linker region between site III and site IV. When more Ca^{2+} was added, the resonances of the Gly residues in the N-terminal domain were also altered until the Ca^{2+} concentration reached 4 equivalents (Figure 3.1). Intermediate-exchange was observed for most Gly residues in the N-terminal domain during this part of the Ca^{2+} titration.

A titration of apo-CaM with Mg^{2+} has also been performed. With the addition of the first equivalent of Mg^{2+}, peak G25 (site I) disappeared while G33 broadened. The change of G23 (site I) was somewhat ambiguous since it overlapped with G96 in the apo-CaM spectrum (Figure 3.1A). The peak for G132 (site IV) decreased when a second equivalent of Mg^{2+} was added, however, with no significant changes in G134 (site IV). CaM was further titrated to 5 equivalents of Mg^{2+} with a new peak for G23 emerging on the spectrum, while peak G96 was broadening (Figure 3.2B). G96 completely disappeared at 8 equivalents of Mg^{2+}, while G33 reappeared at a new position slightly different from the original one. Another new peak for G25 emerged at

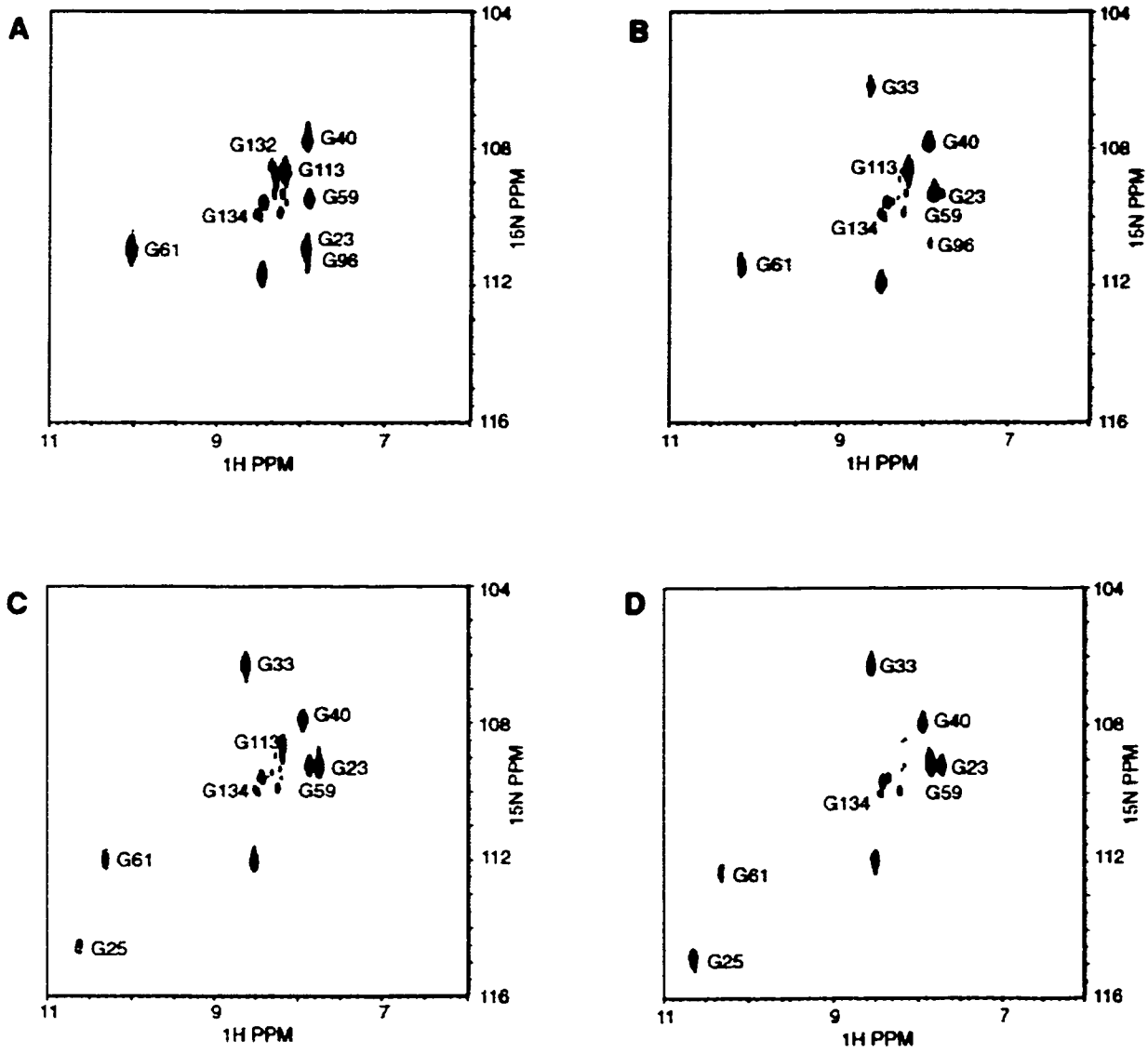

Figure 3.2 2D $^{1}H,^{15}N$ HMQC spectra of the titration of CaM (1.09 mM, pH 6.4) with (A) 1 equivalent, (B) 5 equivalents, (C) 15 equivalents, and (D) 75 equivalents of $MgCl_2$. See Figure 3.1A for the spectrum of apo-CaM.

15 equivalents of Mg^{2+} (Figure 3.2C). No further significant changes were observed in the spectra, except for a decrease of the intensity for G113 when the Mg^{2+} level increased up to 75 equivalents (Figure 3.2D). These data suggest that Ca^{2+}-binding site I located in the N-terminal domain of CaM has the highest affinity for Mg^{2+}. The Ca^{2+}-binding sites in the C-terminal domain, namely site III and IV, displayed a lower affinity for Mg^{2+} ions. Thus, Mg^{2+} has a different site-preference compared to Ca^{2+}. We also performed a titration of CaM with Ca^{2+} in the presence of a high Mg^{2+} concentration (75 equivalents) to investigate if the presence of Mg^{2+} ions affects the Ca^{2+}-binding properties of the protein. Upon addition of the first equivalent of Ca^{2+}, 5 small new peaks emerged; these peaks were at the exact positions of G96, G98, G113, G132, and G134 in the Ca^{2+}-CaM spectrum, suggesting regular incorporation of Ca^{2+} into the C-terminal domain. When the second equivalent of Ca^{2+} was added, the intensity of these new peaks increased(Figure 3.3A). The resonances from the C-terminal domain were at the Ca^{2+}-saturated positions and did not change with the further addition of Ca^{2+} ions. Most peaks of Gly residues in the N-terminal domain were at the same positions as in apo-CaM, except for G23 and G25, indicating that site I was still occupied by Mg^{2+}. These two peaks kept shifting (fast-exchange) when more Ca^{2+} was added until up to 4-6 equivalents while G33 broadened beyond detection (Figure 3.3B). At 10 equivalents of Ca^{2+}, G23 and G25 shifted to final positions and G33 reappeared (Figure 3.3C). At this point, the spectrum superimposed perfectly on the spectrum of Ca^{2+}-saturated CaM. The shifting of the G23 and G25

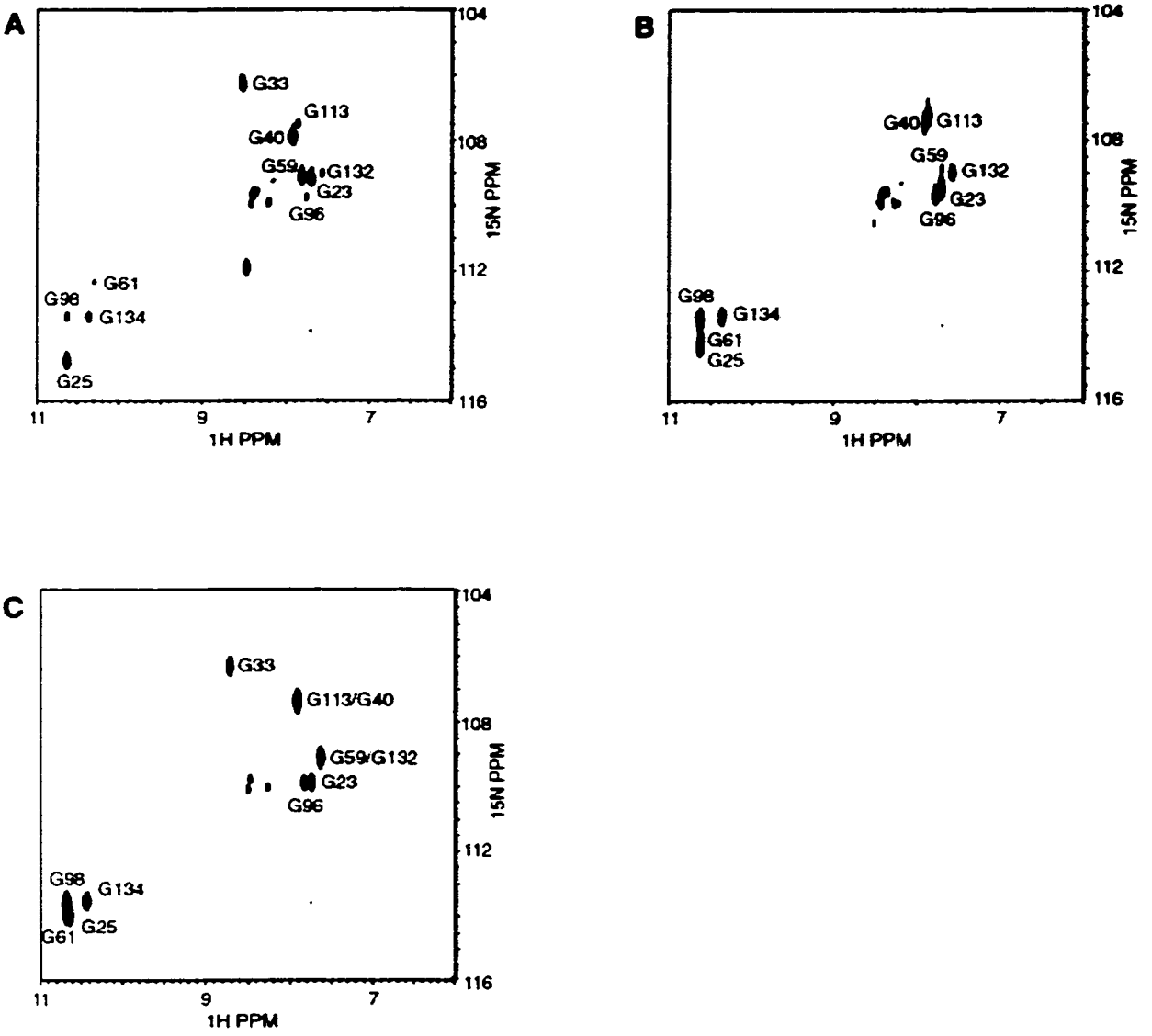

Figure 3.3 2D $^{1}H,^{15}N$ HMQC spectra of the titration of CaM (1.09 mM, pH 6.4) with $CaCl_2$ in the presence of 90 mM $MgCl_2$. (A) 2 equivalents of $CaCl_2$. G23 and G25 are in the positions different from that of apo-CaM (Figure 3.1A) or Ca^{2+}-CaM (Figure 3.1C). (B) 4 equivalents of $CaCl_2$. Note the shifting of G23 and G25, as well as the disappearance of G33. (C) 10 equivalents of $CaCl_2$. See text for details.

resonances indicated fast-exchange between the apo and Ca^{2+}-bound states of the N-terminal domain on the NMR time scale, which further suggested that the binding of Ca^{2+} to the N-terminal domain was relatively weak in the presence of high concentrations of Mg^{2+}.

Intermediate to fast exchange was observed during the titration with Zn^{2+} (Figure 3.4). G23 started shifting and broadening at 1 equivalent of Zn^{2+}, and disappeared at 2 equivalents. G25 and G33 shifted in the same direction while maintaining their intensities until the Zn^{2+} concentration reached 4 equivalents. G59 and G61 also shifted slightly as the level of Zn^{2+} increased from 1 equivalent to 2 equivalents. G132 faded away when 1 equivalent of Zn^{2+} was added. G113 and G134 remained unchanged during addition of the first equivalents, and broadened when the Zn^{2+} concentration exceeded 3 equivalents. G96 was shifting during the whole titration with the same intensity. G40 did not change during the titration of Zn^{2+}. These data suggest that Zn^{2+} ions could interact with CaM; the fast-exchange observed during the titration indicated that the interactions were relatively weak.

Apo-CaM has also been titrated with increasing concentration of K^+ and Na^+. No significant changes were observed in the HMQC spectrum of ^{15}N-Gly labeled CaM during a titration with K^+ up to 150 mM. However, small changes could be detected upon the addition of Na^+ (Figure 3.5). The peaks for G23 and G96 overlap when no Na^+ ions were present; these two peaks began to separate, when the Na^+ concentration was increased to 4-8 equivalents, and evolved into two distinct peaks at over 20 equivalents of Na^+. A small new

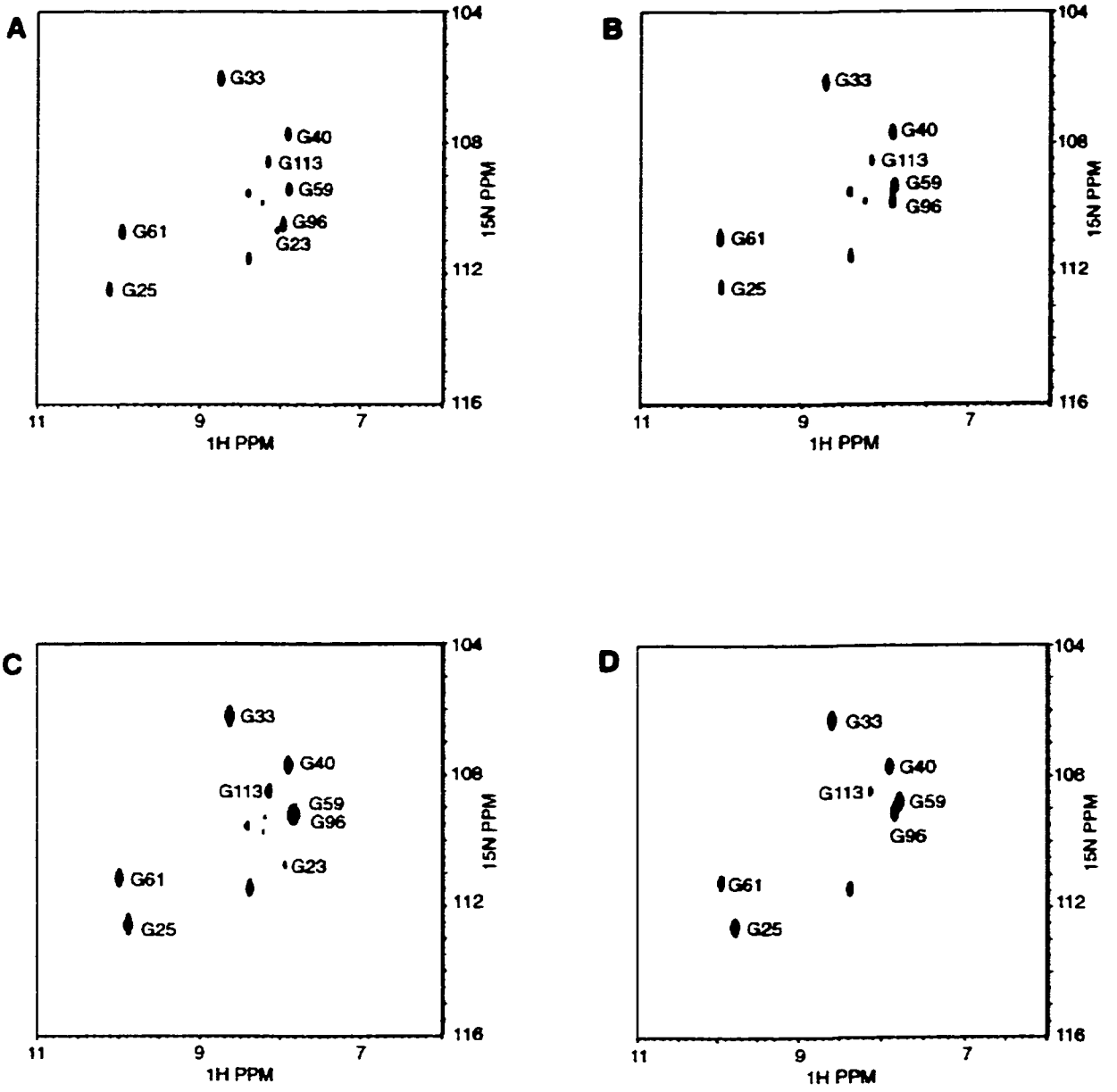

Figure 3.4 2D $^{1}H,^{15}N$ HMQC spectra of the titration of CaM (1.18 mM, pH 6.4) with (A) 1 equivalent, (B) 2 equivalents, (C) 3 equivalents, and (D) 4 equivalents of $ZnCl_2$. See Figure 3.1A for the spectrum of apo-CaM.

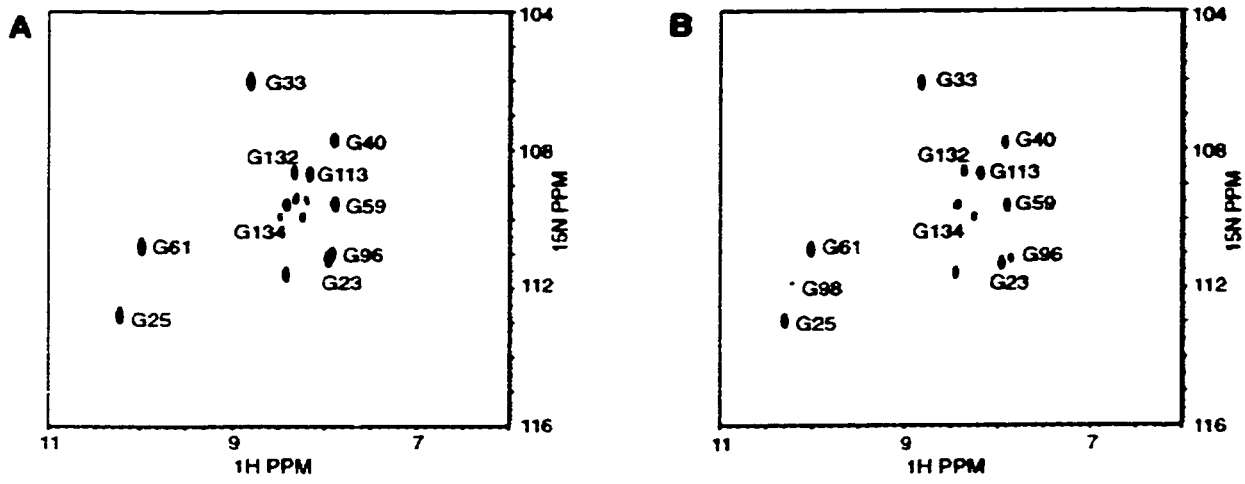

Figure 3.5 2D $^{1}H,^{15}N$ HMQC spectra of the titration of CaM (1.2 mM, pH 6.4) with (A) 6 equivalents and (B) 11 equivalents of NaCl. See Figure 3.1A for the spectrum of apo-CaM.

peak emerged at 10.22 ppm (^{1}H) and 111.89 ppm (^{15}N) when the Na^{+} concentration exceeded 50 equivalents. This new peak probably arose from G98, which was not detectable in the apo-CaM spectrum.

The results obtained during a titration of apo-CaM with Cd^{2+} were similar to those for Ca^{2+}. The resonances of the Gly residues from the C-terminal domain decreased in intensity as soon as Cd^{2+} was added. At 2 equivalents of Cd^{2+}, five new peaks appeared for G96, G98, G113, G132, and G134 (Figure 3.6). The peaks for the N-terminal Gly residues started to change as the titration proceeded. G23, G25, and G59 kept shifting when the Cd^{2+} concentration increased from 2 equivalents to 4 equivalents. G61 had

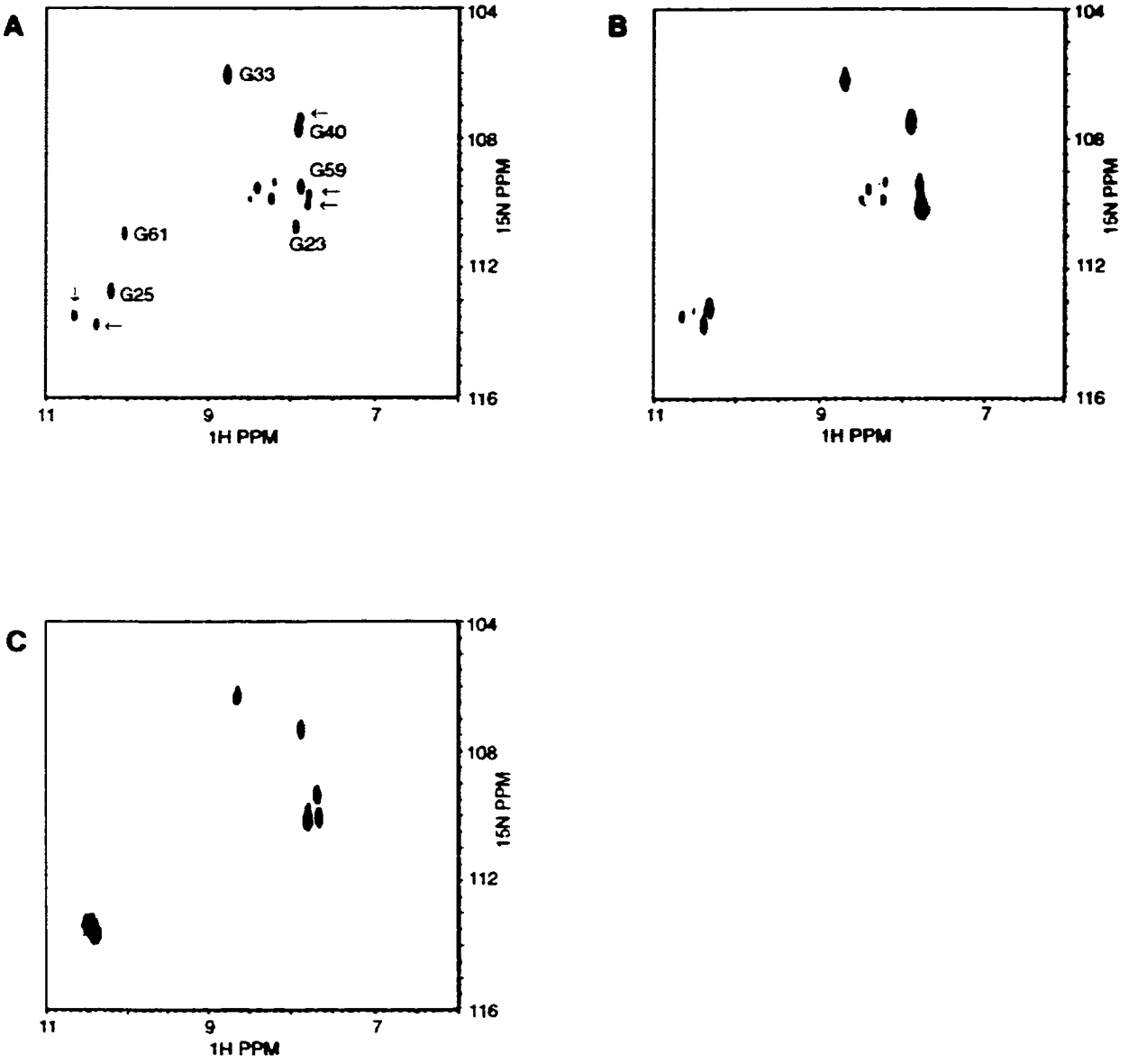

Figure 3.6 2D $^{1}H,^{15}N$ HMQC spectra of the titration of CaM (1.06 mM, pH 6.4) with (A) 2 equivalents, (B) 4 equivalents, and (C) 8 equivalents of $CdCl_2$. See Figure 3.1A for the spectrum of apo-CaM.

disappeared at 3 equivalents of Cd^{2+}, and reappeared at 4 equivalents. Several new peaks at the right-bottom corner of the spectrum kept shifting when Cd^{2+} was further added, suggesting the presence of additional binding sites for this metal ion.

NMR titration of Pb^{2+} could not be performed beyond 2 equivalents because the Pb^{2+} ions caused aggregation and precipitation of CaM. However, the changes in the spectra of the first two equivalents was obvious: G23 (site I), G59 (site II), G96 (site III), and G132 (site IV) disappeared at 1 equivalent of Pb^{2+}, followed by the disappearance of G25 (site I), G61 (site II), G98 (III), and G134 (site IV) at 2 equivalents of Pb^{2+} (Figure 3.7). These data suggest that all four sites of CaM have the same affinity for Pb^{2+} ions. It also seemed

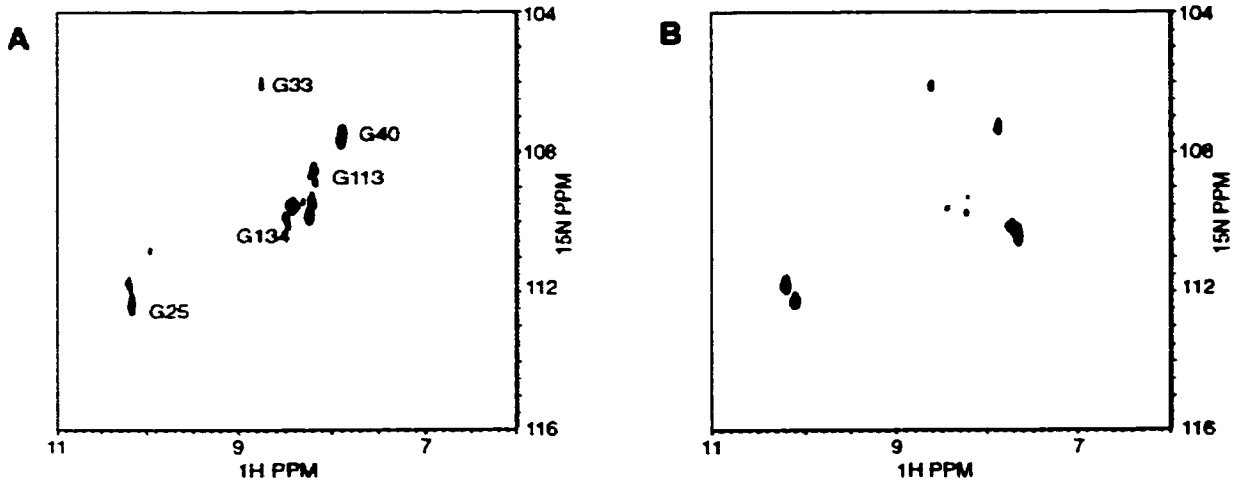

Figure 3.7 2D $^{1}H,^{15}N$ HMQC spectra of the titration of CaM (1.28 mM, pH 6.4) with (A) 1 equivalents and (B) 2 equivalents of $Pb(NO_3)_2$. See Figure 3.1A for the spectrum of apo-CaM.

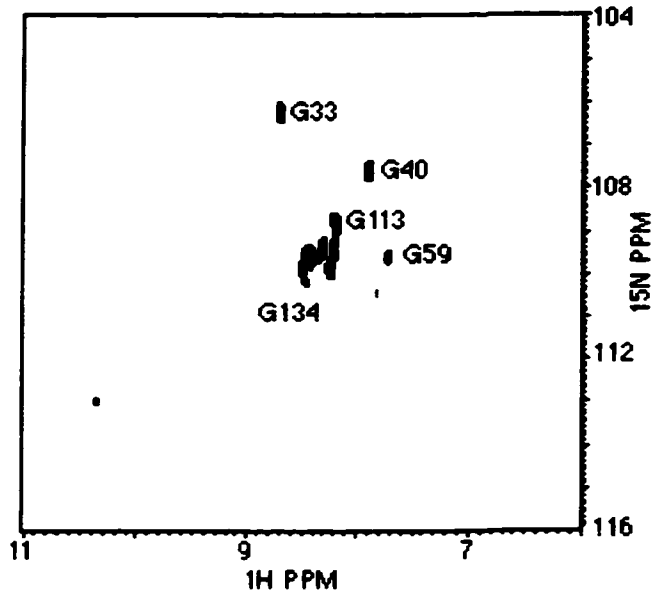

Figure 3.8 2D $^{1}H,^{15}N$ HMQC spectra of the titration of CaM (1.14 mM, pH 6.4) with 1 equivalent $SrCl_2$. See Figure 3.1A for the spectrum of apo-CaM.

that all four sites were affected when the first equivalent of Sr^{2+} was added during a titration with Sr^{2+}. G23, G25, G61, G96, and G132 all decreased, while G33 and G59 shifted to a new position (Figure 3.8). Some of the peaks which had disappeared reappeared in the spectrum when a second equivalent of Sr^{2+} was added; the intensities of these new peaks increased as more Sr^{2+} was added. These data showed that Sr^{2+} binds to CaM in the same manner of Pb^{2+}, which has an equally high affinity for all four sites in CaM.

The titration with Hg^{2+} could be divided into two stages. At low Hg^{2+}

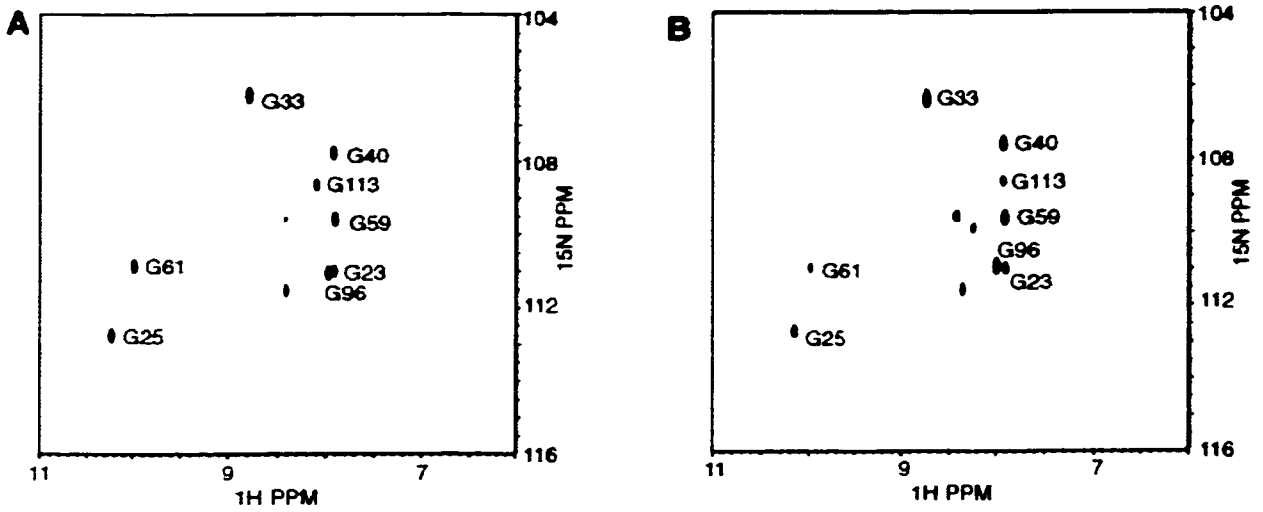

Figure 3.9 2D $^{1}H,^{15}N$ HMQC spectra of the titration of CaM (1.12 mM, pH 6.4) with (A) 3 equivalents and (B) 12 equivalents of $HgCl_2$. See Figure 3.1A for the spectrum of apo-CaM.

concentrations (2 - 3 equivalents), G132 and G134 (site IV) disappeared while G113 slightly shifted (Figure 3.9). No other significant changes were observed until Hg^{2+} level was very high (12 equivalents), when G25 (site I) and G61 (site II) were broadening, while G23 (site I) and G59 (site II) remained unchanged. Thus site IV probably has the highest affinity for Hg^{2+}, while site I and II showed a much lower affinity. Competition experiments showed that Ca^{2+} could readily displace Hg^{2+} and Cd^{2+}, but not Pb^{2+} (data not shown, see also Aramini *et al.* 1996).

In the titration experiments with the largest lanthanide ion La^{3+} and

apo-CaM, G132 and G134 (site IV) were the first resonances to lose intensity (data not shown). The peaks representing the Ca^{2+}-binding sites in the N-terminal domain, G23, G25 (site I), G59, and G61 (site II), also started to lose intensity, followed by the relocating of peak G96 (site III) as the titration proceeded. These results suggested that La^{3+} can bind to all four sites in CaM, however, with different affinity. Site IV showed the highest La^{3+} binding ability, followed by site I and site II, while site III had the lowest affinity for La^{3+}. Apo-CaM has also been titrated by the other diamagnetic lanthanide ion Lu^{3+}. The disappearance of G132 and G134 (site IV) followed the addition of 1 equivalent of Lu^{3+}(Figure 3.10). All the other peaks, except G33, changed position when more Lu^{3+} was added. G23, G25 (site I), G61 (site II), and G113

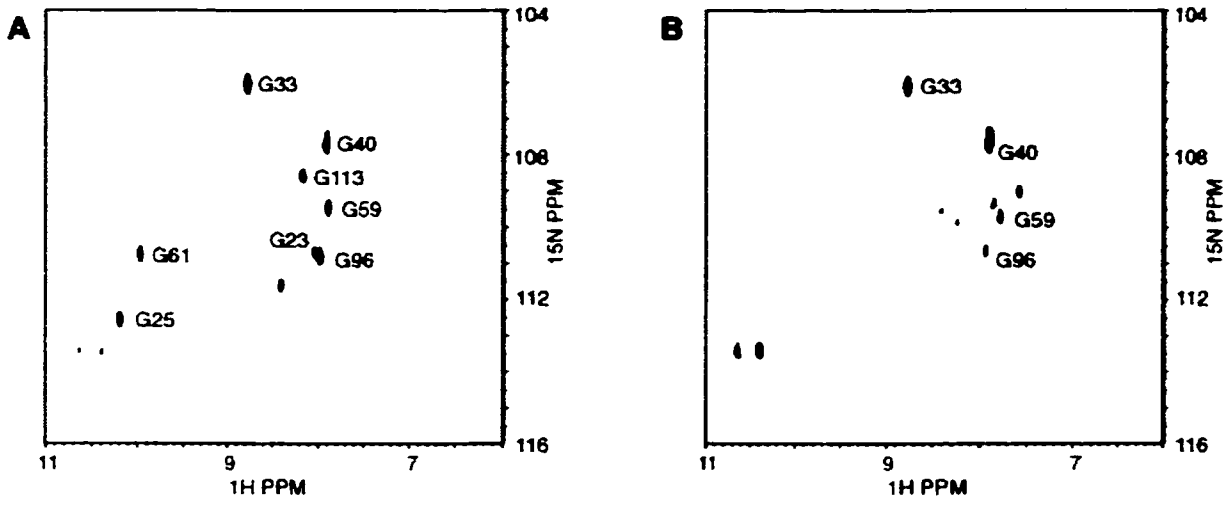

Figure 3.10 2D $^{1}H,^{15}N$ HMQC spectra of the titration of CaM (1.05 mM, pH 6.4) with (A) 1 equivalent and (B) 3 equivalents of $LuCl_3$. See Figure 3.1A for the spectrum of apo-CaM

disappeared with some new peaks emerging. G40, G59 (site II) and G96 (site III) shifted to new positions. These results suggest that site IV has the highest affinity for the smallest lanthanide ion Lu^{3+}, while the other three sites have an almost equal affinity for this metal ion.

The effects of different divalent and trivalent metal ions on the substrate-binding abilities of CaM were investigated by fluorescence spectroscopy. The synthetic MLCK peptide was chosen as a model substrate because it contains a single Trp residue. Thus, the binding of the MLCK peptide to CaM can be monitored by studying the fluorescence change of this Trp residue upon binding to CaM. The binding of Ca^{2+} to CaM induces a major conformational change in the protein, resulting in the exposure of the large hydrophobic surfaces which are essential for the peptide binding. When the MLCK peptide binds CaM, the Trp residue moves from a polar environment into a nonpolar hydrophobic environment (Ikura *et al.* 1992, Crivici & Ikura, 1995), which causes a large blue shift and an increase in the intensity of the emission spectrum (Yuan *et al.* 1998). This large blue shift and intensity change are not observed when the peptide, apo-CaM and a large excess of EDTA are incubated. Some of the emission spectra are shown in Figure 3.11. Unfortunately, the other metal ions in our studies caused protein precipitation during the incubation under these experimental conditions, which significantly lowered the fluorescence intensity (data not shown). However, the blue shift can still be observed for these metal ions (Table 3.3). Our data indicate that most of the divalent and trivalent metal ions can

A

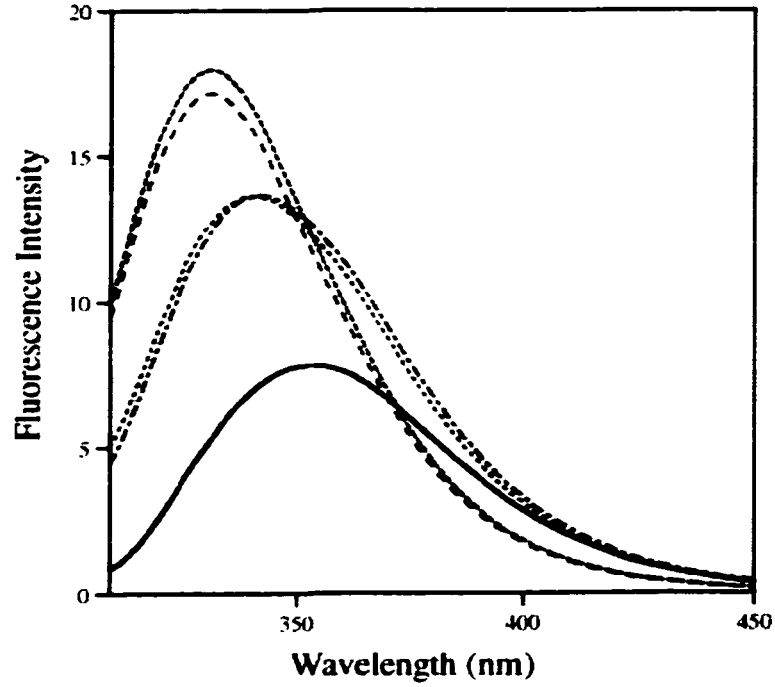
20
15
10
5
0
Fluorescence Intensity
350
400
450
Wavelength (nm)

B

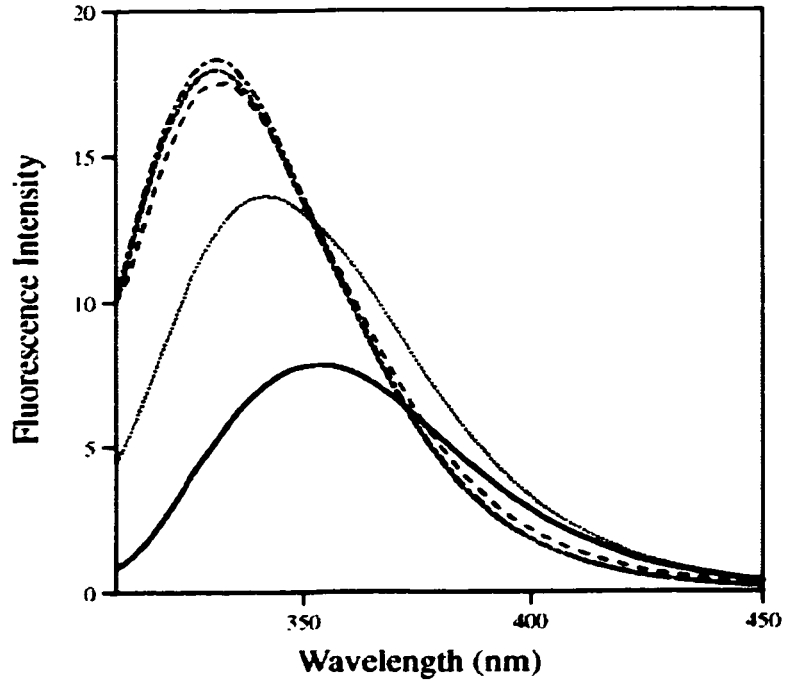
20
15
10
5
0
Fluorescence Intensity
350
400
450
Wavelength (nm)

Figure 3.11 Fluorescence emission spectra showing the effects of various metal ions on the substrate-binding ability of CaM monitored by the fluorescence of the Trp residue in the MLCK peptide. (A) Trp fluorescence of the MLCK peptide (———) shows a larger blue shift and bigger intensity increase when the peptide was incubate with Ca^{2+}-CaM (----------) rather than apo-CaM (-.-.-.-). The spectrum of the sample incubated in presence of Mg^{2+} and Sr^{2+} is shown by (.....) and (-------) respectively. (B) Fluorescence emission spectra of the MLCK peptide (———), the peptide pre-incubated with apo-CaM (.....), and CaM in presence of Ca^{2+} (----------), Zn^{2+} (-------), and Cd^{2+} (-.-.-.-).

Table 3.3 Wavelength of the MLCK peptide emission peak with CaM in the presence of various metal ions.

Metal ions	Wavelength (nm)
None	342
Mg^{2+}	341
Zn^{2+}	334
Cd^{2+}	332
Ca^{2+}	332
Hg^{2+}	340
Sr^{2+}	332
Pb^{2+}	332
La^{3+}	332
Lu^{3+}	334

induce a blue shift and an increase in intensity in the emission spectrum, except for Mg^{2+}, suggesting that most of these metal ions should also be able to activate CaM to some extent.

Discussion

The metal ions included in this study can arbitrarily be divided into four groups: Group A, Ca^{2+}, Mg^{2+}, and Zn^{2+}; Group B, K^{+} and Na^{+}; Group C, Cd^{2+}, Pb^{2+}, and Hg^{2+}; and Group D, Sr^{2+}, La^{3+}, and Lu^{3+}. The divalent metal ions of Group A naturally occur in cells and have relatively high intracellular concentrations; Group B is comprised of monovalent cations that have a high physiological concentration; the metal ions in Group C are serious environmental pollutants and are toxic to cells; Group D includes divalent and trivalent cations that have often been used as calcium analogs in various

studies, such as fluorescence and luminescent spectroscopy (Kilhoffer *et al.* 1980, Wang *et al.* 1982, Mills & Johnson 1985). Our studies on the binding of these metal ions to CaM will shed light on the role that different metal ions can play in Ca^{2+} signal transduction pathways.

In Group A, Ca^{2+} is the natural "substrate" of CaM. The binding of Ca^{2+} to CaM has been well studied. The Ca^{2+} titration in this study (Figure 3.1) confirmed the known Ca^{2+}-binding properties of apo-CaM: at least a ten fold higher affinity for the two C-terminal sites and lower affinity for the N-terminal sites. The slow-exchange observed during the titration indicated the relatively strong binding of Ca^{2+} to the C-terminal lobe of CaM. The intracellular Ca^{2+} concentration is strictly controlled in cells and constantly fluctuate around the level required to saturate CaM (Ohki *et al.* 1993, Vogel 1994). In the case of Mg^{2+}, the situation is rather different. In most multicellular organisms both the intracellular and extracellular free Mg^{2+} concentrations are maintained at approximately 10^{-3} M, i.e. 10^3 - 10^4 fold higher than that of Ca^{2+} (Frausto da Silva & Williams 1991). The high intracellular level of Mg^{2+} suggests that Mg^{2+} may substitute for Ca^{2+} inside cells. Tsai *et al.* (1987) have studied the binding of Mg^{2+} to CaM by magnesium-25 NMR. They found that sites in the N-terminal domain have higher affinities to Mg^{2+}; in their studies they treated sites I and II, and sites III and IV as two sets of equivalent sites. Our data are in general agreement with their conclusions. More precisely, we found that site I, but not site II, in the N-terminal domain has the highest affinity for Mg^{2+}, and that the two C-

terminal domain sites have lower affinities (Figure 3.2). The Mg^{2+}-CaM complex cannot bind to MLCK peptide, a typical target peptide, as our fluorescence experiments demonstrated. The presence of Mg^{2+} ions does not affect the binding of Ca^{2+} to the C-terminal domain of CaM. However, Mg^{2+} can lower the Ca^{2+}-binding affinity of the N-terminal domain because higher Ca^{2+} concentration (10 equivalents) were required to saturate CaM at a high Mg^{2+} level (Figure 3.3). These results are consistent with studies performed by Ohki *et al.* (1997), although these authors suggested that site IV might also be a high affinity site for Mg^{2+}. The existence of some "auxiliary" Mg^{2+}-binding sites in CaM has been suggested. Lafitte *et al.* (1995) found that CaM can bind two Mg^{2+} ions and suggested they bound to 'auxiliary' sites, which are distinct from the four calcium binding loops. However our data show that Mg^{2+} influences the spectra of the Gly residues in the calcium binding loops, suggesting that Mg^{2+} does enter the loops although it does not coordinate like Ca^{2+} because it does not give a conformational change. This is probably related to the well known property of Mg^{2+} to retain its bound H_2O ligands, while Ca^{2+} readily releases its water molecules (Frausto da Silva & Williams, 1991). Furthermore, Ca^{2+} is able to displace Mg^{2+} ions, again arguing against binding of Mg^{2+} to the 'auxiliary' sites. Because the binding of all four Ca^{2+} ions is cooperative in the presence of the substrate enzymes, it is possible that a proportion of CaM is always Ca^{2+}-saturated even when the Ca^{2+} concentration is low. Considering the high intracellular Mg^{2+} level, Ohki *et al.* (1993) suggested that Mg^{2+} can inhibit the formation of the $4Ca^{2+}$CaM-enzyme

complex at lower Ca^{2+} concentrations. Our data support this suggestion: when CaM was half saturated by Ca^{2+} (only the C-terminal domain bound Ca^{2+} ions), CaM could still bind Mg^{2+} in the site I of the N-terminal domain. Because Mg^{2+}-bound CaM is not active, the existence of Mg^{2+} in site I might prevent Ca^{2+} ion from binding to the N-terminal domain to "accidentally" activate CaM when the Ca^{2+} level is low. Thus, the Ca_2-Mg-CaM complex could well be a real form of CaM that exists in the resting cells.

Zn^{2+} is another divalent cation which can have a significant concentration in the cytoplasm (Frausto da Silva & Williams, 1991). Zn^{2+} has been found to be able to activate the CaM-dependent phosphodiesterase to a significant extent (Chao *et al.* 1984). The NMR titration of Zn^{2+} with ^{15}N-Gly labeled CaM displayed fast exchange in the spectra, indicating that the Ca^{2+}-binding loops were affected by addition of Zn^{2+}. However, these data suggest a relatively low affinity for Zn^{2+}. Milos *et al.* (1989) suggested that CaM has six "auxiliary" cation-binding sites which are different from the four "capital" Ca^{2+}-binding sites, and that Zn^{2+} can only bind to the "auxiliary" sites. If this is the case, these "auxiliary" sites must be located in the vicinity of the "capital" sites, i.e., the Ca^{2+}-binding loops. Our fluorescence spectroscopy data showed that Zn^{2+} could also activate CaM, suggesting that the binding of Zn^{2+} may still cause productive conformational changes in CaM. This seems to argue for binding directly to the Ca^{2+}-binding loops.

The ions in Group B, K^+ and Na^+, are by far the highest in concentration among various metal ions inside cells (Frausto da Silva & Williams, 1991). It

had been reported that K^+ can affect the free energy of binding of Ca^{2+} ions to CaM (Linse *et al.* 1991), suggesting that K^+ might interact with CaM. Our experiments directly monitored the Ca^{2+}-binding loops during the titration with the large K^+ ion. However, no significant changes were observed in the spectra, suggesting that the effects of K^+ on CaM were nonspecific and not caused by direct binding to the binding loops. Unlike K^+, univalent Na^+, which is of similar size as Ca^{2+}, has been found to interact with both domains of CaM through "true site-binding" sodium-23 NMR studies (Delville *et al.* 1980). Our data did not totally support this conclusion. The ^{15}N-Gly labeled CaM used in our titrations was very sensitive to any "true site-binding" since each Ca^{2+}-binding loop has two Gly residues in conserved positions. However, only weak interactions were observed between Na^+ and CaM, and these interactions were limited to site III in the C-terminal domain.

In Group C, Cd^{2+} has been proven to be able to serve as a substitute for Ca^{2+} in *in vitro* studies due to their close similarity in ionic radius. Cd^{2+} has frequently been used for cadmium-113 NMR studies because it is a spin 1/2 nucleus which gives simpler NMR spectra than ^{43}Ca, a quadrupolar nucleus (Anderson *et al.* 1983, Thulin *et al.* 1984, Vogel & Forsén 1987). Our titration data proved that the binding of Cd^{2+} to CaM is indeed very similar to that of Ca^{2+}. There were some changes in the spectra when the Cd^{2+} concentrations exceeded 4 equivalents. These could be due to the existence of the "auxiliary" sites to which Cd^{2+} could bind as suggested by Milos *et al.* (1989). The binding of Hg^{2+} to CaM was less significant. Site IV had the highest affinity and sites

I and II had much lower affinities. This was rather different from the other heavy metal ion Pb^{2+}. Pb^{2+} is a toxic ion for cells and has been found to be able to substitute for Ca^{2+} in several proteins (Fullmer *et al.* 1985, Simons 1993, Goldstein 1993). Our data showed that all four Ca^{2+}-binding sites could bind Pb^{2+} simultaneously, which was in agreement with previous lead-207 NMR studies (Aramini *et al.* 1996). Although our fluorescence experiments did not clearly show to what extent Pb^{2+} can activate CaM due to the protein precipitation, Chao *et al.* (1984) demonstrated that Pb^{2+} can activate CaM to over 90%. Thus the toxicity of Pb^{2+} could be caused by its ability to bind and activate CaM. Sr^{2+} appears to bind to CaM in a similar manner as Pb^{2+}, thus the two divalent ions that are significantly larger than Ca^{2+} bind to CaM in a similar manner.

Despite the similarity in size, trivalent lanthanide ions obviously bind to CaM in a different order than calcium; they appear to have a preference for site IV. Thus, caution should be exercised in using this class of metal ions: their favorable spectroscopic properties do not justify their use in this class of proteins, as erroneous results can be obtained (Szebenyi & Moffat 1986, Kumar *et al.* 1991). Similarly the use of Sr^{2+} as a experimental probe with CaM can lead to erroneous results.

As mentioned in the introduction section, cooperativity in the binding of calcium ions is an important feature of CaM. From our studies it appears that of all the metal ions tested, only Cd^{2+} is capable of reproducing these effects. This justifies the extensive use of cadmium-113 in studies of metal

ion binding properties of this class of proteins (Vogel & Forsén 1987, Swain *et al.* 1989).

Fluorescence spectroscopy demonstrated that most of these metal ions could support binding of the MLCK peptide to CaM to some extent, although our NMR studies showed the ions bound to CaM in different manners. The binding of Ca^{2+} to CaM changes the protein from a "closed" conformation to an "open" conformation which exposes a big hydrophobic surface on each domain. This conformational change is critical for proper substrate recognition and subsequent activation. Many metal ions included in this study could interact with CaM in the Ca^{2+}-binding loops, and trigger at least in part the conformational changes resulting in the "open" or a "partially-open" conformation which allows the peptide to bind.

Chapter 4

Melatonin and Serotonin Interactions with Calmodulin: NMR, Spectroscopic and Biochemical Studies

Abstract

It has been reported that the hormone melatonin binds tightly to the ubiquitous calcium-regulatory protein, calmodulin (CaM) with a K_d value around 0.1 nanomolar [Benítez-King *et al.* (1993) Biochim. Biophys. Acta 1290, 191-196]. Normally CaM only binds to target proteins and various 20-residue synthetic peptides encompassing the CaM-binding domain of these target proteins with K_d values ranging between 1.0 micromolar and 0.1 nanomolar. Here we have studied the interaction of melatonin and several structurally related compounds, serotonin, 5-hydroxytryptophan, and tryptophan, to CaM through gel band shift assays, enzymatic competition assays with calcineurin, fluorescence spectroscopy, far and near UV circular dichroism spectropolarimetry and NMR spectroscopy. Fluorescence spectra show that the binding of melatonin is calcium dependent. NMR studies with biosynthetically labeled methyl-^{13}C-Met CaM show that melatonin and the other compounds interact with the hydrophobic cleft regions of the protein. Our NMR data show that melatonin binds to both domains of the dumbbell-shaped CaM, while serotonin appears to bind only to the C-terminal domain.

This binding mode is further substantiated by fluorescence and gel band shift competition experiments with synthetic peptides from myosin light chain kinase and constitutive nitric oxide synthase. Circular dichroism spectra indicate that the secondary structure of CaM is not altered by addition of melatonin. Our data are internally consistent and reveal K_d values in the millimolar range for melatonin. Thus, the binding of these compounds to CaM is substantially weaker than previously reported and is unlikely to be of physiological significance.

Introduction

Calmodulin(CaM) is a well-studied eukaryotic Ca^{2+}-binding protein that plays important roles in a wide variety of cellular processes. It is one of the best characterized components in the Ca^{2+} signaling pathways. In response to higher intracellular Ca^{2+} levels, CaM binds four Ca^{2+} ions and undergoes a major conformational change resulting in the exposure of two hydrophobic regions on the protein surface. CaM can thus activate target enzymes through hydrophobic interactions. To date, more than thirty enzymes have been found to interact with CaM (for reviews, see Vogel & Zhang 1995, Crivici & Ikura 1995, Ikura 1996). The structures of both apo and Ca^{2+}-CaM have been determined (Babu *et al.* 1988, Zhang *et al.* 1995a). The protein is largely made up of α-helices in both forms. It contains two domains which are linked by a long α-helix in the crystal structure and by a flexible linker in solution. There are two Ca^{2+}-binding sites in each domain. Upon binding Ca^{2+}

ions, the helices undergo changes in orientation resulting in the exposure of several hydrophobic residues. CaM interacts with the target enzymes by recognizing amphiphilic α-helices of the enzymes via hydrophobic and ion pair interactions; this interaction does not require conservation of the primary structures of CaM-binding domains. Binding interactions of high affinity have been found between CaM and substrate peptides, usually with K_d values in the nanomolar range (O'Neil & DeGrado 1990).

Considering the importance of CaM in signal transduction pathways, it is of interest to identify potential CaM inhibitors. Indeed, CaM can also bind a number of drugs and hydrophobic compounds other than substrate peptides, such as trifluoperazine and felodipine (Anderson *et al.* 1983, Johnson *et al.* 1986). It has recently been reported that the neurohormone melatonin can also bind to CaM with very high affinity (K_d values around 0.1 nM) (Benítez-King *et al.* 1993). Melatonin is a hormone synthesized and secreted mainly by the pineal gland in a diurnal pattern. Many melatonin receptors have been found in both brain and peripheral tissues, and these receptors show a very high affinity for this tryptophan analog, with K_d values in the low picomolar range. Melatonin can act through these receptors to inhibit intracellular cyclic AMP production by a G-protein coupled mechanism (Morgan *et al.* 1994). In addition to these receptors, melatonin has also been found to interact with cytoplasmic and nuclear proteins including CaM. This suggests that melatonin may also act through modulation of Ca^{2+}-activated CaM (Benítez-King *et al.* 1996). Serotonin, another hormone, is a precursor of melatonin

biosynthesis in the pineal gland. It is widely distributed in both plants and animals, and is implicated in controlling feeding behavior, thermoregulation, sexual behavior, and sleep (Rodriguez-Cabello 1989, Silberstein 1994). Serotonin has a similar structure as melatonin with the methoxy group on the indole ring of melatonin replaced by a hydroxyl group (Figure 4.1).

In this work, we have studied the direct interactions between CaM and melatonin and its naturally occurring structural analogs, serotonin, 5-hydroxytryptophan, and tryptophan (Figure 4.1) by a variety of biochemical and biophysical techniques, including calcineurin assays, native gel band shift assays, fluorescence spectroscopy, circular dichroism (CD) spectropolarimetry, and nuclear magnetic resonance (NMR) spectroscopy. Our data show that

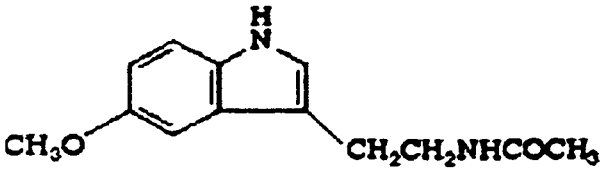

Melatonin

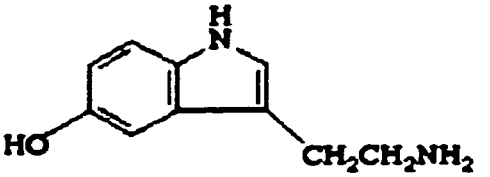

Serotonin

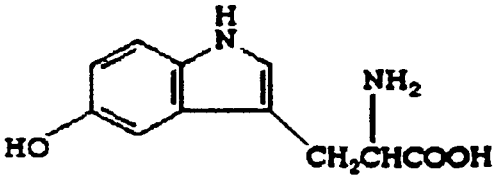

5-Hydroxytryptophan

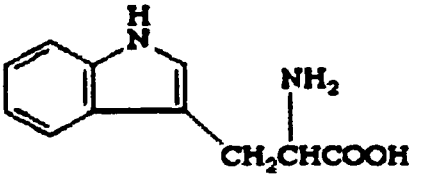

Tryptophan

Figure 4.1 Structures of melatonin and its analogs.

melatonin and its analogs can only interact weakly with CaM and are not likely to serve as CaM antagonists inside cells.

Materials and Methods

Materials

Melatonin, serotonin, 5-hydroxytryptophan and tryptophan were purchased from Sigma. Methyl-^{13}C-methionine and D_2O (99.9%) were purchased from Cambridge Isotope Laboratories. MLCK and cNOS peptides were obtained from the Peptide Synthesis Facility at Queens University (Kingston, ON, Canada). CaM was purified from an *E. coli* strain harboring an expression plasmid containing a synthetic gene for CaM by hydrophobic affinity chromatography. Methyl-^{13}C-Met labeled CaM was prepared as previously described (Zhang *et al.* 1994b, also see Chapter 2).

Fluorescence Spectroscopy Experiments

Fluorescence spectroscopy experiments were performed on a Hitachi F-2000 Fluorescence spectrophotometer at room temperature. The excitation and emission slit widths were 1 nm, and the emission spectra scanning was done at 60 nm/min with an 1-cm path length cuvette. For melatonin and CaM interaction experiments, melatonin (25 μM) was incubated in 10 mM Tris-HCl (pH 7.4), 0.1 M KCl, 500 μM CaM with 2 mM $CaCl_2$ or 10 mM EDTA at room temperature for 30 minutes. This sample was excited at 297 nm and the

fluorescence emission spectra in the range 300 - 450 nm were recorded. For peptide competition experiments, 10 μM MLCK peptide and melatonin of varying concentrations were incubated in 10 mM Tris-HCl (pH 7.4), 0.1 M KCl, 10 μM CaM with 2 mM $CaCl_2$ or 10 mM EDTA at room temperature for 30 minutes. The samples were excited at 297 nm and the emission spectra were recorded in the range 300 - 450 nm.

Circular Dichroism

Circular dichroism (CD) experiments were performed on a Jasco J-715 spectropolarimeter equipped with an Austin computer. All samples were prepared in 10 mM Tris-HCl buffer (pH 7.4) containing 1 mM $CaCl_2$. Each sample was incubated at room temperature for at least 30 minutes before the spectrum was recorded. For far-UV CD experiments, each spectrum was the average of ten scans and the smoothing of base-line-corrected spectra was done by digital filtering. The spectra of 10 μM CaM and/or 10 μm MLCK or cNOS peptides with different concentrations of melatonin or its analogs were recorded between 185 and 255 nm using a cell path length of 1 mm, sensitivity of 20 mdeg/FS, time constant of 2 s, and a scan speed of 50 nm/min. For near-UV experiments, the spectra were recorded between 250 nm and 310 nm. CaM and peptide concentrations were increased to 40 μM for near-UV spectra; and a 10 mm cell path length was used, while each spectrum was the average of twenty scans.

Gel Mobility Shift Assays

Competition for CaM between synthetic CaM-binding peptides and melatonin and its analogs were assayed by determining the relative mobility shifts of CaM by non-denaturing urea polyacrylamide gel electrophoresis using a Bio-Rad mini-gel system (Erickson-Viitanen & DeGrado 1987). Urea gels contained 15% acrylamide, 4 M urea, 0.375 M Tris-HCl (pH 8.8), and 1 mM $CaCl_2$, and was performed under a constant voltage of 100 volts in electrode buffer containing 25 mM Tris, 192 mM glycine (pH 8.3), and 0.1 mM $CaCl_2$. Each sample contained 4 M urea, 100 mM Tris-HCl (pH 7.2), 1 mM $CaCl_2$, and 30 μM CaM in a total volume of 50 μl. For the competition experiments, 30 μM MLCK peptide and various concentrations of melatonin and its analogs were included in the samples. All samples were incubated at room temperature for one hour followed by the addition of 50 μl 50% glycerol and tracer bromophenol blue. 10 μl of each sample was applied to the gel.

Calcineurin Competition Assays

The inhibition by melatonin and its analogs on CaM activation were investigated by enzyme activity assays of calcineurin, a CaM-dependent phosphatase, as described before (Newton *et al.* 1984). Calcineurin, CaM, *p*-nitrophenyl phosphate, melatonin and its analogs were dissolved in assay buffer containing 20 mM Tris-HCl (pH 8.0), 100 mM NaCl, 6 mM $MgCl_2$, 18 μM $MnCl_2$, 1.5 mM $CaCl_2$, 0.45 mM dithiothreitol, and 0.1 mg/ml bovine serum albumin (BSA). The reaction mixture consisted of 0.16 μg/ml

calcineurin, 0.3 μg/ml CaM, 2.5 mM *p*-nitrophenyl phosphate, and different concentrations (typically 1 mM, 0.1 mM, 0.01 mM, and 0.001 mM) of melatonin and its analogs. The rate of production of p-nitrophenolate was monitored at 400 nm at room temperature for 30 minutes.

NMR Spectroscopy

NMR spectra were recorded on a Bruker AMX-500 spectrometer equipped with a Bruker BGU Gradient Unit Z. Stock solutions of melatonin and its analogs (20 to 75 mM) were made in D_2O. CaM samples used for NMR studies were exchanged twice in D_2O. Typically, NMR samples were prepared by dissolving lyophilized CaM in 500 μl of 0.1 M KCl in D_2O. Samples were placed in 5 mm NMR tubes. In each case, the pH was adjusted to pH 7.4 by adding microliter quantities of 0.1 to 2 M KOD or DCl. The concentrations of CaM were determined by optical absorbance using an $\Delta\mathcal{E}^{1\%}_{276/320}$ value of 1.8. During the NMR titration of melatonin and its analogs, small amounts of the stock solution of these compounds were added to the desired concentration at each titration point. The pH value was maintained at pH 7.4 during the titrations. All NMR spectra were collected at 25°C. 1D proton spectra were obtained using the pulse sequence described by Bax *et al.* (1983), and the data were processed on a PowerMac computer by SwaNMR software. 2D (1H, 13C) HMQC experiments were performed using the pulse sequence as previously described (Winder & Wuthrich 1993), and the data were processed on a Silicon Graphics Indy R5000 computer using

NMRpipe software. Typically, each HMQC spectrum was recorded with 128 experiments in F1 and 1024 complex data points in F2.

Results

Melatonin is a fluorophore because it possesses an indole ring. It gives an emission peak at 350 nm when excited at 297 nm (Figure 4.2A). There is no tryptophan residue in CaM, thus CaM does not have any emission peak in the range of 300 - 450 nm when excited at 297 nm. Thus, fluorescence emission spectra can be used to monitor the binding of melatonin to CaM. Usually, a blue shift and an increase in emission intensity can be detected in the emission spectrum when a fluorophore moves from a polar to nonpolar environment (Burstein *et al.* 1973, Permyakov 1993) Accordingly, because of reports on strong melatonin-CaM interactions, dramatic changes in the emission spectra upon binding were expected. However, there were virtually no changes in the emission spectra when 10 μM melatonin was mixed with 10 μM Ca^{2+}-CaM (data not shown). A blue shift of only 5 to 7 nm could be detected at higher concentrations when a large excess of Ca^{2+}-CaM was added (Figure 4.2A). These data suggested that the binding of melatonin to CaM is a weak interaction. As expected, the blue shift was no longer detectable when EDTA was included in the samples (Figure 4.2A), indicating that the binding is Ca^{2+}-dependent. Competition experiments with synthetic peptides encompassing CaM-binding domains have also been performed. The MLCK peptide contains a single tryptophan residue, and the binding of the peptide

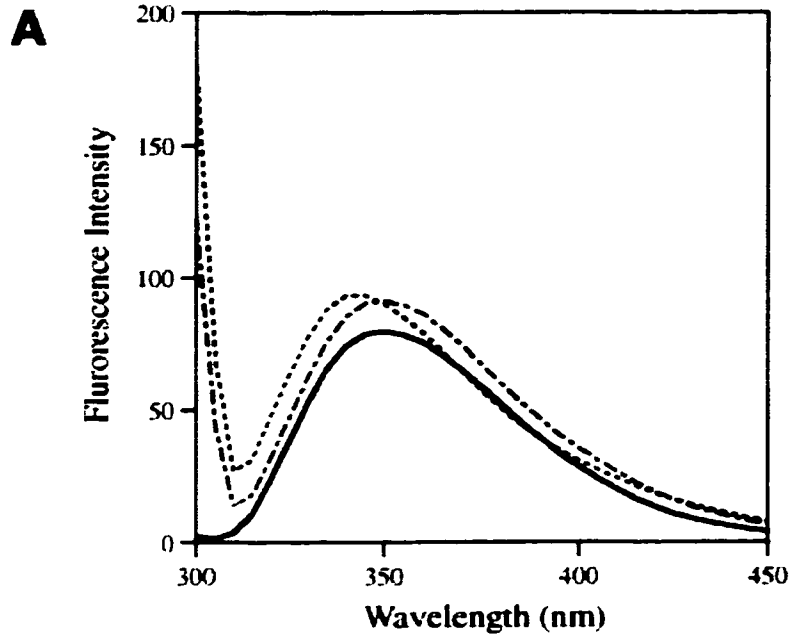
A
200
150
100
50
0
Fluorescence Intensity
300
350
400
450
Wavelength (nm)

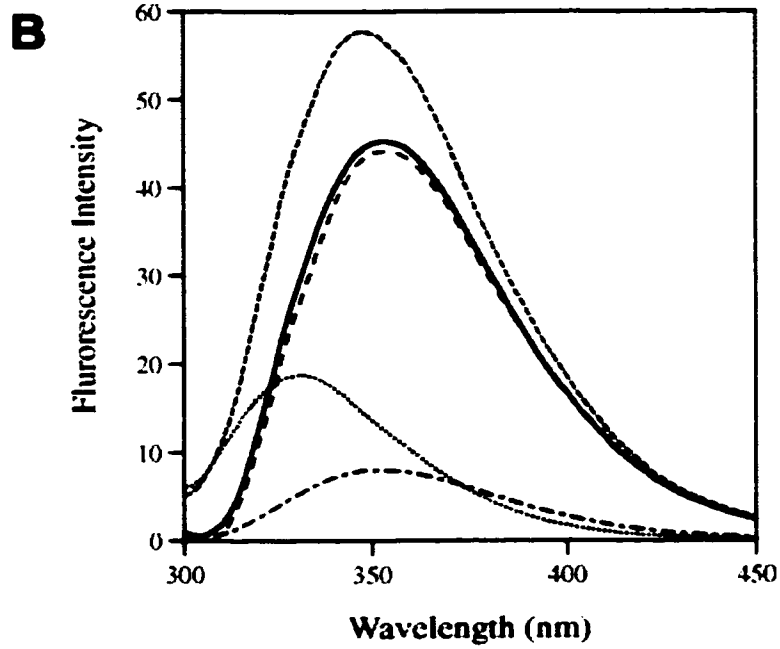
B
60
50
40
30
20
10
0
Fluorescence Intensity
300
350
400
450
Wavelength (nm)

Figure 4.2 Fluorescence spectra showing the Ca^{2+}-dependence of melatonin-binding to CaM and the melatonin-MLCK competition experiments. (A) Melatonin emission peak (———) shows a small blue shift when it interacts with Ca^{2+}-CaM (.....), but not in the presence of EDTA (- - - - - -). (B) MLCK (10 μM) emission peak (- - - - - -) shows a large blue shift and a large increase in intensity when it binds to Ca^{2+}-CaM (.....). The addition of melatonin to MLCK-CaM complex results in a broad peak (----------). The difference spectrum (- - - - -) of this spectrum and the spectrum of MLCK complex superimposes well on the spectrum of melatonin (———).

to CaM can be monitored through the fluorescence change of this tryptophan residue. When the peptide was bound to CaM, the emission spectrum showed a large blue shift (22 nm) and a dramatic increase in intensity (Figure 4.2B). The addition of 10 μM melatonin to the peptide-CaM mixture resulted in a broad emission peak. The difference spectrum of this spectrum and peptide-CaM complex spectrum can be superimposed perfectly on the spectrum of melatonin itself (Figure 4.2B). These data suggested that melatonin does not inhibit peptide binding to CaM when it is at the same concentration as the peptide, which further suggested that melatonin has a lower affinity for CaM than the peptide. Similar fluorescence results were obtained when a complex of CaM and the cNOS peptide were studied after addition of melatonin (data not shown).

This conclusion was further confirmed by CD spectroscopy experiments. The CaM-binding peptides in solution are not structured, thus, they do not give rise to CD bands in the far-UV CD spectra. When a substrate peptide is bound to CaM, it adopts an α-helical conformation. Therefore, the addition of the peptide to a Ca^{2+}-CaM sample enhances the CD spectra (Figure 4.3B). When low concentrations of melatonin were added to Ca^{2+}-CaM, it did not change the protein CD spectra, suggesting that no secondary structure changes were introduced. With higher concentrations of melatonin, CaM samples started to lose their CD signal (Figure 4.3A), probably due to the optical activity of melatonin in the UV range since the same results were obtained when CaM was replaced by BSA. Serotonin and 5-

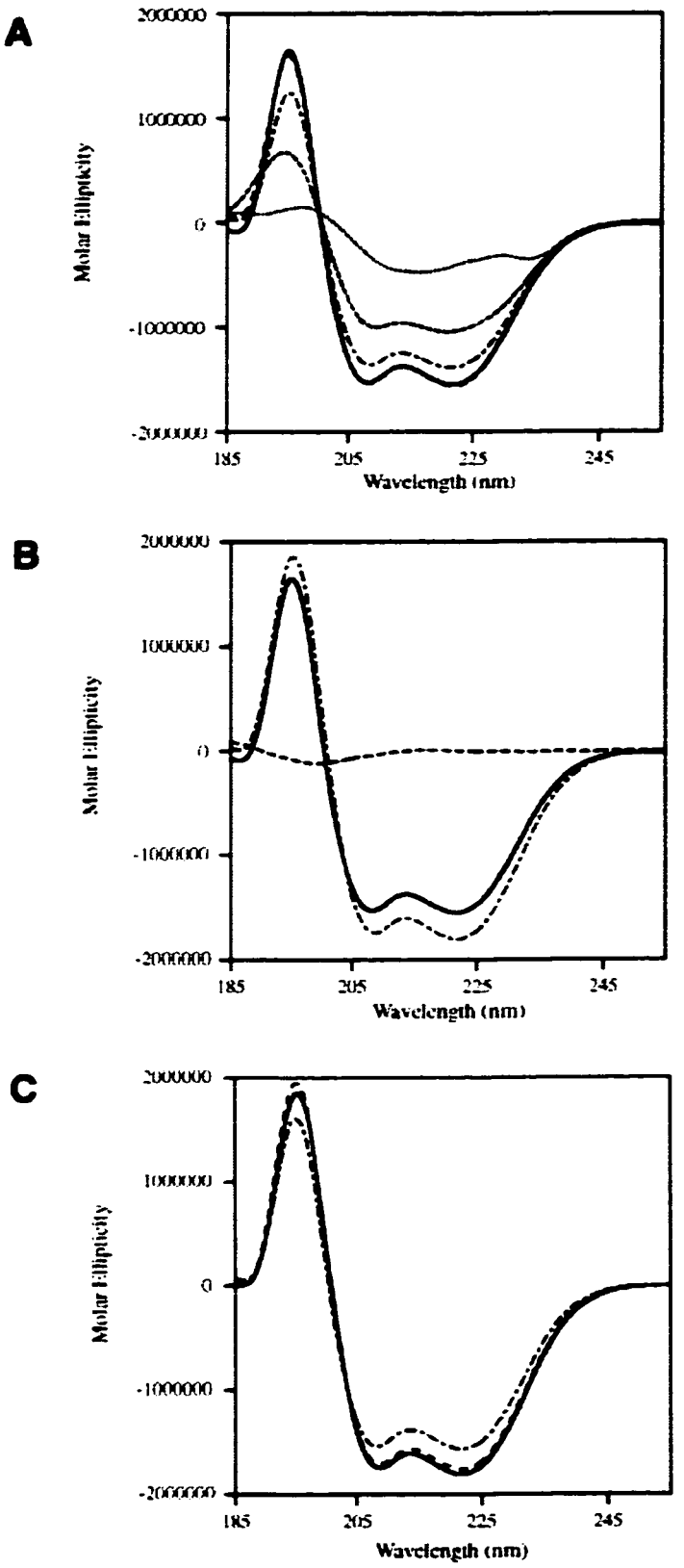
A
2000000
1000000
0
-1000000
-2000000
Molar Ellipticity
185
205
225
245
Wavelength (nm)
B
2000000
1000000
0
-1000000
-2000000
Molar Ellipticity
185
205
225
245
Wavelength (nm)
C
2000000
1000000
0
-1000000
-2000000
Molar Ellipticity
185
205
225
245
Wavelength (nm)

Figure 4.3 Far-UV CD spectra. (A) CaM (10 μM) with different concentrations of melatonin. CaM without melatonin (———), with 10 μM (- - - - -), 100 μM (-.-.-.-), 200 μM (·····), and 1 mM (.....) melatonin. (B) Binding of cNOS peptide to CaM. Free cNOS peptide (-------) does not have strong CD signal. cNOS-CaM complex (-.-.-.-) has stronger CD bands than CaM (———). (C) Melatonin-cNOS competition experiments. The spectrum of 10 μM cNOS-CaM complex (———) does not change by the addition of 10 μM melatonin (- - - - -), which is different from the spectrum of CaM with 10 μM melatonin (-.-.-.-).

hydroxytryptophan revealed similar results in the CD spectra (data not shown). As shown in Figure 4.3C, there were no spectral changes when the same amount of melatonin was added to the peptide-CaM complex, which, again, suggests that melatonin has a lower affinity for CaM than the peptides. There are two characteristic peaks in the near-UV CD spectrum of CaM which arise from Phe and Tyr residues (Gomes *et al.* 2000). Near-UV CD experiments were performed to investigate the effects of the binding of melatonin on these hydrophobic residues. Similar to the results of far-UV CD experiments, no spectral changes were observed when low concentrations of melatonin were added to CaM samples; moreover no new signals for the indole ring of melatonin were found (data not shown).

Calcineurin activity assays have subsequently been used to investigate the inhibition of CaM activation by melatonin and its analogs. As shown in Figure 4.4, CaM activity was only partially inhibited (up to 30%) even when very high melatonin concentrations were used (0.1 - 1 mM). Lower levels of melatonin did not affect CaM activities (Figure 4.4). Melatonin analogs did not show significant inhibition even at the same high concentrations (Figure 4.4). These results were consistent with those of gel band-shift assays. In 4 M urea gel, CaM is not denatured and is able to bind peptides, therefore, CaM and a peptide-CaM complex display different mobilities on the gel (Figure 4.5A, first two lanes). When MLCK peptides were added to CaM sample, no free CaM could be detected on the gel. Melatonin obviously could compete with the peptides for CaM at very high concentrations, as melatonin-bound

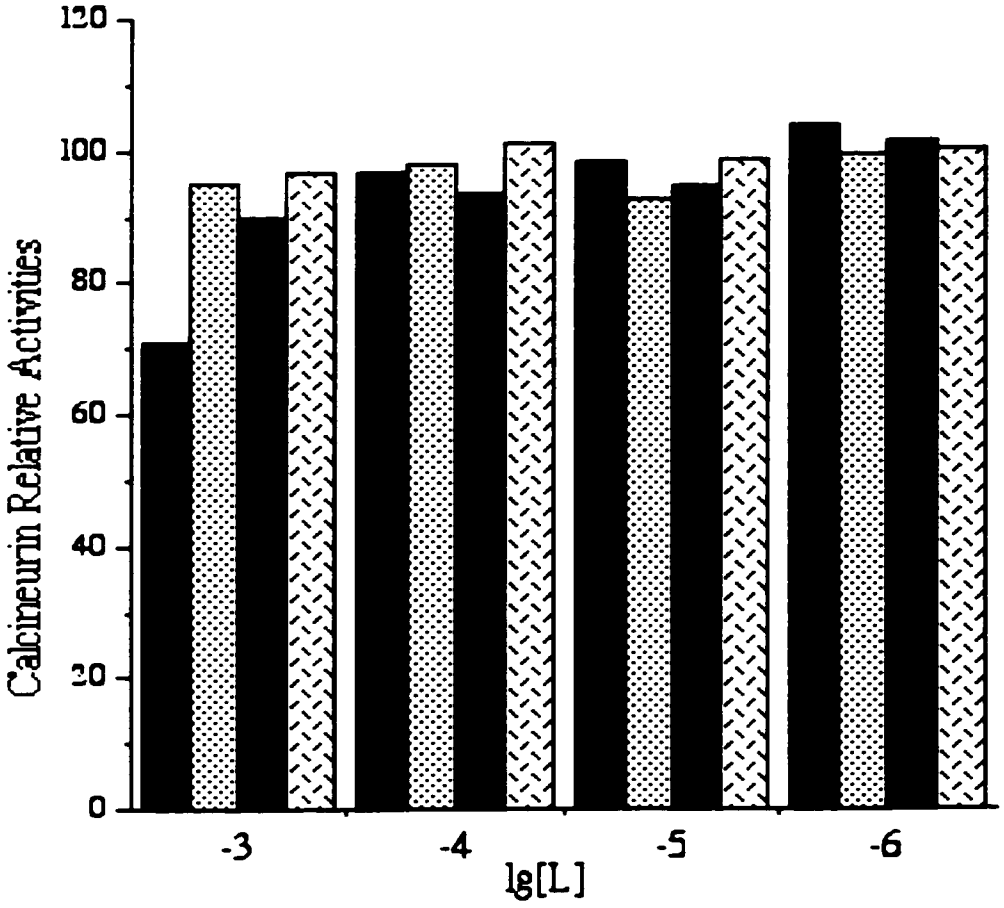

Figure 4.4 The relative activities of calcineurin in the presence of various concentration (M) of ligands (L): melatonin (■), serotonin (▩), 5-hydroxytryptophan (■), and tryptophan (▩). For details of the assay, see materials and methods.

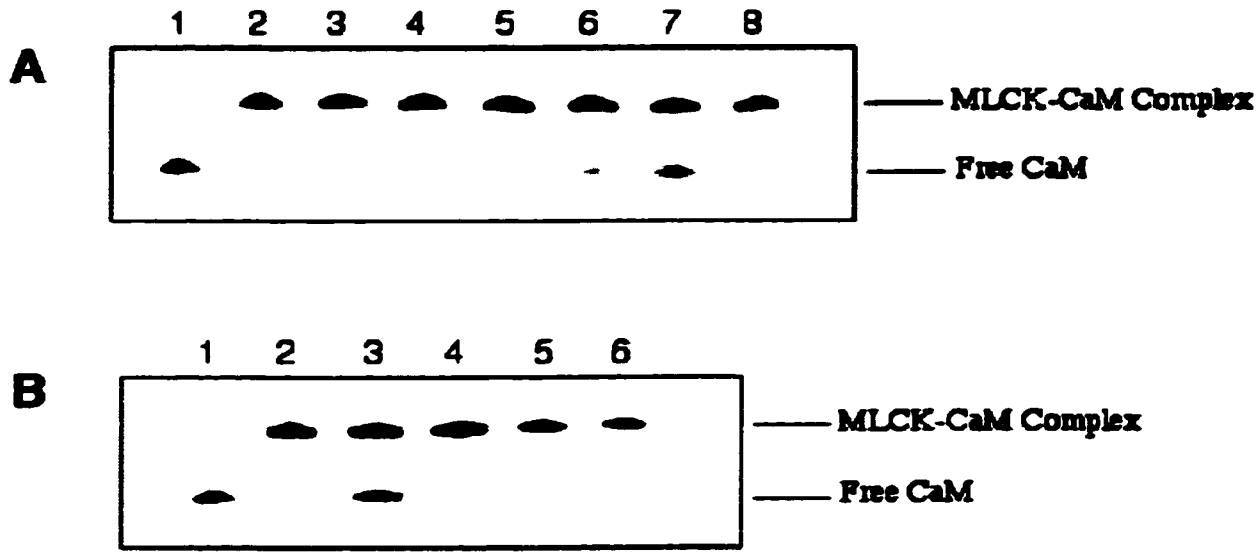

Figure 4.5 Band shift assay on non-denatured urea gel. (A) Electrophoresis of MLCK-CaM (30 μM) with various concentrations of melatonin. Lane 1, Ca^{2+}-CaM; Lane 2 and 8, MLCK-CaM; Lane 3, MLCK-CaM with 30 μM melatonin; Lane 4, MLCK-CaM with 50 μM melatonin; Lane 5, MLCK-CaM with 100 μM melatonin; Lane 6, MLCK-CaM with 500 μM melatonin; Lane 7, MLCK-CaM with 1 mM melatonin. (B) Electrophoresis of MLCK-CaM (30 μM) with 1 mM melatonin or its analogs. Lane 1, Ca^{2+}-CaM; Lane 2 and 8, MLCK-CaM; Lane 3, MLCK-CaM with 1 mM melatonin; Lane 4, MLCK-CaM with 1 mM serotonin; Lane 5, MLCK-CaM with 1 mM 5-hydroxytryptophan; Lane 6, MLCK-CaM with 1 mM tryptophan.

CaM became detectable when high melatonin levels existed in the sample (Figure 4.5A). The same concentrations of serotonin, 5-hydroxytryptophan and tryptophan did not inhibit the binding of the peptide to CaM, and no free CaM can be observed on the gel (Figure 4.5B). Thus the affinity of CaM for melatonin is somewhat higher than that for its analogs.

NMR experiments have been performed to directly study the interactions between CaM and melatonin, serotonin, 5-hydroxytryptophan, and tryptophan. Non-labeled wild-type CaM was titrated by melatonin and monitored by 1D ^{1}H spectra. Figure 4.6 shows the aromatic region of these spectra. Melatonin peaks can be observed after one equivalent was added to the CaM sample. These peaks kept shifting with the addition of melatonin, which indicates that melatonin experiences fast exchange between free and bound states on the NMR time scale. It also suggests that the binding of melatonin to CaM is a weak interaction. Methyl-^{13}C-Met labeled CaM was employed to further investigate the melatonin binding. Met side-chains were selected to be labeled because eight out of the nine Met residues in CaM are located in the hydrophobic patches on the protein surface. Each domain has four Met residues, which contribute as much as 46% to the total hydrophobic surface of Ca^{2+}-CaM (Zhang *et al.* 1995a). The other Met residue, M76, is located in the central linker region. The interactions between melatonin or its analogs and the hydrophobic surface of the Met side-chain labeled CaM should be easily detected by NMR techniques. The melatonin titrations on ^{13}C-labeled protein were monitored by (^{1}H, ^{13}C) HMQC NMR experiments.

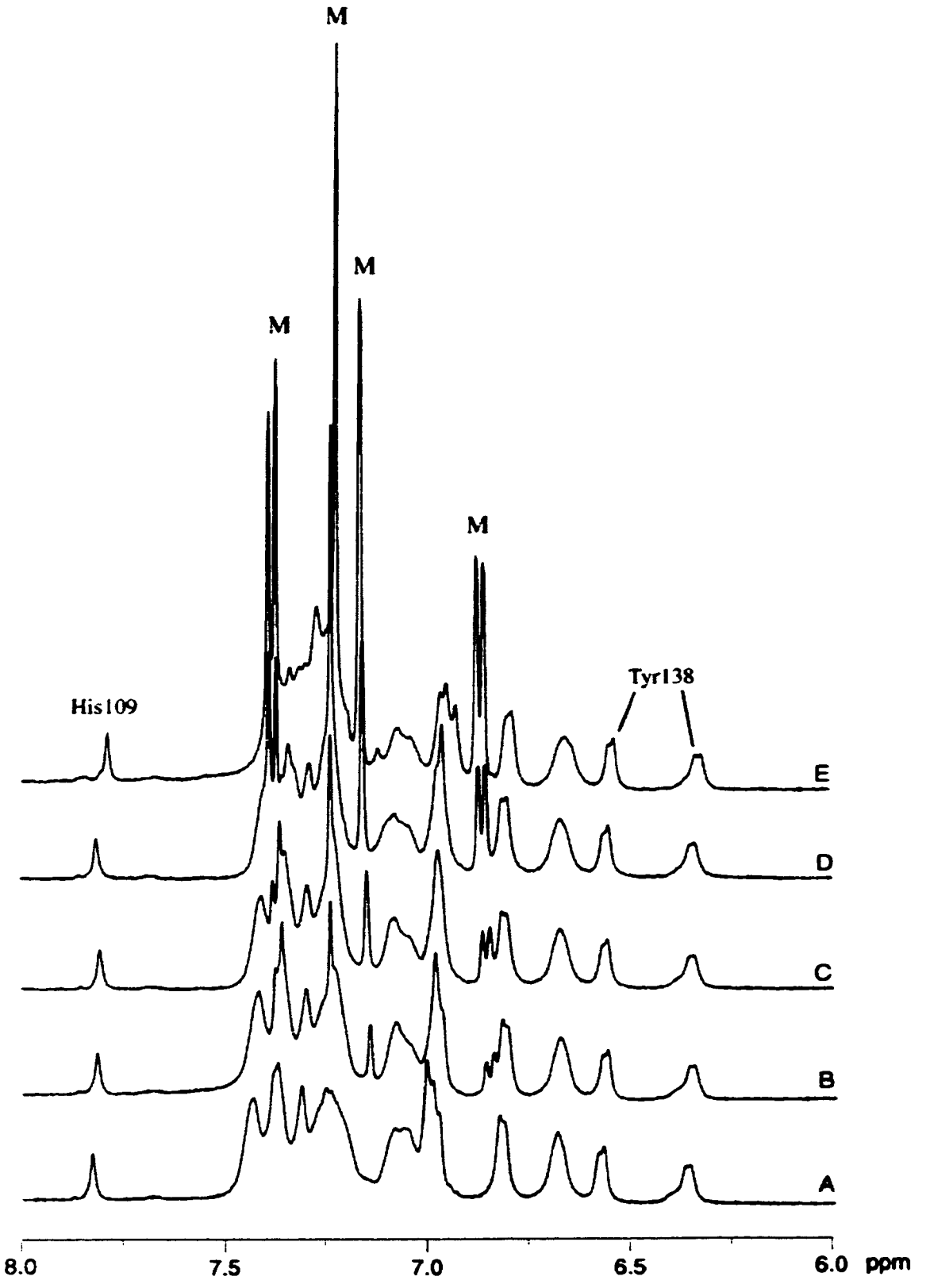
M
M
M
M
His109
Tyr138
E
D
C
B
A
8.0
7.5
7.0
6.5
6.0
ppm

Figure 4.6 Aromatic region of the 1D ^{1}H-NMR spectra of the titration of CaM (1.25 mM, pH 7.4) with (A) 0 equivalent, (B) 0.5 equivalent, (C) 1 equivalent, (D) 2 equivalents, and (E) 6 equivalents of melatonin. Melatonin peaks are marked with "M".

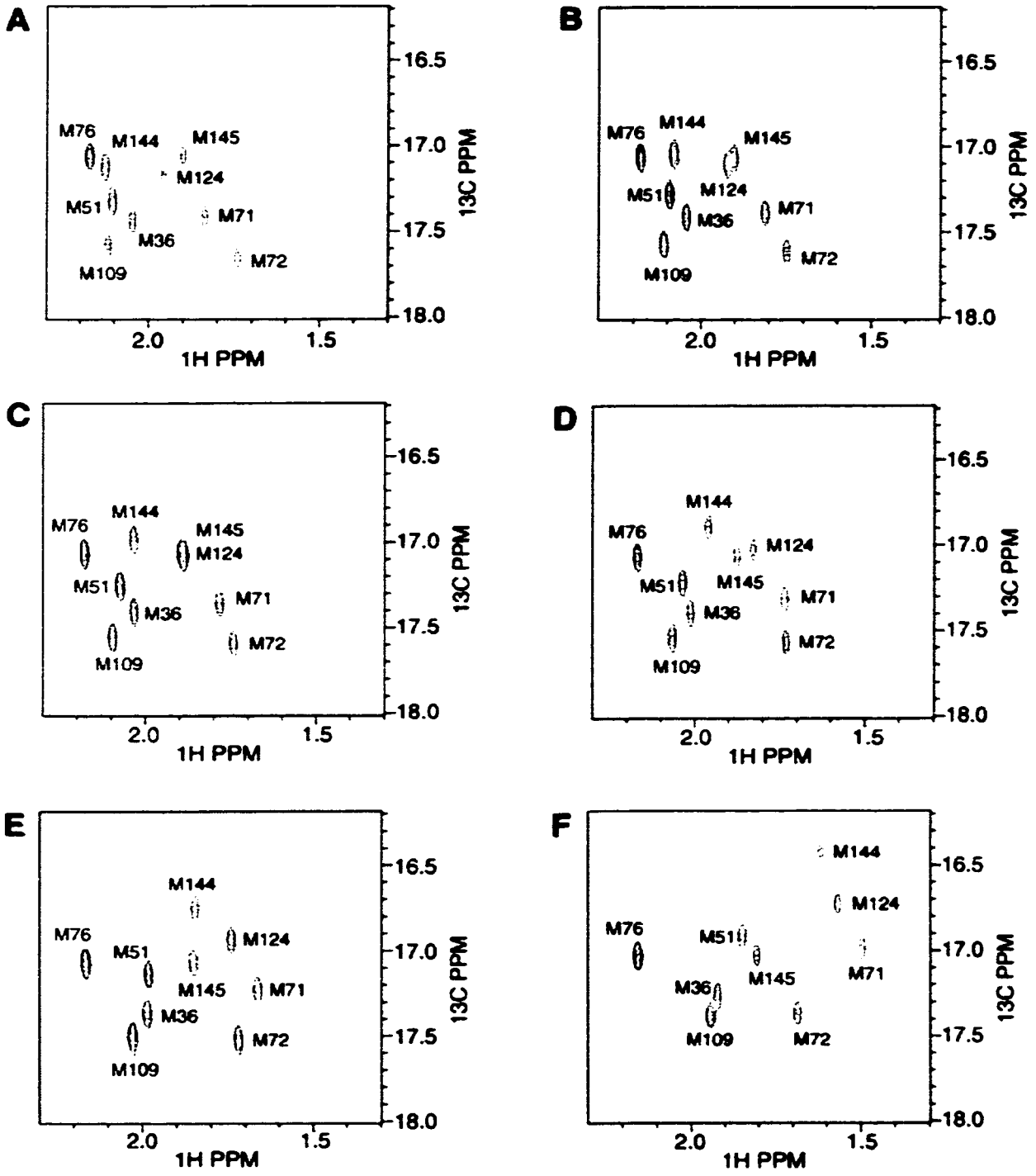
A
M76
M144
M145
M124
M51
M71
M36
M72
M109
16.5
17.0
17.5
18.0
13C PPM
2.0
1.5
1H PPM
B
M76
M144
M145
M51
M124
M36
M71
M72
M109
16.5
17.0
17.5
18.0
13C PPM
2.0
1.5
1H PPM
C
M144
M76
M145
M124
M51
M71
M36
M72
M109
16.5
17.0
17.5
18.0
13C PPM
2.0
1.5
1H PPM
D
M144
M76
M124
M51
M145
M71
M36
M72
M109
16.5
17.0
17.5
18.0
13C PPM
2.0
1.5
1H PPM
E
M144
M76
M124
M51
M145
M71
M36
M72
M109
16.5
17.0
17.5
18.0
13C PPM
2.0
1.5
1H PPM
F
M144
M124
M76
M51
M145
M71
M36
M109
M72
16.5
17.0
17.5
18.0
13C PPM
2.0
1.5
1H PPM

Figure 4.7 2D (^{1}H, ^{13}C) HMQC spectra of the titration of CaM (1.26 mM, pH 7.4) with (A) 0 equivalent, (B) 0.25 equivalent, (C) 0.5 equivalent, (D) 1 equivalent, (E) 2 equivalents, and (F) 6 equivalents of melatonin.

Some of the titration spectra are shown in Figure 4.7. As soon as melatonin was added, all the Met peaks shifted upfield except for M76, the Met residue in the central linker region. Those peaks kept shifting during the whole titration without significant changes in linewidth and intensity. These observations were, again, reflective of typical fast exchange on the NMR time scale. These data suggested that melatonin can interact with both domains of CaM. We plotted the chemical shift change against the melatonin concentrations. Assuming that melatonin binds to both domains of CaM with the same affinity, we have been able to calculate approximate K_d values from chemical-shift versus concentration plots. The estimated K_d values were 2 - 20 millimolar.

Similar NMR titrations have been carried out with serotonin as well. As shown in Figure 4.8, fast exchange was observed in the spectra. Only the peaks in the C-terminal domain showed significant changes during the titration, which suggests that serotonin can only bind to the C-terminal domain of CaM. 5-hydroxytryptophan and tryptophan have also been tested. During the 5-hydroxytryptophan titrations, the HMQC spectra did not show much change with only slight shifting observed on M124 peak (data not shown). In the case of tryptophan, the shifts of M36, M71, M124, and M144 were significant, suggesting again interactions between tryptophan and both domains of CaM.

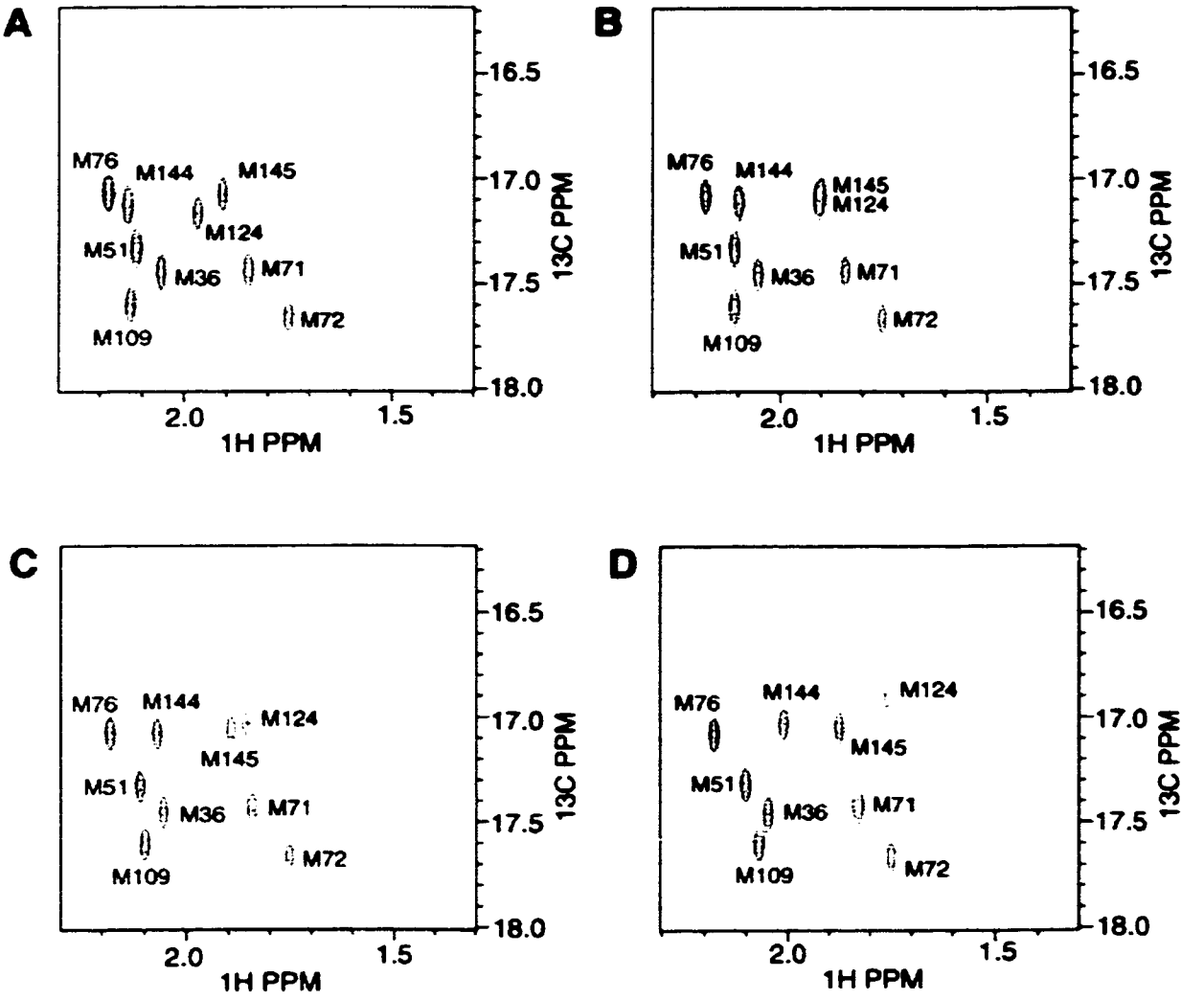

Figure 4.8 2D (^{1}H, ^{13}C) HMQC spectra of the titration of CaM (0.83 mM, pH 7.4) with (A) 0 equivalent, (B) 0.5 equivalent, (C) 1 equivalent, and (D) 2 equivalents of serotonin.

Discussion

CaM modulates a large number of enzymes and proteins by interacting with their CaM-binding domains. Most CaM-binding domains are

amphiphilic α-helices despite the different structures and functions of the target proteins (O'Neil & DeGrado 1990). The binding of synthetic peptides encompassing the amino acid sequence of the CaM-binding domain to CaM has been studied intensively. Several crystal and solution structures of peptide-CaM complexes are available (Crivici & Ikura 1995). Interactions between the hydrophobic cleft in each lobe of CaM and hydrophobic residues on the target peptides are crucial for substrate recognition. CaM has also been shown to bind small compounds, including the neurohormone melatonin. It was reported that melatonin has a very high affinity to Ca^{2+}-CaM with K_d values in the picomolar range (Benítez-King *et al.* 1993), and that melatonin can inhibit Ca^{2+}-CaM-dependent kinase II and phosphodiesterase activities *in vitro* (Benítez-King *et al.* 1991, Benítez-King *et al.* 1996). It was suggested that direct binding of melatonin to CaM was a likely mechanism for the action of melatonin. Here we have presented studies on direct interactions between melatonin and CaM, however, our data do not support the above hypothesis.

Consistent with previous studies, our fluorescence spectroscopy data showed that the binding of melatonin to CaM is Ca^{2+}-dependent. However, melatonin-peptide competition experiments by fluorescence and CD spectroscopy demonstrated that melatonin can not inhibit peptide-binding to CaM at the same concentration, suggesting that melatonin has a significantly lower affinity for CaM than the peptides, which have K_d values in the low nanomolar range. Calcineurin assays and band shift assays also indicated

that melatonin partially inhibits CaM activity only at very high concentrations. This conclusion was confirmed by NMR experiments. Only fast exchange can be observed in both 1D proton and 2D (^{1}H, ^{13}C) HMQC spectra, which suggests that binding of melatonin to CaM is a weak interaction. Moreover, 2D NMR data indicated that melatonin can bind to both lobes of CaM. The approximate K_d values estimated from chemical-shift changes are in the low millimolar range (2 - 20 mM), assuming that melatonin has the same affinity for both domains. This result is different from previous studies (Benítez-King *et al.* 1993), which could due to the different experimental conditions. Our conclusion was also supported by preliminary equilibrium dialysis experiments (data not shown). Thus, it is not likely that the direct interactions between melatonin and CaM would have any significance under physiological conditions. It is more likely that melatonin is involved with CaM through some indirect pathways. It was reported that melatonin modifies CaM cell levels in MDCK and N1E-115 cell lines (Benítez-King *et al.* 1991), suggesting that melatonin could perhaps be involved in controlling CaM synthesis or CaM turnover. On the other hand, evidence has been presented that the activity of serotonin N-acetyl transferase, the rate-limiting enzyme in melatonin synthesis in the chick pineal gland, is related to a calcium/CaM-dependent mechanism, and that melatonin secretion relies on calcium input and output of the cell (Voisin *et al.* 1993, Poblos *et al.* 1996). Clearly, the detailed mechanisms for how CaM modulates melatonin synthesis, or vice versa, have yet to be elucidated. The

actions probably involve some kind of signal transduction pathways, as our results indicate that the direct inhibition of CaM by melatonin is unlikely to be significant *in vivo*.

The melatonin structural analogs, serotonin and 5-hydroxytryptophan, were thought not to interact with CaM because they are more hydrophilic (Benítez-King *et al.* 1993, 1996). Indeed, they did not show any inhibition of CaM activation in calcineurin assays and band shift assays. However, NMR experiments indicate that serotonin can bind to the C-terminal domain of CaM, although very weakly. The rationale for the domain preference of serotonin is presently unknown. Interestingly, unlike serotonin, 5-hydroxytryptophan did not show any significant binding activity to CaM. The only difference between these two compounds is that 5-hydroxytryptophan has an additional carboxyl group on the tail, suggesting that the binding of these compounds to CaM is not solely dependent on the hydrophobic ring. These can be explained by the studies on peptide-CaM interactions. CaM-binding peptides are normally positively charged, hydrophobic α-helices (O'Neil & DeGrado 1990). In addition to hydrophobic interactions, the electrostatic interaction between basic residues on the peptide and acidic residues of CaM also contribute to the binding (Crivici & Ikura 1995, Zhang *et al.* 1995a). In the case of 5-hydroxytryptophan, the extra negative charge from its carboxyl group is likely to be repelled by the negative charges from the acidic residues on CaM surrounding the hydrophobic clefts. Thus, electrostatic repulsion might be the main reason that 5-hydroxytryptophan does not bind to CaM.

Chapter 5

Interactions Between Calmodulin and Anticancer Platinum Drugs

Abstract

Cisplatin and carboplatin are commonly used anti-tumor drugs which attack cancer cells by binding to their DNA. However, these drugs also cause severe side effects which could result from their interactions with proteins or other cellular components. In this work, we have investigated the modification of CaM by these platinum drugs. Cisplatin reacts readily with Met or Met derivatives in solution to form Pt-S bonds which can be detected by UV spectroscopy. Ca^{2+}-CaM has many surface exposed Met residues which are potential targets for cisplatin modification. Indeed, our data demonstrate that cisplatin, as well as carboplatin, binds to the Met sidechains of CaM, forming Pt-S bonds. All nine Met residues in CaM can be modified by cisplatin as indicated by mass spectrometry. NMR data reveal that cisplatin and carboplatin have a higher affinity for the Met residues in the C-terminal domain of the protein. The ability of CaM to bind target peptides is reduced or even abolished by these platinum drugs. Circular dichroism studies show that cisplatin modified CaM retains its secondary structure, consistent with the idea that the inability to bind peptides is the result of modification in the Met-rich interaction surfaces of CaM. Since CaM modulates a large number of signal transduction pathways, CaM-cisplatin adduct formation could be

accountable for many side effects of these anticancer drugs.

Introduction

Cisplatin, cis-$[PtCl_2(NH_3)_2]$, is an extensively used anticancer drug which has proven effective against many kinds of solid tumors, especially testicular and ovarian cancer (Kikuchi *et al.* 1990, Chu 1994, Muggia & Muderspach 1994, Sandler 1998). The intracellular target of cisplatin is believed to be DNA. Cisplatin can cause intra- and inter-strand crosslinks in DNA, and thereby block DNA replication and/or gene transcription, which will further result in cell cycle arrest and programmed cell death (Bancroft *et al.* 1990, Reedijk 1992, Yang *et al.* 1995, Bierbach & Farrell 1998, Elizondo-Riojas *et al.* 1998, Gelasco & Lippard 1998, Lüth *et al.* 1998, Cullinane *et al.* 1999). However, intravenously administered cisplatin has to be transported through the bloodstream and the cell cytoplasm before it can reach the DNA in the cell nucleus; reactions with proteins can occur during the transport process. The chloride ions of cisplatin are relatively labile and can be readily displaced to allow the formation of aquated species, which are often the reactive forms of the compound (Reishus & Martin 1961). Many structural analogs of cisplatin have also been discovered or developed as anticancer drugs, including carboplatin. These drugs share a common feature that two labile platinum ligands are in *cis* position which enables platinum to interact with DNA. Figure 5.1 shows the structures of cisplatin and carboplatin.

Nowadays drug resistance has become a major concern in cancer

treatment. Cell lines from many different kind of tumors have developed resistance to cisplatin and its analogs (Timmer-Bosscha *et al.* 1992, Coukos & Rubin 1998, Fink *et al.* 1998). The dose escalation used to overcome this drug resistance leads to severe multiorgan toxicities, which is one of the main drawbacks of these platinum drugs. One of the reasons for the side effects of cisplatin comes from the fact that the drug can bind to many intra- and extra-cellular components other than DNA. For example, cisplatin has been reported to interact with glutathione, cytochrome c, albumin, metallothionein, alcohol dehydrogenase, and other proteins, as well as with the phospholipid headgroup of phosphatidylserine (Melius *et al.* 1977, Appleton *et al.* 1989, Pattanaik *et al.* 1992, Jiang *et al.* 1996, Jiang *et al.* 1997, Speelmans *et al.* 1997, Zhang *et al.* 1997, Ivanov *et al.* 1998). Cisplatin is particularly reactive

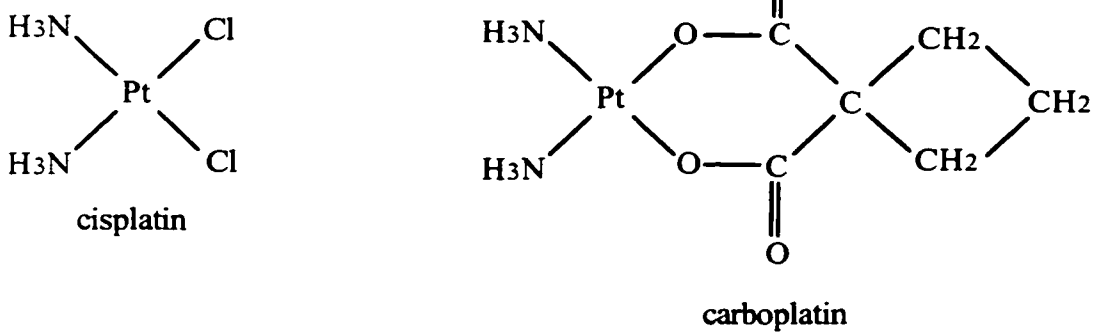

Figure 5.1 Schematic structure of cisplatin and carboplatin.

with proteins with a high sulfur content. Consequently, the binding of cisplatin to the sulfur-containing free amino acids, methionine and cysteine, has been extensively studied (Garoufis *et al.* 1987, Appleton *et al.* 1989, Grochowski & Samochocka 1992, Norman *et al.* 1992, Heudi 1998).

Calmodulin (CaM) is a ubiquitous and versatile Ca^{2+} regulatory protein which modulates a number of cellular signal transduction pathways (Hinrichsen 1993, Vogel 1994, Ikura 1996). When CaM binds Ca^{2+}, it exposes two hydrophobic patches on the protein surface through which CaM can recognize and activate downstream proteins and enzymes. These hydrophobic patches are rich in Met residues, which play an important role in CaM's versatility (Yuan *et al.* 1999). In fact, Met residues contribute as much as 46% of the exposed surface area of the hydrophobic patches on the protein surface (O'Neil & DeGrado 1990, Zhang *et al.* 1995a), which makes them potential targets for platinum drugs. Recent studies have suggested that inhibition of Ca^{2+}-CaM due to direct interactions with cisplatin could play a major role in stomach distention, one of cisplatin's side effects (Jarve & Aggarwal 1997). Since CaM modulates so many cellular activities, the modification by cisplatin or other platinum drugs could also contribute to other side effects of the drugs. Thus, it is of interest to investigate the interactions between CaM and cisplatin more closely. In this work, we have employed a number of biochemical and spectroscopic techniques to study the binding of cisplatin and carboplatin to CaM.

Materials and Methods

Materials

Cisplatin, carboplatin, the pentapeptide methionine enkaphalin (ME) and seleno-methionine were purchased from Sigma. Methyl-^{13}C-methionine and D_2O (99.9%) were obtained from Cambridge Isotope Laboratories. ^{15}N-labeled cisplatin was synthesized by Dr. D. D. McIntyre in our laboratory as described by Kleinberg (1963). MLCK peptide was obtained from the Peptide Synthesis Facility at Queens University (Kingston, ON, Canada). Bacterially expressed CaM was purified as previously described (Zhang *et al.* 1994b).

Fluorescence Spectroscopy

Fluorescence spectroscopy experiments were performed on a Hitachi F-2000 Fluorescence spectrophotometer. CaM (10 μM) was incubated with cisplatin or carboplatin of varying concentrations (0 - 50 molar equivalents) at room temperature for at least five days in 10 mM Tris-Cl buffer (pH 7.4) with 0.1 M KCl and 2 mM $CaCl_2$. MLCK peptide (2 mM) dissolved in the same buffer was then added to these samples to an equal molar concentration of CaM. The samples were incubated at room temperature for another hour before fluorescence spectra were recorded. The excitation wavelength was 297 nm, and emission spectra in the range 300 - 450 nm were recorded. The excitation and emission slit widths were 1 nm, and the emission spectra scanning speed was 60 nm/min with a 1 cm path length cuvette.

Absorption Spectroscopy

UV absorption spectroscopy was used to monitor the binding of cisplatin to Met, N-acetyl-Met, and CaM. For the reactions with the amino acids, the reaction mixture contained 0.58 mM cisplatin and 1.16 mM N-acetyl-Met (or Met) with 0.1 M KCl. The reaction was carried out in a cuvette, and the absorption spectra were acquired at various time intervals. The spectra were recorded from 240 nm to 320 nm at 200 nm/min with a path length of 1 cm. For the reactions with CaM, different amounts of cisplatin were used. The concentration of CaM was determined optically using $\Delta\varepsilon^{1\%}_{280/320}$ = 1.8. CaM (0.25 mM) was mixed with 0, 1, 4, and 25 molar equivalents of cisplatin, respectively, in 0.1 M KCl and 2 mM $CaCl_2$. These samples were incubated at room temperature for at least five days before the absorption spectra were recorded.

Mass Spectrometry

Mass spectrometry was employed to quantify the binding of cisplatin to N-acetyl-Met, ME peptide, and CaM. Electrospray mass spectrometry experiments using a VG triple grad instrument, were performed by Dr. J. Chen and Dr. G. Lajoie in the Biological Mass Spectrometry Laboratory, the University of Waterloo, ON. For the reaction with N-acetyl-Met and ME peptide, 1.5 mM cisplatin was mixed with 0, 1, 2, 4, 10 molar equivalents of N-acetyl-Met or ME peptide in a solution of 100 mM KCl and 10 mM $CaCl_2$.

Samples were incubated at room temperature for five days. For the reactions with CaM, protein samples with various concentrations of cisplatin were prepared as described above for absorption spectroscopy. Before mass spectrometry, the samples were desalted using a DG-10 column (Bio-Rad) after the incubation to remove any remaining free cisplatin, followed by a Chelex-100 (Bio-Rad) column to eliminate Ca^{2+} ions. These samples were then lyophilized and shipped for mass spectrometry.

Circular Dichroism

All circular dichroism (CD) experiments were performed on a Jasco-715 spectropolarimeter. The samples were prepared in 10 mM Tris-Cl buffer (pH 7.4) containing 0.1 M KCl and 1 mM $CaCl_2$. CaM (0.1 mM) dissolved in this buffer was incubated with 0, 1, 4, and 25 equivalents of cisplatin, respectively, at room temperature for at least five days. Excess cisplatin was removed by passage through a DG-10 column (Bio-Rad). The samples were lyophilized and redissolved in 10 mM Tris-Cl buffer (pH 7.4) with 1 mM $CaCl_2$. The modified protein sample was diluted to approximately 10 μM for CD experiments. The CD spectra were recorded between 190 nm to 255 nm using a cell path length of 1 mm. Each spectrum was the average of ten scans and smoothing of base-line-corrected spectra was done by digital filtering.

NMR Spectroscopy

2D NMR experiments were performed on a Bruker AMX-500

spectrometer equipped with a Bruker BGU Gradient Unit Z. 1D NMR experiments were carried out on a Bruker AMX-400 spectrometer. 2D NMR data were processed on a Silicon Graphics Indy 5000 computer using NMRpipe software (Delaglio *et al.* 1995) while 1D data was processed on an X32 workstation with UXNMR software.

NMR spectroscopy was employed to monitor the binding of cisplatin to Met, N-acetyl-Met, and CaM. 1D ^{13}C and ^{195}Pt NMR experiments were performed to study the reaction between cisplatin and the amino acids, Methyl-^{13}C-labeled Met and N-acetyl-Met. Typically, 2 ml of a 6.66 mM cisplatin sample in D_2O was titrated with methyl-^{13}C-labeled Met or N-acetyl-Met at 0, 0.25, 0.5, 0.75, 1, 1.5, 2, 3, and 4 molar equivalents. Immediately after the addition of the ^{13}C-labeled amino acids, a series of 48 ^{13}C NMR spectra were recorded over a period of 24 hr followed by a ^{195}Pt NMR experiment. The pH of the samples was maintained at pH 7.5±0.1 and all the experiments were done at 25°C in a 10-mm NMR tube.

2D NMR experiments were performed to investigate the interaction between cisplatin and CaM. Methyl-^{13}C-Met labeled CaM was titrated with cisplatin and carboplatin. CaM samples used for this study were exchanged twice in D_2O. NMR samples were prepared by dissolving 15 mg CaM into 500 µl D_2O (the final concentration of CaM was determined optically using $\Delta\varepsilon^{1\%}_{280/320} = 1.80$) with 0.1 M KCl, 10 mM $CaCl_2$. Cisplatin (6.66 mM) and carboplatin (50 mM) stocks were prepared in the same solution. The titration was performed at 25°C, and the pH of the samples was maintained at pH 7.4

during the titration (Isotope effects on pH have been ignored). The titration was monitored with ^{1}H, ^{13}C HMQC NMR experiments as previously described (Yuan *et al.* 1999). For each titration point, the sample was incubated at room temperature for at least three days before the HMQC spectra were recorded. ^{15}N-cisplatin was also synthesized so that $^{1}H,^{15}N$ HMQC NMR experiments could be recorded. CaM and ^{15}N-cisplatin stock were prepared in 90%H_2O-10%D_2O with 0.1 M KCl and 10 mM $CaCl_2$. $^{1}H,^{15}N$ HMQC NMR data were recorded using the pulse sequence described by Bax *et al.* (1983). Selenomethionine (SeMet) has also been biosynthetically incorporated into CaM, and similar experiments were carried out on SeMet labeled CaM using $^{1}H,^{77}Se$ HMBC experiments. The experimental details of the $^{1}H,^{77}Se$ HMBC technique for CaM were previously described by Zhang and Vogel (1994). The $^{1}H,^{77}Se$ HMBC experiments were performed at 37°C to improve the quality of the spectra.

Results

Fluorescence Spectroscopy of Peptide Binding

The purpose of this study is to investigate the interaction between the platinum anticancer drugs, cisplatin and carboplatin, and CaM, the ubiquitous secondary messenger protein. The first question to address is whether these platinum drugs affect CaM's activity. Given the importance of CaM in signal transduction pathways, any influence of these drugs on CaM's

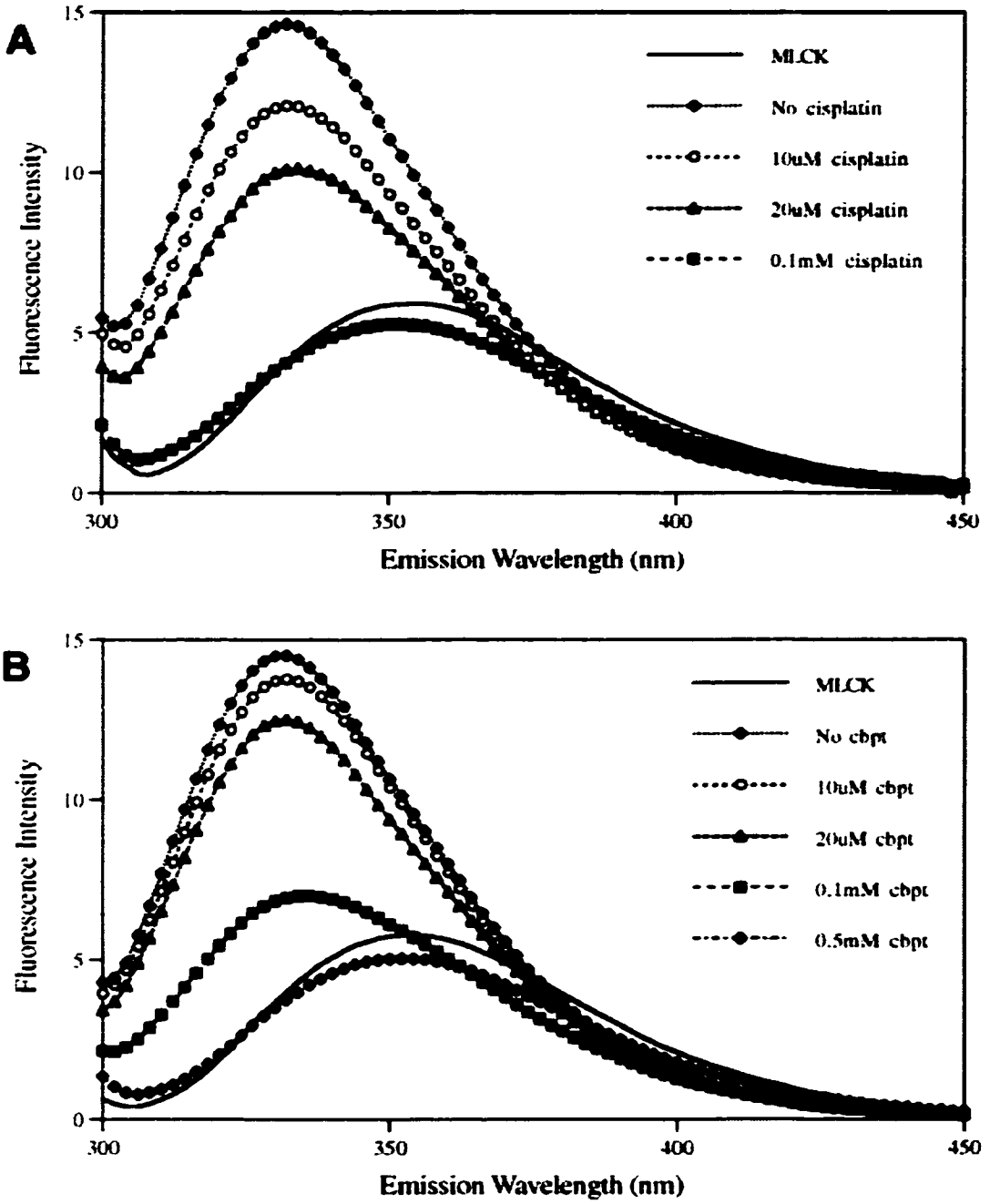

Figure 5.2 Fluorescence spectra. (A) MLCK peptide (10 μM) with an equimolar amount of CaM incubated with various concentrations of cisplatin. (B) MLCK peptide and CaM (10 μM) incubated with various concentrations of carboplatin. Solid lines with no symbol show the spectrum of the free MLCK peptide.

activity could account for wide ranging cellular effects. On the other hand, if these drugs do not have any influence on CaM's activity, the interaction between the drugs and CaM, even if it exists, would not have much physiological significance. CaM's activity is to bind and activate downstream proteins and enzymes after it is saturated with Ca^{2+} ions. Many target enzymes have a 20-residues long CaM-binding domain in their sequence. Synthetic peptides with the sequence from these CaM-binding domains also show very high affinity for CaM, and hence are a good system to study these interactions. In this work, a synthetic peptide containing the CaM-binding domain of skeletal muscle MLCK was used to probe the effects of the platinum drugs on CaM's activity. This peptide possesses a single Trp residue that is absent in CaM. Thus the binding of the peptide to CaM can be monitored by fluorescence spectroscopy. When MLCK peptide binds to CaM, it shows a large blue shift as shown in Figure 5.2A. The emission peak shifts from 355 nm in free MLCK peptide to 332 nm in the CaM-bound form. The intensity of the peak also increases more than two fold. For samples containing CaM incubated with 1 equivalent of cisplatin, the emission peak showed a significant decrease in intensity, suggesting that less MLCK peptide was bound to CaM. With increasing cisplatin (2 equivalents) present, the fluorescence intensity of the emission peak decreased further (Figure 5.2A). When the cisplatin concentration reaches 10 equivalents, the emission spectrum displayed a pattern very similar to that of the free MLCK peptide (Figure 5.2A). These data suggest that cisplatin can inhibit CaM's substrate

binding activity, and the inhibition seems to be dose-dependent. Complete inhibition was obtained with 10 equivalents of cisplatin. The same fluorescence experiment was performed using carboplatin. Carboplatin had similar effects on CaM's ability to bind the MLCK peptide (Figure 5.2B). The emission peak of MLCK peptide decreased in intensity with the presence of 1 equivalent of carboplatin, but was less significant than cisplatin (Figure 5.2). The effect of carboplatin was also concentration-dependent; the intensity of the emission peak decreased further in the presence of higher concentration of carboplatin (Figure 5.2B). Unlike cisplatin, the emission peak still blue shifted from 355 nm to 336 nm at a concentration of 10 equivalents. The binding of the peptide to CaM was fully inhibited at higher carboplatin concentration (Figure 5.2B). Thus, carboplatin can inhibit CaM's activity like cisplatin, but the inhibition is less effective according to these fluorescence data.

Mass Spectrometry of Methionine Enkaphalin and CaM Adducts

The next question is whether the inhibition is caused by direct binding of cisplatin and carboplatin to CaM, or through another mechanism. Cisplatin is an anticancer compound whose reactivity has been studied extensively. The two chloride ligands are very labile and can exchange with hydroxyl groups rapidly in aqueous solution. The two amine groups are more stable, but still replaceable when cisplatin reacts with amino acids and peptides under certain circumstances (Berners-Price & Kuchel 1990, Heudi *et*

al. 1998). Sulfur-atoms in Met and Cys have been found to have a high affinity for cisplatin, although both amino and carbonyl groups can be reactive to platinum(II) as well (Garoufis *et al.* 1987, Lempers & Reedijk 1991). The platinum-sulfur interaction is of particular interest because it is the major interaction between cisplatin and proteins. Cys and Met residues, especially those on the protein surface, are susceptible to platinum modification (Grochowski & Samochocka 1992, Norman *et al.* 1992, Jiang *et al.* 1996, Jiang *et al.* 1997, Heudi 1998).

Mammalian CaM does not have any Cys in its amino acid sequence, which makes Met residues the most likely targets for cisplatin binding. Here we have used mass spectrometry to quantitate the binding of cisplatin to N-acetyl-Met, methionine enkaphalin (ME), and CaM. The reactions were carried out under neutral conditions. Our results indicated that these three molecules can all be modified directly by cisplatin (see below).

To simplify the situation, the pentapeptide ME was used as a model to investigate the binding of cisplatin to a Met sidechain in a protein. Figure 5.3 shows the mass spectrum obtained for 1:1 mixture of cisplatin and ME. ME has a formula weight of 574 Da, while cisplatin is 300 Da. When these two molecules react in solution, the sulfur atom is most likely to replace a chlorine ligand in cisplatin to form a Pt-S bond. The resulting cisplatin-modified ME, ME-$Pt(NH_3)_2Cl$, would have a molecular weight of 838 Da, which is indicated as peak D in Figure 5.3. Since the reaction was carried out in aqueous solution, the chlorine ligand can also readily exchange with water. Therefore,

the resulting compound could also be ME-Pt(NH_3)OH, which has a formula weight of 819 Da (shown as peak C in Figure 5.3). It is also possible that NH_3 groups could be randomly lost; such a loss can occur during the lyophilization or the vacuum/heating step in the electrospray mass spectrometry experiment. If one NH_3 group in species ME-Pt(NH_3)$_2$Cl was removed, the resulting complex, ME-Pt(NH_3)Cl, would have a mass around 820 Da, which also contributes to peak C. For the same reasons, the species in peak C could have the Cl exchanged for OH, or have one OH or NH3 group removed, giving

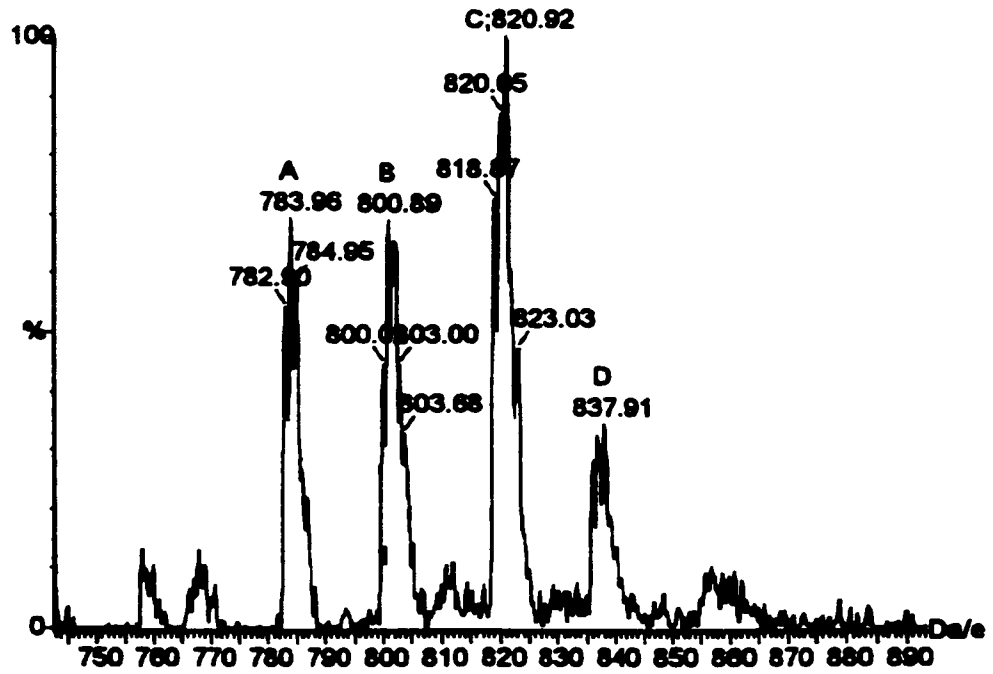

Figure 5.3 Mass spectrum of ME peptide incubated with one equivalent of cisplatin. According to their mass number, these species can be identified as [A] ME-PtNH_3 or ME-PtOH, [B]ME-Pt(NH_3)$_2$, ME-Pt(NH_3)OH or ME-PtCl, [C] ME-Pt(NH_3)$_2$OH or ME-PtNH_3Cl, and [D] ME-Pt(NH_3)$_2$Cl.

rise to the species in peak B with a mass number around 802 Da. Peak A was the result of the species in peak B undergoing a similar change (see the legend of Figure 5.3 for the possible formula of the compounds in these peaks). Since an amine and a hydroxyl group both have a mass number of 17 and chloride is mostly 35 Da, a group of peaks with mass differences of around 17 and multiples thereof would result from cisplatin-modified molecules in the spectrum. Therefore, the multiple peaks observed in the mass spectrum were due to the exchange between Cl and OH group, as well as the random loss of OH or NH_3 group. The isotope composition of cisplatin also has to be considered when interpreting these results. Chlorine has two common isotopes, ^{35}Cl and ^{37}Cl, which are present at 75% and 25%. Normally, platinum has four isotopes, ^{194}Pt, ^{195}Pt, ^{196}Pt, and ^{198}Pt, with natural abundance of 33%, 34%, 25%, and 7%, respectively. Due to the presence of these different isotopes which were not resolved in the present analysis, a linewidth of around 8 Da was expected for each individual peak in the mass spectrum, which was indeed observed in Figure 5.3.

According to previous investigations on the interaction between cisplatin and Met (or N-acetyl-Met), both chloride ligands can be replaced simultaneously by sulfur atoms from Met side chains (Appleton *et al.* 1989, Grochowski & Samochocka 1992, Heudi *et al.* 1998). ME is a pentapeptide containing a single Met residue. If double displacement of chloride ligands happens, cisplatin could cause crosslinking of the peptide. Our results indicated that cisplatin can bind two ME peptides simultaneously when an

excess of peptide is present. Figure 5.4 shows the mass spectrum of a 1:4 mixture of cisplatin and ME. The excess ME is evident from the largest peak in the spectrum (574 Da). The smaller peak with a mass/charge ratio of 671 was identified as a doubly charged species. This species reflects a mass

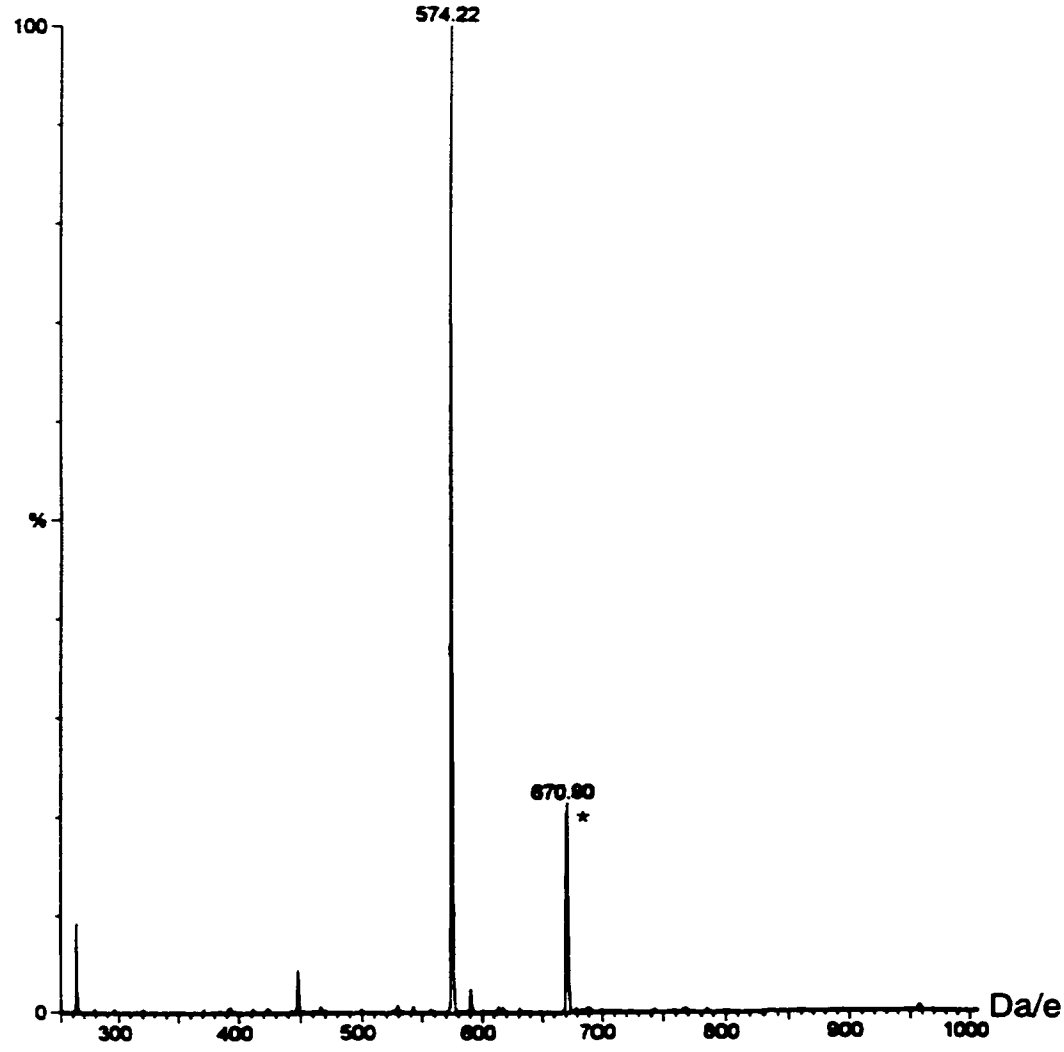

Figure 5.4 Mass spectrum of 1:4 mixture of cisplatin and ME peptide. The peak labeled with an asterisk is doubly charged. See text for details.

number of 1342, which is the exact mass expected for the $Pt(ME)_2$ complex. This result indicates that cisplatin has the capability to bind more than one Met side chain at the same time, which results in crosslinking of peptides and proteins.

The binding of cisplatin to CaM was subsequently investigated by mass spectrometry. Since Ca^{2+}-CaM can give a more complicated mass spectrum than apo-CaM due to the random loss of Ca^{2+} ions during the process, apo CaM was used in these experiments. Apo CaM shows a single peak in the mass spectrum as illustrated in Figure 5.5A. Like the mass spectrum of cisplatin modified ME, the spectra of cisplatin-modified CaM were complicated by the exchange of the Cl group and the random loss of some of platinum's OH and NH_3 ligands. Figure 5.5B shows the spectrum of 1:4 mixture of CaM and cisplatin. Peaks in this spectrum can be divided into three groups. Group A and B represent CaM modified by 2 and 3 cisplatin molecules, respectively. The less intense peaks in group C correspond to CaM containing 4 cisplatins. Within each group, peaks have a mass difference of around 17, suggesting they are the results of exchange and loss of cisplatin ligands as mentioned above. According to their mass, the species that these peaks represent can be identified as indicated in the figure legend. As before, an NH_3 group could also be an OH group since mass spectrometry cannot distinguish between these two groups. In addition, since all protein samples were passed through a desalting column, these data also indicate that the binding of cisplatin to CaM is probably covalent. In agreement with this, the

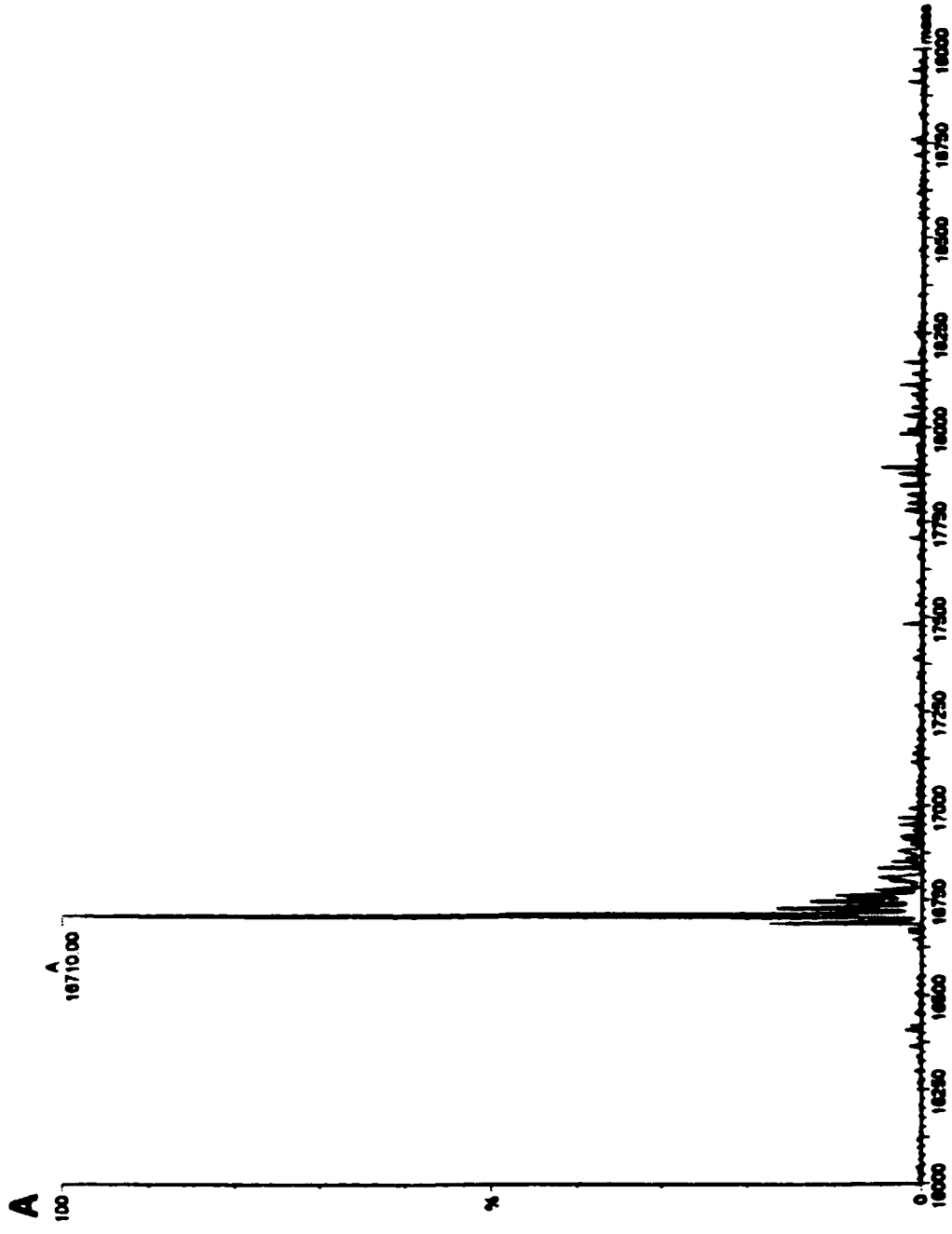
A
100
%
0
A
16710.00
16000
16250
16500
16750
17000
17250
17500
17750
18000
18250
18500
18750
19000
mass

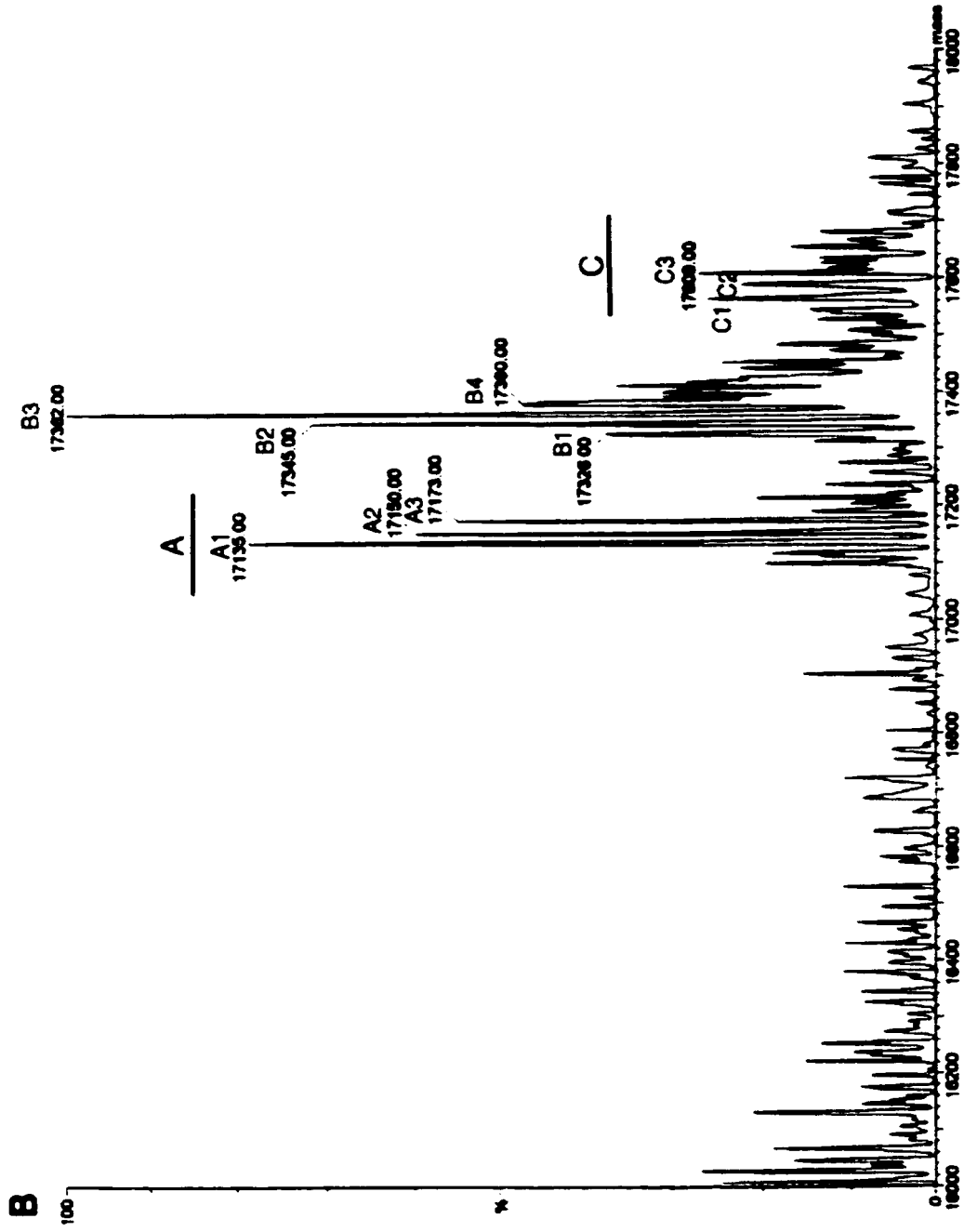
B
A
C
A1
A2
A3
B1
B2
B3
B4
C1
C2
C3
100
%
0
mass

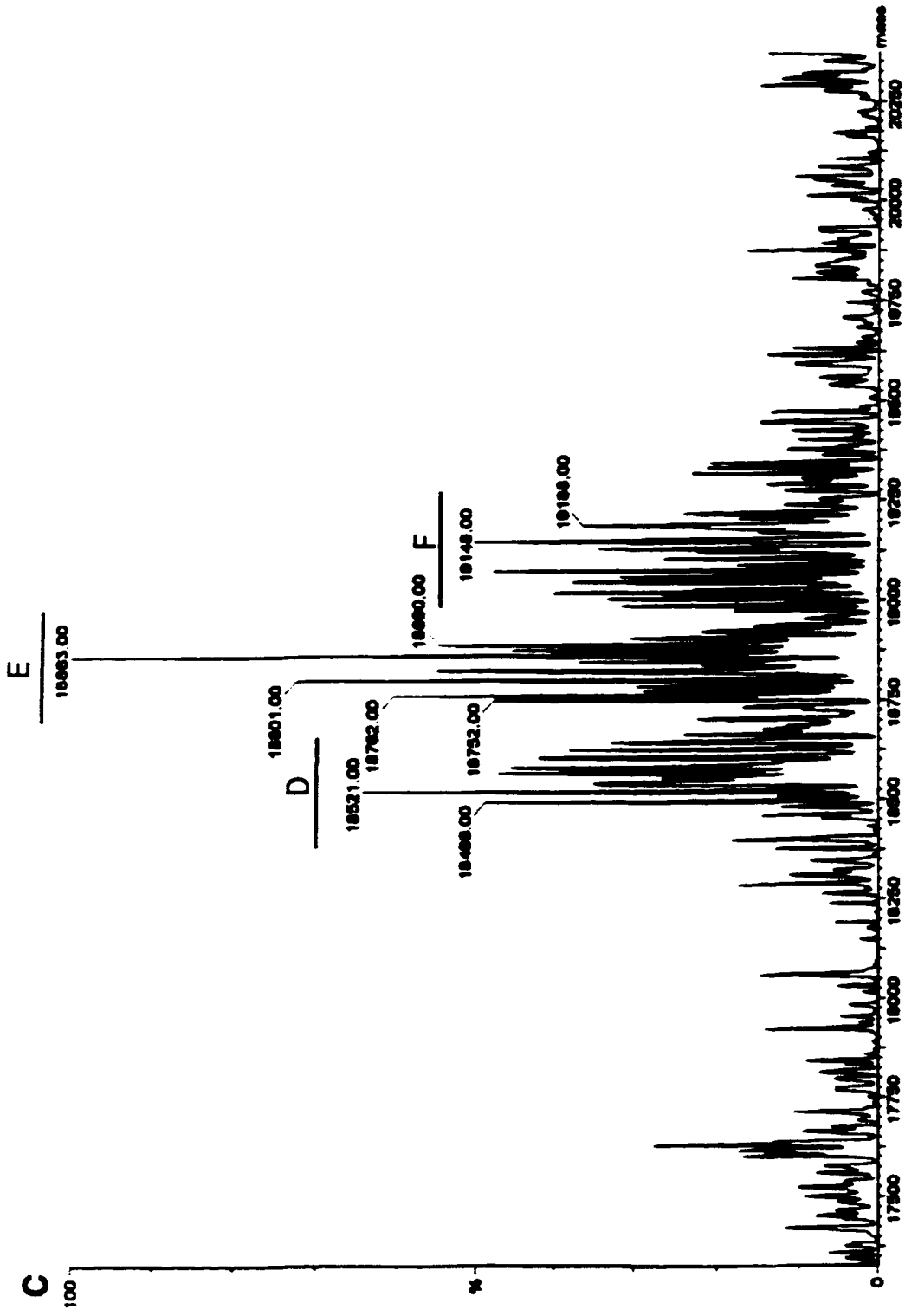
C
100
%
0
17500
17750
18000
18250
18500
18750
19000
19250
19500
20000
20250
mass
E
18863.00
D
18521.00
18762.00
18801.00
18752.00
18496.00
F
18660.00
18148.00
19186.00

Figure 5.5 Mass spectra of cisplatin modified CaM. (A) apo CaM. (B) 1:4 mixture of CaM and cisplatin. Assuming NH_3 is the only platinum ligand other than the Met side chain from CaM, some major species can be identified according to their mass number: [A1] CaM+2Pt+2NH_3; [A2] CaM+2Pt+3NH_3; [A3] CaM+2Pt+4NH_3; [B1] CaM+3Pt+2NH_3; [B2] CaM+3Pt+3NH_3; [B3] CaM+3Pt+4NH_3; [B4] CaM+3Pt+5NH_3; [C1] CaM+4Pt+5NH_3; [C2] CaM+4Pt+6NH_3; and [C3] CaM+4Pt+7NH_3. Please note that the average mass number of Cl atom is 35.5, which is approximately double the mass number of NH_3 group. Cl atom could also be a platinum ligand in these species. For example, A1 could also be CaM+2Pt+Cl. Furthermore, since CaM was modified by more than one cisplatin molecule, the exact format of the bound cisplatin cannot be assigned solely based on these data. For instance, A1 could represent species like CaM-$(PtNH_3)_2$, or CaM-Pt-Pt$(NH_3)_2$. (C) 1:25 mixture of CaM and cisplatin. Group D, E, and F represent CaM modified by 7, 8, and 9 molecules of cisplatin, respectively. See text for more information.

bound platinum could also not be removed from CaM by dialysis or on a metal ion chelating column. CaM can bind more cisplatin as shown in Figure 5.5C which illustrates the mass spectrum obtained for a 1:25 mixture of CaM and cisplatin. This spectrum also has three groups of peaks. Judging from their mass, group D, E, and F represent CaM modified by 7, 8, and 9 cisplatin molecules, respectively. This demonstrates that one CaM molecule can bind up to 9 molecules of cisplatin. Even though a large excess of cisplatin (25 equivalents) was present, no more than 9 equivalents of cisplatin were incorporated. Interestingly, this corresponds to the number of Met residues in CaM. Thus, it seems reasonable to infer from the mass spectrometry data that Met side chains provide the cisplatin binding sites on CaM.

NMR and Absorbance Studies of the Interaction of CaM with Cisplatin

The results in the previous section showed that the reaction between cisplatin and CaM can be investigated with mass spectrometry by examining the mass of the reaction products. The reaction can also be followed independently by monitoring the reactants, cisplatin and Met or Met residues in CaM, which can be achieved by NMR experiments. The time course of the binding of cisplatin to methyl-^{13}C-labeled Met or N-acetyl-Met was monitored by ^{13}C and ^{195}Pt NMR. ^{13}C signals arose from Met (or N-acetyl-Met), and ^{195}Pt signals were from cisplatin. As expected, during the reaction, signals from free Met or cisplatin decreased, while resonances from cisplatin-Met (or N-acetyl-Met) complexes increased (data not shown). Similar NMR studies have been

reported before (Grochowski & Samochocka 1992, Norman *et al.* 1992). Using ^{15}N-labeled cisplatin as a reactant, the binding of this compound to CaM can also be monitored by ^{1}H,^{15}N HMQC NMR experiments (Ivanov *et al.* 1998). The decrease of unreacted cisplatin was obvious from comparing the ^{1}H,^{15}N HMQC spectra of ^{15}N-labeled cisplatin before and after 24 hour reaction with Ca^{2+}-CaM, suggesting that cisplatin was reacting with CaM (data not shown). Therefore, the NMR data also indicated the direct reaction between cisplatin and CaM.

Mass spectrometry and NMR spectroscopy indicated that cisplatin interacts with CaM by direct binding. Does the binding occur through the formation of Pt-S bond since Met residues are the most susceptible targets for cisplatin in CaM? Pt(II)-S bonds display a broad absorbance band below 280 nm which can be detected by UV spectroscopy (Zhang & Tang 1994). Indeed, this absorbance can be easily detected when cisplatin reacts with Met or N-acetyl-Met. Figure 5.6A shows the UV absorption spectrum of a 1:2 mixture of cisplatin and N-acetyl-Met at different time intervals. Cisplatin itself has a very broad absorbance peak around 300 nm, while N-acetyl-Met does not show any absorption in this region. However, when these two substances were mixed, the absorbance below 280 nm increased with time. After a period of 47 hours, the absorption at 250 nm increased from 0.023 to 0.708, and the absorption at 280 nm increased from 0.058 to 0.166. This data clearly indicated that the formation of Pt-S bonds gives rise to a large absorption below 280 nm, therefore UV absorption spectroscopy can be used

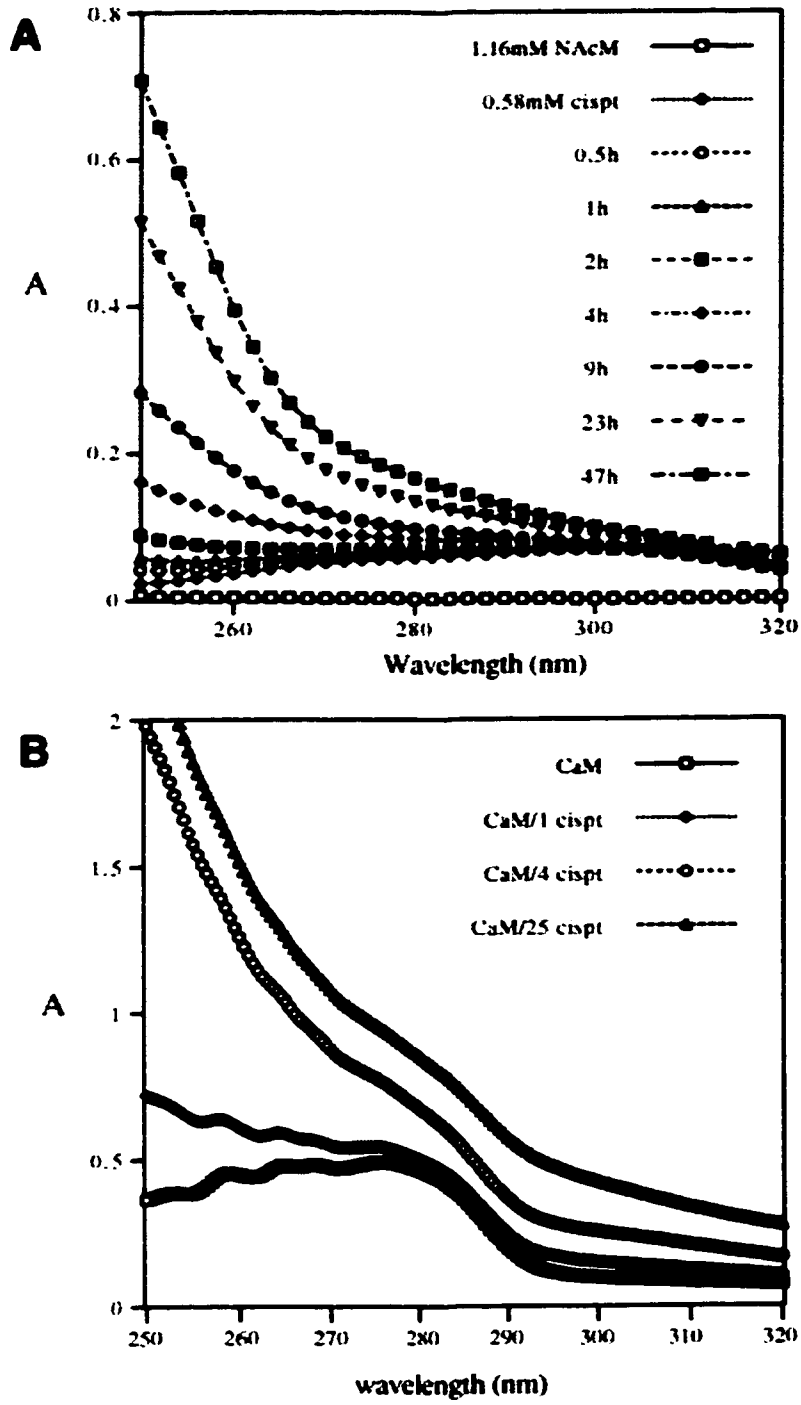

Figure 5.6 UV absorption spectra. (A) 1:2 mixture of cisplatin and N-acetyl-Met at various time intervals. (B) CaM incubated with various concentrations of cisplatin.

to detect the formation of Pt-S bonds between cisplatin and CaM. Figure 5.6B shows the UV spectra of cisplatin-modified CaM. These spectra were recorded on CaM after prolonged incubation with various amounts of cisplatin. The increase of the absorption below 280 nm of the modified CaM is obvious compared to free CaM. These data suggested that the binding of cisplatin to CaM is through the formation of Pt-S bonds. Furthermore, with increased amount of cisplatin in the sample, more Pt-S bonds can be formed (Figure 5.6B).

NMR experiments were performed to further study the binding of platinum drugs to the Met residues of CaM. Methyl-^{13}C-Met was biosynthetically incorporated into CaM to facilitate ^{1}H,^{13}C HMQC NMR experiments. Methyl-^{13}C-Met labeled CaM gives rise to nine well resolved signals in an HMQC spectrum as shown in Figure 5.7A. These nine peaks correspond to the nine Met residues in CaM. The methyl-^{13}C-Met labeled CaM was titrated by cisplatin and carboplatin. After the protein was incubated with 1 equivalent of cisplatin, the nine Met peaks remained at the same positions. However, the Met peaks from the C-terminal domain (M109, M124, M144, and M145) displayed significant broadening. As seen in Figure 5.7B, the intensity of these C-lobe peaks is lower than those from the N-terminal domain. When the concentration of cisplatin was increased to 1.5 equivalents, the broadening of these C-lobe peaks intensified and peaks M109 and M145 broadened beyond detection. Although Met resonances from the N-terminal domain of CaM were still well resolved at this point, the

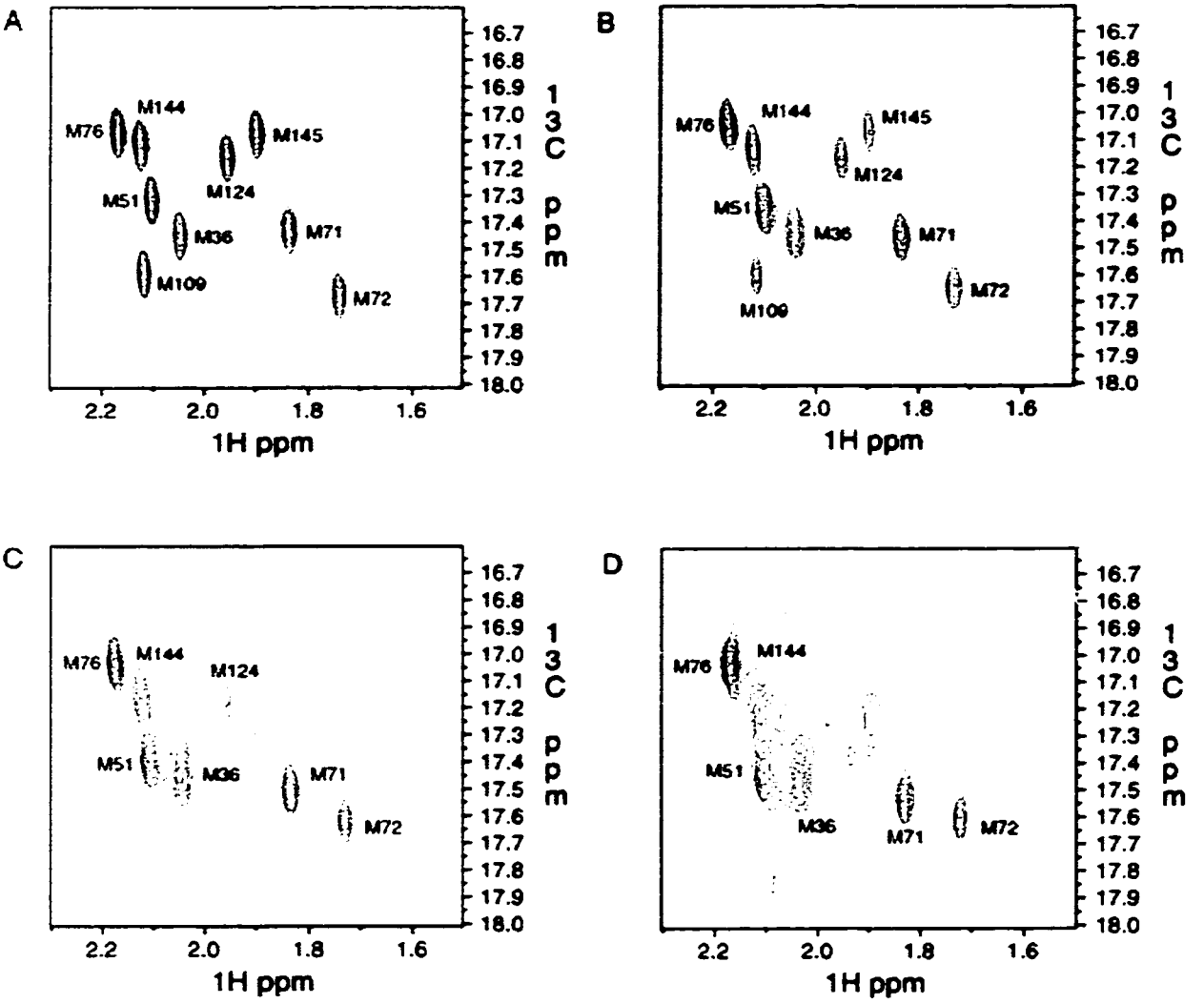

Figure 5.7 $^{1}H,^{13}C$ HMQC spectra of the titration of methyl-^{13}C-Met labeled CaM with (A) 0 equivalent, (B) 1 equivalent, (C) 1.5 equivalent, and (D) 2 equivalents of cisplatin.

linewidth of these peaks was also increasing (Figure 5.7C). The broadening of Met peaks continued at 2 equivalents of cisplatin (Figure 5.7D): at this point, the majority of the C-lobe Met peaks disappeared with M144 showing low intensity; the N-lobe peaks also became broadened. Several very broad new

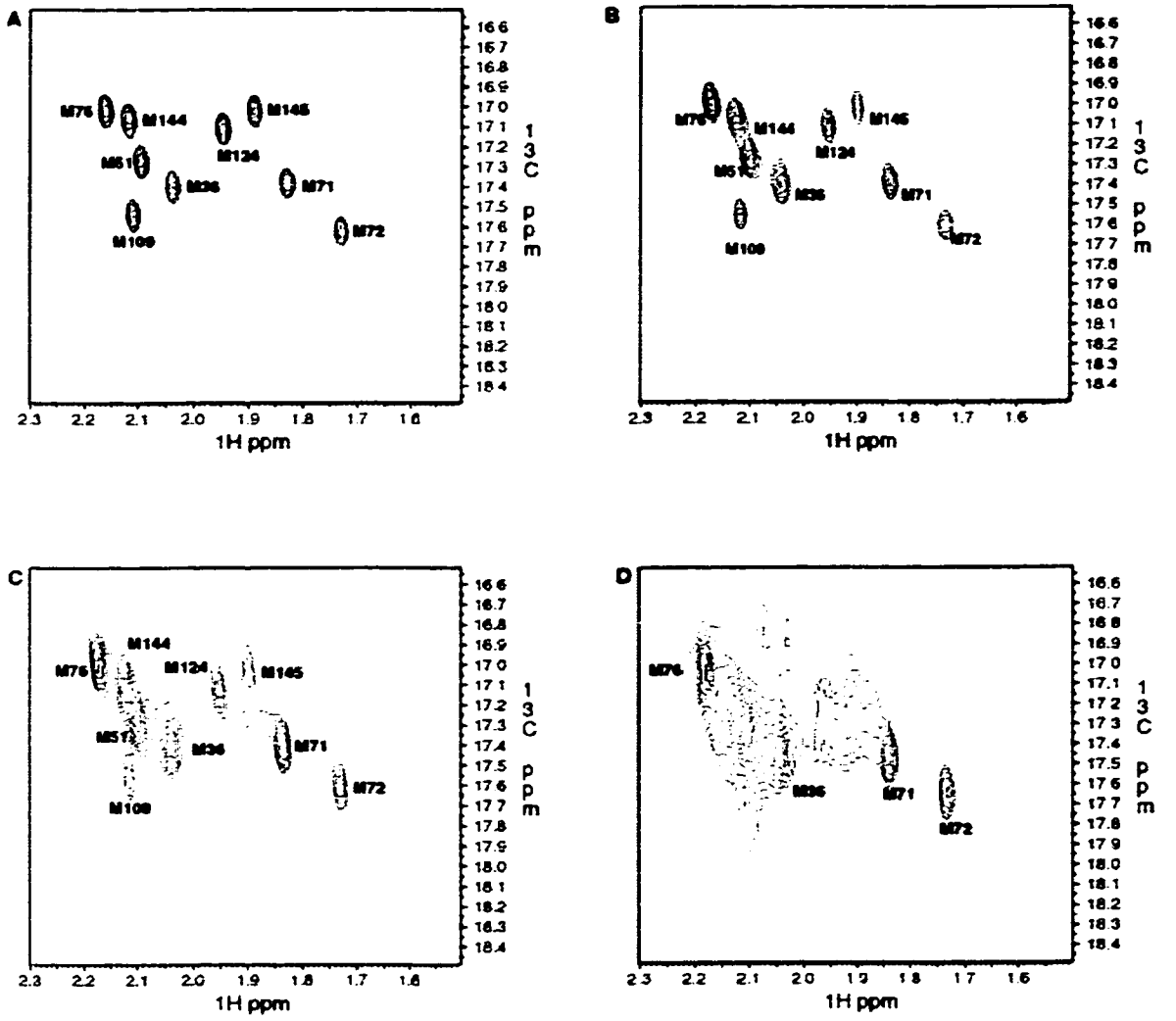

Figure 5.8 $^{1}H,^{13}C$ HMQC spectra of the titration of methyl-^{13}C-Met labeled CaM with (A) 0 equivalent, (B) 1 equivalent, (C) 1.5 equivalent, and (D) 2 equivalents of carboplatin.

peaks arising from cisplatin-modified Met residues became detectable in the spectrum. Eventually, all signals overlapped and could not be resolved (data not shown). Although the titration could not be completed due to these line

broadening problems, these data clearly indicate that the Met residues from the C-terminal domain of CaM were affected first by cisplatin, suggesting that the C-lobe Met residues have higher reactivity with the drug than those from the N-lobe. Similar titration experiments have been carried out with carboplatin. The results of these experiments were quite similar to those of cisplatin. The Met peaks started to broaden when carboplatin was added, and the C-lobe Met signals were affected before those from the N-lobe (Figure 5.8). This result suggests that carboplatin reacts with CaM in a similar manner as cisplatin.

We also used seleno-Met (SeMet) labeled CaM in our studies. SeMet is a structural analog of Met with the sulfur atom replaced by selenium. Selenium is a spin 1/2 nucleus that gives rise to simple sharp NMR signals (Zhang and Vogel 1994). Thus, using SeMet labeled CaM enables us to study the "sulfur" atom by NMR. Figure 5.9 shows the $^{1}H,^{77}Se$ HMBC spectra of SeMet labeled CaM titrated by cisplatin. SeMet of untreated CaM shows nine well-resolved peaks corresponding to the nine SeMet residues of CaM. Unfortunately, like the NMR titration of methyl-^{13}C-Met labeled CaM, line broadening became so severe that the spectral titration data could not be interpreted beyond 2 equivalents of cisplatin. As seen in Figure 5.9, the signals from the C-lobe of the protein are affected first by cisplatin. A new peak at 2.02 ppm (^{1}H) and 74.4 ppm (^{77}Se) was detected at 1 equivalent of cisplatin, which probably arose from modified SeMet residues. Thus, the results from these experiments are consistent with the results of the NMR

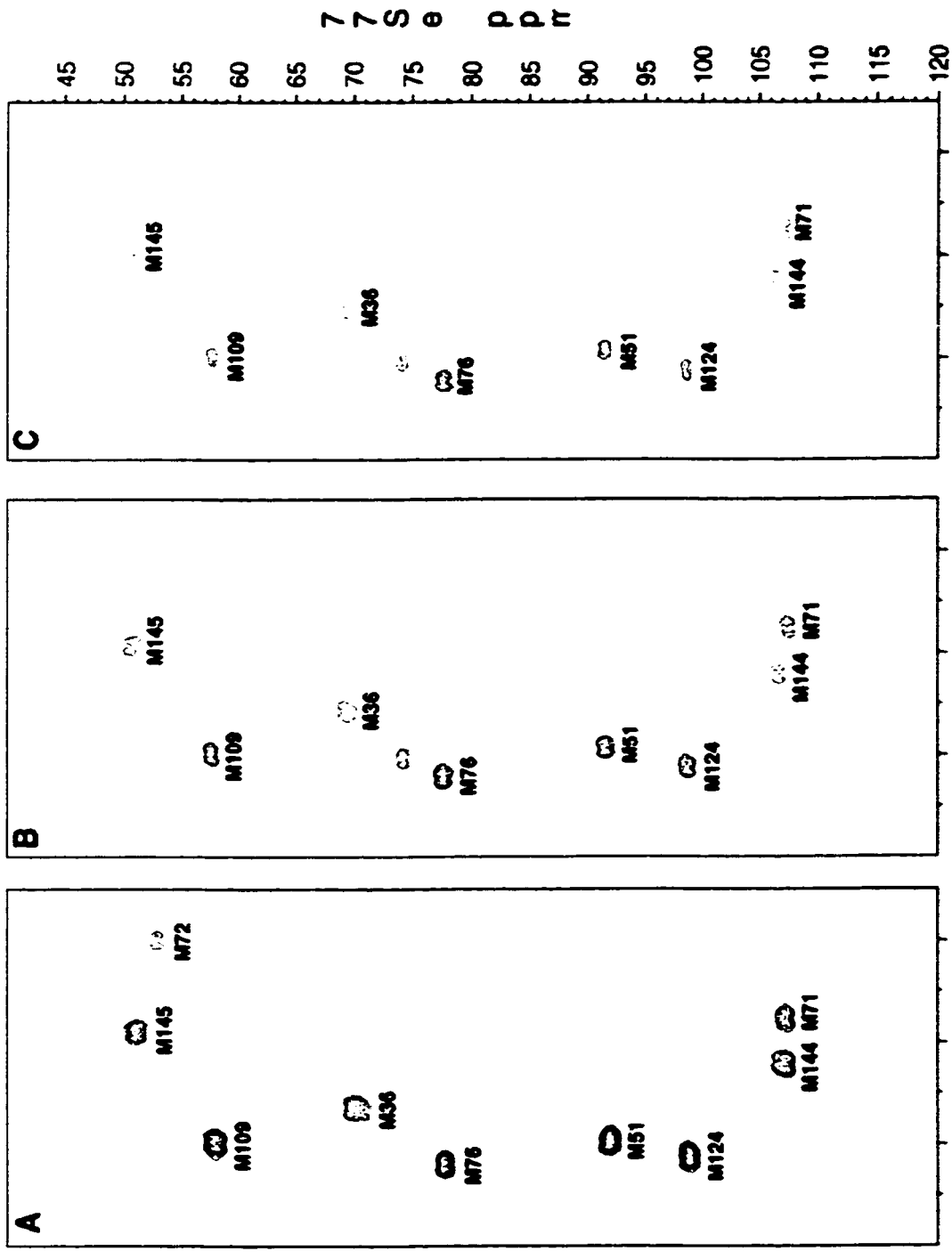

Figure 5.9 1H,77Se HMBC spectra of the titration of SeMet labelled CaM with (A) 0 equivalent, (B) 1 equivalent, and (C) 1.5 equialent of cisplatin.

titration on methyl-^{13}C-Met labeled CaM.

Circular Dichroism of Cisplatin Modified CaM

Circular dichroism (CD) spectroscopy was employed in this study to investigate the effects of cisplatin on the secondary structure of CaM and its bound peptides. CaM is largely an α-helical protein whose CD spectrum has

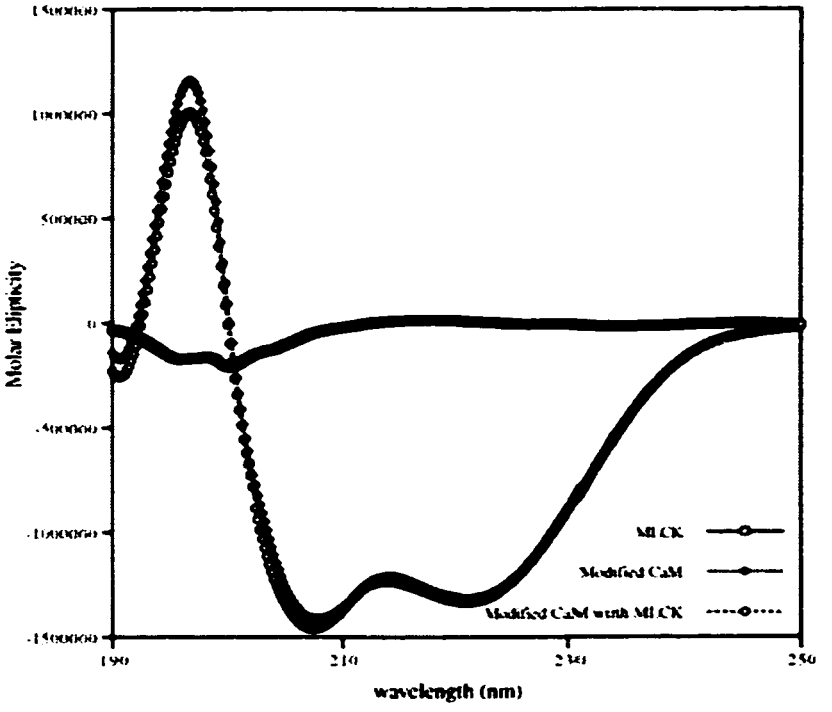

Figure 5.10 Far-UV CD spectra of the mixture of MLCK peptide to cisplatin-modified CaM. No signal enhancement is observed in the presence of the peptide.

characteristic α-helical peaks, containing two negative bands at 222 nm and 208 nm, respectively, and a positive band at 195 nm (see Chapter 2). CD spectra of CaM modified by different number of cisplatin molecules were recorded. Bands from CD spectra of modified CaM have the same shape and characteristics as free CaM (data not shown), suggesting that the modification of cisplatin does not significantly change the secondary structure of CaM. This result was somewhat expected since cisplatin interacts with CaM through its Met side chains, which has little effect on the protein's backbone conformation. Thus, the CD spectra of CaM are not altered by the binding of cisplatin. CD experiments can also be used to study the peptide binding ability of CaM. A free target peptide is virtually unstructured in solution so that it does not have strong CD signals. When the peptide is bound to CaM, it adopts an α-helical structure which significantly enhances the α-helical CD signals at 208 and 222 nm (Ouyang & Vogel 1998, also see Chapter 2). However, for cisplatin-modified CaM, the addition of MLCK peptide did not have any effect on the CD signals, suggesting that peptide-binding to CaM did not occur (Figure 5.10). These data are in agreement with the outcome of the fluorescence experiments.

Discussion

Cisplatin is a potent anticancer drug that has been extensively used for chemotherapy treatment. The antitumor mechanism of platinum drugs is believed to be related to their capacity to bind to DNA, which has been the

focus of many investigations (Rosenberg 1985, Pinto & Lippard 1985). Cisplatin can cause intra- and inter-strand crosslinks in DNA, which destabilizes the DNA structure and leads to cell cycle arrests or cell death (Gelasco & Lippard 1998, Bauer *et al.* 1998, Sánchez-Perez *et al.* 1998, Zlatanova *et al.* 1998). Recently, much attention has been paid to the study of the mechanism of the drug-resistance found in many tumor cell lines (Zamble & Lippard 1995, Gosland *et al.* 1996, Potapova *et al.* 1997, Patrik & Turchi 1998, Li *et al.* 1998). The major drawbacks of the platinum anticancer drugs are their severe side effects; these are the result of the binding of the drug to many cellular components other than DNA. Cisplatin has been found to have a particularly high reactivity with sulfur-containing amino acids, which makes proteins with surface-exposed Met or Cys side chains potential targets for cisplatin modification (Grochowski & Samochocka 1992, Norman *et al.* 1992, Jiang *et al.* 1996, Jiang *et al.* 1997, Heudi 1998). CaM is an important Ca^{2+} regulatory protein that falls into this category. Jarve and Aggarwal (1997) proposed that inhibition of CaM through cisplatin-modification could play a major role in stomach distention, one of cisplatin's side effects. The motility of stomach and pyloric sphincter smooth muscle depends on acetylcholine release and nitric oxide (NO) synthesis; and both acetylcholine release and NO synthesis are regulated by CaM. Consequently, these authors suggested that cisplatin can cause stomach distention by inhibiting CaM activity (Jarve & Aggarwal 1997).

In this work, we have studied the direct interaction between CaM and

cisplatin, as well as its analog, carboplatin. Fluorescence and CD experiments clearly demonstrated a reduced substrate-binding ability for modified CaM. As little as one equivalent of cisplatin already displayed a significant effect on CaM. These results support the suggestion of Jarve and Aggarwal (1997) that cisplatin interacts with CaM directly thereby inhibiting its activity. Carboplatin, a related platinum anticancer drug, also shows inhibition of CaM's activity, but not as pronounced as cisplatin under the same experimental conditions. This difference was not totally unexpected, as carboplatin has also been found to have a lower reactivity with DNA than cisplatin (Reedijk 1996). Carboplatin's reduced reactivity with CaM could be one of the contributing factors to the reduced toxicities of this drug compared to cisplatin.

Mass spectrometry was used in our study to investigate the mode and extent of binding of cisplatin to CaM. Mass spectrometry provided us with the most direct method to detect cisplatin-modified products. As shown in Figure 5.3, cisplatin binds to ME, a single Met-containing peptide. Cisplatin-modified peptide tends to lose several of its platinum-bound ligands, therefore, there are several peaks in the spectrum. Cisplatin has two labile chloride ligands, suggesting that it can simultaneously bind more than one Met residues. Indeed, cisplatin could bind two ME peptides simultaneously in the presence of excess peptide (Figure 5.4). Cisplatin-modified CaM can also be detected by mass spectrometry. Groups of peaks representing CaM modified by a different number of cisplatin molecules were observed in the

mass spectra, although the random loss of the platinum ligands made the analysis a little complicated (Figure 5.5). Nevertheless, our mass spectrometry results unambiguously demonstrated that cisplatin can modify CaM by direct binding. More interestingly, each CaM molecule seems to bind a maximum of nine molecules of cisplatin even in the presence of a large excess of the drugs (Figure 5.5C). Since there are nine Met residues in CaM, this result implies that Met residues provide the cisplatin binding sites on CaM, and that all Met residues can be modified.

The binding of cisplatin to Met residues through the formation of Pt-S bonds was studied by absorbance spectroscopy. When CaM was modified by cisplatin, its absorption spectrum changed drastically. The increased absorbance below 280 nm indicated that the drug binds to CaM through Pt-S bonds. The binding of cisplatin to Met residues explains the inhibition of CaM by the drug. CaM is a dumbbell-shaped protein that contains two lobes. Upon binding Ca^{2+} ions, each domain exposes a large hydrophobic patch on the protein surface. These hydrophobic surfaces are the major interface for CaM and substrate protein interactions (O'Neil & DeGrado 1990, Vogel 1994, Ikura 1996). Met residues play a significant role in target-recognition since they make up to 46% of the hydrophobic surfaces on Ca^{2+}-CaM (Zhang *et al.* 1995a). If cisplatin binds to Met residues, its large platinum atom will prevent Met sidechains from contacting the target protein. Moreover, since the ligands on platinum are labile, such a modification on Met residues will introduce charges into the hydrophobic patches which can drastically disturb

the hydrophobic interactions between CaM and its substrates.

Methyl-^{13}C-Met and SeMet labeled CaM were titrated by cisplatin and carboplatin to study the binding of these drugs to the Met side chains in more detail. The titration could not be followed reliably beyond two equivalents because of severe line broadening. Such severe line broadening of ^{1}H and ^{13}C NMR signals has also been observed in NMR studies concerning interaction of cisplatin and glutathione (Appleton *et al.* 1989, Berners-Price & Kuchel 1990). These authors suggested that the line broadening of glutathione signals may be due to overlap of resonances from coordinated glutathione molecules in slightly different environments, and a consequence of exchange at an intermediate rate (on the NMR time scale) between different coordinated glutathione environments (Berners-Price & Kuchel 1990). Appleton *et al.* (1989) attributed the broadened signal in the complex *cis*-$[\{(NH_3)_2Pt(u\text{-}SG)\}_2]^{2+}$ to an interconversion of the two isomers of the S-bridged dimer via inversion at the S atom. The line broadening in our NMR experiments could be caused by similar processes. The cisplatin molecule is still reactive after binding to one Met side chain. For example, it can bind another Met side chain which can cause intermolecular crosslinks between two ME peptides (Figure 5.4). In the case of CaM, many Met residues are located very close together on the surface of the protein, for instance, the sulfur atoms of M71 and M72 are separated by only 5 Å in the structure. Thus it is possible that cisplatin can bind simultaneously to more than one Met side chain in CaM leading to intramolecular crosslinks. Cisplatin can

also react with other atoms in the protein after binding to Met side chains. Shi *et al.* (1999) recently reported structures of cisplatin-modified dipeptides. They noted that the N atom from the peptide bond amide group was reactive to Pt(II) under some circumstances. Such a reaction could also be possible in proteins since Met side chains are very flexible. In addition, Pt(II) is capable of binding to the O atom from peptide bond carbonyl groups. Although the Pt-O interaction is weaker than other reactions mentioned, it could be one of the sources for line broadening. Such additional reactions would give rise to the "loss" of NH_3 and OH ligands seen by mass spectrometry. If the reaction with another atom happens after cisplatin binds to one Met residue, it constrains the flexibility of the Met side chain, which would result in two possible orientations of the methyl group of the side chain (Grochowski & Samochocka 1992). Therefore, each of the nine Met residues in CaM could have many different coordinated environments upon cisplatin binding. Intermediate exchange rate between these different environments would contribute further to line broadening in our NMR experiments. Be that as it may, our experiments demonstrate that the resonances from the C-terminal domain of CaM were affected first by the addition of the platinum drugs, suggesting that cisplatin and carboplatin bind preferentially to the C-terminal lobe of the protein. Although, the reason for such domain preference is presently unclear, several other compounds also show a higher affinity for the C-domain when binding to CaM, such as the neurohormone, serotonin, for example (Ouyang & Vogel 1998a, also see Chapter 4).

In summary, our study unambiguously indicates that covalent interactions between CaM and the platinum drugs are formed under relatively benign conditions; and that such modifications by the drugs can cause inhibition of CaM's capacity to activate target proteins; cisplatin and carboplatin form Pt-S bonds with Met sidechains, and all nine Met residues of CaM are susceptible to the modification; clearly, cisplatin and carboplatin have higher affinity for the C-terminal lobe of CaM. It is unclear what the intracellular concentration of cisplatin is during the cancer treatment. However, it does appear to reach DNA in the nucleus. In future work, it needs to be demonstrated that these reactions that can occur *in vitro* also play a role *in vivo*, before we can conclude that reactions with CaM contribute to the toxicity of these platinum anticancer drugs.

Chapter 6

Calmodulin-Melittin Interactions: An Half Molecule Approach Reveals Two Opposite Binding Orientations

Abstract

Melittin, a bee venom peptide, can form an amphipathic α-helical structure. It has been shown to bind to calcium-saturated calmodulin (CaM) with high affinity, and has frequently been used as a model peptide to mimic CaM-binding domains from selected CaM-activated target proteins. Here we have used a variety of biophysical techniques to study the interaction of CaM with melittin. In addition, we used half molecules of the dumbbell-shaped CaM [TR1C (1-75) and TR2C (78-148)] as well as the melittin fragments [MLN (1-14) and MLC (14-26)] to dissect sites of interaction between these two intact molecules. Cadmium-113 NMR was used to analyze the response of the four bound metal ions of CaM to addition of peptide(s); the appearance of minor peaks suggested that two distinct protein peptide complex conformers existed. Cadmium-113 and proton NMR experiments showed that MLC has a higher affinity than MLN for both the C- and N-terminal lobes of CaM. Far-UV circular dichroism studies revealed that CaM and its isolated lobes induce the formation of α-helical structure in bound melittin, MLC and MLN. Near-UV CD data indicated that the unique Trp19 residue of melittin does not enter the hydrophobic clefts of CaM in a same manner as typical target peptides such as those derived from myosin light chain kinases. Nevertheless, blue shifts and Stern-Volmer quenching data obtained in

target peptides such as those derived from myosin light chain kinases. Nevertheless, blue shifts and Stern-Volmer quenching data obtained in fluorescence experiments of the Trp19 residue, as well as photochemically induced dynamic nuclear polarization NMR experiments, show that the Trp enters a hydrophobic environment and is shielded from solvent upon binding to CaM. Taken together our data suggest that melittin can bind to CaM with two distinct orientations, with the C to C alignment preferred over the N to C orientation. In addition the complex is distinct from other CaM targets with known structures because of a different interaction of CaM with the Trp19 residue of melittin.

Introduction

Melittin is a 26-residue toxic peptide from the venom of the European honey bee *Apis mellifera* which has significant hemolytic activity (for reviews, see Habermann, 1972; Dempsey, 1990). The three-dimensional structure of melittin has been studied extensively, both by X-ray crystallography and by nuclear magnetic resonance (NMR) spectroscopy (Dempsey, 1990). Melittin is a random coil peptide in aqueous solution at low ionic strength, but it forms a monomeric α-helix in organic solvents such as methanol or a tetrameric α-helical bundle in aqueous solutions of high ionic strength (Dempsey, 1990). In the latter case, melittin forms an amphiphilic α-helix with a 20° to 60° bend in the middle of the peptide caused by the presence of the Pro14 residue. The amphiphilic nature of melittin makes it a good model peptide to study calmodulin-target peptide interactions.

Calmodulin (CaM) is a ubiquitous Ca^{2+}-regulatory protein which can

calmodulin-target peptide interactions.

Calmodulin (CaM) is a ubiquitous Ca^{2+}-regulatory protein which can bind and activate more than 80 different target proteins (for reviews, see Vogel, 1994; Crivici & Ikura, 1995; Vogel & Zhang, 1995; Ikura, 1996; Zhang & Yuan, 1998). CaM adopts a dumbbell-shaped structure with two lobes connected by a central linker region (Babu *et al.* 1988; Kuboniwa *et al.* 1995; Zhang *et al.* 1995a). Each lobe of CaM contains two helix-loop-helix, so-called EF-hand, Ca^{2+}-binding motifs with the central part of the two Ca^{2+}-binding loops forming a small β-sheet. Upon binding of two Ca^{2+} ions, each lobe of CaM exposes a Met-rich hydrophobic patch for target protein binding (Yuan *et al.* 1999). Tryptophan or other large hydrophobic residues of various target proteins enter these hydrophobic methionine-lined clefts, when these proteins bind to CaM (Meador *et al.* 1992, 1993; Ikura, 1992; Yuan *et al.* 1998; Weljie & Vogel, 2000). The CaM-binding sequence in typical target proteins usually contain a stretch of ~20 amino acids which has the potential to form a basic amphiphilic α-helix upon binding to Ca^{2+}-CaM (O'Neil & DeGrado, 1990; Ikura *et al.* 1992; Meador *et al.* 1992, 1993; Zhang *et al.* 1994a).

Melittin is a good model peptide for studying CaM-target protein interactions. It is rather hydrophobic and contains five positively charged residues and no negatively charged residues (Table 6.1). In addition it is capable of forming an amphiphilic α-helical structure (Dempsey, 1990). The interaction between Ca^{2+}-CaM and intact melittin has already been studied by various spectroscopic and biochemical techniques (Comte *et al.*

Maulet & Cox, 1983; McDowell *et al.* 1985; Seeholzer *et al.* 1986, 1987; Caday & Steiner, 1986; Steiner *et al.* 1986; Sanyal *et al.* 1988; Kataoka *et al.* 1989; Itakura & Iio, 1992; Fisher *et al.* 1994; Liu *et al.* 1994; Scaloni *et al.* 1998). Melittin can form a 1:1 complex with Ca^{2+}-CaM (Comte *et al.* 1983), as recently confirmed by electrospray mass spectrometry (Veenstra *et al.* 1998). It forms an α-helix upon binding to Ca^{2+}-CaM, as demonstrated by CD difference spectroscopy (Maulet & Cox, 1983; McDowell *et al.* 1985) and isotope-edited infrared spectroscopy (Fabian & Vogel, unpublished observations; Zhang *et al.* 1994a). Proton NMR studies have shown that the binding of melittin to Ca^{2+}-CaM involves both lobes of Ca^{2+}-CaM (Seeholzer *et al.* 1986). Upon binding to melittin, the overall structure of the Ca^{2+}-CaM-melittin complex becomes globular, in contrast to the extended dumbbell-shape of Ca^{2+}-CaM in solution (Kataoka *et al.* 1989). The binding orientation of melittin with respect to Ca^{2+}-CaM has been studied primarily by fluorescence spectroscopy and proteolysis and crosslinking studies (Steiner *et al.* 1986; Sanyal *et al.* 1988; Itakura & Iio, 1992; Scaloni *et al.* 1998). These studies suggested that the C-terminal end of melittin probably binds to the C-lobe of Ca^{2+}-CaM, which is in the opposite orientation of the well characterized CaM-binding domains of myosin light chain kinase and CaM-dependent protein kinase II (Ikura *et al.* 1992; Meador *et al.* 1992, 1993). Since there is currently no high-resolution structure available for the Ca^{2+}-CaM-melittin complex, we decided to further study the Ca^{2+}-CaM-melittin interaction using a

CaM and from melittin, and we studied their interactions by cadmium-113 and proton NMR spectroscopy, as well as near-UV and far-UV circular dichroism (CD) and fluorescence spectroscopy.

Cadmium-113 NMR spectroscopy is an excellent method to study metal ions bound to Ca^{2+}-binding proteins (Vogel & Forsén, 1986; Summers, 1988; Coleman, 1993; Öz *et al.* 1998; Clarke & Vogel, 2000). Cadmium-113 is a nucleus with a magnetic spin 1/2 and a natural abundance of 12.26%. The Cd^{2+} ion has an ionic radius of 0.97 Å, which is very close to that of the Ca^{2+} ion (0.99 Å). The chemical shift of $^{113}Cd^{2+}$ is very sensitive to its ligand residues and the overall structure of the protein, and ^{113}Cd NMR has been used extensively to study calcium-binding proteins, and their complexes. X-ray structures of Cd^{2+}-substituted calcium-binding helix-loop-helix proteins, such as parvalbumin and troponin C have been solved and these are nearly identical to the structures of the Ca^{2+}-saturated proteins (Swain *et al.* 1989; Rao *et al.* 1996). Proton NMR titration experiments with Ca^{2+} and Cd^{2+} reveal identical conformational changes in intact CaM for the two metal ions (Vogel & Forsén, 1986). As a classical helix-loop-helix calcium-binding protein, CaM has already been studied by ^{113}Cd NMR spectroscopy (Forsén *et al.* 1980; Andersson *et al.* 1983a; Thulin *et al.* 1984; Linse *et al.* 1986; Ikura *et al.* 1989; Ohki *et al.* 1993; Zhang *et al.* 1995b; Brokx & Vogel, 2000; Clarke & Vogel, 2000). Cadmium-113 NMR has also been used to study the calcium-binding sites and structural changes in other calcium-binding proteins such as parvalbumin (Drakenberg *et al.* 1978; Bjornson *et al.* 1985), troponin C (Ellis *et al.* 1984, 1988; Drakenberg *et al.* 1987),

et al. 1984, 1988; Drakenberg *et al.* 1987), calbindin D_9K (Vogel *et al.* 1995), bovine prothrombin (Kingsley Hickman *et al.* 1986), proteolytic enzymes such as trypsin (Adebodun & Jordan, 1989), as well as lactalbumin and related calcium-binding lysozymes (Berliner *et al.* 1983; Aramini *et al.* 1995). Collectively these studies have shown that the large ^{113}Cd chemical shift scale provides a very sensitive monitor of the protein structural changes.

Here, we have studied the interaction between Ca^{2+}-CaM and melittin. We generated the half-CaM molecules TR1C (1-75) and TR2C (78-148) by limited trypsin proteolysis and expression of a truncated gene (Fabian *et al.* 1996), and we chemically synthesized the half-melittin peptides MLN (1-14) and MLC (14-26) (Table 6.1). Cadmium-113 and proton NMR spectroscopy were employed to determine the orientation, relative affinity, and the presence of multiple conformers using the above half molecules, as well as the intact

```
          *             *
MEL  GIGAVLKVLTTGLPALISWIKRKRQQ
             #           #

MLN  GIGAVLKVLTTGLP-NH2

MLC              ac-PALISWIKRKRQQ
```

Table 6.1 Primary structures of MEL, MLC and MLN peptides. (*indicated proposed anchoring residues, and # indicates another set of potential anchoring residues similar to the CaMKII peptide)

CaM protein and the complete melittin peptide. Far-UV CD studies were

CaM protein and the complete melittin peptide. Far-UV CD studies were used to show induction of α-helical structure upon the binding of the peptides to CaM and its fragments. In addition, near-UV CD studies, fluorescence spectroscopy and photo-CIDNP NMR were used to study the environment of the Trp19 residue of melittin in the complexes. Photo-CIDNP NMR provides a unique tool to study surface exposure of aromatic residues in proteins and their complexes (Kaptein, 1982;Vogel, 1983). Our studies confirm that melittin binds mostly to Ca^{2+}-CaM in a parallel orientation, but that a second N to C orientation is possible. Moreover our results show that the Trp residue of MEL interacts in an unusual fashion with CaM, compared to other target peptides.

Materials and Methods

Materials

CaM was expressed in *E. coli* from a plasmid harboring a synthetic mammalian CaM gene, and the purification of CaM was as described before (Waltersson *et al.* 1993; Zhang & Vogel, 1993). The N-lobe of CaM (TR1C, residues 1-75) and the C-lobe of CaM (TR2C, residues 78-148) were generated and purified using published procedures (Fabian *et al.* 1996). Melittin was obtained from Sigma Chemical Company, and it was further purified to >95% purity by reverse phase HPLC. The two halves of the melittin peptide, the N-terminal half (MLN) and the C-terminal half (MLC) peptides were commercially synthesized at the Core Facility for Protein/DNA Chemistry at Queens University, Kingston, Canada. The peptide sequence for MLN is GIGAVLKVLTTGLP-NH_2, and the MLC

peptides were commercially synthesized at the Core Facility for Protein/DNA Chemistry at Queens University, Kingston, Canada. The peptide sequence for MLN is GIGAVLKVLTTGLP-NH_2, and the MLC peptide sequence is Ac-PALISWIKRKRQQ (Table 6.1). The acetyl and carboxamide group were introduced to remove end charges that are not present in intact MEL. The purity of both peptides was >95%, as judged by analytical HPLC, mass spectrometry and one dimensional ^1H NMR spectroscopy. The concentration of CaM was calculated using an extinction coefficient $\Delta\varepsilon_{276/320}^{1\%}$=1.8. The concentrations of TR1C and TR2C were determined using molar extinction coefficient ε_{258} =1073 M^{-1} cm^{-1} and ε_{276}=2666 M^{-1} cm^{-1}, respectively, which were obtained from quantitative amino acid analysis. The different wavelength used for the TR1C peptide reflects the fact that it possesses no Tyr residues, leaving Phe as the only aromatic residue. The concentrations of stock solutions of MLC and MEL were determined spectrophotometrically from the Trp absorbance, while that of MLN required the use of quantitative amino acid analysis.

Cadmium-113 NMR Spectroscopy

Cadmium-113 NMR spectra were acquired on a Bruker AM400 widebore NMR spectrometer equipped with a 10 mm broadband probe. All spectra were recorded at a frequency of 88.75 MHz. Isotopically enriched ^{113}CdO (94.8%) was purchased from MSD Isotopes. A 100 mM stock solution of $^{113}Cd(ClO_4)_2$ (pH≈1 in D_2O) was used for the preparation and titration of the samples. All ^{113}Cd NMR samples were prepared in 25% (v/v) D_2O, 100 mM KCl, 20 mM Tris, pH 7.50±0.05 (not corrected for the isotope

of $^{113}Cd(ClO_4)_2$ (pH≈1 in D_2O) was used for the preparation and titration of the samples. All ^{113}Cd NMR samples were prepared in 25% (v/v) D_2O, 100 mM KCl, 20 mM Tris, pH 7.50±0.05 (not corrected for the isotope effects). The ^{113}Cd NMR acquisition parameters were as follows: a 45° flip angle, acquisition time 0.14 s, relaxation delay 0.5 s or 5 s, sweep width 30 KHz, 8 K data points, and 70,000 scans. The temperature of all experiments was 298° K. The total acquisition time for each 0.5 s delay experiment was 12 h and 40 min. Each free induction decay (FID) was zero-filled once and an exponential line broadening of 30 Hz was applied prior to Fourier transformation. All ^{113}Cd spectra were referenced to external 100 mM $^{113}Cd(ClO_4)_2$ in D_2O.

Proton NMR Spectroscopy

One-dimensional (1D) ^1H NMR spectra were acquired on a Bruker AMX500 NMR spectrometer equipped with a 5 mm broadband probe. All NMR samples contained ~ 0.5 mM CaM, TR1C or TR2C, 10 mM $CaCl_2$, 100 mM KCl in 99.9% D_2O, pH (pD) 7.50±0.05 (not corrected for the isotope effects). The ^1H NMR acquisition parameters are as follows: a relaxation delay of 1.5 s, sweep width 6024 Hz, 8 K data points, and 128 scans. The temperature of all experiments was 298 K. Each FID was zero-filled once and an exponential line broadening of 1 Hz was applied prior to Fourier transformation. Proton NMR spectra were referenced to sodium 3-(trimethylsilyl)-propionate-2,2,3,3-d_4 as 0 ppm.

Photo CIDNP

Photo CIDNP

Photo CIDNP experiments were used to detect solvent exposed Tyr, His, and Trp residues (Kaptein 1982). Photo-CIDNP spectra of melittin, CaM, and the melittin-CaM complex were recorded for protein or peptide samples (1 - 2 mM) containing 0.4 mM flavin dye. The same buffer as used for proton NMR experiments was used. Irradiation of the sample was done through a fibre optic cable from an argon ion laser (Spectra Physics model 164), using an 1 sec irradiation time. 16 scans were normally acquired, as photo bleaching of the dye prevented further aquisitions. Alternating light and dark free induction decays were collected. After Fourier transformation and subtraction these gave the photo-CIDNP difference spectra.

Circular Dichroism

CD experiments were performed on a Jasco-715 spectropolarimeter. The sample buffer for these experiments contained 10 mM Tris-Cl (pH 7.4), 100 mM KCl, and 1 mM $CaCl_2$. All samples were incubated at room temperature for at least 30 minutes before the spectrum was acquired. Far-UV CD spectra were recorded between 200 and 250 nm, using a cell path length of 1 mm. The protein/peptide concentration used for far-UV experiments was 0.01 mM. Near-UV CD spectra were recorded from 250 nm to 320 nm, using a cell path length of 10 mm. The protein/peptide concentration used for near-UV CD experiments was 0.05 mM. Each spectrum was the average of twenty scans, and smoothing of the base-line-corrected spectra was done by digital filtering.

corrected spectra was done by digital filtering.

Fluorescence Spectroscopy

Fluorescence spectroscopy experiments were performed on a Hitachi F-2000 fluorescence spectrophotometer. A peptide/protein concentration of 10 mM was used. Samples were incubated at room temperature for at least 30 minutes before the spectrum was recorded. The excitation and emission bandpasses were 1 nm, and the emission spectra scanning was done at 60 nm/min with a 1 cm path length cuvette. The excitation wavelength was set at 297 nm, and emission spectra were recorded in the range 300 - 450 nm. The buffer used for these experiments was the same as in the CD experiments. For fluorescence quenching experiments, the fluorescence intensity at the emission peak was recorded right after microliter amounts of 4 M acrylamide stock solution were added into the sample. Acrylamide was titrated into the sample from 0 to 0.2 M.

The fluorescence quenching data were analyzed according to Stern-Volmer equation (Eftink & Ghiron 1976):

$$F_0/F=1 + Ksv[Q]$$

where F_0 and F are the fluorescence intensities in the absence and the presence of quencher (Q), respectively. Ksv is the Stern-Volmer quenching constant, which is a measure for the accessibility of the tryptophan to acrylamide. This Ksv was calculated as the slope of the Stern-Volmer plot.

Results

Cadmium-113 NMR of the Interaction Between Melittin and CaM

Results

Cadmium-113 NMR of the Interaction Between Melittin and CaM

We first studied the interaction between MEL and CaM by ^{113}Cd NMR spectroscopy. As shown in Figure 1A, CaM saturated with four Cd^{2+} ions displays two ^{113}Cd NMR resonances at -88.4 ppm and -114.4 ppm, respectively (Figure 6.1). These two signals originate from the two high-affinity Ca^{2+}-binding sites in the C-lobe of CaM, while the signals from the two weak-affinity Ca^{2+}-binding sites in the N-lobe of CaM are in fast exchange with free Cd^{2+} (Andersson *et al.* 1983b; Thulin *et al.* 1984), or alternatively involved in a conformational exchange process, involving the N-terminal domain of CaM (Forsén *et al.* 1986). When MEL was titrated gradually into the Cd^{2+}_4-CaM sample, the two signals from the C-terminal domain of CaM decreased and a new set of four peaks appeared at the same time (Figure 6.1). No chemical shift changes were observed for the resonances in either set, which indicates that these two groups of resonances display slow exchange on the ^{113}Cd NMR time scale. This is consistent with the nanomolar binding affinity reported for the MEL and Ca^{2+}-CaM complex (Comte *et al.* 1983). The four resonances in the 1:1 complex of MEL-CaM originate from the four different Cd^{2+} ions in the metal ion-protein-peptide complex. The integration of these four peaks indicates that their total intensity is less than two times the area of the two peaks in the Cd^{2+}_4-CaM spectra. This could be due to the relaxation delay in the experiments not being long enough to allow full relaxation

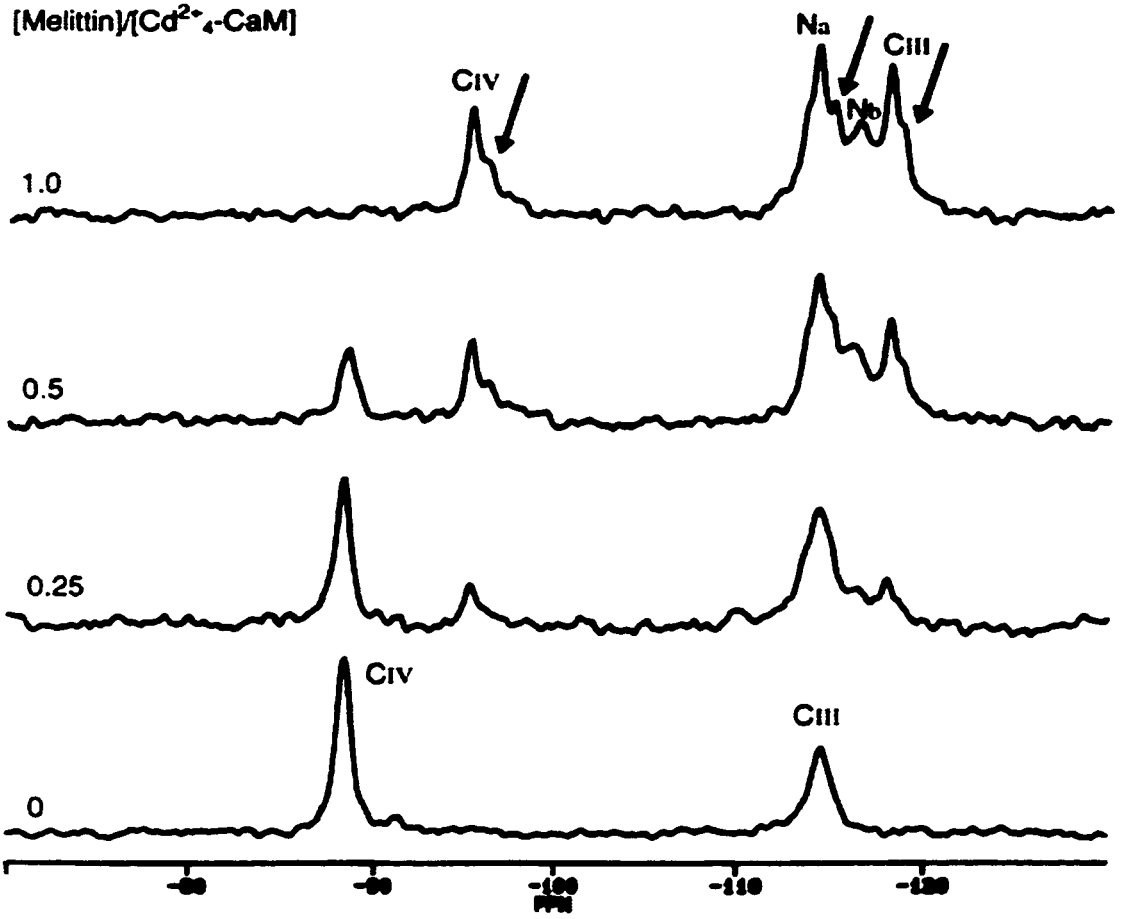

each spectrum.

1995b). Therefore, we also performed the same experiments with a 5 s relaxation delay, and the area under the four resonances in the MEL-Cd^{2+}_4-CaM complex is close to two times that of the two resonances in the Cd^{2+}_4-CaM (data not shown). This behavior was very similar to other CaM-peptide complexes that we have studied before (Zhang *et al.* 1995b). In the top panel of Figure 6.1 several minor peaks are also indicated by arrows.

CaM (data not shown). This behavior was very similar to other CaM-peptide complexes that we have studied before (Zhang *et al.* 1995b). In the top panel of Figure 6.1 several minor peaks are also indicated by arrows. These indicate the presence of a distinct second form of the MEL-CaM complex. Spectral simulations suggest that this second form is present at 15-20% of the total.

We also carried out a ^{113}Cd NMR titration with a sample containing MEL and apo-CaM. During the titration, the four Cd^{2+} resonances of the Cd^{2+}_4-CaM-MEL complex increased simultaneously in intensity up until four equivalent Cd^{2+} ions were added (data not shown). This titration experiment indicates that the four Cd^{2+} binding sites in CaM possess a similar Cd^{2+}-binding affinity in the presence of the MEL peptide, thus the presence of MEL induces cooperativity in Cd^{2+} binding between the N- and C-lobes of CaM. The same experiments have been conducted before for the CaM-binding domain peptide derived from myosin light chain kinase and neuronal nitric oxide synthase (Linse *et al.* 1986; Ikura *et al.* 1989; Zhang *et al.* 1995b), giving similar results.

Cadmium-113 NMR of the Interactions Between MEL and TR1C or TR2C

Next, we conducted titration experiments with MEL and either TR1C or TR2C. As shown in Figure 6.2A, no resonances were visible in the Cd^{2+}_2-TR1C sample due to exchange broadening processes (Andersson et al 1983b; Forsén *et al.* 1986). When MEL was titrated into this solution, two ^{113}Cd NMR signals appeared at -113.6 ppm and -117.2 ppm, respectively

These two resonances can be attributed to the two Cd^{2+} ions bound to the two metal binding sites in TR1C in the MEL-TR1C complex. Clearly the binding of MEL to TR1C slows down the off rate of Cd^{2+} bound to TR1C, thus increasing its Cd^{2+}-binding affinity to TR1C. Alternatively it reduces the conformational exchange rate between two TR1C conformers (Forsén *et al.* 1986).

As expected from the results obtained with intact CaM the titration of MEL to $Cd^{2+}{}_2$-TR2C showed slow exchange on the ^{113}Cd NMR time scale, two new resonances appeared at -92.2 ppm and -117.3 ppm, respectively (Figure

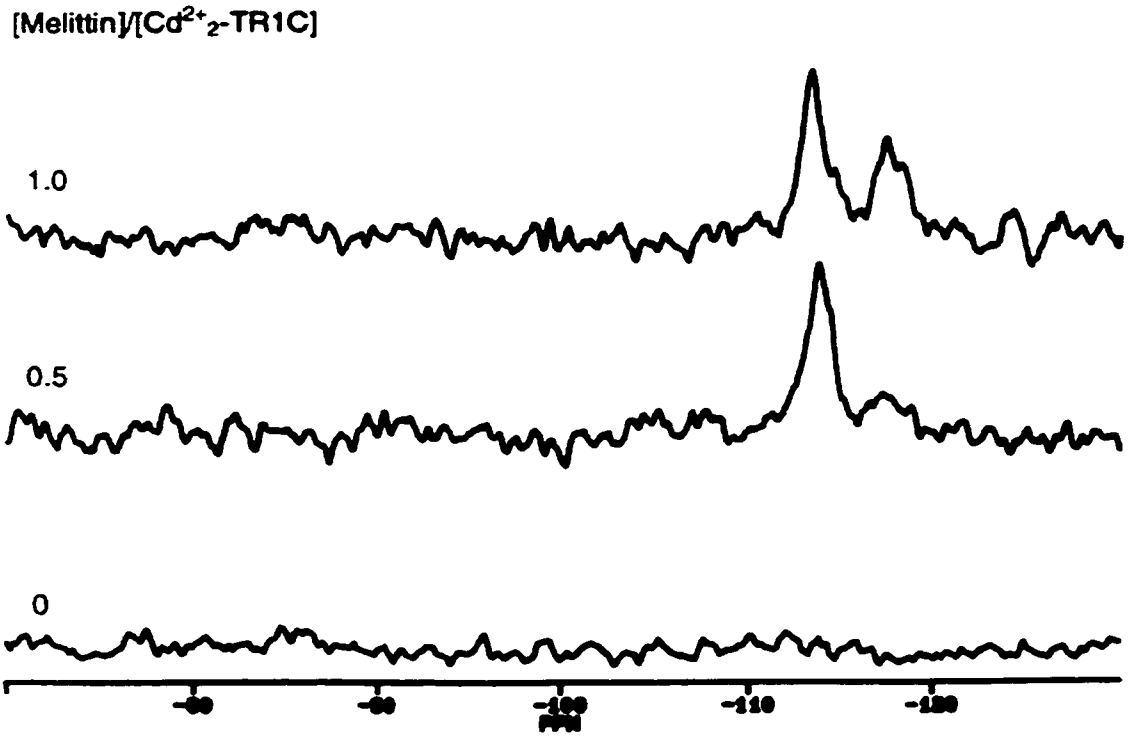

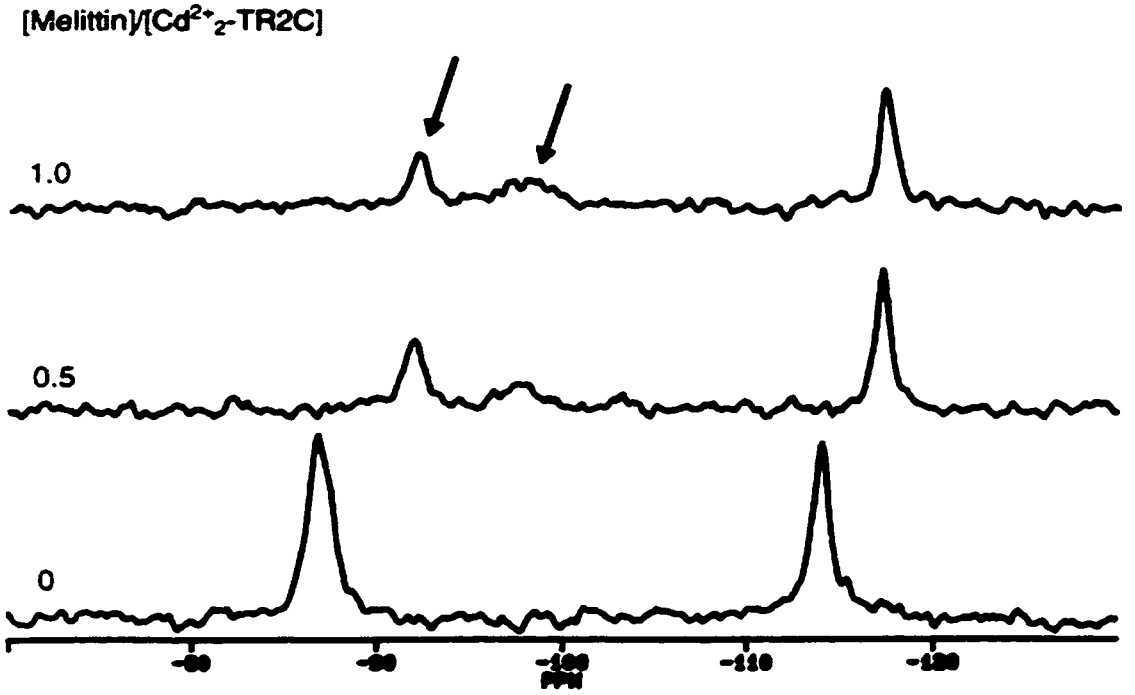

Figure 6.3 1D ^{113}Cd NMR spectra of the titration of melittin on Cd^{2+}_2-TR2C.

6.3). It was obvious that two TR2C fragments can bind simultaneously to one MEL molecule, since the two resonances from Cd^{2+}_2-TR2C disappeared completely after only 0.5 equivalent of MEL was added. The two signals at -92.2 ppm and -117.3 ppm most probably originate in the two Cd^{2+}-binding sites in TR2C bound to the C-half of MEL, and the broad resonance at -97 ppm likely represents the Cd^{2+} ions in the second TR2C fragment bound to the N-half of MEL, because the C-half of MEL (MLC) has a higher binding affinity to TR2C than the N-half of MEL (MLN) (see below).

We decided to chemically synthesize the half melittin molecules

affinity to TR2C than the N-half of MEL (MLN) (see below).

We decided to chemically synthesize the half melittin molecules MLN and MLC to further study the interaction between MEL and CaM. Titration of Cd^{2+}_4-CaM with either MLN or MLC demonstrated that each CaM molecule can bind up to two molecules of either MLN or MLC, with the possibility that each lobe of CaM binds one molecule of MLN or MLC. However, the spectra acquired were complicated and can not be explained straightforwardly (data not shown). Therefore we decided to study the interaction between MLN and MLC with the separated lobes of CaM, TR1C and TR2C.

Cadmium-113 NMR Studies of the Interaction Between MLN and TR1C or TR2C

The MLN peptide is composed of the first 14 residues of MEL and was used to titrate both TR1C and TR2C, each in the presence of two equivalents of Cd^{2+} ions. No resonance was observed in the MLN-Cd^{2+}_2-TR1C complex, suggesting a relatively weak binding nature between these two components. We also did not observe any resonances when the acquisition temperature was lowered to 283 K (data not shown).

When the MLN peptide was titrated into Cd^{2+}_2-TR2C, two signals from Cd^{2+}_2-TR2C move, indicating that the binding of the peptide is in the fast exchange regime on the ^{113}Cd NMR time scale (data not shown). The two signals have chemical shifts at -92.7 ppm and -117.2 ppm, respectively, in the

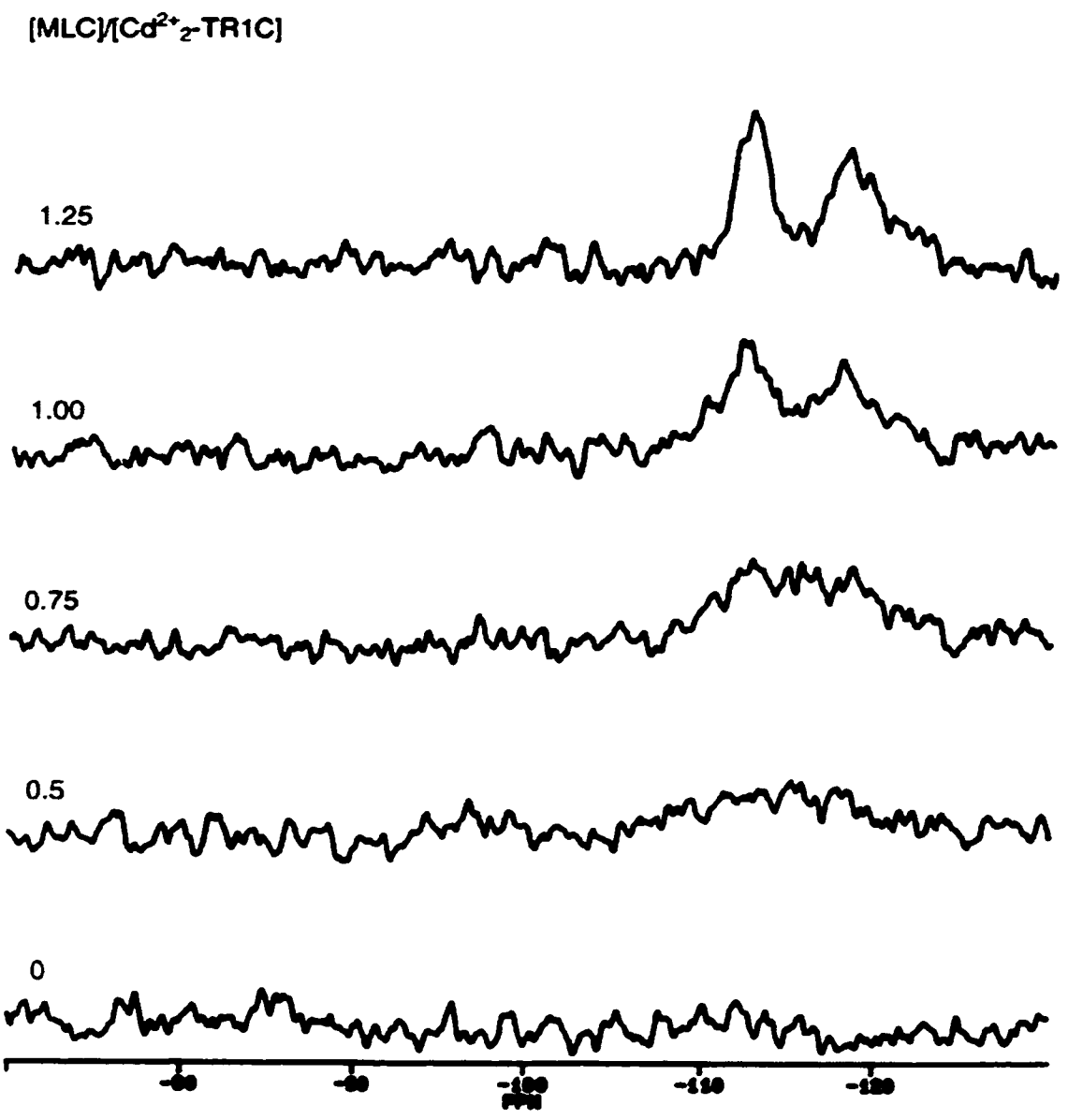
A [MLC]/[Cd2+2-TR1C]
1.25
1.00
0.75
0.5
0
PPM

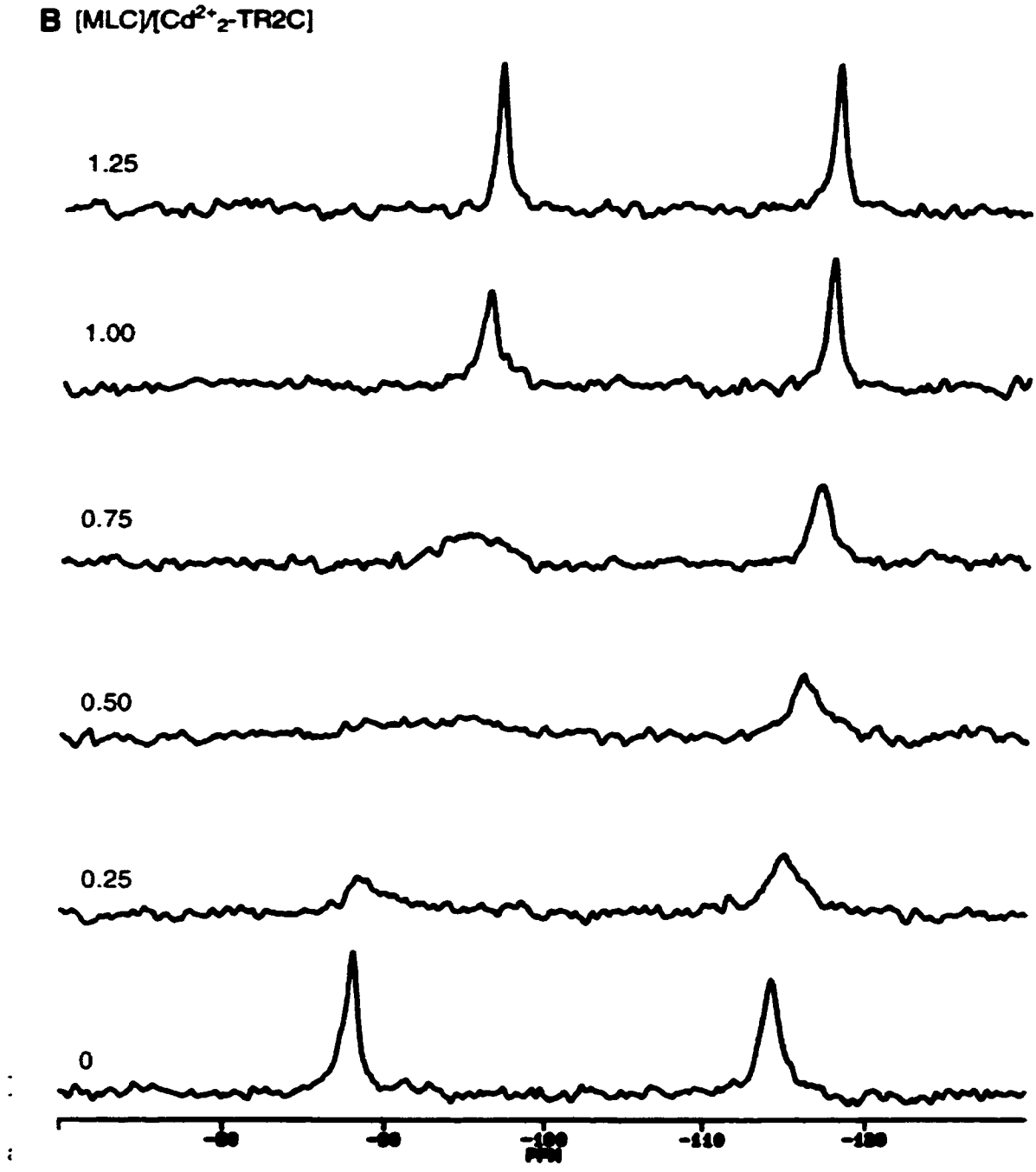
B [MLC]/[Cd2+2-TR2C]
1.25
1.00
0.75
0.50
0.25
0

Table 6.2 The Chemical Shift Values Measured for the Protein-bound ^{113}Cd Resonances

Protein	[MEL]: [Protein]	[MLN]: [Protein]	[MLC]: [Protein]	Chemical shift (ppm)				Exchange Rate
				CIII	NI	NII	CIV	
CaM	0			-88.4	no'	no	-114.4	Slow/Fast
CaM	1			-96.1	-115.0	-116.3	-118.7	Slow
TR1C	0				no	no		Fast
TR1C	1				-113.6	-117.2		
TR1C		1			no	no		Fast
TR1C			1		-112.3	-117.9		
TR2C	0			-87.5			-114.2	Slow
TR2C	1			-92.2			-117.3	Slow
TR2C		1		-92.7			-117.2	Fast
TR2C			1	-96.4			-117.8	Intermediate

'no: not observable due to exchange broadening (for discussion see Forsén et al., 1986).

1:1 MLN-

Th

of the melittin peptide, and it was also titrated with TR1C and TR2C in the

1:1 MLN-Cd^{2+}_2-TR2C complex (Table 6.2).

The MLC peptide comprises of the last 13 amino acid residues of the melittin peptide, and it was also titrated with TR1C and TR2C in the presence of two equivalents of Cd^{2+} ions. As shown in Figure 6.4A, two ^{113}Cd signals appeared in the spectra in the course of the titration of MLC peptide to Cd^{2+}_2-TR1C. The two resonances have chemical shift values at -112.3 ppm and -117.9 ppm; these are similar to the chemical shifts of the two resonances observed in the MEL-Cd^{2+}_2-TR1C complex (Figure 6.2). The above titration experiments suggest that the binding of MLC to Cd^{2+}_2-TR1C is relatively strong, and that the binding of MLC increased the binding affinity of Cd^{2+} ions bound to Cd^{2+}_2-TR1C.

When the MLC peptide was titrated into Cd^{2+}_2-TR2C, we observed a distinct pattern in the spectra (Figure 6.4B). The two resonances from Cd^{2+}_2-TR2C first experienced broadening and changes in chemical shift during the titration. At the end of the titration the two resonances sharpened again for the 1:1 MLC-Cd^{2+}_2-TR2C complex with a chemical shift -96.4 ppm and -117.8 ppm, respectively (Figure 6.4B, Table 6.2). These titration results demonstrate that the binding of the MLC peptide to Cd^{2+}_2-TR2C is in the intermediate exchange regime on the ^{113}Cd NMR time-scale. Assuming similar on rates, this indicates that the MLC, TR2C interaction is the strongest detected between MLN or MLC and TR1C or TR2C by ^{113}Cd NMR spectroscopy, suggesting that the binding of the C-lobe of MEL-like-MLC to the C-lobe of CaM (TR2C) triggers the binding process.

Proton NMR Studies of the Interaction Between MLN or MLC and TR1C or

Proton NMR Studies of the Interaction Between MLN or MLC and TR1C or TR2C

In order to confirm that the results obtained by ^{113}Cd NMR spectroscopy were consistent with those recorded for CaM in the presence of calcium instead of cadmium, we also conducted some titration experiments with CaM, TR1C and TR2C in the presence of calcium, using one-dimensional proton NMR spectroscopy to study their mutual interactions.

The binding of MLN and MLC to Ca^{2+}_4-CaM showed fast exchange on the proton NMR time scale. Either peptide can bind to Ca^{2+}_4-CaM with a 2:1 ratio, i.e., two molecules of peptide can bind to one molecule of Ca^{2+}_4-CaM (data not shown). This observation is consistent with the ^{113}Cd NMR studies (see above). The first molecule of either MLN or MLC binds to the C-lobe of Ca^{2+}_4-CaM, as evidenced by the change in the chemical shift of the Tyr138 E proton resonance at 6.33 ppm in the 1D ^1H NMR spectra. The second molecule of MLN or MLC apparently binds to the N-lobe of Ca^{2+}_4-CaM, since the Tyr138 E proton resonance does not change any further beyond a 1:1 peptide-protein ratio (data not shown, also see below).

The titration of MLN and MLC to Ca^{2+}_2-TR1C is in the fast exchange regime on the proton NMR time scale (data not shown). Next we performed a competition experiment using the MLC peptide which was titrated into 1:1 ratio MLN-Ca^{2+}_2-TR1C complex. The proton NMR spectra became very similar to the 1:1 MLC-Ca^{2+}_2-TR1C complex, as the MLC concentration is

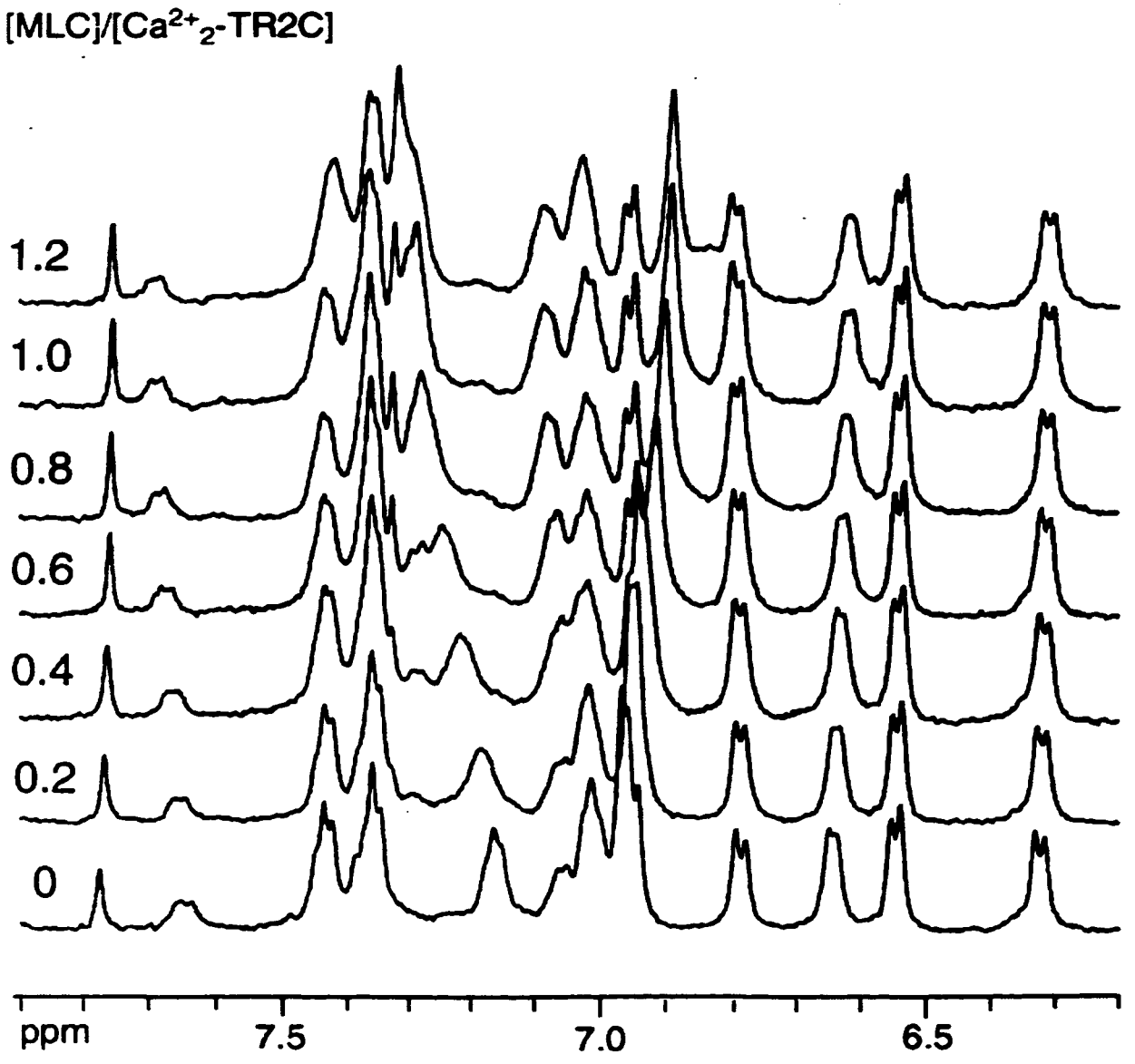
[MLC]/[Ca2+2-TR2C]
1.2
1.0
0.8
0.6
0.4
0.2
0
ppm
7.5
7.0
6.5

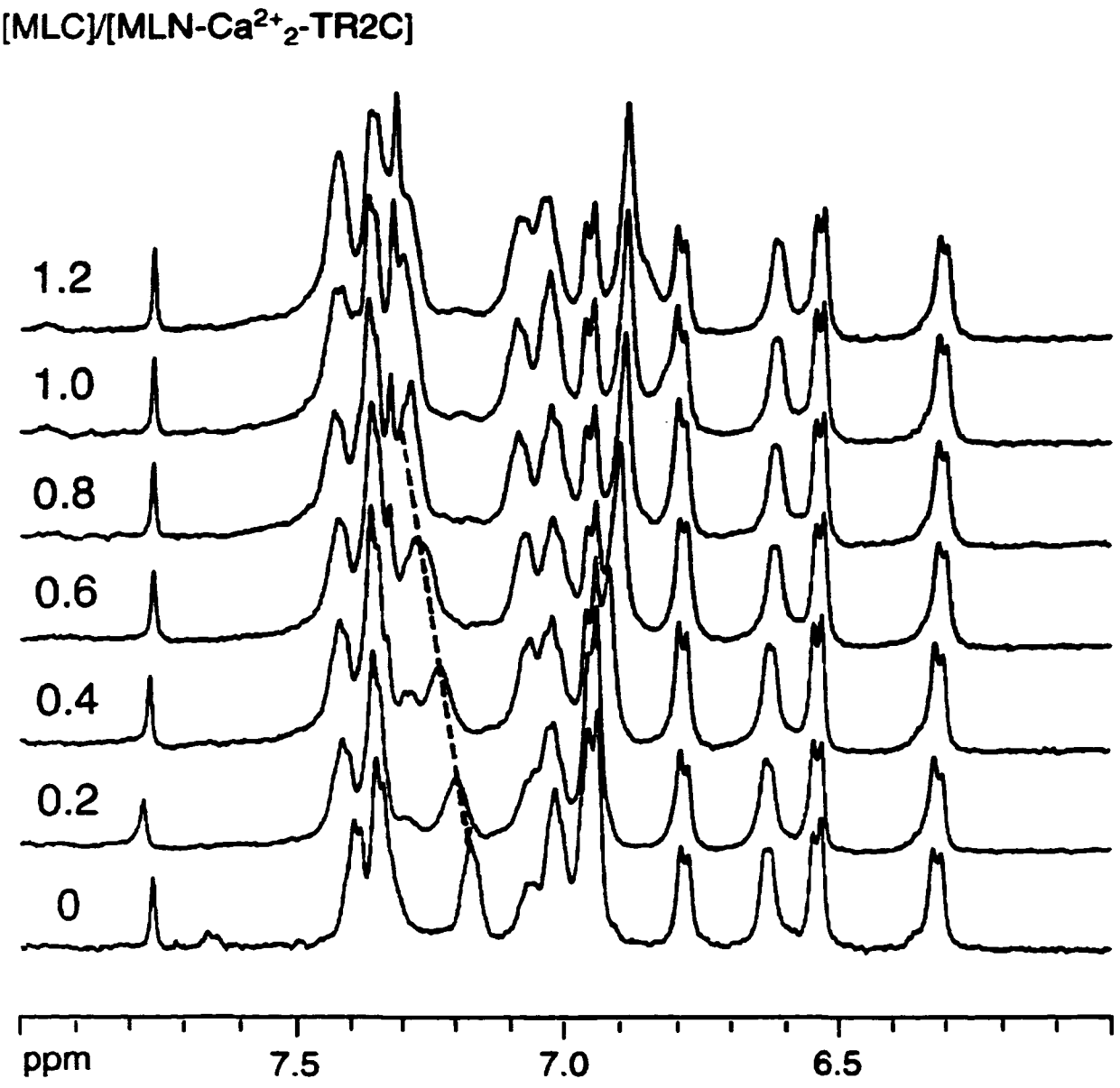

increased. For example, the peak around 7.5 ppm appears in the course of the titration, which resembles the spectrum of the 1:1 MLC-Ca^{2+}_2-TR1C complex (data not shown). Thus the MLC peptide has a stronger binding

increased. For example, the peak around 7.5 ppm appears in the course of the titration, which resembles the spectrum of the 1:1 MLC-Ca^{2+}_2-TR1C complex (data not shown). Thus the MLC peptide has a stronger binding affinity for Ca^{2+}_2-TR1C than the MLN peptide.

Similar results were also obtained for the TR2C fragment. Both MLN and MLC bind to Ca^{2+}_2-TR2C in the fast exchange regime on the proton NMR time scale (Figure 6.5, data not shown). When the MLC peptide was competitively titrated into a sample of the 1:1 MLN-Ca^{2+}_2-TR2C complex, we also observed that the spectra gradually changed to a spectrum which more closely resembles the spectrum of the 1:1 MLC-Ca^{2+}_2-TR2C complex (Figure 6.6). The shifts of the Phe141 side-chain C3,5H resonances are clearly labeled in the spectra (Figure 6.6). Thus we observe that MLC also binds to Ca^{2+}_2-TR2C more tightly than MLN. The above proton NMR titration experiments carried out in the presence of calcium clearly confirmed and complemented the results obtained by ^{113}Cd NMR spectroscopy.

Often the interactions between CaM and its target peptides are conveniently studied by biosynthetically labeling the methyl groups of the Met residues of CaM with isotopically carbon-13 labeled material and studying these by two dimensional proton-carbon correlated NMR experiments (e.g. Yuan *et al.* 1999 and references therein). However in the case of melittin, very broad resonances in the carbon dimension were observed for the complex, making this approach not effective in this instance (data not shown). This result was unexpected, as, for several other CaM binding domains, a well-defined spectrum for the Met residues

domains, a well-defined spectrum for the Met residues is obtained (e.g. Yuan *et al.* 1999). Proton NMR spectra of Met methyl residues can be conveniently recorded by spin echo NMR spectroscopy because of the singlet nature of this resonance (Vogel *et al.* 1990; Brockbank & Vogel, 1990). By adding the oxidant H_2O_2 surface exposed Met residues are converted to Met sulfoxide, which can be conveniently followed by proton NMR, because of the downfield shift of the peak for the sulfoxide. Following addition of MEL, 8 peaks collapse into one large peak, only Met76 located in the linker region of the protein remains (Huque 1989, Yuan *et al.* 2000). Addition of a large excess of H_2O_2 shows that Met76 rapidly oxidizes, but that the peak for the other 8 Met groups is unaffected, suggesting that binding of MEL covers up the two Met-rich patches of CaM.

The surface exposure of the Tyr99, Tyr138, and His107 residues of CaM and the Trp19 residue of MEL were studied by photo-CIDNP NMR experiments. Photo-CIDNP difference spectra (Huque 1989, Yuan *et al.* 2000) show that the Tyr99, Tyr138 and the His107 residue of mammalian CaM are all surface exposed as revealed by the increased emission or absorption peaks (for a detailed description of this technique see Kaptein, 1982). Our results clearly show that the Trp19 residue is exposed for the isolated MEL peptide, but in the complex its NH indole proton becomes inaccessible to the photo activated dye used for excitation, indicative of burial of the Trp sidechain. At the same time however, the Tyr99, Tyr138, and His107 residues remain exposed in the complex (Huque 1989, Yuan *et al.* 2000).

Fluorescence studies of the Binding of Melittin and MLC to CaM, TR1C and

Fluorescence studies of the Binding of Melittin and MLC to CaM, TR1C and TR2C

Because CaM is devoid of any Trp residue one can use Trp fluorescence of the unique Trp residue in the melittin and MLC peptides to study the peptide protein interactions (Ouyang & Vogel, 1998; Yuan *et al.* 1998; Weljie & Vogel, 2000). The Trp residues of many target-domain peptides of CaM enter the C-terminal hydrophobic cleft of CaM, becoming virtually completely shielded from the solvent (Meador *et al.* 1992; Ikura *et al.* 1992). Figure 6.7A shows that the Trp of MEL experiences a blue shift from 354 to 332 nm upon binding to CaM as well as a small increase in intensity. This indicates binding of the Trp sidechain to a hydrophobic region of CaM, and our result is consistent with earlier reports (Steiner *et al.* 1980; Sanyal *et al.* 1988; Weljie & Vogel, 2000). Subsequently we studied the binding of MLC to intact CaM. A similar blue shift is observed, in addition the results confirm that 2 equivalents of MLC can bind to intact CaM (see Figure 6.7B). When MLC was added to TR1C and TR2C a blue shift from 354 nm to 348 nm and 344 nm respectively was observed. However only a slight enhancement of the fluorescence intensity was noted (Figure 6.7C).

We also probed the exposure of the Trp residues of CaM bound MEL and MLC by fluorescence quenching experiments with added acrylamide, which has previously been shown to be an efficient quenching reagent in this system (Saryal *et al.* 1988, Gomes *et al.* 2000). In order to provide a direct

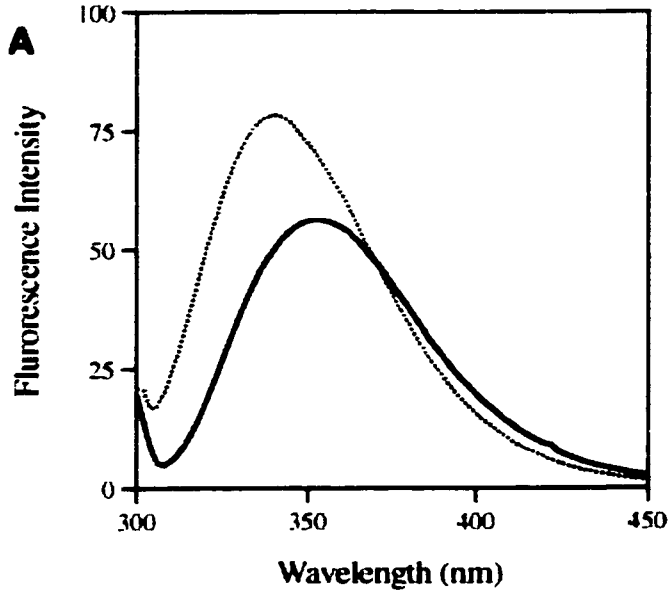
A
100
75
50
25
0
Fluorescence Intensity
300
350
400
450
Wavelength (nm)

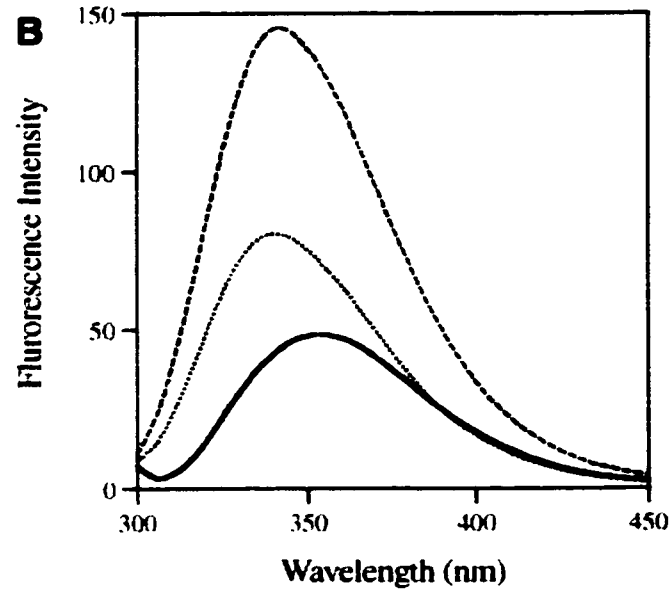
B
150
100
50
0
Fluorescence Intensity
300
350
400
450
Wavelength (nm)

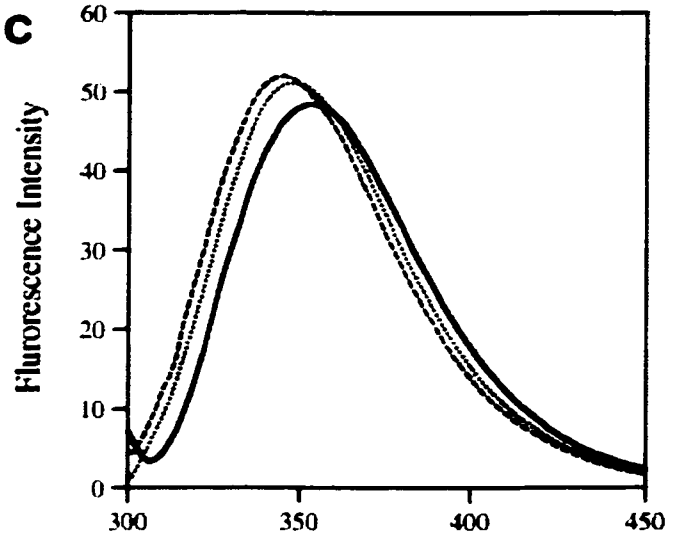

Figure 6.7 Fluo inding to CaM and its fragments. (A) emission spectra of melittin(———) and melittin-CaM complex(.....). (B) MLC (———), 1MLC-CaM (.....), and 2MLC-CaM (----------). (C) MLC (———), and its complexes with TR1C (.....) and TR2C (----------).

comparison to a peptide with a known CaM-complex structure, we also studied in parallel the binding of the skeletal muscle MLCK peptide. Representative results are shown in Figure 6.8, and the relative Stern-Volmer coefficients are given in the Figure legend. These data show that the Trp residues of MEL and MLC are well protected when bound to intact CaM. Protection factors were quite similar to those obtained for the MLCK peptide.However, for MLC bound to TR1C and TR2C, only the latter complex

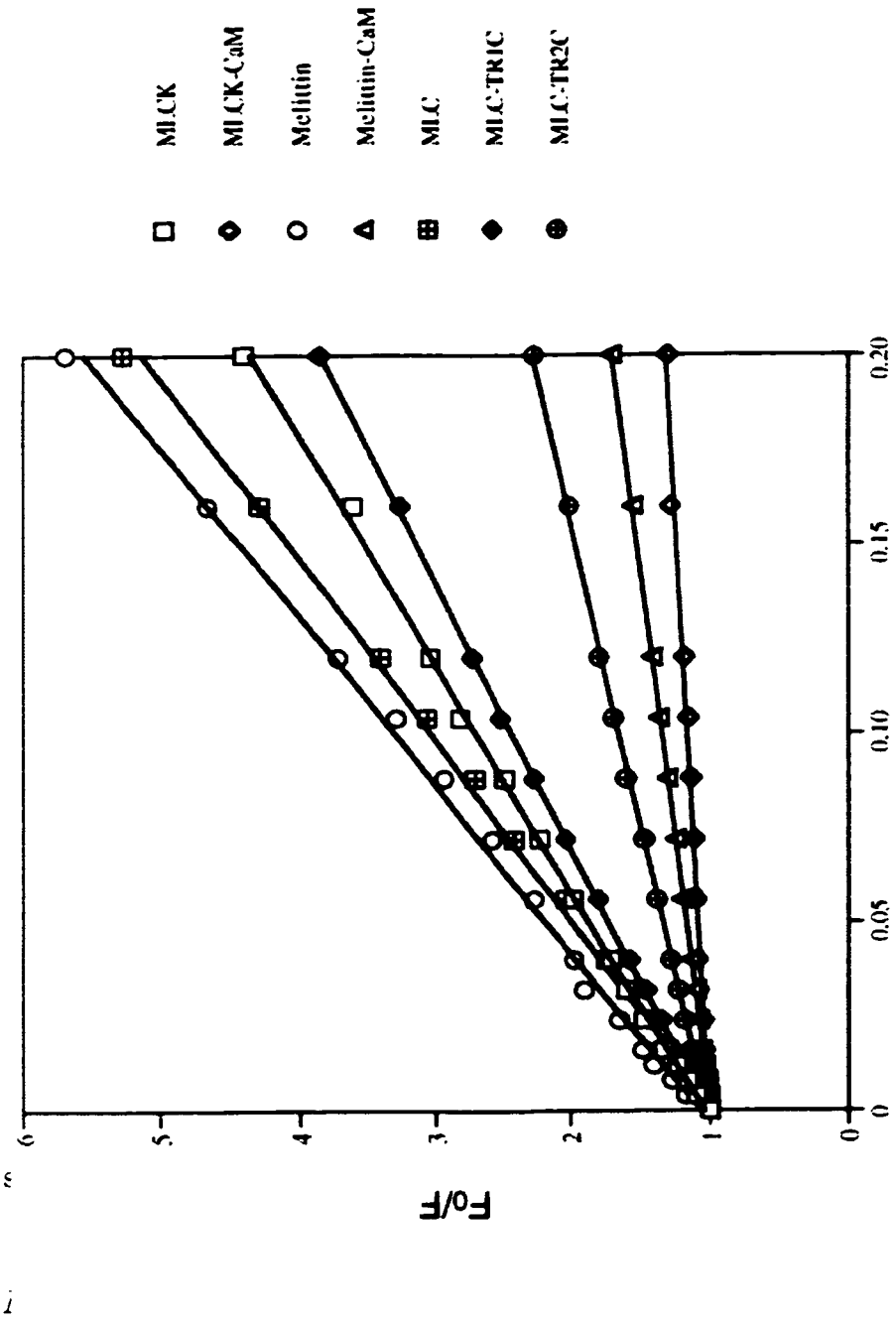

Figure 6.8 Stern-Volmer plot of melittin, MLC, and MLCK with CaM and its fragments. The Stern-Volmer coefficients are as following: MLCK peptide, 17; melittin peptide, 22; MLC peptide, 21; MLCK-CaM complex, 2; melittin-CaM complex, 4; MLC-TR1C complex, 1.4; MLC-TR2C complex, 6; 1MLC-CaM complex, 5 (not shown); and 2MLC-CaM complex, 6 (not shown).

shows significant protection (see Figure 6.8).

Near-UV and Far-UV circular dichroism studies of CaM, TR1C, TR2C and MEL and MLC interactions

Binding of Trp residues of target peptides to CaM can also be studied with near-UV CD measurements. For the Trp residues of target peptides derived from MLCK (Martin *et al.* 1996), CaM kinase I (Gomes *et al.* 2000) or cyclic nucleotide phosphodiesterase (Yuan *et al.* 1999b), a very characteristic bound Trp positive signal is observed between 285 and 310 nm. However, earlier near-UV CD studies of the MEL CaM interaction only showed a faint negative band around 280 nm (Maulet and Cox, 1983). This result was at variance with the near-UV studies of the other target peptides as listed above. However when we repeated the experiment we also noted only a slight extra negative peak for the CaM-bound MEL (see Figure 6.9A). The Phe residues of CaM are affected by the MEL binding as shown before (Maulet and Cox, 1983; Martin *et al.* 1996, Gomes *et al.* 2000, Yuan *et al.* 1999b) as evidenced by the enhanced negative peaks for Phe between 260 and 270 nm. Binding of one or two equivalents of MLC to intact CaM does not give rise to large changes, however very small positive peaks can be observed in the region between 285 and 310 nm (see Figure 6.9B), where other target peptides give similar, but much more intense peaks. Finally in Figure 6.9C we compare the near-UV CD spectra for TR1C, TR2C and CaM. As expected, the Tyr peak around 280 nm is only present for TR2C, which contains the two Tyr residues

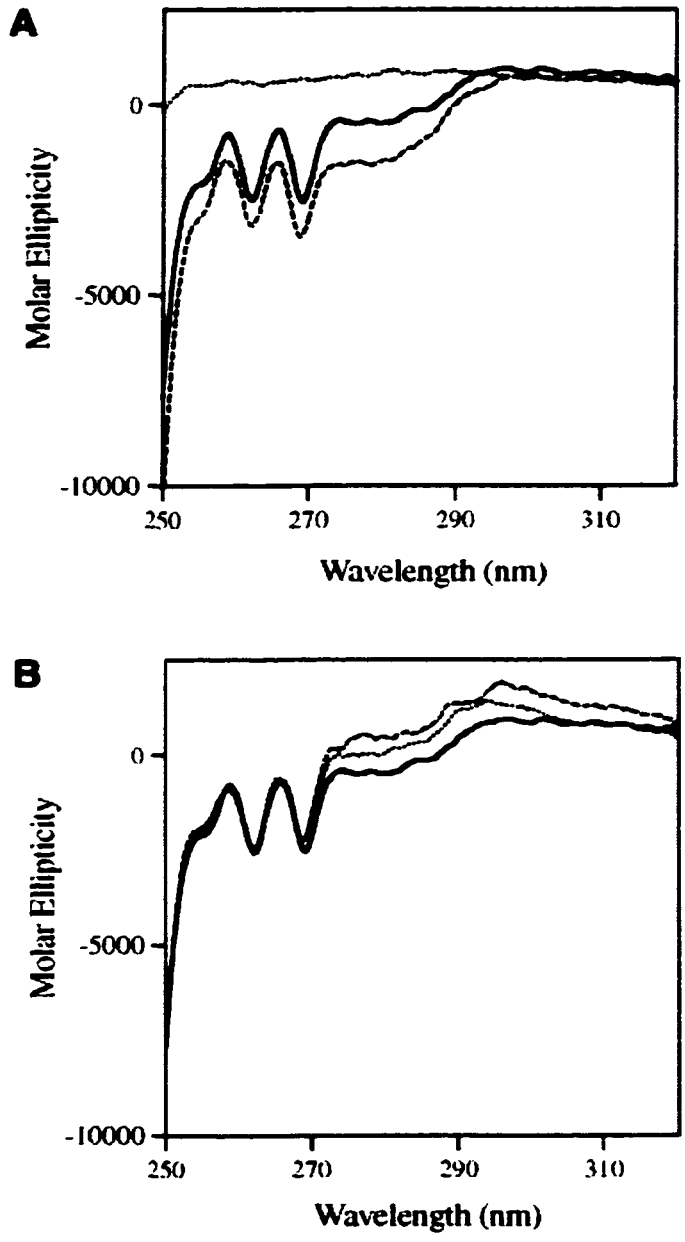
A
0
-5000
-10000
Molar Ellipticity
250
270
290
310
Wavelength (nm)
B
0
-5000
-10000
Molar Ellipticity
250
270
290
310
Wavelength (nm)

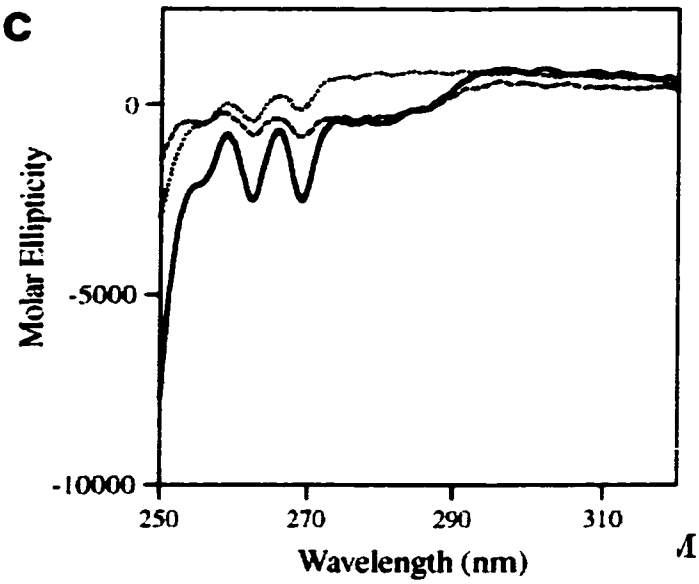

Figure 6.9 Near- *M* (———) and melittin-CaM complex (---------). (B) CaM (———) complexed with one (.....) and two (---------) MLC. (C) CaM (———) and its fragments TR1C (.....) and TR2C (---------).

of mammalian CaM, whereas TR1C is devoid of such residues. Addition of MLC to TR1C or TR2C did not produce any changes in the near-UV CD spectra that could be reliably detected (data not shown).

Far-UV CD spectra of MEL, MLN or MLC, bound to CaM, TR2C and TR1C were recorded as well to study the formation of α-helical structures upon binding of these peptides to the proteins. Far-UV CD spectra show the absence of α-helical structure in the isolated MEL and MLC peptides (see Figure 6.10A). When one equivalent of MEL is added to CaM, a substantial increase in the negative ellipticity around 208 and 222 nm is observed, indicative of α-helix formation in the peptide. Likewise our data show that the peptide becomes α-helical when the first and second equivalent of MLC binds to CaM (see Figure 6.10A). When MLC binds to

increase in the negative ellipticity around 208 and 222 nm is observed, indicative of α-helix formation in the peptide. Likewise our data show that the peptide becomes α-helical when the first and second equivalent of MLC binds to CaM (see Figure 6.10A). When MLC binds to TR2C the formation of α-helical bound peptide structure is also noted (see Figure 6.10B), but no such enhancement of α-helicity is obtained when MLC is added to TR1C (data not shown). When MLN is added to either TR1C, TR2C or CaM, induction of α-helical structure can be observed in all three instances (Figure 6.10C-E).

Discussion

In this work, we have studied the interaction between CaM and melittin by NMR and optical spectroscopy methods. We have dissected the interactions between these two components using half molecules, both from CaM and from melittin. The NMR titration experiments indicate that the MLC peptide binds with a higher affinity to both the TR1C and the TR2C fragments than the MLN peptide (Figure 6.4 and 6.5). Among them, the MLC peptide binds to TR2C fragment with the highest affinity, as demonstrated by ^{113}Cd NMR spectroscopy (Figure 6.4B). Far-UV CD data show that all peptides become α-helical upon binding to CaM, TR1C and TR2C, with the exception of the MLC TR1C complex (Figure 6.10). Our NMR results indicate that the orientation of melittin binding to Ca^{2+}-CaM is mostly in a parallel orientation, i.e., the C-terminal end of melittin will bind preferentially to the C-lobe of Ca^{2+}-CaM. The parallel C to C orientation of the CaM-MEL complex

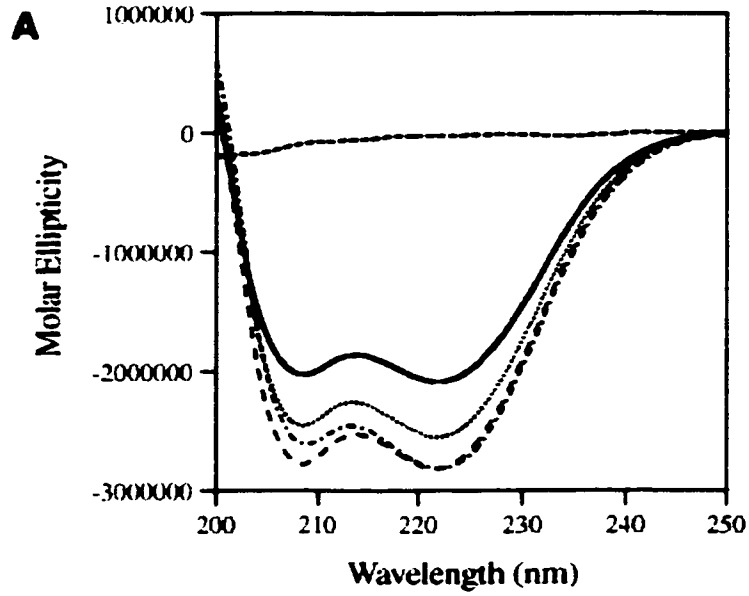
A
1000000
0
-1000000
-2000000
-3000000
Molar Ellipticity
200
210
220
230
240
250
Wavelength (nm)

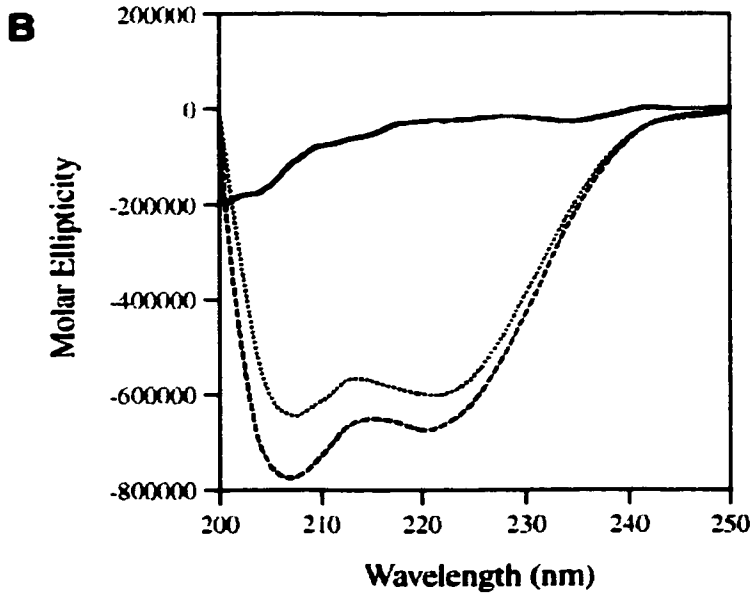
B
200000
0
-200000
-400000
-600000
-800000
Molar Ellipticity
200
210
220
230
240
250
Wavelength (nm)

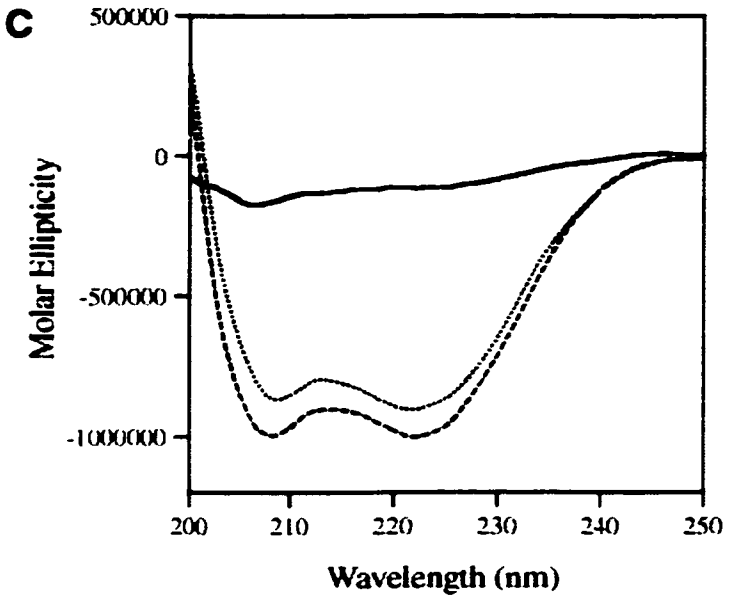
C
500000
0
-500000
-1000000
Molar Ellipticity
200
210
220
230
240
250
Wavelength (nm)

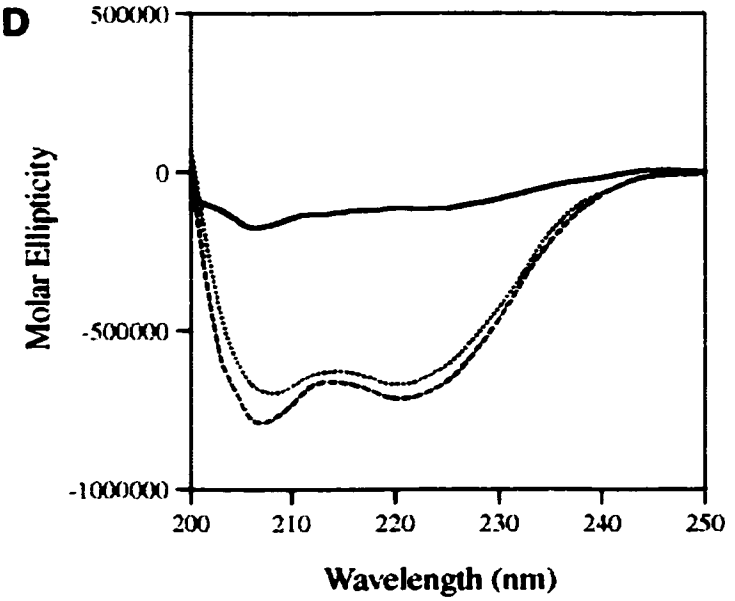
D
500000
0
-500000
-1000000
Molar Ellipticity
200
210
220
230
240
250
Wavelength (nm)

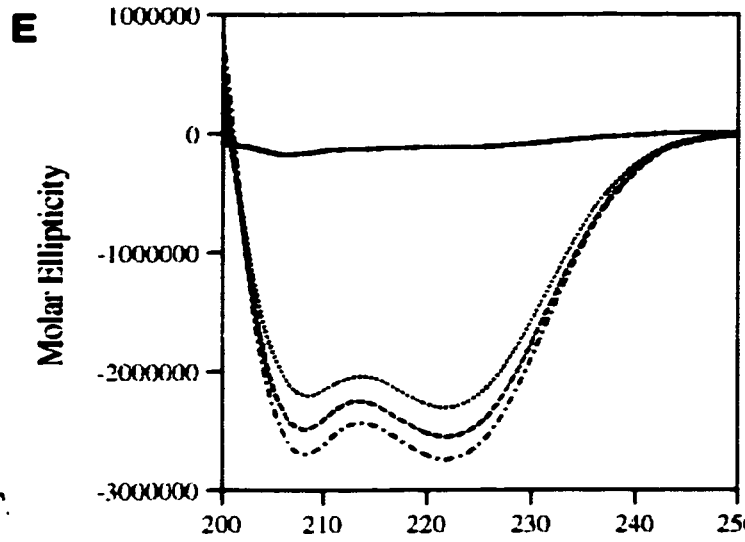

Figure 6.10 F ——), 1MLC-CaM (.....), - -) complexes. (B) MLC (——), TR2C (.....), and MLC-TR2C (.....) complex. (C) MLN (——), TR1C (.....) and MLN-TR1C complex (.....). (D) MLN (——), TR2C (.....) and MLN-TR2C complex (.....). (E) CaM (.....) complexed with one (.....) and two (.....) MLN, and free MLN is represented by a solid line.

appears to be an exception amongst the CaM-peptide complexes studied to date. Most other CaM-binding peptides characterized bind with a regular α-helical structure and show an anti-parallel N to C binding orientation with respect to Ca^{2+}-CaM. This includes CaM-binding peptides derived from MLCK, CaM-dependent protein kinase II, neuronal nitric oxide synthase, phosphofructokinase and CaM-dependent protein kinase I (Ikura *et al.* 1992; Meador *et al.* 1992, 1993, Zhang *et al.* 1995b, P. Bayley personal communication; Yuan and Vogel, unpublished results). In the case of CaM kinase kinase, the opposite orientation is found, but this

Meador *et al.* 1992, 1993, Zhang *et al.* 1995b, P. Bayley personal communication; Yuan and Vogel, unpublished results). In the case of CaM kinase kinase, the opposite orientation is found, but this peptide binds with a partial helical-turn like structure (Osawa *et al.* 1999). Another distinct 2:1 helical coiled-coil structure was found for the complex of CaM with the petunia glutamate decarboxylase peptide (Yuan and Vogel, 1998). Thus the α-helical C to C oriented melittin Ca^{2+}-CaM complex represents yet another distinct protein complex among the various CaM-binding peptides. Early studies, using fluorescence spectroscopy, crosslinking, proteolysis and ^{1}H NMR spectroscopy, also are consistent with a parallel CaM-MEL orientation (Steiner *et al.* 1986; Sanyal *et al.* 1988; Seeholzer *et al.* 1987; Itakura and Iio, 1992; Scaloni *et al.* 1998).

The data in Figure 6.1 reveal that two slowly exchanging conformers are present for the MEL-CaM complex in approximately a 85%-15% ratio. This reflects the sensitivities of the ^{113}Cd chemical shift to subtle changes in the overall structure. As described above the C-terminal region of MEL strongly prefers to bind to the C-terminal domain of CaM, giving rise to the major species. However, MLC also binds effectively to the N-terminal domain of CaM with a greater affinity than MLN. Hence an opposite orientation of MEL with respect to both lobes of CaM is clearly feasible based on cadmium-113 and proton NMR data, explaining the presence of the minor peaks. Consistent with this is the outcome of the fluorescence and far-UV CD data (Figure 6.8, 6.9, and 6.10), which reveal that two MLC peptides can bind simultaneously to one CaM molecule. Likewise two MLN can bind to one CaM, being consistent with the notion

simultaneously to one CaM molecule. Likewise two MLN can bind to one CaM, being consistent with the notion of two oppositely oriented conformers. Earlier preliminary proton NMR spectra have also indicated the presence of multiple conformers for the MEL-CaM complex (Seeholzer *et al.* 1986). These multiple coexisting conformations will make it difficult to determine the solution structure of the complex by NMR methods.

Recently, Bayley and colleagues suggested that an α-helical CaM-binding region of a target protein can in principle choose one of two possible binding orientations when it is docked to Ca^{2+}-CaM (Barth *et al.* 1998), given the approximate two-fold symmetry in the structures of the Ca^{2+}-CaM-MLCK peptide complex (Ikura *et al.* 1992; Meador *et al.* 1992). Also Persechini *et al.* (1994) have reported activation studies with fragments of CaM, which illustrate the symmetry of the CaM-binding domains in intact target enzymes of CaM. Interestingly, Shoemaker *et al.* (1990) reported that the inversion of the CaM binding domain in MLCK still created a functional kinase activated by CaM, although the CaM concentration required for half-maximal activity was increased. Thus the correct orientation between target proteins and CaM may contribute to the high affinity and binding specificity between them. Our studies on melittin show that the major form of the CaM-MEL complex adopts a parallel binding orientation, and the minor conformer probably in the opposite orientation.

Tryptophan residues often play an important role in the interaction between CaM and target peptides (e.g. Yuan *et al.* 1998a). Mutation of Trp to smaller aliphatic hydrophobic residues in the CaM-binding domains of

smaller aliphatic hydrophobic residues in the CaM-binding domains of target proteins often reduces their affinity for calmodulin. Also basic residues of the peptide play an important role and they are interacting with acidic sidechains of CaM residues, to help orient the peptide. Tryptophan sidechains of CaM-binding domains often associate with the hydrophobic cleft on the C-terminal end of calcium-CaM (e.g. Ikura *et al.* 1992; Meador *et al.* 1992, 1993; Yuan *et al.* 1998), although they have also been found bound to the hydrophobic cleft of the N-terminal domain of CaM (Osawa et al.; Yuan and Vogel, 1998). Therefore, the $W^{19}IKRKR^{24}$ motif in the C-terminal part of melittin can be implicated as an important region to initiate the peptide binding to Ca^{2+}-CaM. However, early results from ultraviolet circular dichroism (near-UV CD) spectroscopy suggested that the single Trp19 residue in melittin was not intimately involved in the interaction with Ca^{2+}-CaM (Maulet and Cox, 1983). In contrast, intermolecular fluorescence quenching experiment using a CaM variant containing the unnatural amino acid analog selenomethionine in place of methionine residues suggested that the Trp19 residue of melittin binds in the vicinity of the Met-rich hydrophobic surface of Ca^{2+}-CaM (Weljie and Vogel, 2000). Furthermore, fluorescence quenching experiments with acrylamide show that the Trp residue of melittin becomes essentially fully buried as expected upon binding to CaM (Maulet and Cox, 1983; Sanyal *et al.* 1988).

Here we have reinvestigated the near-UV CD spectra of CaM bound MEL; in addition MLC was studied in the same fashion as well (Figure 6.9). Our results clearly corroborate the unusual nature of the Trp-19

Our results clearly corroborate the unusual nature of the Trp-19 MEL near-UV CD spectrum (Maulet and Cox, 1983), as opposed to other CaM-binding domain peptides (see above). The near-UV CD spectra obtained with TR1C and TR2C make it unlikely that the two opposite orientations of MEL with respect to CaM give rise to offsetting contributions to the Trp near-UV CD spectrum of the intact protein, suggesting that the Trp of MEL is not bound to CaM in the same fashion as that of MLCK for example. On the other hand however, the fluorescence quenching and photo-CIDNP experiments with MEL and MLC clearly reveal that the Trp-19 residue becomes almost completely buried upon binding to the C-terminal domain of CaM. Earlier results from our group have also shown that the Trp of MEL is bound closely to the Met residues in the hydrophobic pockets of CaM (Weljie and Vogel, 2000). This is in qualitative agreement with our Met oxidation data (Yuan *et al.* 2000) which shows that MEL binds on top of the two Met-rich regions of CaM, quite similar to other CaM-binding domain peptides (Yuan *et al.* 1999a). Collectively therefore these data suggest that perhaps the Trp sidechain of MEL is bound in a different orientation in the complex than MLCK, PDE, and CaM Kinase I peptides. In this respect it is interesting that the Trp sidechain of a Ca^{2+}-pump peptide binds in a different orientation to CaM as MLCK (Elshorst *et al.* 1999).

Completion of the preliminary X-ray structural analysis should reveal the details of how the Trp19 residue in melittin and basic residues in the sequence play a role in the binding CaM (Quiocho *et al.* 1997). A remaining question is what residues in melittin interact with the N-terminal region of CaM and further stabilize the major parallel

question is what residues in melittin interact with the N-terminal region of CaM and further stabilize the major parallel orientation. Small angle X-ray studies show that the binding of melittin to calcium-CaM is accompanied by a structural collapse (Kataoka et al. 1989); such a collapse is not observed when the proper anchoring residue for the binding to the N-terminal domain is missing (Elshorst *et al.* 1999). Hence, by analogy to other CaM binding peptides, we suggest that the Leu-residue which is 13 residues upstream from the Trp residue of MEL will act in this capacity.

In conclusion, this work has demonstrated that useful information can be obtained about CaM-peptide interactions by using half molecules of melittin and CaM. This approach can be further applied to regulatory calcium-binding protein peptide interactions, as more CaM-target proteins and CaM-related proteins emerge in the future.

Chapter 7

Interactions Between Calmodulin and LLP Segments from HIV-1 Transmembrane Protein

Abstract

Lentivirus lytic peptides (LLP) are cytoplasmic segments found close to the C-terminus of the transmembrane glycoprotein of human immunodeficiency virus (HIV), which play an important role in single-cell cytolysis and infectivity. These peptides also display calmodulin (CaM)-binding activities, which were examined in this work. Two LLP peptides derived from two distinct HIV-1 isolates, LLP-1A, as well as its mutant C837S, and LLP-1E, were studied. Circular dichroism (CD) experiments demonstrated that these peptides have a strong propensity to form an α-helical conformation, and that they bind to CaM as an α-helix. Fluorescence spectroscopy showed that the single Trp residue in the LLP-1E peptide enters one of the hydrophobic pockets on CaM's surface, and is well shielded from the solvent. However, this Trp sidechain might adopt a different orientation than typical CaM-binding peptides, such as MLCK and PDE peptides, when it binds to CaM, as revealed by near-UV CD data. Fast to intermediate exchange rates were observed in NMR experiments when these peptides bind to CaM, indicating that they have a lower affinity for CaM than model peptides such as MLCK. Furthermore, small angle X-ray spectroscopy results

elucidated that the CaM-LLP-1A peptide complex was not as compact as CaM-MLCK peptide complex, as it probably adopts a more extended conformation. It is likely that the LLP peptides bind to CaM in a different way from typical model CaM-binding peptides, as subtle differences can be detected by the various spectroscopic methods used. These findings will help further understand HIV pathogenesis.

Introduction

Acquired immunodeficiency syndrome (AIDS) is a chronic, usually fatal, disease which is caused by human immunodeficiency virus (HIV). HIV primarily affects the immune and nervous systems. One characteristic of HIV infection is progressive depletion of T lymphocytes which express the CD4 cell-surface marker (Barré-Sinoussi *et al.* 1983, Popovic *et al.* 1984, Levy *et al.* 1984, Gallo 1987, Garry *et al.* 1988, Levy 1988, Garry 1989). A steady state seems to be achieved, consisting of a rapid turnover of lymphocytes concomitant with rapid viral production and clearance (Ho *et al.* 1995, Wei *et al.* 1995). This steady state eventually shifts with a loss of the ability of the immune system to replace CD4+ cells. Although great progress has been made in AIDS research in recent years, the mechanisms leading to dysfunction and eventual death of HIV-infected cells are still not completely understood. In the early state of the infection, T-cell membrane permeability increases, particularly to calcium ions (Cloyd & Lynn 1991), suggesting the potential involvement of CaM in HIV cytotoxicity. Recent studies also

implied that one potential mechanism for the accelerated loss of CD4+ cells is an increased rate of apoptosis, a process which could be modulated by CaM (Zhang *et al.* 1994, Pan *et al.* 1996, Micoli *et al.* 2000). Thus, understanding the role of CaM in HIV infection is critical to an understanding of HIV pathogenesis.

The envelope glycoproteins of HIV play an important role both in early and late stages of viral infection (Sodroski *et al.* 1986, Stein *et al.* 1987, McKeating & Willey 1989). The glycoprotein of HIV-1 is first synthesized as a precursor polypeptide, gp160, which is then cleaved intracellularly to give rise to a surface (SU) glycoprotein designated as gp120, and a transmembrane (TM) protein, referred to as gp41 (Allan *et al.* 1985, Veronese *et al.* 1985, Ranajit *et al.* 1988, Willey *et al.* 1988). These two subunits remain noncovalently associated after cleavage (Helseth *et al.* 1991). The gp120 subunit functions to recognize CD4 and a coreceptor on the surface of T lymphocytes, and gp41 subsequently undergoes conformational changes that mediate fusion of the viral membrane and the target cell membrane (Chan & Kim 1998, Turner & Summers 1999).

The gp41 glycoprotein has an ectodomain, a linker region, a transmembrane domain, and a long cytoplasmic tail (Wyatt & Sodroski 1998, Turner & Summers 1999). This is schematically depicted in Figure 7.1. A segment with a relatively large hydrophobic moment has been identified in the cytoplasmic domain of gp41 (Eisenberg & Wesson 1990). This segment tends to fold into an amphiphilic α-helix (Srinivas *et al.* 1992, 1993), like

CaM-binding domains in many CaM targeting proteins. In fact, *in vitro* studies have shown that the full length gp41 protein binds CaM, whereas a truncated TM protein lacking this segment does not bind CaM (Miller *et al* 1993). Addition of this peptide to membrane preparations causes it to bind and form an α-helix (Wray *et al.* 1999). Interestingly, similar amphiphilic α-helical segments have also been found in HIV-2 and simian immunodeficinecy virus (SIV) (Table 7.1). Mutated viruses with truncated gp41 proteins are infectious and induce cell fusion but do not cause extensive single cell killing (Kong *et al.* 1988, Kodama *et al.* 1989, Lee *et al.* 1989, Kowalski *et al.* 1991), suggesting that CaM may be involved in the cytopathology of HIV and related

LLP-1A	RVIEVVQGACRAIRHIPRRIRQGLERIL
C837S	----------S----------
LLP-1E	RVIEVAQGAWRAILHIPRRIRQGFERS
SIV	DLWETLRRGGRWILAIPRRIRQGLELTL
SIV-W3F	--F----------
SIV-W12F	----------F----------
HIV-2	GFWGTLGQIGRGILAVPRRIRQGAEIAL

Table 7.1 Primary structures of the LLP-1 peptides from HIV-1 (first three peptides), SIV and HIV-2. The LLP-1A peptide is derived from HIV-1 isolate HXB2R. The C837S peptide is engineered according to the sequence of the LLP-1A with a single Cys to Ser mutation. The LLP-1E peptide is derived from HIV-1 isolate TN243; the residues which are different from LLP-1A are underlined in the LLP-1E sequence. The SIV-W3F and SIV-W12F peptides are different Trp to Phe mutants of the SIV peptide. The HIV-2 peptide listed here is derived from HIV-2 isolate ST.

viruses.

Synthetic peptide homologues of the amphiphilic region near the C-terminus of HIV-1 gp41 glycoprotein are often referred to as LLP-1 (lentivirus lytic peptide). This peptide displays both cytolytic and CaM-binding

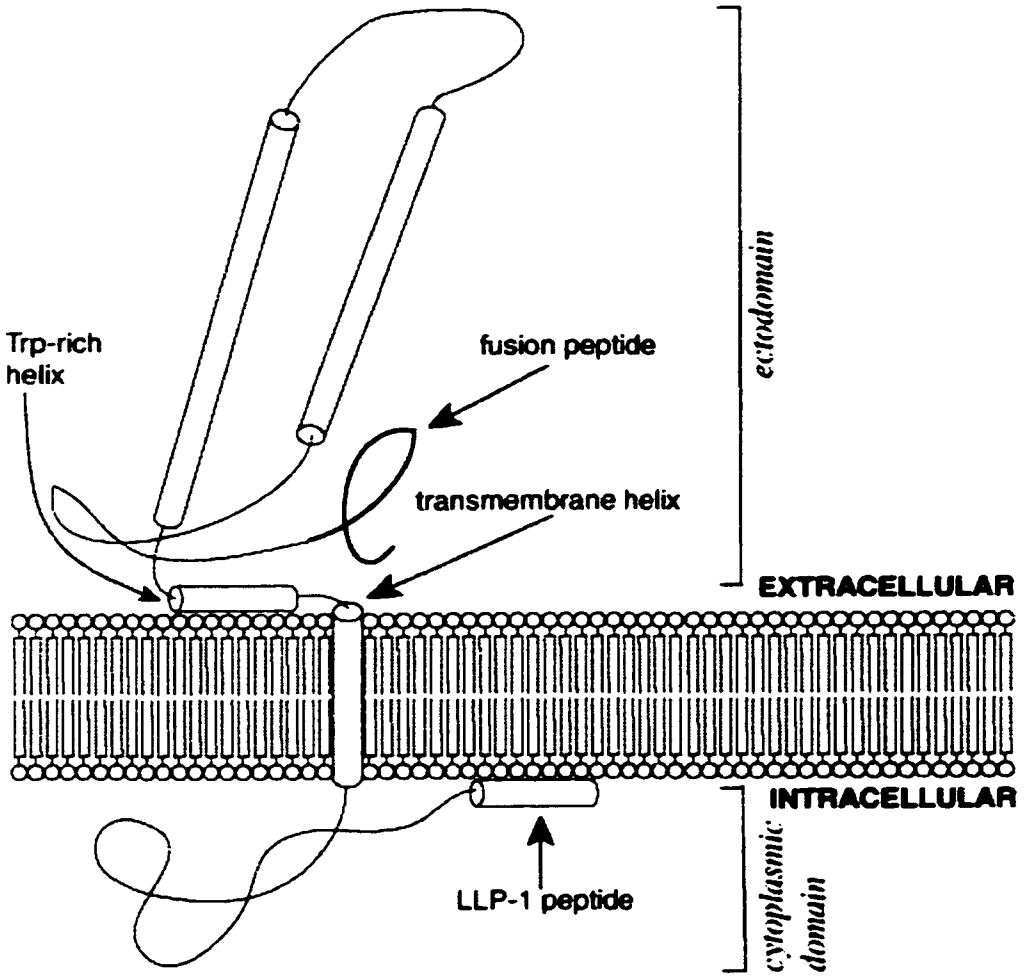

Figure 7.1 Schematic of the predicted structure of the gp41 protein from HIV-1. The gp41 protein forms a trimer on the membrane (only one subunit is illustrated here). The structure of the ectodomain has been determined (Chan *et al.* 1997, Weissenhorn *et al.* 1997). The LLP-1 peptide is located near the C-terminus of the gp41 protein.

properties (Miller *et al.* 1993c, Srinivas *et al.* 1993, Tencza *et al.* 1995, 1997). In this work, we have studied the CaM-binding properties of two LLP-1 peptides using various spectroscopic techniques.

Materials and Methods

Materials

Methyl-^{13}C-labeled Met and D_2O (99.9%) were purchased from Cambridge Isotope Laboratories. Other chemicals and reagents were obtained from Sigma. Synthetic peptides used in this work, which were purified by HPLC, were generous gifts from Dr. R. C. Montelaro (University of Pittsburgh School of Medicine). Sequences of peptide LLP-1A and LLP-1E were derived from the C-terminal amphiphilic helical segments of HIV-1 isolates HXB2R and TN243, respectively. C837S is an engineered mutant of LLP-1A with a single Cys residue substituted by a Ser residue (Tencza *et al.* 1997); it was used instead of the wild type peptide in lengthy experiments where disulfide formation between two peptides could occur. Bacterially expressed CaM was purified as described before (Zhang and Vogel 1993).

Circular Dichroism

Circular dichroism (CD) experiments were performed at room temperature on a Jasco J-715 spectropolarimeter as described earlier (Ouyang & Vogel 1998a). For titration experiments with 2,2,2-

trifluoroethanol (TFE), the LLP-1 (10 μM) peptides were dissolved in various TFE solution (0%, 10%, 20%, 30%, 40%, 60% and 80%) with a final peptide concentration of 10 μM, and far-UV CD spectra (185 nm - 255 nm) were recorded for these samples. CD spectra were acquired in both the far-UV (200 nm - 250 nm) and near UV (250 nm - 320 nm) region for the LLP-1E and its complexes with CaM.

Fluorescence Spectroscopy

The LLP-1E peptide possesses a single Trp residue in its sequence which makes it suitable for intrinsic fluorescence experiments. The concentration of LLP-1E was determined optically by using ε_{280}=5500 M^{-1}. The LLP-1E samples were prepared at 10 μM in 10 mM Tris-HCl (pH 7.4), 0.1 M KCl, and 1 mM $CaCl_2$. For CaM-peptide complexes, 12 μM CaM was included in the sample to ensure complete saturation of the peptide. Fluorescence emission spectra were recorded as previously described (Ouyang & Vogel 1998b). For fluorescence quenching experiments, microliter amounts of a 4 M acrylamide stock solution were titrated into the sample (1 ml). Fluorescence intensity at the emission peak was then recorded. The fluorescence quenching data were analyzed as described in Chapter 6.

Gel Band Shift Assays

The binding of target peptides to CaM can be studied by non-denaturing urea gel electrophoresis. The urea gel used in this work contains

15% acrylamide, 4 M urea, 0.375 M Tris-HCl (pH 8.8), and 1 mM $CaCl_2$. CaM (30 μM) samples were prepared in a volume of 50 μl containing 4 M urea, 25 mM Tris-HCl (pH 7.4), and 1 mM $CaCl_2$. For CaM-peptide complexes, 30 μM CaM and 35 μM peptide (LLP-1A or LLP-1E) were prepared in the same sample; the slight excess of peptide should give rise to a complete band shift. All samples were incubated at room temperature for one hour before 50 μl of 50% glycerol was added to each sample. 10 μl of each sample was applied to the gel. The gel was run at a constant voltage of 100 V as previously described (Ouyang & Vogel 1998a).

NMR Experiments

NMR spectra were recorded on a Bruker AMX-500 spectrometer equipped with a Bruker BGU Z Gradient unit. Methyl-^{13}C-Met labeled CaM samples were prepared in D_2O, containing 0.1 M KCl, 10 mM $CaCl_2$. Peptide (LLP-1E and C837S) samples were prepared in the same solvent. Methyl-^{13}C-Met labeled CaM was titrated with these peptides by adding 0, 0.5, 1, and 1.2 equivalents. The sample was then incubated at room temperature for an hour at each titration point before a 2D ^{1}H, ^{13}C HMQC spectrum was acquired. 2D ^{1}H, ^{13}C HMQC NMR spectra were recorded as previously described (Ouyang & Vogel 1998a). The pH was maintained at pH 7.4 throughout the titration process, and the isotope effect on the pH value was not corrected. The titrations were performed at 25 °C. For CaM samples with 1.2 equivalents of LLP-1E or C837S, the ^{1}H,^{13}C HMQC spectra were recorded at various

temperatures (5.5 °C, 16.5 °C, 23.5 °C, 37 °C, and 45 °C).

Small Angle X-ray Spectroscopy

Small angle X-ray spectroscopy (SAXS) experiments were performed by Dr. H. Yoshino from Sapporo Medical University, Japan. SAXS data were obtained using the BL-10C instrument at the Photon Factory in the National Laboratory for High Energy Physics at Tsukuba, Japan. The sample buffer contained 50 mM Tris-HCl (pH 7.5), and 120 mM NaCl. Appropriate amounts of $CaCl_2$ were added into the sample according to the CaM concentration, while 1 mM EDTA was included in the buffer for apo-CaM samples. The sample volume was 70 µl, and the temperature was maintained at 25 °C during the data acquisition. The radius of gyration (R_g) was calculated from the scattering data in the very small angle region by the Guinier method (Guinier & Fournet 1955). The pair-distribution function, P(r), is calculated by a direct Fourier transformation as described by Yoshino *et al.* (1996).

Results

Circular Dichroism

CD experiments have been performed in both the far-UV and near-UV region. Far-UV CD spectra are often used to determine the secondary structure of polypeptides (Kelly & Price 1997). Free linear peptides usually do

not adopt any stable secondary structure in aqueous solution, therefore LLP-1A in water does not display any characteristic CD band in the far-UV region (Figure 7.3). TFE is known to induce the α-helical conformation in polypeptides, and can be used to study the α-helical propensity of a peptide (Zhang *et al.* 1993). Far-UV CD spectra were recorded for the LLP-1 peptide in various aqueous TFE mixtures. As shown in Figure 7.2, the peptide shows a significant CD signal in the far-UV region, with a positive peak around 190 nm and two negative peaks at 208 nm and 222 nm respectively. These signals are typical CD signals for α-helical structures, indicating that the LLP-1A

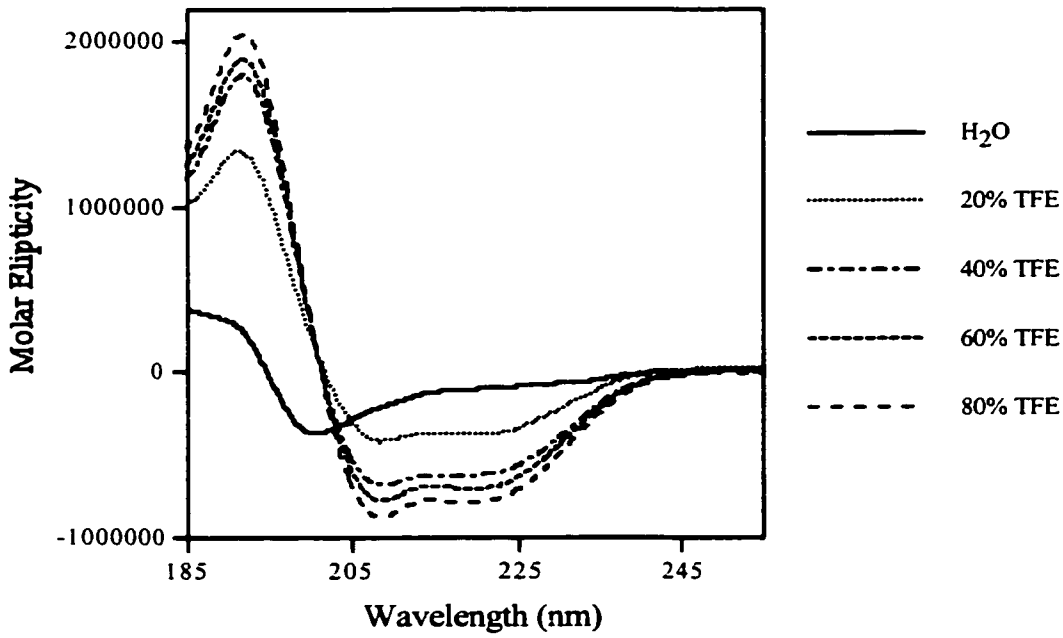

Figure 7.2 Far-UV spectra of the LLP-1A peptide in aqueous solutions containing varying amounts of TFE (v/v).

peptide forms an α-helix in TFE solution, which suggests that this peptide has a tendency to adopt an α-helical conformation. A similar result was obtained for the LLP-1E peptide (data not shown).

Far-UV CD experiments can also be used to monitor the formation of peptide-CaM complexes. Most target peptides form an α-helix when they are bound to CaM, which enhances the negative ellipticity signals of CaM in the far-UV region (Ouyang & Vogel 1998a, also see Chapter 2). Figure 7.3A shows the far-UV CD spectra of CaM, LLP-1A, and the CaM-LLP-1A complex. The enhancement of the CD signal of CaM is obvious after the binding of the peptide. Similar results were obtained with the LLP-1E peptide (data not shown). These data suggests LLP-1A and LLP-1E bind to CaM as α-helices, like most CaM target peptides.

Near-UV CD spectropolarimetry has been proven a useful technique to study the aromatic residues in proteins (Kelly & Price 1997). The near-UV spectrum of CaM displays characteristic peaks arising from its Phe and Tyr residues (Figure 7.3B). CaM is devoid of Trp residues, therefore no signal originating from Trp is detected in CaM's spectrum. Many of CaM's targeting peptides have a Trp residues in their sequence, for example, the CaM-binding domains from CaM kinase I, MLCK, and PDE. The Trp residue in the free peptide usually does not give rise to significant CD signals in the near-UV range. When the CaM kinase I peptide binds to CaM, the Trp residue is anchored in the hydrophobic pocket of CaM, and is now in asymmetric environment which induces its near-UV CD spectrum. The Trp residue in such

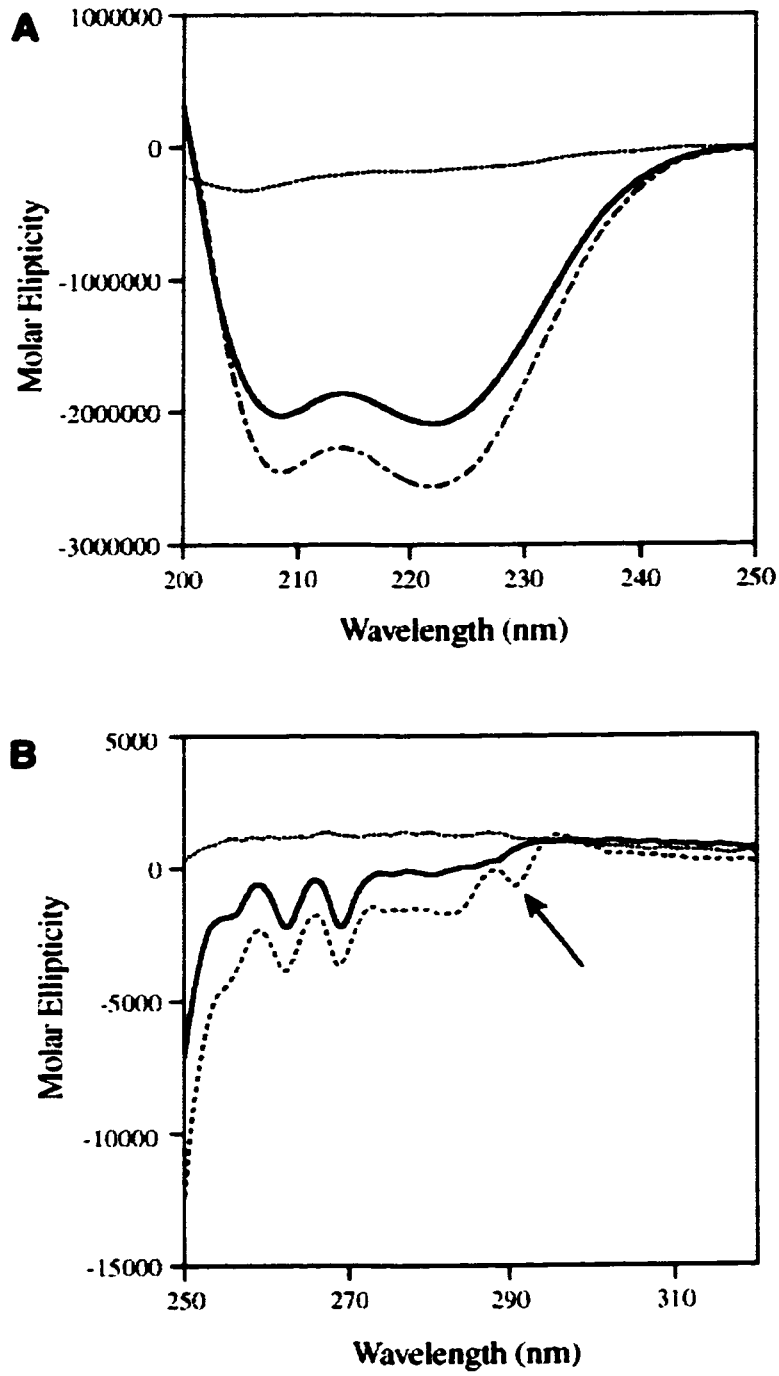

Figure 7.3 (A) Far-UV CD spectra of LLP-1A (dotted line), CaM (solid line), and the CaM-LLP-1A complex (dotted and dashed line). (B) Near-UV CD spectra of LLP-1E (dotted line), CaM (solid line), and the CaM-LLP-1E complex (dashed line). Note the negative peak indicated by an arrow (see text for more details).

a complex normally has a strong positive CD signal around 300 nm (Barth *et al.* 1998, Yuan & Vogel 1998, Yuan *et al.* 1999b, Brokx & Vogel 2000, Gomes *et al.* 2000). When the LLP-1E peptide binds to CaM, the negative signals below 300 nm are enhanced, and a small negative peak was observed around 300 nm as indicated by the arrow in Figure 7.3B. This data is quite different from what was reported for other CaM-binding domain peptides like CaM kinase I, PDE, MLCK, and PGD, which may suggest that the Trp residue in LLP-1E is not anchored to CaM in the same manner as in these peptides. However, it does partially resemble the results obtained with melittin (see Chapter 6).

Fluorescence Spectroscopy and Quenching Experiments

The Trp residue in the LLP-1E peptide makes it convenient to monitor the interaction of LLP-1E and CaM by fluorescence spectroscopy. When excited at 297 nm, the Trp residue in the free peptide has an emission peak around 350 nm (Figure 7.4A). This emission peak displayed a blue shift to around 330 nm when the peptide was bound to CaM. Additionally, the intensity of the emission peak also increased drastically (Figure 7.4A). This phenomena has been observed for many other Trp-containing CaM targeting peptides, for example, the MLCK, CaM Kinase I, and PDE peptides (Ouyang & Vogel 1998b, Yuan *et al.* 1999b, Gomes *et al.* 2000). The blue shift and the increase of the emission peak indicates that the Trp sidechain of LLP-1E enters one of the two hydrophobic pockets on the CaM surface.

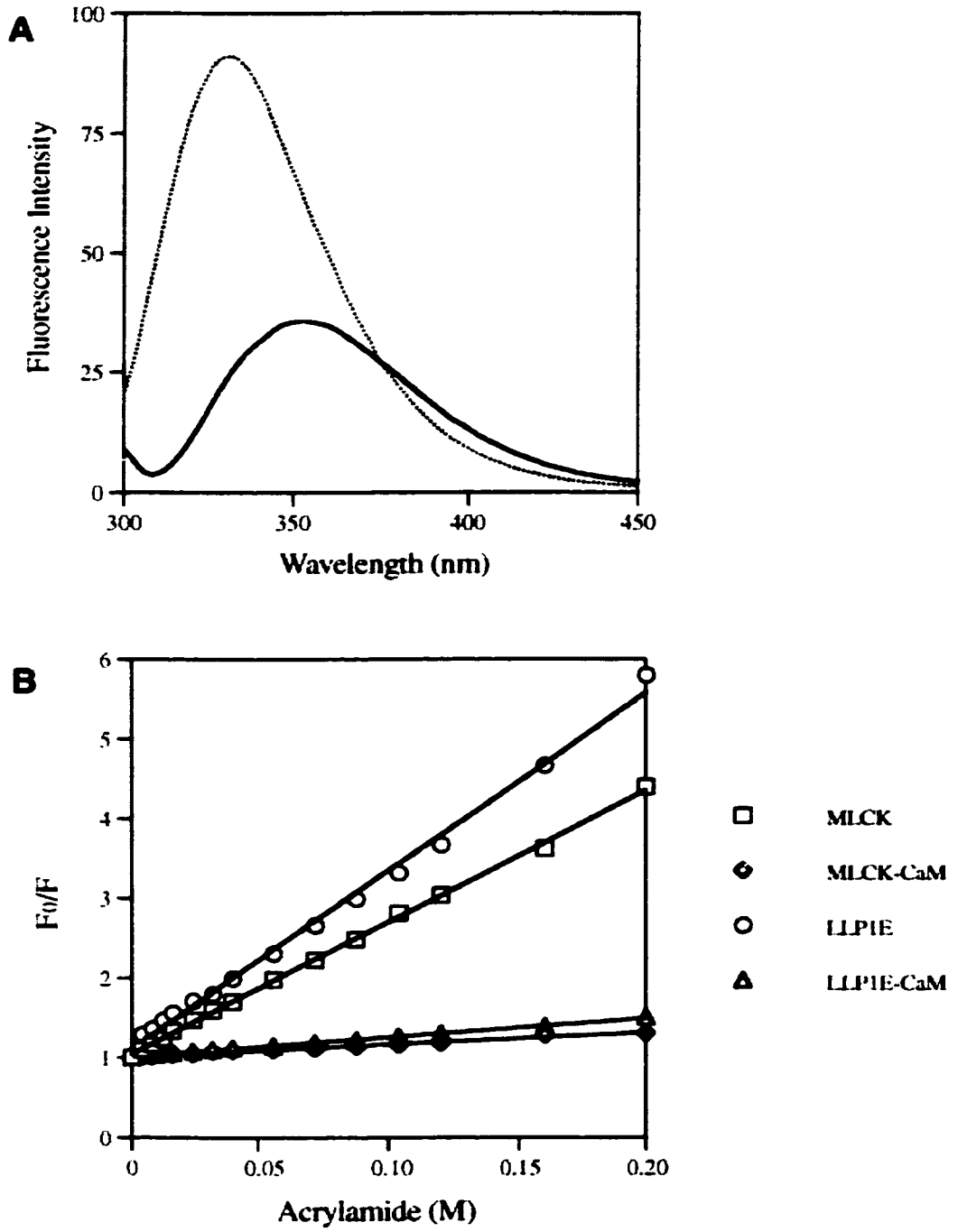

Figure 7.4 (A) Emission spectra of LLP-1E peptide (solid line) and its complex with CaM (dotted line). (B) Stern-Volmer plot of the quenching experiment on LLP-1E peptide and its complex with CaM. Data on the MLCK peptide is also shown for comparison.

Fluorescence quenching experiments were also performed to investigate the solvent exposure of the Trp sidechain. The quenching reagent used in this work was acrylamide. Figure 7.4B shows the Stern-Volmer plot obtained for the quenching experiment. In the free peptide, the Trp sidechain is largely exposed to the solvent, therefore its fluorescence can easily be quenched by acrylamide. Thus, the Stern-Volmer constant for the Trp in the free LLP-1E peptide is relatively large (22.4 M^{-1}). When the peptide binds to CaM, the Stern-Volmer constant becomes much smaller (2.4 M^{-1}), suggesting that the Trp sidechain is buried in the CaM-peptide complex and is not accessible to the solvent (Figure 7.4B). The acrylamide quenching effects on LLP-1E were very similar to those observed for the MLCK peptide whose 3D structure has been determined for its complex with CaM (Figure 7.4B, also see Chapter 6). The Trp residue in the MLCK peptide is anchored into CaM's hydrophobic cleft, and is well protected from the solvent (Ikura *et al.* 1992). The similarity of fluorescence spectra and acrylamide quenching observed for the LLP-1E and MLCK peptides suggests that the Trp residue in LLP-1E is making close contact with CaM and is shielded from the solvent.

Gel Band Shift Assays

Many CaM-binding peptides which have high affinity for CaM can be conveniently studied on a nondenaturing native gel since the CaM-peptide complexes are less mobile on the gel (Ouyang & Vogel 1998a, also see Chapter 2). However, the complexes of the LLP-1 peptides with CaM could

not be detected in 1:1 CaM/peptide mixture using this method, although such a complex was observed for melittin and cNOS under identical conditions (see Figure 2.5). This data suggests that both the LLP-1 peptides have a lower affinity for CaM than other CaM-binding peptides, which is consistent with our NMR results (see below), and with titration studies with dansyl-CaM (Teneza *et al.* 1997).

NMR Experiments

Peptide LLP-1E and C837S were titrated into methyl-^{13}C-Met labeled CaM. Since eight out of all nine Met residues in CaM are located in the hydrophobic patches on the protein surface, Met resonances are very sensitive to peptide binding. Figure 7.5 shows the 2D ^{1}H,^{13}C HMQC spectra of the titration of LLP-1E on methyl-^{13}C-Met labeled CaM. Met resonances are well resolved in free CaM (Figure 7.5A). When 0.5 equivalent of the LLP-1E peptide was added to the sample, all the Met signals were broadened, although M76 was less affected than the other residues (Figure 7.5B). Meanwhile, no new peaks were detected in the spectrum, suggesting the line broadening was caused by intermediate exchange rates. The spectrum changed drastically as the peptide concentration was increased to one equivalent (Figure 7.5C). Generally, all peaks became broader, and many resonances shifted to new positions. The LLP1-E peptide was titrated to 1.2 equivalents to saturate CaM (Figure 7.5D). The spectrum changed slightly with two very broad peaks emerging. Most resonances in the spectrum were

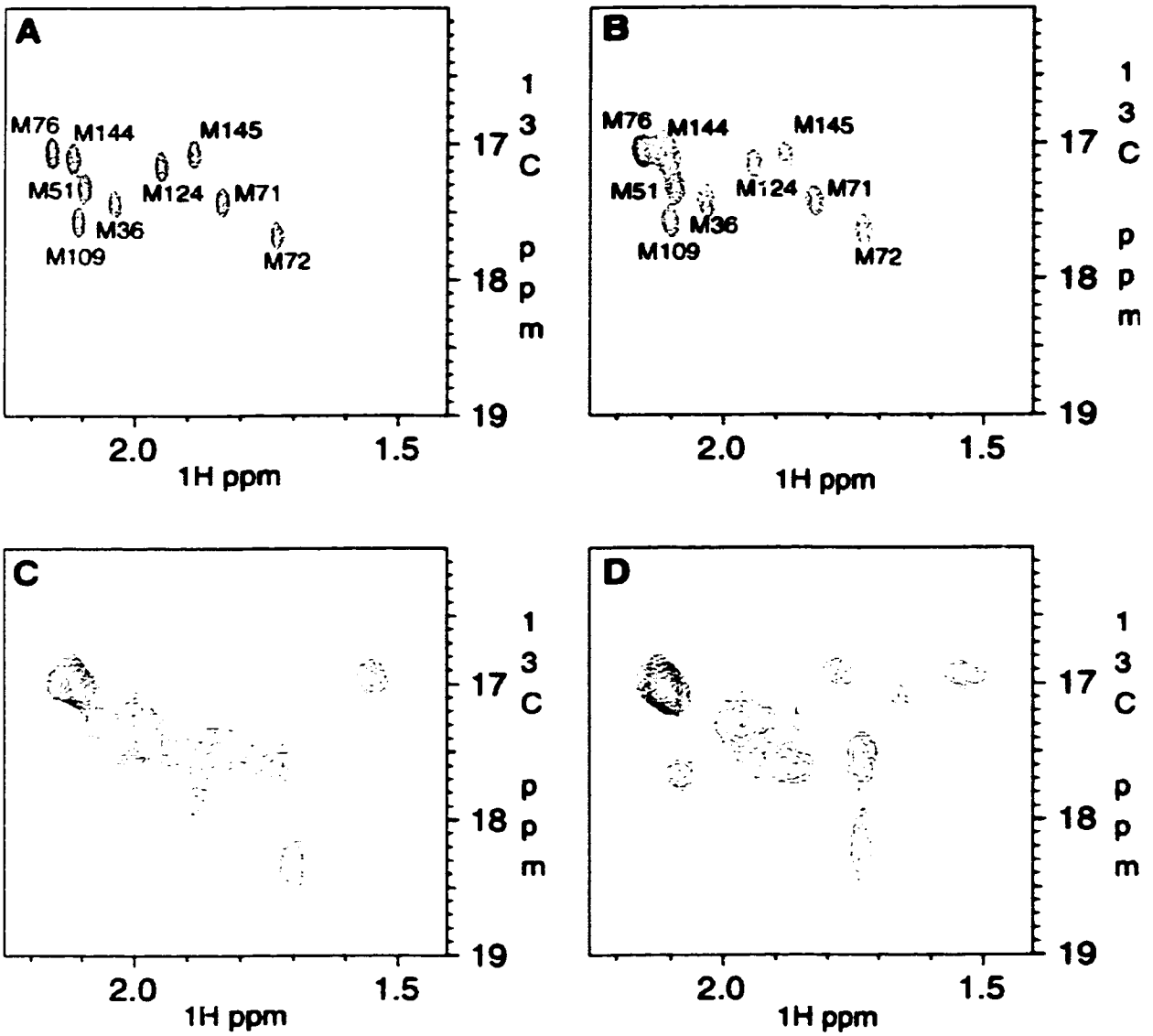

Figure 7.5 2D $^{1}H,^{13}C$ HMQC spectra of methyl-^{13}C-Met labeled CaM with (A) 0, (B) 0.5, (C) 1, and (D) 1.2 equivalents of the LLP-1E peptide. These spectra were recorded at 23.5 °C.

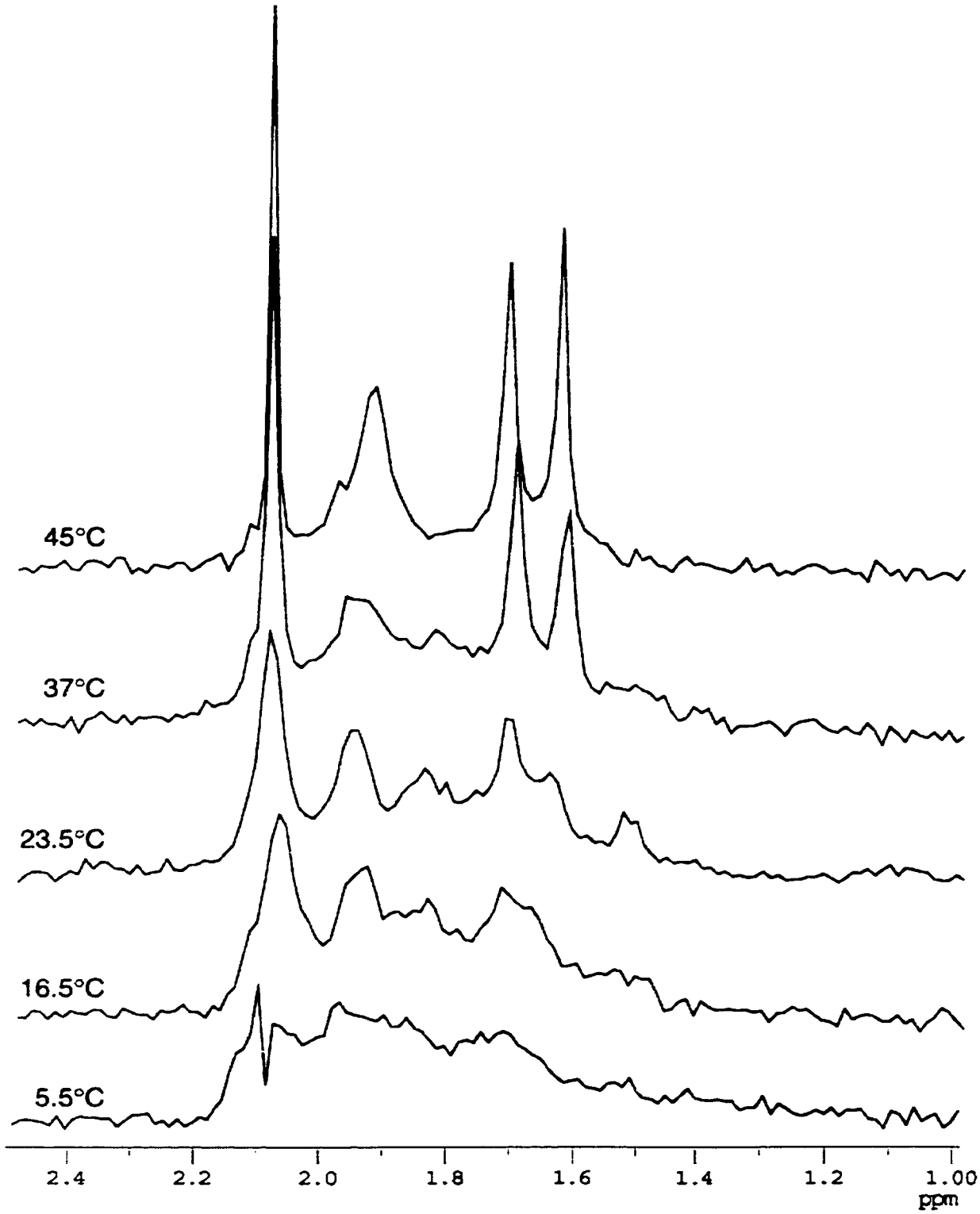

Figure 7.6 1D ^{1}H HMQC spectra of methyl-^{13}C-Met labeled CaM complexed with the LLP-1E peptide (1:1.2 ratio) at different temperatures.

much broader than those from free CaM (Figure 7.5A). One resonance was relatively sharper than others, which is on the top left of the spectrum. This resonance originated from Met76, which is located in the central linker region of CaM instead of the hydrophobic patches, like the other Met residues.

To verify if the line broadening problem observed in the titration process was a result of intermediate exchange, the $^{1}H,^{13}C$ HMQC NMR experiments were also performed at various temperatures. The exchange rates increase giving narrow resonances as the temperature goes up, or vice versa. If the temperature can be adjusted to a point which results in slow or fast exchange, the line broadening problem can be overcome. Figure 7.6 shows

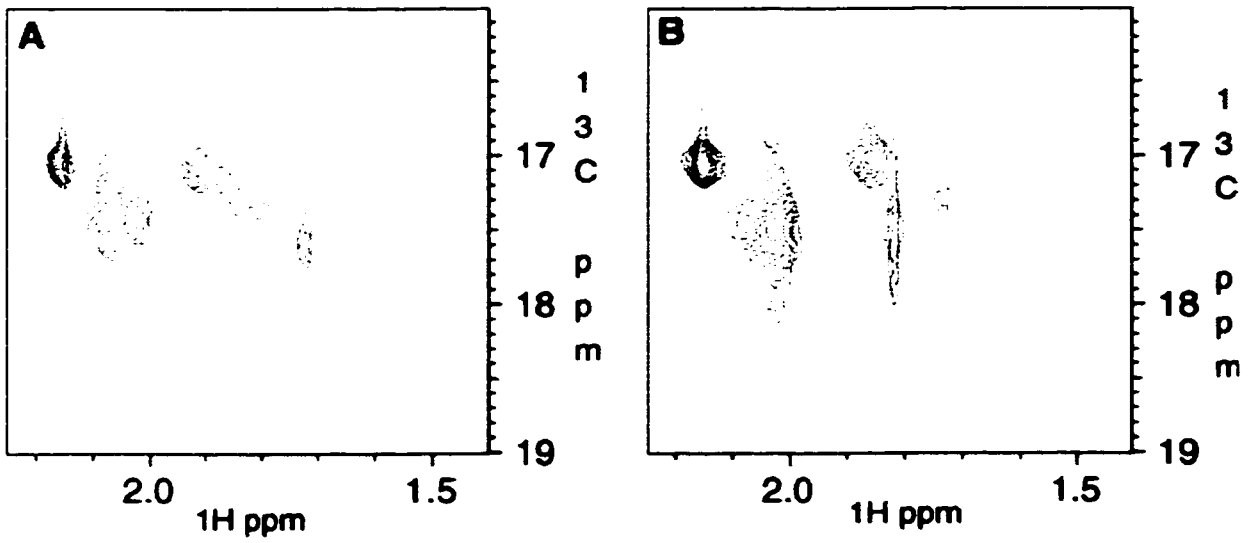

Figure 7.7 2D $^{1}H,^{13}C$ HMQC spectra of methyl-^{13}C-Met labeled CaM with (A) 0.5 and (B) 1.2 equivalent of C837S at 25 °C. .

the 1D ^{1}H HMQC spectra of methyl-^{13}C Met labeled CaM with 1.2 equivalents of LLP-1E peptide at different temperatures. This figure clearly shows that the Met signals become sharper as the temperature is increased. Met resonances were broadened and badly overlapped at 5.5 °C, while they were sharp at 37 °C or 45 °C where a fast exchange rate in the NMR time scale

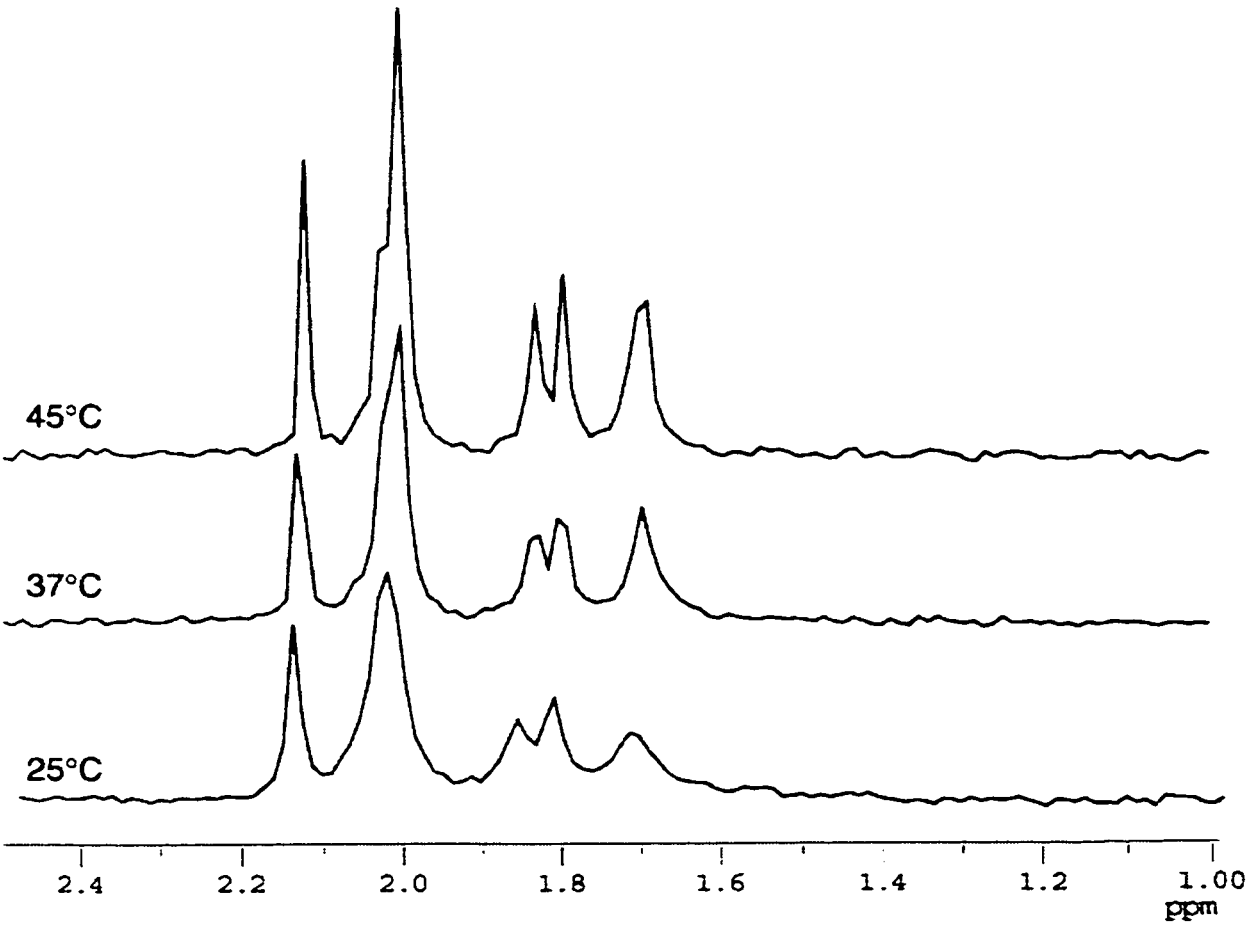

Figure 7.8 1D ^{1}H HMQC spectra of methyl-^{13}C-Met labeled CaM complexed with the C837S peptide (1:1.2 ratio) at different temperatures.

was achieved. These data suggests that the line broadening observed for the peptide-CaM complex at 23.5° C was a result of an intermediate exchange rate.

Similar experiments were performed with the C837S peptide. Figure 7.7 shows the $^{1}H,^{13}C$ HMQC spectra of the titration of C837S with CaM. Very similar results to the LLP-1E peptide titration were obtained as an intermediate to fast exchange rate was observed during these experiments. Figure 7.8 displays the 1D ^{1}H HMQC spectra of CaM with 1.2 equivalents of the C837S peptide at various temperatures, which is also similar to the results obtained before.

SAXS Experiments

The radius of gyration (R_g) value calculated from the small angle X-ray scattering data gives a simple geometric measure of how extended the protein is in solution. Normally, the R_g value is 20.0 Å for apo-CaM, and 21.2 Å for Ca^{2+}-saturated CaM. When CaM binds a target peptide such as the MLCK peptide, the R_g value decreases significantly, to 16.4 Å for the CaM-MLCK peptide complex (Yoshino *et al.* 1996, Trewhella & Krueger 2000). This

Table 7.2 R_g Values of CaM-LLP-1A peptide complex

	EDTA	1Ca	2Ca	3Ca	4Ca	5Ca
Rg(Å)	20.5	23.1	21.6	21.1	20.8	21.1

decrease in the R_g value suggests that CaM forms a more globular complex with the MLCK peptide, consistent with the NMR structure (Ikura *et al.* 1992). Table 7.2 shows the R_g values of CaM and its complexes with the LLP-1A peptide. Only a slight decrease in the R_g values were observed for the Ca^{2+}-CaM-peptide complex (20.8 Å and 21.1 Å for $4Ca^{2+}$-CaM and $5Ca^{2+}$-CaM respectively), which was quite distinct from what was obtained for the CaM-MLCK peptide complex. This data suggests that the complex of CaM formed with the LLP-1A peptide was not collapsed as the one with the MLCK peptide.

P(r) is another parameter determined from SAXS data that is often used to investigate protein structure. P(r) is extremely sensitive to the overall shape of the scattering particle, and to the relationships between domains and repeating structures (Trewhella 1992, Trewhella & Krueger 2000). The P(r) function of CaM has a major peak around 18 Å, and a minor peak around 40 Å, which is characteristic for a dumbbell shaped structure. P(r) goes to zero at a value corresponding to the maximum dimension of the particle, *dmax*. The measured *dmax* for free Ca^{2+}-CaM is 69 Å (Trewhella & Krueger 2000). When CaM binds the MLCK peptide, it forms a globular shaped complex whose P(r) functions displays a single symmetric peak. In the meantime, a reduction of 20 Å in *dmax* was also observed for the complex (Trewhella 1992, Trewhella & Krueger 2000). Figure 7.9 shows the P(r) functions measured for CaM complexes with the LLP-1A peptide. When the availability of Ca^{2+} ions was low (0 - 1 equivalent), the P(r) functions remained very similar to those of free

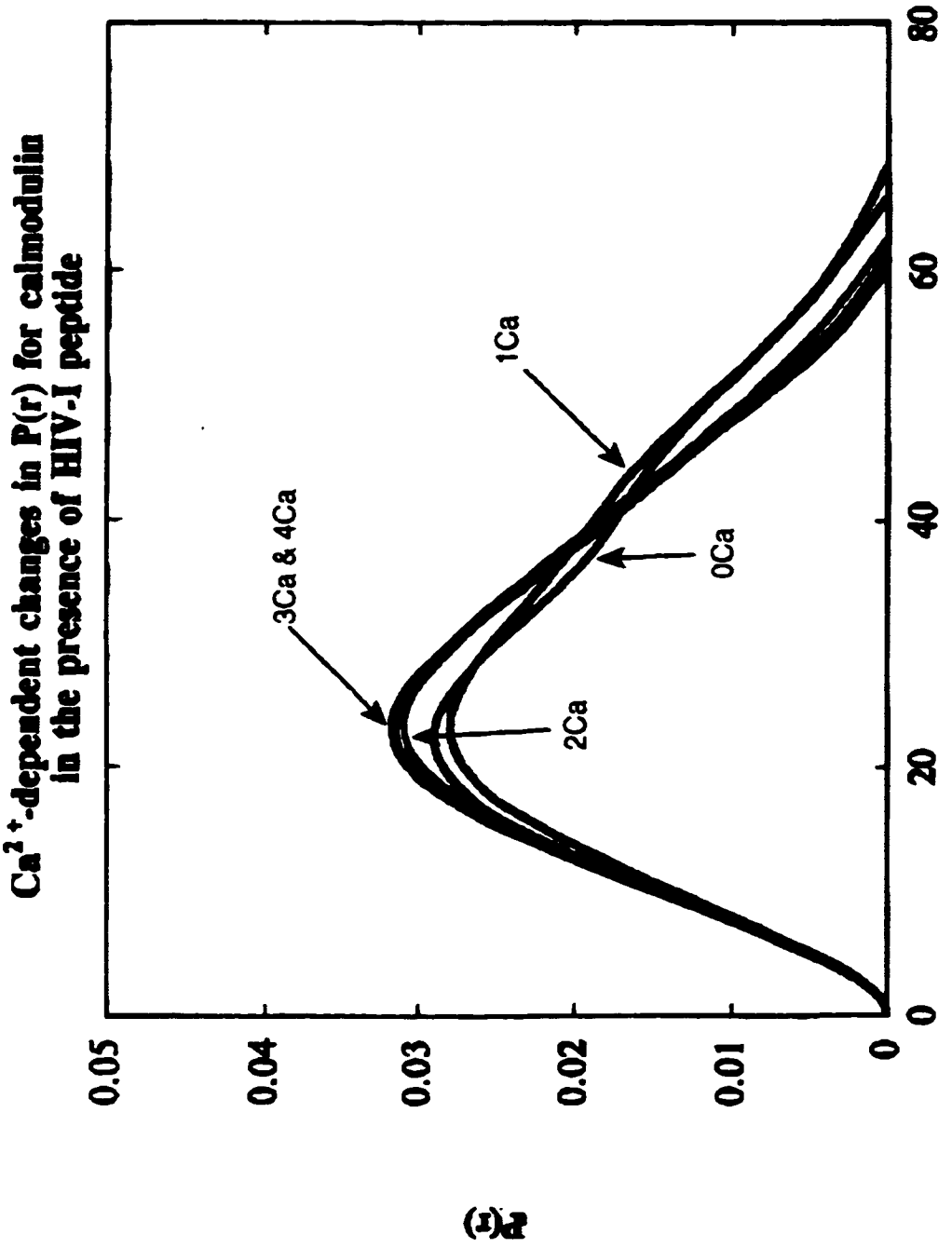

Figure 7.9 P(r) functions of the CaM-LLP-1 complex with various calcium concentrations.

CaM with clear observation of the minor peak around 40 Å (Figure 7.9). When the Ca^{2+} concentration was increased, this minor peak disappeared as the P(r) functions displayed a single peak, indicating a CaM-peptide complex was formed. However, the *dmax* measurement of this complex (around 61 Å) was only slightly lower than that of free CaM (69 Å). These data suggests that the complex of CaM and LLP-1A peptide has a different shape from the CaM-MLCK peptide complex, which is probably more compact.

Discussion

The transmembrane glycoprotein (gp41) of HIV possesses a segment in its cytoplasmic domain that has CaM-binding properties. In this work, we have studied the interaction of CaM with peptides derived from these segments in different HIV-1 isolates using various approaches. The structural information on TM proteins suggests that these segments have a tendency to form α-helical structures (Srinivas *et al*. 1992, Koenig *et al*. 1999). Indeed, our far-UV CD data indicated that the LLP1 peptides adopt α-helical conformation in TFE solutions (Figure 7.2). Moreover, our data suggests that these peptides bind to CaM with an α-helical structure (Figure 7.3A). This data is in agreement with the results obtained for a related SIV peptide (Yuan et al. 1995). Among the peptides included in this work, the LLP1-E peptide is of special interest for spectroscopic studies since it possesses a single Trp residue in its sequence. A single Trp residue has been found in several CaM binding peptides, which shows characteristic properties in CD

and fluorescence experiments. Near-UV CD is a useful method to study the aromatic residues in peptide-protein complexes. The Trp residue in the free peptide normally does not give rise to a strong CD signal. However, the Trp residue in several typical CaM-binding peptides, such as the MLCK, CaM Kinase I, and PDE peptides, show prominent positive CD bands around 300 nm when they bind CaM. In the near-UV CD spectrum of the CaM-LLP1-E peptide complex, only a small negative band was observed at 300 nm (Figure 7.3B). This result implies that the microenvironment around the Trp sidechain in this complex is distinct from those of other well-studied model peptides, although our fluorescence experiments indicated that the Trp sidechain enters the hydrophobic cleft in CaM's binding site and was well protected from the solvent (Figure 7.4 and 7.5). Interestingly, a similar phenomenon has been observed for melittin, another CaM-binding peptide (see Chapter 6). Melittin has a Trp residue close to its C-terminus, which is quite unique among CaM-binding peptides. Despite tight binding, the near-UV CD spectrum of CaM-melittin complex also lacks the positive signal around 300 nm. We propose that this unusual observation might be due to a distinct orientation of the Trp sidechain in the hydrophobic pocket. This could also be the case for the LLP1-E peptide. In fact, it has been found that not all Trp residue anchors into the hydrophobic cleft of CaM in the same manner. For example, the Trp residue in the CaM-binding domain of the Ca^{2+}-pump enters the hydrophobic cleft with a different angle than other known structures (Elshort *et al.* 1999). If the Trp residue adopts a distinct angle, the

microenvironment around it would be altered which may result in different CD properties, as was observed in the case of the LLP-1E and melittin peptides. It is also possible that there is some flexibility in the complex and that the Trp sidechain is not firmly anchored in the hydrophobic pocket. This interpretation might be consistent with the NMR data discussed below.

Fast to intermediate exchange rates were observed when these LLP-1 peptides were titrated into methyl-^{13}C-Met labeled CaM (Figure 7.5, 7.6, 7.7, and 7.8), which are an indication of relatively weak interactions. A close comparison of the NMR titrations of the C837S and LLP-1E peptides with CaM revealed that a faster exchange rate was observed for the C837S peptide, indicating that the LLP-1E peptide has a higher affinity for CaM than the C837S peptide. Slow exchange rates are normally observed when the binding is strong, for instance, the cerebellar nitric oxide synthase or the CaM Kinase I peptide (Zhang *et al.* 1995a, Yuan & Vogel, unpublished results). Our results presented here are consistent with previous report by Tencza *et al.* (1997). These authors have measured the binding constants of a series of LLP-1 peptides to dansyl-CaM. Most of their LLP-1 peptides (or mutants) have K_d values in the range from 20 nM to 200 nM. More specifically, LLP-1A, C837S, and LLP-1E have a K_d value of 100 nM, 70 nM, and 15 nM, respectively (Tencza *et al.* 1997). Thus, these peptides have a lower affinity for CaM than typical model CaM-binding peptides, such as MLCK or CaM Kinase I peptides, which have a K_d values around 1 nM (O'Neil & DeGrado 1990). It should be pointed out that although the CaM-binding affinities of

these HIV peptides are lower than some typical CaM-binding peptide, it does not mean they cannot affect CaM-dependent pathways *in vivo*. First of all, CaM is such a versatile protein regulating a large number of substrate enzymes. Peptides derived from the CaM-binding domains of some CaM target proteins have significantly lower affinity than the model peptides mentioned above. For example, the CaM-binding peptide from the Ca^{2+} pump has a K_d value of 600 nM for CaM (Enyedi *et al.* 1989), which is much higher than those of the LLP peptides. Target proteins like this could be readily affected by the introduction of the LLP segments from HIV. Secondly, the K_d values are normally obtained *in vitro*, which could be quite different from the conditions *in vivo*. Moreover, the separated peptides do not always behave exactly like the whole protein. Proteins normally have a higher binding affinity for CaM than isolated peptides. Therefore, it is impossible to tell which CaM-modulated pathway HIV will interfere with simply from the CaM-binding constants of the LLP peptides. Nevertheless, with K_d values in the lower nanomolar range, it is likely that many CaM-regulated pathways would be affected by HIV. In fact, the co-localization of HIV-1 gp160 and CaM within a cell has been reported (Radding *et al.* 1996), suggesting that CaM-TM interaction indeed occurs *in vivo*.

The SAXS data obtained for the CaM-LLP-1A peptide complex was significantly distinct from that of CaM-MLCK peptide complex. The SAXS parameters of the CaM-MLCK complex had a R_g value around 16 Å, d_{max} around 40 Å, and symmetric P(r) functions, which were quite different from

free CaM (Trewhella 1992). All these SAXS data indicate that the CaM-MLCK complex is a compact spherical globule. The SAXS data collected for the CaM-LLP-1A complex didn't display such drastic changes when compared to free CaM. Both R_g and *dmax* only decreased slightly. The most significant change is the disappearance of the minor peak in the P(r) functions of the CaM-LLP-1A complex, which suggests the complex is no longer a two-lobed object like free CaM. Taken together, the LLP-1A peptide probably binds to CaM to form a complex with a more extended overall shape than the CaM-MLCK complex.

It has not been established how the binding of LLP-1 segments to CaM will affect the infected cell or HIV itself. Given that LLP-1 is a competitive inhibitor of CaM-dependent phosphodiesterase (Miller *et al.* 1993c), a number of CaM-dependent pathways could be perturbed. Although still under debate (Prati *et al.* 1997), some investigators believe that CaM-TM interaction may also be involved in the increasing apoptosis rate of HIV-infected T cells (Pan *et al.* 1996, Micoli *et al.* 2000).

In conclusion, our work indicates that the LLP segments from the glycoprotein of HIV bind to Ca^{2+}-CaM in a different manner compared to typical model CaM binding peptides. For example, the Trp residue in LLP-1E probably enters into the hydrophobic cleft of CaM with a different orientation or is more mobile. The CaM-LLP-1 complex is likely to adopt a more extended conformation than the CaM-MLCK complex. The finding of these subtle differences certainly furthers our understanding of possible HIV-infection

mechanisms, which may eventually lead to improved therapies for AIDS treatment.

Chapter 8

M-domain of *Escherichia coli* ffh Protein: Cloning, Expression, Purification, and Structural Modeling

Abstract

The ffh protein of *E. coli* is a structural homologue of mammalian SRP54, a key component of the signal recognition particle, which is responsible for recognizing the signal sequence of nascent secretory or membrane proteins. The Met-rich domain (M-domain) of ffh protein is believed to bind signal sequences in a sequence-independent manner, which resembles the interactions between CaM and its target peptides. In both cases, the peptides are of a basic hydrophobic nature, but have no obvious amino acid sequence homology. We attempted to express and purify the M-domain in this work. The M-domain was successfully overexpressed as an fusion protein in both the Maltose Binding Protein and Thioredoxin Fusion systems. A portion of the fusion proteins formed inclusion bodies. No expression of the M-domain was observed when using the pCaM plasmid. The high hydrophobicity and intrinsic flexibility of the M-domain made it difficult to purify after it was cleaved from the fusion protein. Homology modeling was also performed on the M-domain from *E. coli*, using the crystal structure of the ffh protein from *T. aquaticus* as a template. The comparative modeling indicates that the M-domain possesses a large hydrophobic surface for

binding the signal sequence. The majority of the Met residues are located in this hydrophobic cleft, implying that, as in CaM, the Met sidechains, with their unique hydrophobicity and flexibility, play an important role in the sequence-independent substrate recognition ability of the M-domain.

Introduction

Signal Sequence Many proteins have to be positioned at the right location to fulfill their tasks. Some proteins are located in the cytoplasm, some are secreted to the outside, while others are resident in membranes. However, all proteins are synthesized by the same cytosolic ribosome pool, therefore a protein sorting and translocating system is required. This system must distinguish secretory and membrane proteins from cytosolic proteins, and then direct them into or out of the cell membrane. Secretory and membrane proteins in both prokaryotic and eukaryotic cells possess an N-terminal "signal sequence" on the nascent polypeptide, which distinguishes them from cytoplasmic proteins. Such a signal sequence can be endoproteolytically removed by a signal peptidase during or after the translocation process (Wei & Stader 1994, Paetzel *et al.* 1998). One intriguing feature of these sequences is that they share little amino acid sequence homology. Even the length of signal sequences for different proteins varies (Von Heijne 1985, Gennity *et al.* 1990). Despite these variations in length and amino acid sequence, however, signal sequences seem to be functionally interchangeable. Recombinant proteins composed of a signal sequence from

one organism and a mature secretory protein from another organism are frequently exported without difficulty (Yost *et al.* 1983, Jabbar & Nayak 1987, Wingren *et al.* 1996).

Although signal sequences vary in overall length and primary structure, they do share some common features. Signal sequences from all species display three structurally dissimilar regions: a positively charged N-terminal region, a central highly hydrophobic region and a more polar C-terminal region (Gierasch 1989, Gennity *et al.* 1990). The N-terminal region is mostly responsible for the length variation of signal sequences: it can be as short as 1 residue, or as long as 17 residues. Nevertheless, the N-terminal region always carries a net positive charge (a mean value of +1.7 in both eukaryotes and prokaryotes). This charge comes from basic residues in prokaryotes, while in eukaryotes, the positively charged N-terminus can also make a contribution (Von Heijne 1985). The central hydrophobic region, also called the "h-region", also varies in length and composition. The h-region is rich in hydrophobic residues, such as Leu, Ala, Met, Val, Ile, Phe and Trp, although it may contain an occasional Pro, Gly, Ser or Thr residue; it is 7 to 15 residues long and serves as a hydrophobic core for signal sequences. There is no internal sequence homology among various h-regions, and statistical analysis suggests that overall hydrophobicity is the major requirement for the h-region. In fact, introduction of a charged residue into this region significantly affects the function of the signal sequence, regardless of the specific position of the mutation (Gierasch 1989, and references therein). Immediately following the

h-region is the C-terminal region whose hydrophobicity is sharply reduced. The C-terminal region is normally 5 to 7 residues long, and always contains a signal peptidase recognition site, Ala-X-Ala (Gierasch 1989, Gennity *et al.* 1990, Wei & Stader 1994). It is generally believed that the C-terminal region of a signal sequence provides the cleavage site for signal peptidase; the h-region is the main binding site for recognition by the translocation machinery; and that the N-terminal region can interact with the surface of membranes (Gierasch 1989). The h-region is the true hallmark of signal sequences which distinguishes nascent secretory and membrane proteins from cytoplasmic proteins.

Signal Recognition Particle In mammalian cells, the synthesis of secretory and membrane proteins takes place on ribosomes that are bound to the rough ER membrane, and protein translocation and integration occur cotranslationally, i.e. simultaneously with ongoing protein synthesis (Walter & Johnson 1994). Since all the other proteins are synthesized on ribosomes that are free in the cytosol, a mechanism is needed to selectively direct the ribosomes for secretory or membrane protein synthesis to the ER membrane. The signal recognition particle (SRP) and its receptor on the ER membrane have been identified as key components for such a system (Walter & Blobel 1980, 1981). In eukaryotic cells, the targeting of most proteins to the ER membrane is mediated by SRP-targeting pathway although alternative routes have been suggested (Rapoport *et al.* 1996, De Gier *et al.* 1997). A

detailed model for the SRP-mediated translocation process has been proposed (Walter *et al.* 1984, Walter & Schekman 1986, Rapoport 1992, Sanders & Schekman 1992). When a signal sequence of a nascent polypeptide emerges from the ribosome, it is recognized by SRP. This recognition results in strong interactions between SRP and the ribosome, which stops further synthesis of the nascent polypeptide chain (this step is also called "elongation arrest"). Subsequently the "arrested" complex is translocated to the ER membrane. Once SRP interacts with the SRP receptors on the ER membrane, the ribosome binds to the translocon in the membrane. The SRP then dissociates from the ribosome and is released from the ER membrane. The translation of the nascent polypeptide resumes in the translocon-bound ribosome, presumably through a gated aqueous pore on the translocon (Walter & Johnson 1994). SRP plays a key role in this process by selecting and targeting the ribosomes that are synthesizing secretory and membrane proteins to the ER membrane.

Human SRP is a cytosolic ribonucleoprotein complex which consists of one 7S RNA molecule, called SRP RNA, and six different polypeptides with molecular masses of 9, 14, 19, 54, 68, and 72 kD, which are designated SRP9, SRP14, SRP19, SRP54, SRP68, and SRP72, respectively (Walter & Johnson 1994, Rapoport *et al.* 1996). The SRP RNA is the central component of SRP: it provides the backbone for the assembly of the SRP proteins; it may also mediate SRP's association with the ribosome and the SRP receptor. The protein components assemble along the SRP RNA to form a rod shaped

complex. SRP9 and SRP14 bind to SRP RNA as a heterodimer whose function is probably involved in elongation arrest after SRP binds to the ribosome (Walter & Blobel 1983, Siegel & Walter 1985). SRP68 and SRP72 also bind to SRP RNA as a stable heterodimer which might mediate the association with the SRP receptor on the ER membrane (Siegel & Walter 1988, Patel & Austen 1996). Both SRP19 and SRP54 bind to SRP RNA individually. SRP19 seems to promote the binding of SRP54 to SRP RNA since SRP54 and SRP RNA can not form a stable complex without SRP19 (Miller *et al.* 1993). SRP54 is the key component in SRP since its main function is to specifically recognize and bind signal sequences (Hauser *et al.* 1995). SRP54 is the only SRP component that becomes photo-cross-linked to the signal sequence of a nascent polypeptide (Krieg *et al.* 1986, Kurzchalia *et al.* 1986). SRP54 also mediates the release of the signal sequence and the dissociation of SRP from the SRP receptor which make it available for a next translocation cycle (Connolly *et al.* 1991, Miller *et al.* 1993).

SRP54 attracts more research interest than the other SRP proteins because it plays a key role in the signal recognition process. In fact, SRP54 alone has been shown to be able to bind signal sequences (Hauser *et al.* 1995). Amino acid sequence analysis predicted that SRP54 contains a putative N-terminal GTP-binding domain (called "G-domain") and a C-terminal Met-rich domain, often referred to as "M-domain" (Bernstein *et al.* 1989). The GTP-binding domain has an unusual GTP-binding motif which has not been found in other GTP-binding proteins except SRP receptors (Bernstein *et al.* 1989).

Hydrolysis of GTP is not required for signal sequence binding or targeting of the ribosome to the ER membrane (Zopf *et al.* 1993, Rapiejko & Gilmore 1994). However, the GTPase activity plays a role in the dissociation of SRP from the SRP receptors (Walter & Johnson 1994). The smaller C-terminal M-domain is more important in function. M-domain possesses an RNA-binding site which is necessary for SRP54 to interact with SRP RNA (Römisch *et al.* 1990). The M-domain also contains the signal sequence binding site since the signal sequence can be photocrosslinked to the M-domain rather than the G-domain (Zopf *et al.* 1990, High & Dobberstein 1991).

The M-domain's ability to recognize so many signal sequences with different primary structures is very intriguing. The interactions between SRP and the signal sequences are basically sequence-independent. Such sequence-independent interactions have also been found in one other example of protein-protein interactions: CaM and its multiple substrates (O'Neil & DeGrado 1990). The M-domain and CaM have one thing in common: they both are Met-rich proteins. In fact, M-domain of SRP54 has an even higher Met content (11%) than CaM (5.6%), which suggests that its Met residues could make a unique contribution to the recognition of the signal sequence (Figure 8.1, see also chapter 1).

Protein Translocation in E. coli and the ffh Protein Protein targeting and translocation in bacteria was initially believed to be mediated solely through the Sec-dependent pathway. The Sec pathway in *E. coli* has been

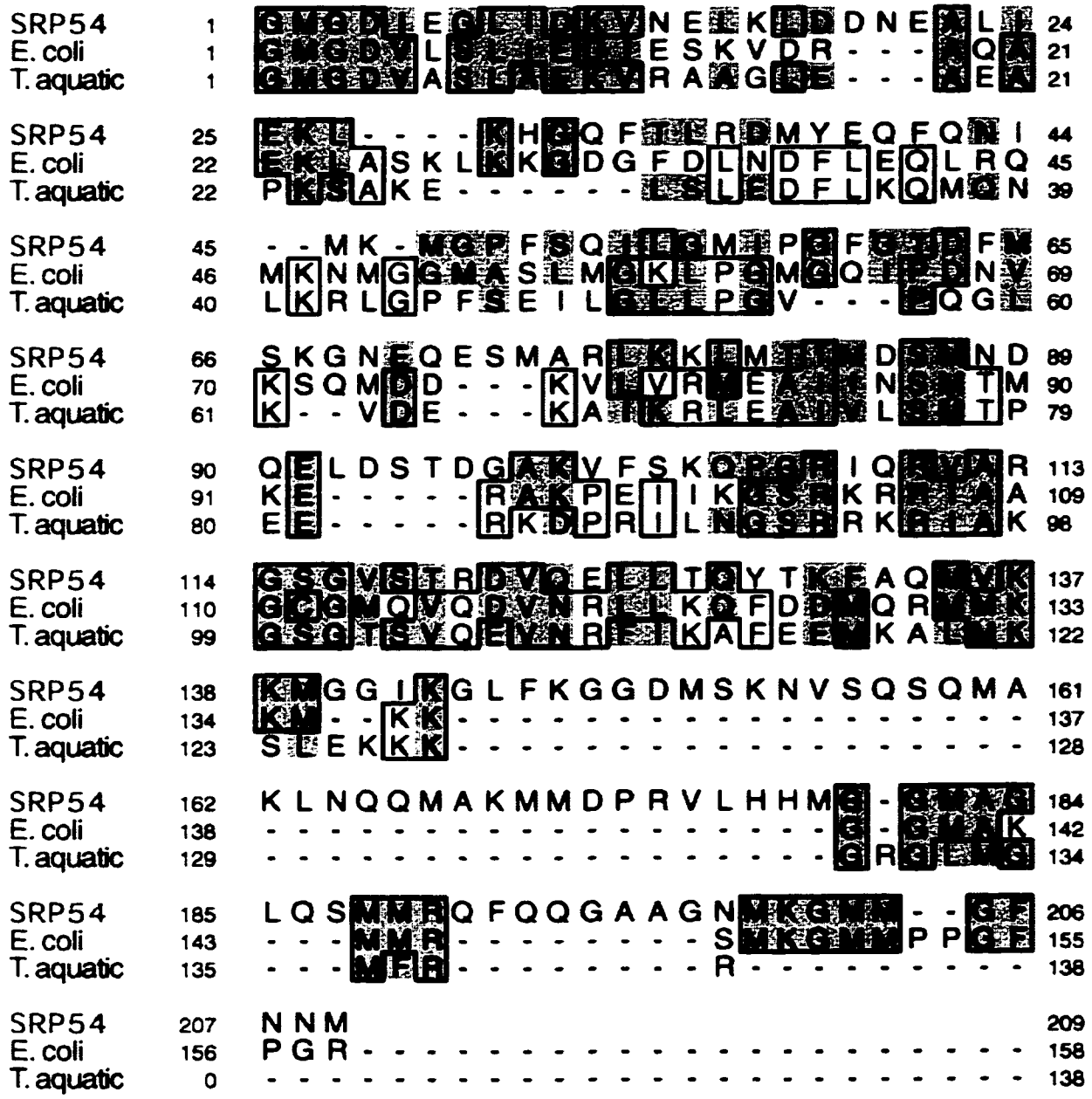

Figure 8.1 Sequence alignment of the M-domains of human SRP54, *E. coli* ffh, and *T. aquaticus* ffh. The identical sequences are boxed, while the homologous sequences are shaded.

extensively studied. There is a proteinaceous translocon in the cytoplasmic membrane of *E. coli* which consists of the core components SecY, SecE, and SecG. Substoichiometric components of the translocon, such as SecD, SecF, and yaiC are also required for efficient translocation. The Sec pathway uses a cytosolic chaperone, SecB, that binds post-translationally at a late translational stage to the mature region of pre-proteins (Kumamoto & Francetic 1993). SecB targets pre-proteins to the membrane by binding to SecA with high affinity. Although SecA is not an integral part of the *E. coli* translocon, it is considered a part of the dynamic structure of the translocon during the translocation process. After the pre-protein binds to the membrane-embedded translocon, SecB is released from the pre-protein as the ATPase of SecA mediates the ATP-driven post-translational translocation (Economou & Wickner 1994, Economou *et al.* 1995).

While the Sec pathway has been established as the main translocation pathway in *E. coli*, an SRP pathway has recently been discovered when a previously uncharacterized *E. coli* protein was found to have strong sequence homology to SRP54 in mammalian cells (Bernstein *et al.* 1989). This protein was named ffh (fifty-four homologue). In the meantime, another *E. coli* protein, FtsY, has also been found to resemble SRα, an SRP receptor protein on the ER membrane in eukaryotic cells (Connolly & Gilmore 1989). More recently, a 4.5S RNA has been found to show strong homology to 7S SRP RNA, and the 4.5S RNA and ffh form a ribonucleoprotein complex (Poritz *et al.* 1990, Ribes *et al.* 1990). This ffh/4.5S RNA ribonucleoprotein complex is

also able to bind signal sequences (Luirink *et al.* 1992). The finding of ffh, 4.5S RNA and FtsY suggests that the SRP pathway is a common protein targeting and translocation pathway that is conserved from bacteria to mammals. Miller *et al.* (1994) demonstrated that the ffh/4.5S RNA indeed interacts with FtsY with high affinity. The binding of ffh/4.5S RNA ribonucleoprotein to FtsY is GTP-dependent. This interaction results in the stimulation of GTP hydrolysis which can be inhibited by synthetic signal peptides. These properties resemble those of mammalian SRP and its receptor, which strongly suggests that the *E. coli* ffh/4.5S RNA ribonucleoprotein and FtsY have functions in protein targeting and translocation pathway similar to their mammalian counterparts.

The full physiological significance of the *E. coli* SRP pathway is still not clear. Some research has shown that the ffh protein is necessary for efficient protein export, which may affect the bactera's growth and viability (Philips & Silhavy 1992, Samuelsson *et al.* 1995). Although the *E. coli* SRP pathway is believed to function similarly to its mammalian counterpart, there are some obvious differences. Although ffh protein closely resembles SRP54, no homologues of other eukaryotic SRP proteins have been found in *E. coli*. Moreover, *E. coli* 4.5S RNA is smaller than the 7S SRP RNA in mammalian cells, which possesses the binding loops for the other SRP proteins, SRP9, SRP14 and SRP19 (Walter & Johnson 1994). Therefore, the ffh/4.5S ribonucleoprotein complex seems to be sufficient to perform the protein targeting process in *E. coli*. Thus, elongation arrest (mediated by SRP9 and

SRP14 in mammalian cells, see above) does not occur in *E.coli*. While the SRP pathway is believed to mediate cotranslational translocation (Powers & Walter 1997), there must be a time window in *E. coli* where protein synthesis is taking place before the ribosome is directed to the membrane. Nevertheless, sequence analysis indicated that ffh and SRP54 are closely related with relatively high homology (31% sequence identity, see Figure 8.1). Bernstein *et al.* (1993) have even shown that ffh protein can substitute for SRP54 in a mammalian SRP complex. Ffh assembles efficiently with other SRP components to form a chimeric ribonucleoprotein. Although such a complex is not able to promote the protein translocation across the membrane, it does specifically recognize the signal sequence of a nascent polypeptide, and it can arrest elongation of the preprotein like a normal mammalian SRP complex. On the other hand, SRP54 can also recognize signal sequences when introduced in E. coli, although it does not interact with FtsY (Patel & Austen 1996). Thus, ffh and SRP54 are at least partially functionally interchangeable, suggesting that they have similar structure.

Structural Studies on ffh and its M-domain Ffh protein , with a molecular weight around 48 kDa, is a slightly smaller protein than eukaryotic SRP54. Ffh and SRP54 share high sequence homology, with 31% identity and 60% similarity (Bernstein *et al.* 1989, Figure 8.1). To completely understand how SRP54 or ffh protein functions, it is necessary to resolve their 3D structures. There are only two ways to determine protein structure at present,

X-ray crystallography and NMR spectroscopy. A large quantity of protein is required for success in either approach. Therefore, a protein usually has to be cloned and overexpressed in *E. coli* or another microorganism to provide enough material for structure determination. To date, most of the interest has been focused on the ffh protein even though SRP54 was better characterized functionally (of course, the cloning and expression of SRP is also under way, for example, see Gowda *et al.* 1998).

Sequence analysis predicted two distinguishable domains in the ffh protein, a G-domain and an M-domain (Berstein *et al.* 1989). Freymann *et al.* (1997) recently determined the X-ray structure of the GTP-free G-domain of ffh protein. These authors cloned ffh from *Thermus aquaticus* and expressed it in *E. coli*. Limited proteolysis using elastase was performed on ffh to separate the G-domain from the M-domain. The G-domain was then purified and crystallized. The crystal diffracted at 2.05 Å resolution, and the molecular structure was determined. It is now clear that the so-called "G-domain" actually contains two distinct, yet closely associated domains. On the N-terminal side of the GTPase domain (G-domain), there is a bundle of four antiparallel α-helices, which is called the "N-domain". The N-domain tightly associates with the G-domain by opening the helix bundle at one end, allowing sidechains of the G-domain to complete packing of its hydrophobic core. A ten-residue peptide that links the two domains is packed tightly against the protein surface. The function of the N-domain has yet to be elucidated. There are some indications that the N-domain might promote efficient signal

sequence binding in SRP54 (Newitt & Bernstein 1997). The core GTPase fold of Ffh is a five-stranded β-sheet surrounded by α-helices. The binding of GTP and GDP induces a significant conformational change in the G-domain (Farmery *et al.* 1997, Freymann 1999), although the exact function of such a conformational change is still not clear. The crystal structure of the NG-domain of FtsY, the Ffh receptor, has also been determined, showing that the NG-domain from Ffh and FtsY are very similar in structure. The SRP-type GTPases are now being regarded as a distinct subfamily of GTPase (Montoya *et al.* 1997).

Freymann *et al.* (1997) did not include the M-domain in their original crystallography studies probably because the intact ffh protein proved difficult to crystallize. The initial structural information about the M-domain came from inspection of the amino acid sequence (Bernstein *et al.* 1989). These authors predicted that the M-domain of ffh possesses three amphiphilic α-helices. One face of these helices is highly hydrophobic with many Met residues, while the other side of is polar, and contains several charged residues. It was believed that the hydrophobic side of these helices could form a hydrophobic groove on the protein surface, which serves as a signal peptide binding site. Oh *et al.* (1996) chemically synthesized a 25-residue-long peptide corresponding to one of the proposed Met-rich amphiphilic helices and studied it by CD and NMR spectroscopy. They found that this linear peptide formed an appreciable amount of α-helical structure even in aqueous solution, and that this α-helical conformation was stabilized

in aqueous TFE cosolvent solutions. This investigation supported the secondary structure prediction by Bernstein *et al.* (1989). This chapter describes our attempts to clone and overexpress the M-domain of *E. coli* ffh in order to study the structure of the M-domain by NMR spectroscopy.

Recently, Keenan *et al.* (1998) succeeded in crystallizing the entire ffh protein from the thermophilic bacterium *T. aquaticus* in the presence of detergents. The ffh protein crystallized as a trimer under these conditions. A protein structure at 3.2 Å resolution was obtained from these crystals. This structure missed eleven amino acids in the linker region between the G-domain and the M-domain and seven residues at the C-terminus of the M-domain due to weak electron density. Nevertheless, this is the first 3D structure that is available for the M-domain of entire SRP family proteins. In this crystal structure, the M-domain consists of four amphiphilic helices organized around a small hydrophobic core. There is a deep hydrophobic groove on the surface of the M-domain which has been predicted for signal sequence binding. The M-domain also has a highly positively charged helix-turn-helix motif for RNA binding. All in all, the crystal structure indicated that the M-domain possesses the predicted features.

It has to be pointed out that the ffh from *T. aquaticus* is quite different from that of *E. coli* in primary structure although these two proteins are homologues. One prominent feature of the M-domain is its unusually high content of Met residues which is the reason why this domain was named M-domain (Bernstein *et al.* 1989). However, many of the Met residues in the *T.*

aquaticus Ffh protein are substituted by other amino acids, such as Leu, Phe, and Val (Figure 8.1). There are twenty-one Met residues in E. coli M-domain, while only six are present in *T. aquaticus* M-domain. Although the overall hydrophobicity of M-domain remains similar, the amino acid side chain flexibility would be quite different. Using *T. aquaticus* M-domain as a template, we performed computer modeling on *E. coli* M-domain in this study to better illustrate the role Met residues play in the nonsequence specific signal recognition.

Materials and Methods

Materials

The maltose-binding protein (MBP) fusion protein cloning kit was obtained from New England Biolabs. The ThioFusion cloning kit was purchased from Invitrogen. All the restriction endonuclease with buffer and PCR reagent were purchased from BRL. All the PCR primers were synthesized in Dr. M. Moloney's lab (University of Calgary). Other chemicals and reagents were obtained from Sigma.

Cloning and Expression of E. coli M-domain

This study was initiated by Dr. M. Zhang, a former student in our lab, who amplified the ffh M-domain gene from *E. coli* chromosomal DNA using the polymerase chain reaction (PCR). The primers used for PCR contained the

sequences GCGTGAGCTCGGCATGGGC (forward) and GACGAGCACATCC-CGGTGCCAAAA (backward). The later was a gift from Dr. S. L. Wong (University of Calgary). The PCR products were digested by Elc136II and EcoRI; and Maltose Fusion System (New England Biolabs) vector pMAL was digested by StuI and EcoRI. The M-domain gene was then ligated to the pMal vector followed by transformation into TB1 competent cells. Single colonies was inoculated and grown the next day on fresh LB-plates. Miniscreen and restriction enzyme digestions were performed to confirm the correct insertion of the M-domain gene into pMAL.

Expression and Purification of M-domain using the Maltose Fusion System

The *E. coli* strain harboring pMAL with the M-domain gene was activated by streaking on a LB plate. Cells were grown on the plate at 30 °C for 16 - 18 hours before a single colony was picked and inoculated into 1 L LB media with 50 mg ampicillin. Initially, the temperature for the cell culture and protein induction was 37 °C. Lower temperatures, such as 25 °C, 28 °C, 30 °C, and 33°C, were attempted later to avoid the formation of inclusion bodies. We have found that 30 °C was most suitable for avoiding inclusion bodies while achieving relatively high protein expression. Typically, the cells were grown overnight until the OD_{600} was around 0.8 when 160 mg/L IPTG were added to the cell culture. Protein was induced for five hours before the cells were harvested by centrifugation.

The cells were resuspended into 40 ml cold lysate buffer containing 50

mM Tris-HCl, pH 7.4, with 100 mM KCl, 1 mM EDTA, 1 mM DTT, and 1mM PMSF. Cell lysis was achieved by french pressing the cells which were resuspended twice. The cell debris was spun down at 4 °C at 20,000 rpm for 20 minutes. The supernatant was applied to an amylose column (20 ml) which was equilibrated with the same buffer. The column was washed with the buffer for at least ten bed volumes, followed by five volumes of a buffer containing 50 mM Tris-HCl, pH 7.4, with 500 mM NaCl, 1 mM EDTA, and 1 mM DTT. The column was then washed with washing buffer containing 50 mM Tris-HCl, pH 7.4, and 50 mM NaCl. The protein was eluted from the column using washing buffer containing 10 mM maltose.

Cloning and Expression of M-domain using pCaM

The M-domain gene also was cloned into pCaM, the vector used to express CaM, to be expressed alone. The M-domain gene was amplified with PCR from the plasmid we used in Maltose Fusion System. pMAL with M-domain gene was purified from TB1 strain using the normal alkaline method (Sambrook *et al.* 1989). The forward primer was CTGCTCGAGGAAG-GAGGCGAATTCTATGGGCGACGTACTGTC, and the backward primer was GGGGAGCTCCTATTAGCGACCAGGGAAG. In each PCR cycle, the reaction temperatures were 94°C, 72°C, and 50°C for denaturation, extension, and annealing, respectively. The sample was kept at each temperature for 60 seconds for each cycle. A total of thirty cycles were used. The PCR products were purified with EasyPrep PCR Product Prep Kit (Pharmacia). The vector

pCaM was purified from *E. coli* strain MM294 with EasyPrep Plasmid Prep Kit (Pharmacia). The purified PCR products and pCaM were then digested with XhoI and SstI under conditions recommended by the manufacturers. The digested DNA was applied to a low melting temperature agarose (LMTA) gel and separated. DNA fragments of the pCaM vector and the M-domain gene were cut out and melted together at 65°C for 2-3 minutes. The volume of LMTA was measured followed by the addition of water. Ligase (BRL) was added at the concentration recommended by the manufacturer. The ligation was performed overnight at room temperature. The ligation mixture was melted at 65°C for 2-3 minutes followed by transformation to freshly made MM294 competent cells. Culture media containing transformed cells (50 μl and 300 μl) were plated to two ampicillin LB plates respectively. These plates were incubated overnight at 37°C, and single colonies were inoculated and grown in fresh LB medium (2 ml) containing ampicillin. Plasmids from these cells were purified and subjected to restriction enzyme digestion to check the insertion.

The expression of M-domain from the pCaM system was conducted in a similar fashion as CaM. A single colony was inoculated into 50 ml LB media with ampicillin. The cells were allowed to grow at 30°C in a shaker for five to six hours until the cell density measured by OD_{600} reached a range of 0.8 to 1.0. The temperature was then increased to 37°C, and 8 mg isopropyl-β-d-thiogalactopyranoside (IPTG) was added to induce the production of M-domain. The cells were grown for another 3 to 4 hours for protein induction. 1

ml of cell culture was transferred into a microtube, then the cells were spun down using a microcentrifuge. The pellet was resuspended into 100 µl sample buffer, and 10 µl was applied to an SDS gel to check the expression.

Cloning and Expression of M-domain Using ThioFusion System

The M-domain gene was also cloned into the ThioFusion System (Invitrogen). The overall cloning strategy was similar as stated in the last section. The M-domain gene was amplified from pMAL using the following primers: GGGGTACCCCTCGGCATGGGCGAC (forward) and GGGCTGCAG-CTATTAGCGACCAGGGAAG (backward). The PCR products and the vector pTrxFus were digested by KpnI and PstI, respectively. The enzyme digested PCR products and pTrxFus were separated in LMTA and ligated as described in the last section. The strain used in this system was GI724, and the competent cells were prepared with FSB transformation solution and DMSO using the protocol supplied by the manufacturer. The transformed cells harboring the M-domain/thioredoxin construct were again cultured at various temperatures to find a suitable condition to avoid inclusion bodies. A culture temperature of 30 °C was chosen to express the fusion protein. Normally, a singly colony was picked from an RG plate and inoculated into 5 ml RG media where the cells grew overnight. The cell culture was then transferred into 50 ml RG media and let grow for 2 - 3 hours until the OD_{550} reached 0.5. L-tryptophan was added to the cell culture (final concentration was 100 µg/ml) to induce expression of the fusion protein. The cells were grown for another

five hours before they were harvested by centrifugation.

The purification methods recommended by the manufacturer were attempted. For both osmotic and heat shock methods, the *E. coli* strain GI724 containing pTrx which expresses wild-type thioredoxin was used as a positive control. Osmotic shock solutions were supplied by Invitrogen. Osmotic shock solution #2 was also used for the heat shock method. The expression and purification results were analyzed by SDS-PAGE gel.

Sequence Homology Modeling of the M-domain from *E. coli*

The sequence homology modeling of ffh M-domain was performed using an on-line server (http://www.expasy.ch). The template structures of the M-domain from *T. aquaticus* were obtained from the Protein Data Bank (Keenan *et al.* 1998). The modeling procedures were carried out by SWISS-MODEL Version 3.5 (Peitsch 1995, 1996, Guex & Peitsch 1997). The structure generated from this program was analyzed by the program WHATIF version 19970813-1517.

Results and Discussion

To effectively perform protein structural studies using NMR spectroscopy, a good protein expression and purification system has to be established. The protein has to be efficiently overexpressed at high yields, and the purification process should be relatively simple since yield decreases over a number of purification steps. Moreover, all possible denaturing procedures

should be avoided since protein in its "natural" state is desired for structural studies. Therefore, a good system should not involve inclusion bodies because recovering proteins from inclusion bodies often requires denaturing conditions.

We first attempted to express and purify M-domain through the MBP fusion system. The cloning was successful and the fusion protein was overexpressed (Figure 8.2A). One of the problems encountered in this system was the appearance of inclusion bodies. A number of culturing temperatures were tested to decrease inclusion bodies in the cell. It was found that most

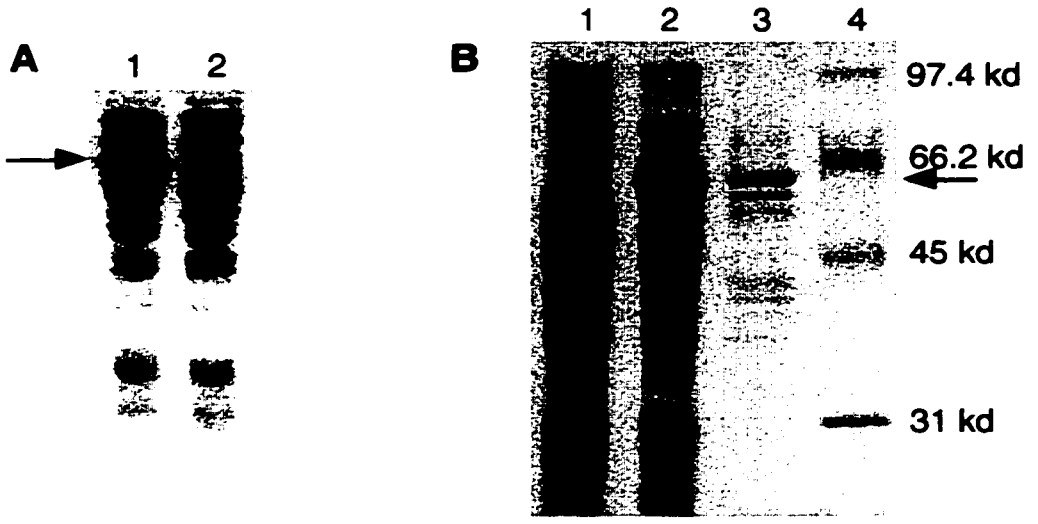

Figure 8.2 Expression and purification of the fusion protein in the MBP fusion system. (A) The over expression of the fusion protein. Lanes 1 and 2 show the cell lysate after and before induction by IPTG. (B) Purification of the fusion protein by the amylose column. Lanes 1 and 2 are the cell lysate before and after the protein induction. Lane 3 shows the sample after the amylose affinity column. Lane 4 shows molecular weight (MW) markers.

of the fusion protein was soluble when the expression temperature was lowered to 30 °C. However, the lower temperature also slowed down the cell growth. Therefore, a longer induction period (five to six hours) was used.

The purification started with the use of an amylose column, which is designed for this system. According to the manufacturer, one amylose column can greatly purify the fusion protein. The protease Factor Xa can be used after this step to cleave the M-domain from the MBP fusion protein. Then a second amylose column can be used to separate the MBP domain from the protein of interest. An amylose column did purify our fusion protein to some extent. However, there were still many impurities after this step (Figure 8.2B). Factor Xa was then used to cleave the fusion protein. Initially, the proteolysis was carried out under the conditions recommended by the the manufacturer.

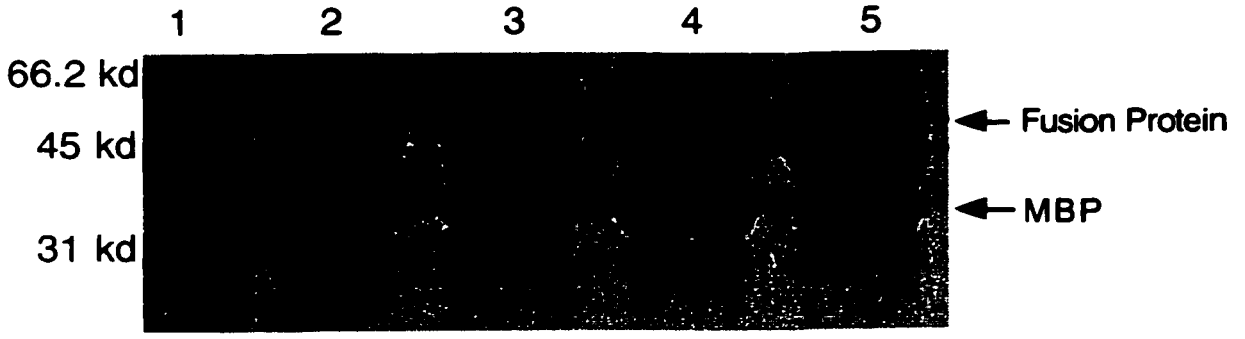

Figure 8.3 Factor Xa digestion of the fusion protein under different conditions. Lane 1 shows the MW marker; lanes 2 and 3 show the samples before and after Factor Xa digestion under the condition recommended by the manufacturer; lanes 4 and 5 show the samples after the digestion in the presence of Ca^{2+} and EDTA, respectively.

However, we found that factor Xa was not very effective using these conditions. A number of experiments were performed to find the most effective conditions. Figure 8.3 shows an SDS-PAGE with proteolysis samples under several conditions. It was found that the addition of the Ca^{2+} ion into the reaction mixture can promote the enzyme reaction.

However, even though the fusion protein could be cleaved by Factor Xa, a large amount of M-domain was still difficult to obtain. As shown in Figure 8.4, the band for the M-domain is very faint compared to the fusion protein and MBP. It seemed that some of the M-domain was also degraded because

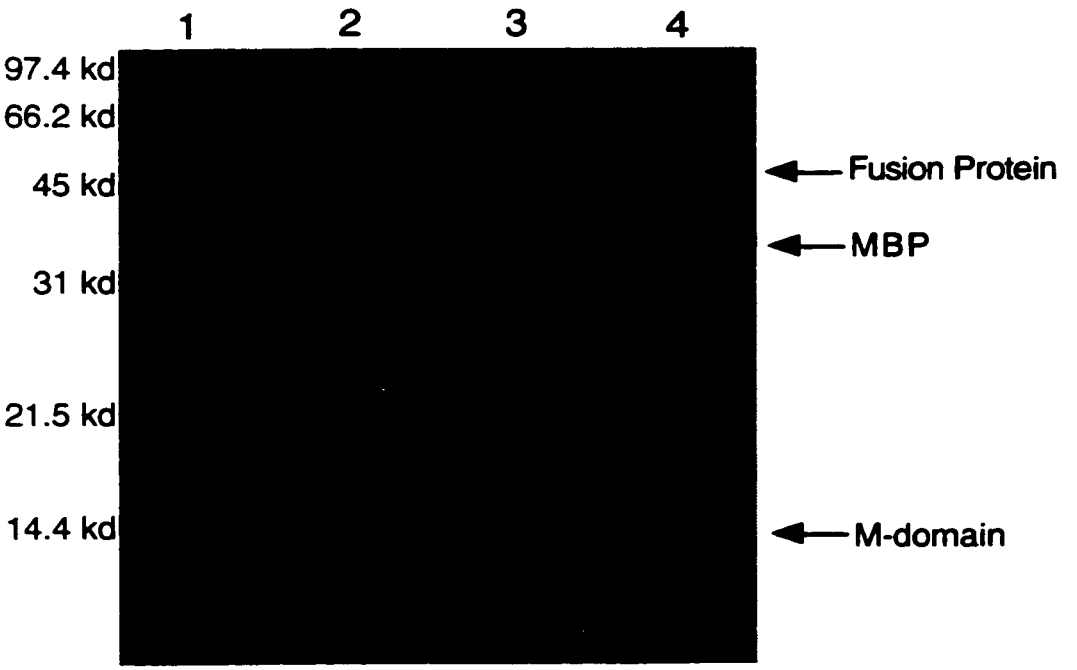

Figure 8.4 Factor Xa digestion of the fusion protein. Lane 1 is the MW marker; lane 2 is the sample before the digestion; lanes 3 and 4 are the samples after a 2-hour digestion.

many bands of smaller proteins can be detected on the gel (Figure 8.4). No detectable amount of the M-domain could be collected after passing this mixture through a second column of amylose.

Another fusion protein system was attempted to express and purify the M-domain. The M-domain gene was cloned into ThioFusion system provided by Invitrogen. The cloning and expression were successful, and the fusion protein could be highly overexpressed in the cell (Figure 8.5). N-terminal amino acid sequencing confirmed that the overexpressed protein wasthe desired fusion protein. Although the system is designed to improve the protein's solubility and avoid

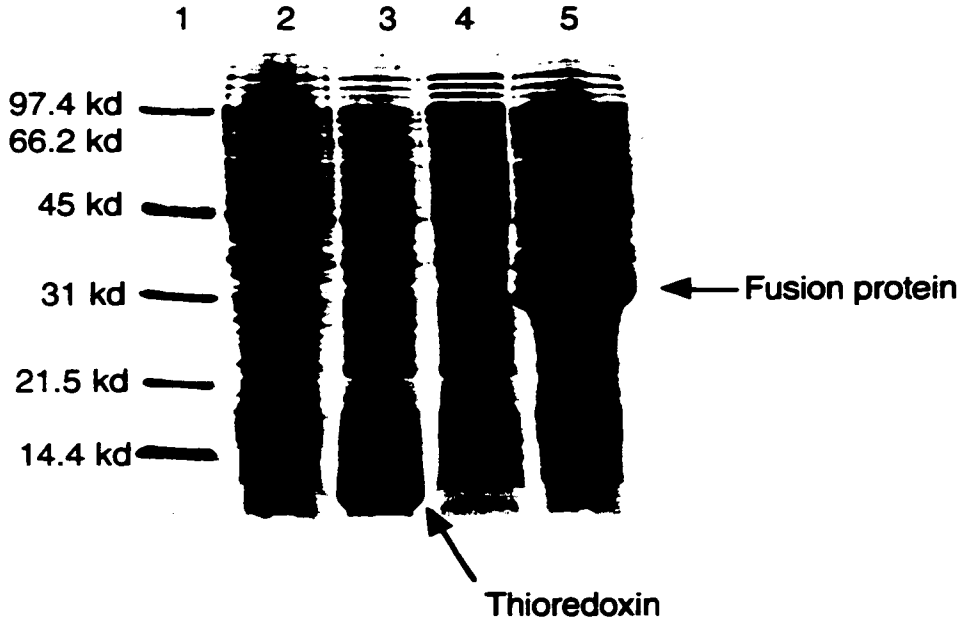

Figure 8.5 Overexpression of the fusion protein in ThioFusion system. Lane 1, MW marker; lane 2, cells containing pAL-781 (negative control); lane 3, cells containing pTrx (positive control); lane 4 and 5, cells harboring engineered plasmid before and after the protein induction by Trp.

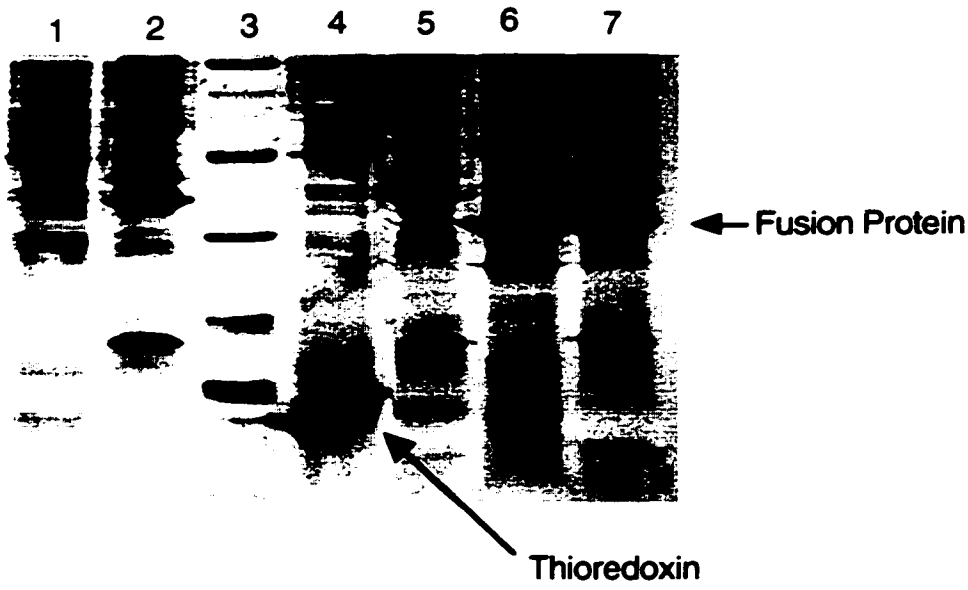

Figure 8.6 Check for inclusion bodies in the ThioFusion system. All cells were broken by the sonication and freeze-thaw method, followed by centrifugation at 4 °C (20, 000 rpm, 25 minutes). Both the supernatant and cell pellet were applied to the SDS-PAGE. Lanes 1 and 2, the supernatant and the pellet of cells containing pAL-781 (negative control); lane 3, MW marker; lanes 4 and 5, the supernatant and the pellet of cells with pTrX (positive control); lanes 6 and 7, the supernatant and the pellet of cells containing the fusion protein. Note that the fusion protein is present both in the supernatant and cell pellets, indicating that a portion of the fusion protein is in the "inclusion bodies".

inclusion bodies, the latter was still a problem at the normal expression temperature. Once again, 30 °C seemed to be the most suitable for protein expression, although there is still a portion of fusion protein in the inclusion bodies (Figure 8.6).

The ThioFusion system also offers a simple purification process which would work for most fusion proteins when used according to the manufacturer. One of the purification approaches involves an osmotic shock. Basically, the cells were osmotically shocked by transferring from a high ionic strength buffer to a low ionic strength buffer which should result in the release of the fusion protein of interest from the periplasm. Therefore, the fusion protein can be purified by spinning down the cells. We have included both a negative and a positive control in our experiments. The negative control was the GI724

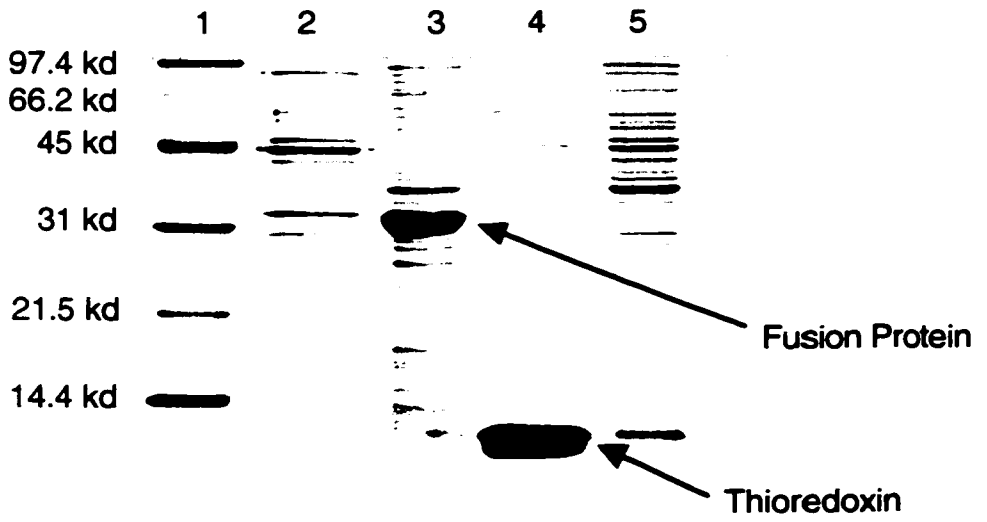

Figure 8.7 Purification of the fusion protein by osmotic shock. If osmotic shock is successful, the fusion protein should be released from the cell and appear in the supernatant. Lane 1, MW marker; Lanes 2 and 3, supernatant and cell pellet of cells expressing fusion protein. Note that the fusion protein is still in the cell pellet after the osmotic shock; lanes 4 and 5, supernatant and cell pellet of cells harboring pTrx (positive control). Note that the wild type thioredoxin is released from the cell, and is present in the supernatant.

strain containing the pAL-781 plasmid which does not contain thioredoxin or M- domain gene. The positive control is GI724 with pTrx which expresses wild type thioredoxin. Figure 8.7 shows the results of the osmotic shock experiments. Clearly the fusion protein could not be released from the cell, in contrast to the wild type thioredoxin. The other purification method recommended by the manufacturer is heat shock. This method takes advantage of the heat stability of thioredoxin by incubating the cell lysate at

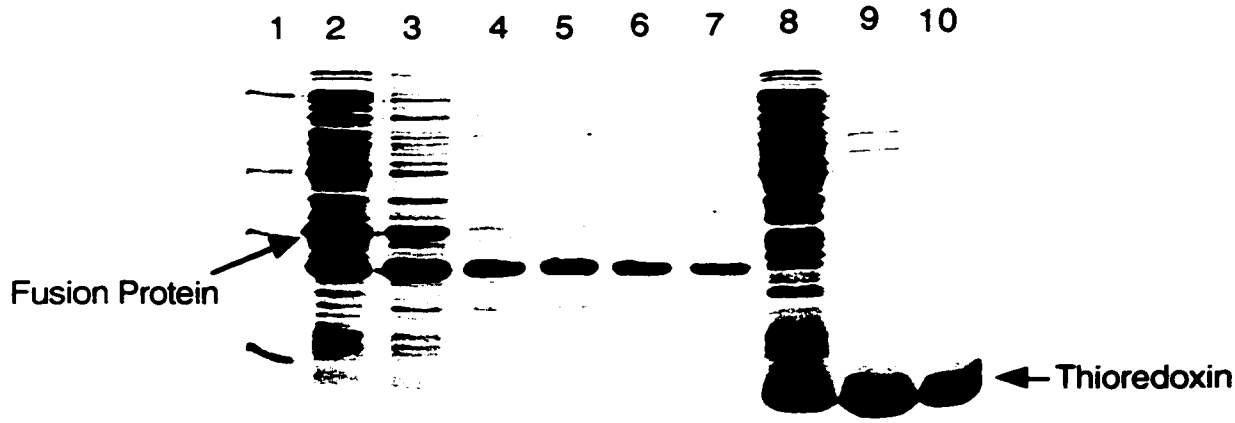

Figure 8.8 Purification of the fusion protein using the heat shock method. The cells were broken by french press; the cell debris was removed by centrifugation. The supernatant was then subject to heat shock at 80 °C. The samples were centrifuged after the heat shock to remove denatured proteins. The supernatant of these samples were analyzed by SDS-PAGE. Lane 1, MW marker; lane 2 to 7, cell lysate containing the fusion protein after the heat shock for 0, 0.5, 1, 2, 5, and 10 minutes, respectively; lane 8 to 10, cell containing expressed thioredoxin after the heat shock of 0, 2, and 10 minutes.

80 °C for a certain period of time. Figure 8.8 shows the results of the heat shock experiments. Although thioredoxin itself is highly stable, the fusion protein did not show any higher stability than most other proteins.

Several other purification methods have also been attempted on both MBP and Thioredoxin fusion proteins, for instance, ion exchange and hydrophobic interaction chromatography. However, no approach was found to significantly improve the purification of these fusion proteins and the subsequent release of the M-domain. Therefore, we have also attempted to express the M-domain alone in pCaM, the plasmid for expressing CaM. No protein expression was detected although restriction analysis and sequencing of the construct demonstrated that the gene was successfully cloned into the plasmid. The M-domain, if expressed by itself, might be quickly degraded in cell because this protein is intrinsically flexible (Ribes *et al.* 1990). Therefore, it seemed that the unusual hydrophobicity and flexibility of M-domain makes it difficult to purify either intact or as a fursion protein. Recently, it has been shown that the M-domain is unstable (Zhang & Gierasch 1997). Only when 4.5S RNA was included could stable protein be purified. All our work was done in the absence of RNA, explaining why we met little success in our attempt at obtaining pure protein.

Keenan *et al.* (1998) have recently crystallized the ffh protein from *T. aquaticus* in the presence of detergents. The protein forms a trimer in the crystal, and the structure was resolved at 3.2 Å resolution. Using this structure as a template, automated homology modeling was performed on the

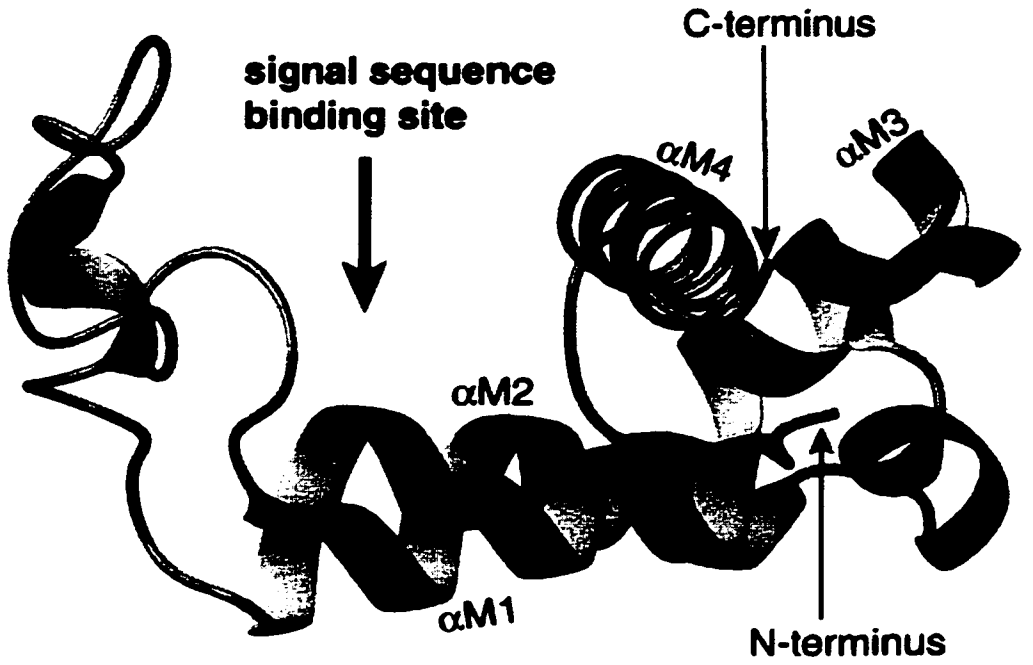

Figure 8.9 Predicted structure of the M-domain from *E. coli* obtained by homology modeling. Ribbon representation shows the signal sequence binding site with a long loop on one side, and α-helices on the other side.

M-domain of the *E. coli* ffh protein. Figure 8.9 illustrates the ribbon structure computed for the *E. coli* M-domain. The overall structure of the M-domain from *E. coli* is very similar to that from *T. aquaticus*. The M-domain contains four long α-helices around a small hydrophobic core. Two antiparallel helices, αM1 and αM2, form the base of a deep groove. The most striking feature of this structure is the 24 residue-long loop which forms on one end of the groove. In the middle of this long loop, there is a short helical structure which is not seen in the *T. aquaticus* M-domain. The other end of the groove is formed by

helices αM3 and αM4. Most hydrophobic residues of the M-domain are located between this long loop and the helix bundle, which provide a large hydrophobic groove on the protein surface. According to the 3D structure of the *T. aquaticus* ffh, the G-domain is located on the opposite side of the helix bundle, which means this hydrophobic groove is not buried between the domains. This hydrophobic groove is believed to be the signal sequence peptide binding site (Keenan *et al.* 1998). The major contribution to this hydrophobic cleft is made by the long loop which is very flexible according to the modeling. The flexibility allows the long loop to adjust its orientation and distance to the helix bundle, which enables the hydrophobic groove to accommodate substrate peptides of different size and conformation.

Compared to *E. coli* ffh or human SRP54, many Met residues in *T. aquaticus* ffh have been replaced by other hydrophobic amino acids, such Leu or Ile. With its long unbranched sidechain, Met has more flexibility than Leu or Ile, which is more suitable for sequence-independent protein-protein interactions (Vogel 1994, also see Chapter 1). Therefore, it is not surprising that most of the Met sidechains in *E. coli* M-domain are located in the hydrophobic groove (Figure 8.10). The Met residues can provide extra flexibility for the binding site to accommodate different sidechains from the substrate peptides. It is believed that in *T. aquaticus* such extra flexibility might not be necessary since the archaeon lives in a high temperature environment, increasing the intrinsic flexibility of the protein. The modeling results reveal that the Met residues of *E. coli* ffh are ideally positioned to

provide a large sequence-independent peptide binding area, which bears some resemblance to the Met-rich CaM-peptide binding surface.

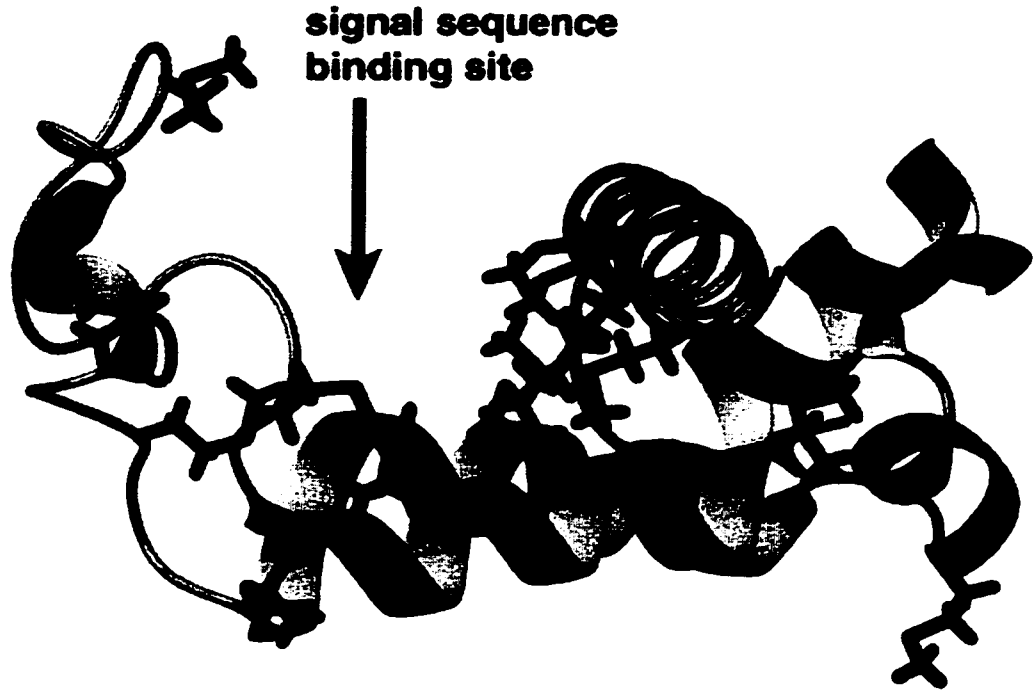

Figure 8.10 Predicted structure of the *E. coli* M-domain with the Met sidechains. This structure is obtained by homology modeling based on the crystal structure of the ffh protein from *T. aquaticus* at 3.2 Å resolution. The positions of the Met side chains may not be accurate.

Chapter 9

Concluding Remarks

As mentioned at the beginning of this dissertation, most of the work described herein involved studies of CaM-mediated interactions. CaM is a versatile Ca^{2+}-regulatory bi-lobal protein in eukaryotic cells, which modulates a number of essential cellular activities. CaM has attracted significant research interest for two decades. It is generally believed that CaM has three "natural" forms inside a cell, apo-CaM, Ca^{2+}-CaM, and CaM-substrate complexes. The "natural" ligand and activator for CaM is calcium, while the "natural" substrates are the CaM-target proteins that are present in the cell. These studies on CaM were largely focused on the ligand and substrate-binding properties of this ubiquitous yet versatile protein. However, the research presented in this dissertation was focused on the "unusual" interactions of CaM. These include the binding of many other metal ions to CaM, the interactions between CaM and drugs or hormones, and some novel CaM-binding peptides from HIV. Even melittin, which is considered as a model CaM-binding peptide because of its high CaM-binding affinity, is actually unique because it can bind to CaM with a different orientation. The studies on these "unusual" interactions were certainly helpful to completely understand this important and versatile protein.

CaM is a Ca^{2+}-regulatory protein whose "natural" ligand is calcium.

CaM binds calcium tightly with fast kinetics, which not only enables it to pass on the calcium signal promptly, but also avoids prolonged activation of the downstream enzymes. Given the importance of CaM in signal transduction pathways, it is surprising that CaM has a broad specificity for metal ions. Many metal ions can substitute for calcium in CaM based on their similarity in ionic radius. We have studied the metal ion binding properties of CaM using NMR and fluorescence spectroscopy (see Chapter 3). Metal ions with high physiological intracellular concentration, such as K^+, Na^+, Mg^{2+} and Zn^{2+}, normally have low affinity for CaM, as shown in our studies. These metal ions can be easily replaced by Ca^{2+} so that they won't interfere with calcium signaling in cells.

Ca^{2+} "activates" CaM by changing the interhelical angles within each lobe of the protein (Zhang *et al.* 1995), which further results in the exposure of a large hydrophobic cleft on each domain of the protein. These hydrophobic areas are the major interface for recognizing substrate peptides and proteins. Many metal ions in our test are capable of causing such conformational changes in CaM and enable CaM to bind MLCK peptide, as shown in our fluorescence experiments (Figure 3.11). This could explain the toxicity of some heavy metal ions, for example, Pb^{2+}. Lead binds to CaM very tightly so that it can not be replaced by calcium which could result in prolonged activation of CaM's substrate proteins and enzymes that would be toxic to the cell.

The hydrophobic surfaces on Ca^{2+}-CaM play a major role in substrate recognition. These surfaces could interact with molecules other than the

substrates. The neurohormone melatonin has been reported to interact with CaM through these hydrophobic patches, and thereby inhibit its activity (Benìtez-King *et al.* 1993). We investigated this interactions with several biochemical and biophysical methods, including CD, fluorescence, and NMR spectroscopy, gel band shift assay and calcineurin activity assay. Some of melatonin's structural analogs were also included on our studies. Our results consistently demonstrated that the interactions between these molecules and CaM are very weak, and so saturation can only occur at very high concentrations. Thus, these compounds are not likely to interfere with CaM's activity *in vivo*.

We have also studied the binding of two other compounds, cisplatin and carboplatin, to CaM. These compounds are widely used anticancer platinum drugs, which have been found to react with the sulfur-containing amino acids, Cys and Met. Since CaM was a Met rich protein and Met plays an important role in substrate recognition, it is of interest to study if these drugs can modify CaM. Indeed, our investigation demonstrated that these platinum drugs bind to CaM tightly, and their binding sites on CaM are the Met sidechains. Such a modification drastically reduces CaM's activity since it introduces a large group onto the substrate-binding sites of the protein. Our studies also showed that cisplatin and carboplatin bind to CaM covalently through Pt-S bonds. No mechanism has been found that can reverse such a modification *in vivo*, which means once these drugs binds to CaM, they are not released. Given that CaM modulates so many signal transduction pathways,

it is therefore possible that the modification of CaM by cisplatin and carboplatin is accountable for some of the toxic side effects of these drugs.

The interactions between melittin and CaM were also studied. Melittin is a bee venom peptide which has been found to have very high affinity for CaM. What distinguishes melittin from other CaM-binding model peptides is that this peptide has a single Trp residue in its sequence, and this Trp is located at the C-terminal part of the peptide. Many CaM-binding peptides have a Trp residue, however, the Trp residue is normally located in the N-terminal part of the sequence (Figure 1.5). The different location of this Trp residue suggests a distinct binding property for melittin. Normally, this Trp reside is anchored into the hydrophobic cleft in the C-lobe of CaM showing an "antiparallel" binding alignment. The situation is more complicated in the case of melittin. Our results indicated that the majority of the peptide binds to CaM with a "parallel" orientation: the C-terminal part of the peptide binds to the C-lobe of CaM, which is distinct from all known CaM-peptide complexes. In this project, we used a so-called "half-molecule" approach which means we utilized CaM and its isolated lobes, TR1C and TR2C, and melittin and its half-molecules, MLN and MLC, to investigate the binding of the peptide to CaM. Our study demonstrated that this is a very effective approach and could be used to study the binding of other natural target peptides to CaM.

We investigated the interactions between CaM and several novel CaM-binding peptides from the HIV glycoprotein. The LLP peptides are derived

from an α-helical segment close to the C-terminus of the HIV transmembrane gp41 protein. These peptides have the propensity to form α-helical structures, and they all bind to CaM although there are variations in their sequence for different HIV isolates. Small angle X-ray scattering data revealed that the LLP-1 peptide forms a more extended complex with CaM, compared to the CaM-MLCK peptide complex. The near-UV CD spectrum also suggested that the single Trp residue in LLP-1E peptide may enter a hydrophobic cleft of CaM with a different orientation than what has been seen for typical CaM-binding peptides.

This disseretation included studies on another protein, the M-domain of ffh protein from *E. coli*. The ffh protein is the bacterial homologue of the central component of the signal recognition particle, SRP54, in mammalian cells. The ffh protein recognizes the signal peptide from a nascent polypeptide and initiates the translocation process. The M-domain is the part of the protein that carries out the signal peptide recognition. We tried to express and purify the M-domain in different fusion systems, and also determined a structural model of the protein using a homology-based approach. It is likely that M-domain has a large hydrophobic cleft on its surface which is suitable for signal peptide binding.

Why were these two completely different subjects, CaM and M-domain, included in one dissertation? Although CaM and M-domain differ from one another both functionally and structurally, these two proteins have one thing in common: they both recognize their substrates independently of their amino

acid sequences. Although basic residues are one noteworthy feature of the peptide recognized, both proteins bind their substrates largely through hydrophobic interactions. This is not surprising because hydrophobic interaction is more suitable for sequence-independent protein recognition than other kinds of protein-protein interactions, like hydrogen bonds or electrostatic interaction which provide directionality and specificity to the interactions. Electrostatic interactions require oppositely charged amino acid sidechains which are restricted to Asp, Glu and Arg, Lys, and His. Hydrogen bonds are also normally found between certain residues, such as Ser, Thr and Asn/Gln. Among the twenty natural amino acids, hydrophobic amino acids (9) outnumber other kinds, such as negatively (2), or positively (3) charged, or polar (6) amino acids. Thus, sequence-independent protein-protein recognition is more likely to occur through hydrophobic interactions.

Hydrophobic residues are normally found in the core of a protein which is not accessible to solvent. Most proteins do not have a large hydrophobic surface. The hydrophobic surfaces on proteins have to be certain sizes to obtain enough stacking forces to achieve strong protein-protein interactions. CaM and M-domain both have unusually large hydrophobic patches on their surface to facilitate substrate recognition. It is impossible for one or two hydrophobic residues to form strong interactions. That probably is the reason why melatonin and its analogs do not bind tightly to CaM (Chapter 3).

Flexibility is another necessity for sequence-independent interaction. A protein has to be able to constantly adjust itself in order to recognize different

substrates, of different shape and length. For CaM, the long flexible central α-helix allows its two lobes to adjust themselves upon substrate-binding. The overall structure of the M-domain is flexible. In addition, part of the hydrophobic surface on M-domain is made up by a unusually large loop which gives the binding site extra flexibility. Furthermore, the hydrophobic patches on the surface of these two proteins are rich in Met residues. With its long unbranched side chain and a slightly longer C-S bond (compared to C-C bond), Met is more flexible than either Ile or Leu, making it more suitable for the binding site to accommodate different amino acids. Moreover, because of the sulfur atom in Met, this sidechain is highly polarizable (Gellman 1991, Zhang & Vogel 1994). Hence it acts like a hydrophobic residue when bound to target proteins, or in apo-CaM, while Met has "polar" character when interacting with water as in Ca^{2+}-CaM. This feature markedly contributes to the stability of CaM in its physiologically different forms.

Sequence-independent interaction is a very interesting motif in protein-protein interaction. It offers an effective way to modulate cellular pathways. For example, when CaM is "activated" by calcium, it can recognize many downstream proteins and enzymes resulting in wide ranging cellular effects. It is economical for the cell because it does not need a range of secondary messenger proteins for each pathway. The same applies to the M-domain: only one SRP is required to recognize most signal sequences. Thus sequence-independent interactions are a necessity in such cases, and it appears that CaM and the M-domain are perfectly "designed" for this kind of interaction.

References

Adebodun, F. and Jordan, F. 1989 Multinuclear magnetic resonance studies on the calcium (II) binding site in trypsin, chymotrypsin, and subtilisin. *Biochemistry* 28, 7524-7531.

Agell N, Aligue R, Alemany V, Castro A, Jaime M, Pujol MJ, Rius E, Seratosa J, Taules M and Bachs. 1998 New nuclear functions for calmodulin. *Cell Calcium* 23, 115-121.

Allen BG and Walsh MP. 1994 The biochemical basis of the regulation of smooth muscle contraction. *Trends Biochem. Sci.* 19, 362-368.

Allen JS, Coligan JE, Bari F, McLane MF, Sodroroski JG, Rosen CA, Haseltine, WA, Lee TH, and Essex M. 1985 Major glycoprotein antigens that induce antibodies in AIDS patients are encoded by HTLV-III. *Science* 228, 1091-1093.

Andersson A, Drakenberg T, Thulin E, and Forsén S. 1983a A ^{113}Cd and ^{1}H NMR study of the interaction of calmodulin with D600, trifluoperazine and some other hydrophobic drugs, *Eur. J. Biochem.* 134, 459-465.

Andersson A, Forsén S, Thulin E, and Vogel HJ. 1983b Cadmium-113 nuclear magnetic resonance studies of proteolytic fragments of calmodulin: assignment of strong and weak cation binding sites. *Biochemistry* 22, 2309-2313.

Appleton TG, Connor JW, Hall JR, and Prenzler PD. 1989 NMR study of the reactions of the cis-diamminediaquaplatinum(II) cation with glutathione and amino acids containing a thiol group. *Inorg. Chem.* 28, 2030-2037.

Aramini JM, and Vogel HJ 1998 Quadrupolar metal ion NMR studies of metalloproteins. Biochem. *Cell Biol.* 76, 210-222.

Aramini JM, Germann MW, Vogel HJ 1997 Soft-pulsed aluminum-27 quadrupolar central transition NMR studies of ovotransferrin. *J. Magn. Reson.* 129, 111-114.

Aramini JM, Hiraoki T, Ke Y, Nitta K, and Vogel HJ. 1995 Cadmium-113 NMR studies of bovine and human alpha-lactalbumin and equine lysozyme. *J. Biochem.* (Tokyo) 117, 623-628.

Aramini JM, Hiraoki T, Yazawa M, Yuan T, Zhang M, Vogel HJ. 1996 Lead-207 NMR: a novel probe for the study of calcium-binding proteins. *J Biol Inorg Chem* 1, 39-48.

Babu YS, Sack JS, Greengrough TJ, Bugg CE, Means AR and Cook WJ. 1985 Three-dimensional structure of calmodulin. *Nature* 315, 37-40.

Babu YS, Bugg CE and Cook WJ. 1988 Structure of calmodulin refined at 2.2 Å resolution. *J. Mol. Biol.* 204, 191-204.

Badminton MN, Kendall JM, Rembold CM and Campbell AK. 1998 Current evidence suggests independent regulation of nuclear calcium. *Cell Calcium* 23, 79-86.

Bancroft DP, Lepre CA, and Lippard SJ. 1990 ^{195}Pt NMR kinetic and mechanistic studies of cis- and trans-diamminedichloroplatinum(II) binding to DNA. *J. Am. Chem. Soc.* 112, 6860-6871.

Barbato G, Ikura M, Kay LE, Pastor RW, Bax A. 1992 Backbone dynamics of calmodulin studied by ^{15}N relaxation using inverse detected two-dimensional NMR spectroscopy: the central helix is flexible. *Biochemistry* 31, 5269-5278.

Barré-Sinoussi F, Chermann JC, Rey F, Nugeyre MT, Chamaret S, Gruest J, Dauguet C, Axler-Blin C, Vézinet-Brun F, Rouzioux C, Rozenbaum W, and Montagnier L. 1983 Isolation of a T-lymphoxyte retrovirus from a patient at risk for acquired immunodificiency syndrome (AIDS). *Science* 220, 868-871.

Barth A, Martin SR, and Bayley PM. 1998 Specificity and symmetry in the interaction of calmodulin domains with the skeletal muscle myosin light chain kinase target sequence. *J. Biol. Chem.* 273, 2174-2183.

Bauer C, Peleg-Shulman T, and Gibson D, and Wang HJ. 1998 Monofunctional platinum amine complexes destabilize DNA significantly. *Eur. J. Biochem.* 256, 253-260.

Bax A, Griffey RH, and Hawkins BL. 1983 Correlation of proton and nitrogen-15 chemical shifts by multiple quantum NMR, *J. Magn. Reson.* 55, 301-315.

Benítez-King G, Huerto-Delgadillo L, and Antón-Tay F 1991 Melatonin modifies calmodulin cell levels in MDCK and N1E-115 cell lines and inhibits phosphodiesterase activity in vitro, *Brain Res.* 557, 289-292.

Benítez-King G, Huerto-Delgadillo L, and Antón-Tay F. 1993 Binding of ^{3}H-

melatonin to calmodulin, *Life Sci.* 53, 201-207.

Benítez-King G, Ríos A, Martínez A, and Antón-Tay F. 1996 In vitro inhibition of Ca^{2+}/calmodulin-dependent kinase II activity by melatonin, *Biochim. Biophys. Acta* 1290, 191-196.

Berliner LJ, Ellis PD, and Murakami K 1983 Manganese (II) electron spin resonance and cadmium-113 nuclear magnetic resonance evidence for the nature of the calcium binding site in alpha-lactalbumins. *Biochemistry* 22, 5061-5063.

Berner-Price SJ and Kuchel PW 1990 Reaction of cis- and trans-$[PtCl_2(NH_3)_2]$ with reduced glutathione studied by ^{1}H, ^{13}C, ^{195}Pt and ^{15}N-{^{1}H} DEPT NMR. *J. Inorg. Biochem.* 38, 305-326.

Bernstein HD, Poritz MA, Strub K, Hoben PJ, Brenner S, and Walter P. 1989 Model for signal sequence recognition from amino-acid sequence of 54K subunit of signal recognition particle. *Nature* 340, 482-486.

Bernstein HD, Zopf D, Freymann DM, and Walter P. 1993 Functional substitution of the signal recognition particle 54-kDa subunit by its Escherichia coli homolog. *Proc. Natl. Acad. Sci.* 90, 5229-5233.

Berridge MJ. 1997 Elementary and global aspects of calcium signaling. *J. Exp. Biol.* 200, 315-319.

Bezprozvanny I and Ehrlich BE. 1995 The insotol 1,4,5-triphosphate receptor. *J. Membr. Biol.* 145, 205-216.

Bierbach U and Farrell N. 1998 Structural and reactivity studies on the ternary system guanine/methionine/trans-[$PtCl_2(NH_3)L$](L=NH_3, quinoline): implications for the mechanism of action of nonclassical trans-platinum antitumor complexes. *J. Biol. Inorg. Chem.* 3, 570-580.

Bjornson ME, Corson DC, and Sykes BD. (1985) 13C and 113Cd NMR studies of the chelation of metal ions by the calcium binding protein parvalbumin. *J. Inorg. Biochem.* 25, 141-149.

Blumenthal DK, Takio K, Edelman AM, Carbonneau H, Titani K, Walsh KA, and Krebs EG. 1988 Identification of the calmodulin-binding domain of skeletal muscle myosin light chain kinase. *Proc Natl Acad Sci USA* 82, 3187-3197.

Brokx RD, and Vogel HJ. 2000 Peptide and metal ion dependent association of isolated helix-loop-helix calcium binding domains: studies of thrombic fragments of calmodulin. Protein Science (in press).

Burstein EA, Vedenkia NS, and Ivkova MN. 1973 Fluorescence and the location of tryptophan residues in protein molecules, *Photochem. Photobiol.* 18, 263-279.

Caday CG, and Steiner RF. 1986 The interaction of calmodulin with melittin. *Biochem. Biophys. Res. Commun.* 135, 419-425.

Carafoli E. 1987 Intracellular calcium homeostasis. *Ann. Rev. Biolchem.* 56, 395-433.

Carafoli E. 1994 The signaling function of Ca^{2+} and its regulation. *J. Hyperten.*

12, S47-S56.

Carafoli E, Nicotera P and Santella L. 1997 Calcium signaling in the cell nucleus. *Cell Calcium* 22, 313-319.

Chan DC, and Kim PS. 1998 HIV entry and its inhibition. *Cell* 93, 681-684.

Chan DC, Fass D, Berger JM, and Kim PS. 1997 Core structure of gp41 from the HIV envelope glycoprotein.*Cell* 89, 263-273.

Chao SH, Suzuki Y, Zysk JR, Cheung WY. 1984 Activation of calmodulin by various metal cations as function of ionic radius. *Mol Pharmacol* 26, 75-82.

Chattopadhyaya R, Meador WE, Means AR and Quiochon FA. 1992 Calmodulin structure refined at 1.7 A resolution. *J. Mol. Biol.* 228, 1177-1192.

Chin D, Winkler KE, and Means AR 1997 Characterization of substrate phosphorylation and use of calmodulin mutants to address implications from the enzyme crystal structure of calmodulin-dependent protein kinase I. *J. Biol. Chem.* 272, 31235-31240.

Chu G. 1994 Cellular response to cisplatin: the roles of DNA-binding proteins and DNA repair. *J. Biol. Chem.* 269, 787-790.

Clapham DE. 1995 Ca^{2+} signaling. *Cell* 80, 259-268.

Clarke TE, and Vogel HJ. 2000 In Calcium binding proteins protocols. Ed. H. J. Vogel, *Meth. Mol. Biol.* (in press).

Cloyd MW, and Lynn WS. 1991 Perturbation of host-cell membrane is a primary mechanism of cytopathology. *Virology* 181, 500-511.

Coleman JE. 1993 Cadmium-113 nuclear magnetic resonance applied to metalloproteins. *Methods Enzymol.* 227, 16-43.

Comte M, Maulet Y, and Cox JA. 1983 Ca^{2+}-dependent high-affinity complex formation between calmodulin and melittin. *Biochem. J.* 209, 269-272.

Connolly T, and Gilmore R. 1989 The signal recognition particle recepter mediates the GTP-dependent displacement of SRP from the signal sequence of the nascent poly peptide. *Cell* 57, 599-610.

Connolly T, Rapiejko PJ, and Gilmore R. 1991 Requirement of GRP hydrolysis for dissociation of the signal recognition particle from its receptor. *Science* 252, 1171-1173.

Coukos G and Rubin SC. 1998 Chemotherapy resistance in ovarian cancer: new molecular perspectives. *Obstet. Gynecol.* 91, 783-792.

Crivici A and Ikura M. 1995 Molecular and structural basis of target recognition by calmodulin. Annu. Rev. Biophys. Biomol. Struct. 24, 85-116

Cullinane C, Mazur SJ, Essigmann JM, Phillips DR, and Bohr VA. 1999 Inhibition of RNA polymase II transcription in human cell extracts by cisplatin DNA damage. *Biochemistry*38, 6204-6212.

Danielson MA, and Falke JJ 1996 Use of 19F NMR to probe protein structure

and conformational changes. *Annu. Rev. Biophys. Biomol. Struct.* 25,163-195.

David AD 1997 Two dimensional nuclear magnetic resonance and biochemical studies of fluorinated calmodulins. M. Sc. thesis, University of Calgary.

Dawson AP. 1997 Calcium signaling: how do IP3 receptors work? *Curr. Biol.* 7, R544-R547.

Delaglio F, Grzesiek S, Vuister GW, Zhu G, Pfeifer J, and Bax A. 1995 NMRPipe: a multidimensional spectral processing system based on UNIX pipes. *J. Biomol. NMR* 6, 277-293.

Delville A, Grandjean J, Laszlo P, Gerday C, Brzeska H, Drabikowski W. 1980 Sodium-23 nuclear magnetic resonance as an indicator of sodium binding to calmodulin and tryptic fragments, in relation to calcium content. *Eur J Biochem* 109, 515-522.

Dempsey CE. 1990 The actions of melittin on membranes. *Biochim. Biophys. Acta* 1031, 143-161.

Drabikowski W, Brzeska H and Venyaminow AY. 1982 Tryptic fragments of calmodulin. Ca^{2+}- and Mg^{2+}-induced conformational changes. *J. Biol. Chem.* 257, 11584-11590.

Drakenberg T, Lindman B, Cave A, and Parello, J. 1978 Non-equivalence of the CD and EF sites of muscular parvalbumins. A 113Cd NMR study. *FEBS Lett.* 92, 346-350.

Drakenberg T, Forsén S, Thulin E, and Vogel HJ. 1987 The binding of Ca^{2+},

Mg^{2+} and Cd^{2+} to tryptic fragments of skeletal muscle troponin C. Cadmium-113 and proton NMR studies. *J. Biol. Chem.* 262, 672-678.

Economou A, and Wickner W. 1994 SecA promotes preprotein translocation by undergoing ATP-driven cycles of membrane insertion and deinsertion. *Cell* 78, 835-843.

Economou A, Pogliano JA, Beckwith J, Oliver DB, and Wickner W. 1995 SecA membrane cycling at SecYEG is driver by distinct ATP binding and gydrolysis events and is regulated by SecD and SecF. *Cell* 83, 1171-1181.

Edwards RA, Walsh MP, Sutherland C, and Vogel HJ 1998 Activation of calcineurin and smooth muscle myosin light chain kinase by Met-to-Leu mutants of calmodulin. *Biochem. J.* 331,149-152

Eftink MR, and Ghiron. 1976 *J. Phys. Chem.* 80, 486-493.

Eisenberg D, and Wesson M. 1990 The most highly amphiphilic alpha-helices include two amino acid segments in human immunodeficiency virus glycoprotein 41. *Biopolymers* 29,171-177.

Elizondo-Riojas MA, Gonnet F, Chottard JC, Girault JP, and Kozelka J. 1998 The TpG chelate of cis(diammineplatinum) forms two head-to-head rotamers in H_2O solution. *J. Biol. Inorg. Chem.* 3, 30-43.

Ellis PD, Strang P, and Potter JD. 1984 Cadmium-substituted skeletal troponin C. Cadmium-113 NMR spectroscopy and metal binding investigations. *J. Biol. Chem.* 259, 10348-10356.

Ellis PD, Marchetti PS, Strang P, and Potter JD. 1988 Cadmium-substituted skeletal troponin C metal binding investigations and sequence assignment of the cadmium-113 resonances. *J. Biol. Chem.* 263, 10284-10288.

Elshorst B, Hennig M, Forsterling H, Diener A, Maurer M, Schulte P, Schwalbe H, Griessinger C, Krebs J, Schmid H, Vorherr T, and Carafoli E. 1999 NMR solution structure of a complex of calmodulin with a binding peptide of the Ca^{2+} pump. *Biochemistry* 38, 12320-12332.

Enyedi A, Vorherr T, James P, McCormick DJ, Filoteo AG, Carafoli E, and Penniston JT. 1989 The calmodulin binding domain of the plasma membrane Ca2+ pump interacts both with calmodulin and with another part of the pump. *J. Biol. Chem.* 264, 12313-12321.

Erickson-Viitanen S, and DeGrado WF. 1987 Recognition and cherecterization of calmodulin-binding sequences in peptides and proteins, *Methods Enzymol.* 139, 455-478.

Farmery M, Macao B, Larsson T, Samuelsson T. 1997 Binding of GTP and GDP induces a significant conformational change in the GTPase domain of Ffh, a bacteria homologue of the SRP 54 kDa subunit. *Biochim. Biophys. Acta* 1385, 61-68.

Fink D, Aebi S, and Howell SB. 1998 The role of DNA repair in Drug resistance. *Clin. Cancer Res.* 4, 1-6.

Fisher PJ, Prendergast FG, Ehrhardt MR, Urbauer JL, Wand AJ, Sedarous SS, McCormick DJ, and Buckley PJ. 1994 Calmodulin interacts with amphiphilic peptides composed of all D-amino acids. *Nature* 368, 651-653.

Forsé S, Thulin E, Drakenberg T, Krebs J, and Seamon K. 1980 A 113Cd NMR study of calmodulin and its interaction with calcium, magnesium and trifluoperazine. *FEBS Lett* 117, 189-194.

Forsén S, Vogel HJ, and Drakenberg T. 1986 in Calcium and Cell Function (Cheung, W. Y., eds.) Vol. VI, pp113-157, Academic Press, New York.

Frausto de Silva JJR and Williams RJP. 1991 The Bioinorganic Chemistry of the Elements. Oxford: Clarendon press.

Freymann DM, Keenan RJ, Stroud RM, and Walter P. 1997 Structure of the conserved GTPase domain of the signal recognition particle. *Nature* 385, 361-364.

Freymann DM, Keenan RJ, Stroud RM, and Walter P. 1999 Functional changes in the structure of the SRP GTPase on binding of GDP and Mg^{2+}GDP. *Nature Struct. Biol.* 6, 793-801.

Fullmer CS, Edelstein S, Wasserman RH. 1985 Lead-binding properties of intestinal calcium-binding protein. *J Biol Chem* 260, 6816-6819.

Galione A and White A. 1994 Ca^{2+} release induced by cyclic ADP-ribose. *Trends Cell Biol.* 4, 431-436.

Gallo RC 1987 The AIDS virus. *Sci. Am.* 256, 47-56.

Garoufis A, Haran R, Pasdeloup M, Laussac JP, and Haddjiliadis N. 1987 Interaction of cis-$Pt(ino)_2Cl_2$ with amino acids. *J. Inorg. Biochem.* 31, 65-79.

Garry RF 1989 Potential mechanisms for the cytopathic properties of HIV. AIDS 3, 683-694.

Garry RF, Gottlieb AA, Zuckerman KP, Pace J, Frank T, and Bostick DA. 1988 Cell surface effects of HIV. *Biosci. Rep.* 8, 35-48.

Gelasco A and Lippard SJ. 1998 NMR solution structure of a DNA dodecamer duplex containing a cis-diammineplatinum(II) d(GpG) intrastrand cross-link, the major adduct of the anticancer drug cisplatin. *Biochemistry* 37, 9230-9239.

Gellman S. 1991 The role of methionine residues in the sequence-independent recognition of nonpolar protein surfaces. *Biochemistry* 30, 6633-6636.

Gennity J, Goldstein J, and Inouye M. 1990 Singal peptide mutants of escherichia coli. *J. Bioenergetics Biomembranes* 22, 233-268.

Gierasch LM. 1989 Signal sequences. *Biochemistry* 28, 923-930.

Gilchrist JSC, Czubryt MP and Pierce GN. 1994 Calcium and calcium-binding proteins in the nucleus. *Mol. Cell. Biochem.* 135, 79-88.

Goldstein GW. 1993 Evidence that lead acts as a calcium substitute in second messenger metabolism. *Neuro Toxicol* 14, 97-102.

Gomez A, Barnes J, and Vogel HJ. 2000 submitted for publication.

Gosland M, Lum B, Schimmelpfennig J, Baker J and Doukas M. 1996

Insights into mechanisms of cisplatin resistance and potential for its clinical reversal. *Pharmacotherapy* 16, 16-39.

Gowda K, Black SD, Moeller I, Sakakibara Y, Liu M, and Zwieb C. 1998 Protein SRP54 of human signal recognition particle: cloming, expression, and comparative analysis of functional sites. *Gene* 207, 197-207.

Grochowski T and Samochocka K. 1992 Structural characterization of platinum(II)-methionine complexes in aqueous solution. *J. Chem. Soc. Dalton Trans.* 1992, 1145-1149.

Guex N, and Peitsch MC. 1997 SWISS-MODEL and the Swiss-PdbViewer: an environment for comparative protein modelling. *Electrophoresis* 18, 2714-2723.

Guinier A, and Fournet G. 1955 Small-angle Scattering of X-rays. John Wiley & Sons, New York.

Habermann E. 1972 Bee and wasp venoms. *Science* 177, 314-321.

Hauser S, Bacher G, Dobberstein B, and Lutcke H. 1995 A complex of the signal sequence binding protein and the SRP RNA promotes translocation of nascent proteins. *EMBO J.* 14, 5485-5493.

Helseth E, Olshevsky U, Furman C, and Sodroski J. 1991 Human immunodeficiency virus type 1 gp120 envelope glycoprotein regions important for association with the gp41 transmembrane glycoprotein. *J Virol.* 65, 2119-2123.

Heudi O, Cailleux A, and Allain P. 1998 Kinetic studies of the reactivity between cisplatin and its monoaquo species with L-methionine. *J. Inorg. Biochem.* 71, 61-69.

High S, and Dobberstein B. 1991 The signal sequence interacts with the methionine-rich domain of the 54-kD protein of signal recognition particle. *J. Cell Biol.* 113, 229-233.

Hinrichsen RD. 1993 Calcium and calmodulin in the control of cellular behavior and mobility. *Biochim. Biophys. Acta* 1155, 277-293.

Hiraoki T, Vogel HJ. 1987 Structure and function of calcium-binding proteins. *J. Cardiovasc Pharm* 10, S14-S31.

Ho DD, Neumann AU, Perelson AS, Chen W, Leonard JM, and Markowitz M. 1995 Rapid turnover of plasma virions and CD4 lymphocytes in HIV-1 infection. *Nature* 373, 123-126.

Huque MDE. 1989 NMR studies of calmodulin. Ph. D. dessertation, University of Calgary.

Ikura M. 1996 Calcium binding and conformational response in EF-hand proteins. *Trends Biochem. Sci.* 21, 14-17.

Ikura M, Hasegawa N, Aimoto S, Yazawa M, Yagi K, and Hikichi K. 1989 113Cd-NMR evidence for cooperative interaction between amino- and carboxyl-terminal domains of calmodulin. *Biochem. Biophys. Res. Commun.* 161, 1233-1238.

Ikura M, Hiraoki T, Hikichi K, Mikuni T, Yazawa M, Yagi K. 1983 Nuclear magnetic resonance studies on calmodulin: calcium-induced conformational change. *Biochemistry* 22, 2573-2579.

Ikura M, Spera S, Barbato G and Bax A. 1991 Secondary structure and side-chain 1H and 13C resonance assignments of calmodulin in solution by heteronuclear multidimensional NMR spectroscopy. *Biochemistry* 30, 9216-9228.

Ikura M, Clore GM, Gronenborn AM, Zhu G, Klee CB and Bax A. 1992 Solution structure of a calmodulin-target peptide complex by multi-dimensional NMR. *Science* 256, 632-638.

Itakura M, and Iio T. 1992 Static and kinetic studies of calmodulin and melittin complex. *J. Biochem.* (Tokyo) 112, 183-191.

Ivanov AI, Christodoulou J, Parkinson JA, Barnham KJ, Tucker A, Woodrow J, and Saddler PJ. 1998 Cisplatin binding sites on human albumin. *J. Biol. Chem.* 273, 14721-14730.

Jabbar MA and Nayak DP. 1987 *Mol. Cell. Biol.* 7, 1476-1485.

Jaffe LF. 1993 Classes and mechanisms of calcium waves. *Cell Calcium* 14, 736-745.

Jarve RK and Aggarwal SK. 1997 Cisplatin-induced inhibition of the calcium-calmodulin complex, neuronal nitric oxide synthase activation and their role in stomach distention. *Cancer Chemother. Pharmacol.* 39, 341-48.

Jiang L, Tang G, and Tang W. 1996 The interaction between cytochrome c and trans-[$PtCl_2(NH_3)_2$]. *J. Chem. Soc. Dalton Trans* 1996, 2223-2226.

Jiang L, Yu C, Tang G, and Tang W. 1997 Studies on the interaction between cytochrome c and cis-[$PtCl_2(NH_3)_2$]. *J. Inorg. Biochem.* 65, 73-77.

Johnson JD, Wittenauer LA, Thulin E, Forsén S, Vogel HJ. 1986 Localization of a felodipine (dihydropyridine) binding site on calmodulin. *Biochemistry* 25, 2226-2231.

Kaptein R. 1988 *Biol. Magn. Reson.*4, 145-188.

Kataoka M, Head JF, Seaton BA, and Engelman DM. 1989 Melittin binding causes a large calcium-dependent conformational change in calmodulin. *Proc. Natl. Acad. Sci. USA* 86, 6944-6948.

Kawasaki H and Kretsinger 1994 Calcium-binding proteins. *Protein Profile* 1,343-390.

Keenan RJ, Freymann DM, Walter P, and Stroud RM. 1998 Crystal strucature of the signal sequence binding subunit of the signal recognition particle. *Cell* 94, 181-191.

Kelly SM, and Price NC. 1997 The application of circular dichroism to studies of protein folding and unfolding. *Biochim. Biophys. Acta* 1338, 161-185.

Kikuchi Y, Iwano I, Miyauchi M, Sasa H, Nagata I, and Kuki E. 1990 Restorative effects of calmodulin antagonists on reduced cisplatin uptake by cisplatin-resistant human ovarian cancer cells. *Gynecol. Oncol.* 39, 199-203.

Kilhoffer MC, Demaille JG, Gerard D. 1980 Terbium as a luminescent probe of calmodulin calcium-binding sites. *FEBS Lett* 116, 269-272.

Kingsley-Hickman PB, Nelsestuen GL, and Ugurbil K. 1986 113Cd NMR study of bovine prothrombin fragment 1 and factor X. *Biochemistry* 25(11), 3352-3355

Kleinberg J. 1963 Cis- and trans-dichlorodiammine-platinum(II). *Inorg Syntheses* 7, 239-245.

Klemper MS. 1985 An adenosine triphosphate-dependent calcium uptake in human neutrophil lysosomes. *J. Clin. Invest.* 76, 303-310.

Kodama T, Wooley DP, Naidu YM, Kestler HW III, Daniel MD, Li Y, and Desrosiers RC. 1989 Significance of premature stop codons in env of simian immunodeficiency virus. *J Virol.* 63, 4709-4714.

Koenig BW, Ferretti JA, and Gawrish K. 1999 Site-specific deuterium order parameters and membrane-bound behaviour of a peptide fragment from the intracellular domain of HIV-1 gp41. *Biochemistry* 38, 6327-6334.

Kondo R, Tikunova SB, Cho MJ, and Johnson JD 1999 A point mutation in a plant calmodulin is responsible for its inhibition of nitric-oxide synthase. *J. Biol. Chem.* 274, 36213-36218

Kong L, Lee S, Kappes JC, Parkin JS, Dechker D, Hoxie J, Hahn BH, and Shaw GM. 1988 West African HIV-2-related human retrovirus with attenuated cytopathicity. *Science* 240, 1525-1529.

Kowalski M, Bergeron L, Dorfman T, Haseltine W, and Sodroski J. 1991 Attenuation of human immunodeficiency virus type 1 cytopathic effect by a mutation affecting the transmembrane envelope glycoprotein. *J. Virol.* 65, 281-291.

Kretsinger RH, and Nockolds CE. 1973 Carp muscle calcium-binding protein II. Structure determination and general description. *J. Biol. Chem.* 248, 3313-3326.

Krieg UC, Walter P, and Johnson AE. 1986 Photocrosslinking of the signal sequence of nascent preprolatin to the 54-kilodalton polypeptide of the signal recognition particle. *Proc. Natl. Acad. Sce. USA.* 83, 8604-8608.

Kuboniwa H, Tjandra N, Grzesiek S, Ren H, Klee CB, Bax A. 1995 Solution structure of calcium-free calmodulin. *Nature Struct Biol* 2, 768-776.

Kumamoto CA, and Francetic O. 1993 Highly selective binding of nascent polypeptide by an escherichia coli chaperone protein in vivo. *J. Bacteriol.* 175, 2184-2188.

Kumar VD, Lee L, Edwards BF. 1991 Refined crystal structure of ytterbium-substituted carp parvalbumin 4.25 at 1.5 Å, and its comparison with the native and cadmium-substituted structures. *FEBS Lett* 283, 311-316.

Kurzchalia TV, Wiedmann M, Girshovich AS, Bochkareva ES, Bielka H, adn Rapoport TA. 1986 The signal sequence of nascent preprolactin interacts with the 54K polypeptide of signal recognition particle. *Nature* 320, 634-636.

Lafitte D, Capony JP, Grassy G, Haiech J, Calas B. 1995 Analysis of the ion binding sites of calmodulin by electrospray ionization mass spectrometry. *Biochemistry* 34, 13825-13832.

Lee HC. 1994 Cyclic ADP-ribose - a new member of a super family of signallin cyclic-nucleotides. *Cell Signall.* 6, 591-600.

Lee S, Hu W, Fisher AG, Looney DL, Kao VF, Mitsuya H, Ratner L, and Wong-Staal F. 1989 Role of the carboxy-terminal portion of the HIV-1 transmembrane protein in viral transmission and cytopathogenicity. *AIDS Res Hum Retroviruses* 5, 441-449.

Levy JA 1988 The mysteries of HIV: challenges for therapy and prevention. *Nature* 333, 519-522.

Levy JA, Hoffman AD, Kramer SM, Landis JA, Shimabukuro JM, and Oshiro LS 1984 Isolation of lymphocytopathic retroviruses from San Francisco patients with AIDS. *Science* 225, 840-842.

Lempers EL, and Reedjik J. 1991 Interactions of platinum amine compounds with sulfur-containing biomolecules and DNA fragments. *Adv. Inorg. Chem.* 37, 175-217.

Li Q, Gardner K, Zhang L, Tsang B, Bostick-Bruton F, and Reed E. 1998 Cispaltin induction of ERCC expression in A2780/CP70 human ovarian cancer cells. *J. Biol. Chem.* 273, 23419-23425.

Linse S, Drakenberg T, and Forsén S. 1986 Mastoparan binding induces a structural change affecting both the N-terminal and C-terminal domains of

calmodulin. A 113Cd-NMR study. *FEBS Lett.* 99, 28-32.

Linse S, Helmersson A and Forsen S. 1991 Calcium binding to calmodulin and its globular domains. *J. Biol. Chem.* 266, 8850-8854.

Liu Y, and Storm DR. 1989 Dephosphorylation of neuromodulin by calcineurin. *J. Biol. Chem.* 264, 12800-12804.

Liu L, Yan H, Ni A, Cheng X, and He B. 1994 Interaction of calmodulin with synthetic deletion peptides of melittin. *Int. J. Peptide Protein Res.* 43, 107-112

Luirink J, High S, Wood H, Giner A, Tollervey D, and Dobberstein B. 1992 Signal-sequence recognition by an Escherichia coli ribonucleoproein complex. *Nature* 359, 741-743.

Lüth MS, Freisinger E, Glahé, Müller, and Lippert B. 1998 Taking advantage of right angles in N1,N7-diplatinated purine nucleobases: toward molecular squares, rectangles, and Meanders. *Inorg. Chem.* 37, 3195-3203.

Marsden B, Shaw G and Sykes BD. 1990 Calcium binding proteins, elucidating the contributions to calcium affinity from an analysis of sequences variants and peptide fragments. *Biochem. Cell Biol.* 68, 587-601.

Maulet Y, and Cox JA. 1983 Structural changes in melittin and calmodulin upon complex formation and their modulation by calcium. *Biochemistry* 22, 5680-5686.

McDowell L, Sanyal G, and Prendergast FG. 1985 Probable role of amphiphilicity in the binding of mastoparan to calmodulin. *Biochemistry* 24,

2979-2984.

McKeating JA, and Willey RL. 1989 Structure and function of the HIV envelope. *AIDS* 3 (suppl 1), S35-S41.

Meador WE, Means AR and Quiocho FA. 1992 Target enzyme recognition by calmodulin: 2.4 Å structure of a calmodulin-peptide complex. *Science* 257, 1251-1255.

Meador WE, Means AR and Quiocho FA. 1993 Modulation of calmodulin plasticity in molecular recognition on the basis of crystal structures. *Nature* 262, 1718-1721.

Melius P, McAuliffe CA, Photaki I, and Sakarellou-Daitsiotou M. 1977 Interactions of platinum complexes, peptides, methionine and dehydrogenases. *Bioinorg. Chem.* 7, 203-210.

Micoli KJ, Pan G, Wu Y, Williams JP, and Cook WJ. 2000 Requirement of calmodulin binding by HIV-1 gp160 for enhanced FAS-mediated apoptosis. *J. Biol. Chem.* 275, 1233-1240.

Miller JD, Wilhelm H, Gierasch L, Gilmore R, and Walter P. 1993a GTP binding and hydrolysis by the signal recognition particle during initialtion of protein translocation. *Nature* 366, 351-354.

Miller JD, Bernstein HD, and Walter P. 1994 Interaction of E. coli Ffh/4.5S ribonucleoprotein and FtsY mimics that of mammalian signal srecognition particle and its receptor. *Nature* 367, 657-659.

Miller MA, Cloyd MW, Liebmann J, Rinaldo CR Jr, Islam KR, Wang SZS, Mietzner TA, and Montelaro RC. 1993b Alterations in cell membrane permeability by the lentivirus peptide (LLP-1) of HIV-1 transmembrane protein. *Virology* 196, 89-100.

Miller MA, Mietzner TA, Cloyd MW, Robey WG, and Montelaro RC. 1993c Identification of a calmodulin-binding and inhibitory peptide domain in the HIV-1 transmembrane glycoprotein. *AIDS Res. Hum. Retroviruses* 9, 1057-1066.

Mills JS, Johnson JD. 1985 Metal ions as allosteric regulators of calmodulin. *J Biol Chem 260*, 15100-15105.

Milos M, Comte M, Schaer JJ, Cox JA. 1989 Evidence for four capital and six auxiliary cation-binding sites on calmodulin: divalent cation interactions monitored by direct binding and microcalorimetry. *J Inorg Biochem* 36, 11-25.

Montoya G, Svensson C, Luirink J, and Sinning I. 1997 Crystal structure of the NG domain from the signal-recognition particle receptor FtsY. *Nature* 385, 365-368.

Morgan PJ, Barrett P, Howell HE, and Helliwell R. 1994 Melatonin receptors: location, molecular pharmacology and physiological significance, *Neurochem. Int.* 24, 101-146.

Muggia FM and Muderspach L. 1994 Platinum compounds in cervical and endometrial cancers: focus on carboplatin. *Semin. Oncol.* 21, 35-41.

Newitt JA, and Bernstein HD. The N-domain of the signal recognition particle

54-kDa subunit promotes effecient signal sequence binding. *Eur. J. Biochem.* 245, 720-729.

Newton DL, Oldewurtel MD, Krinks MH, and Shiloach J. 1984 C.B. Klee, Agonist and antagonist properties of calmodulin fragments, *J. Biol. Chem.* 259, 4419-4426.

Nicotera P, and Orrenius S. 1998 The role of calcium in apoptosis. *Cell Calcium* 23, 173-180.

Norman RE, Ranford JD, and Sadler PJ. 1992 Studies of platinum(II) methionine complexes: metabolites of cisplatin. *Inorg. Chem.* 31, 877-888.

Norris V, Grant S, Freestone P, Canvin J, Sheikh FN, Toth I, Trinei M, Modha K and Norman RI. 1996 Calcium signaling in Bacteria. *J. Bacteriol.* 178, 3677-3682.

Oh D, Yi G, Chi S, and Kim H. 1996 Structure of a methionine-rich segment of Escherichia coli Ffh protein. *FEBS Lett.* 395, 160-164.

Ohki S, Iwamoto U, Aimoto S, Yazawa M, Hikichi K. 1993 Mg^{2+} inhibits formation of $4Ca^{2+}$-calmodulin-enzyme complex at lower Ca^{2+} concentration. *J Biol Chem* 268, 12388-12392.

Ohki S, Ikura M, and Zhang M. 1997 Identification of Mg^{2+}-binding sites and the role of Mg^{2+} on target recognition by calmodulin. *Biochemistry* 36,4309-4316.

O'Neil KT and DeGrado WF. 1990 How calmodulin binds its targets: sequence

indepedent recognition of amphiphilic a-helices. *Trends Biochem. Sci.* 15, 59-64.

O'Neil KT, Erickson-Viitanen S, and DeGrado WF. 1989 Photolabeling of calmodulin with basic, amphiphilic alpha-helical peptides containing p-benzoylphenylalanine. *J. Biol. Chem.* 264, 14571-14578.

Onek LA and Smith RJ. 1992 Calmodulin and calcium mediated regulation in prokaryotes. *J. Gen. Microbiol.* 138, 1039-1049.

Osawa M, Tokumitsu H, Swindells MB, Kurikara H, Orita M, Shibanuma T, Furuya T, and Ikura M. 1999 A novel target recognition revealed by calmodulin in complex with Ca^{2+}-calmodulin-dependent kinase kinase. *Nature Struct. Biol.* 6, 819-824.

Ouyang H, and Vogel HJ. 1998a Melatonin and serotonin interactions with calmodulin: NMR, spectroscopic and biochemical studies. *Biochim. Biophys. Acta* 1383, 37-47.

Ouyang H, and Vogel HJ. 1998b Metal ion binding to calmodulin: NMR and fluorescence studies. *Biometals* 11, 213-222.

Öz G, Pountney DL, and Armitage IM. 1998 NMR spectroscopic studies of I = 1/2 metal ions in biological systems. *Biochem. Cell Biol.* 76, 223-234.

Pablos MI, Agaopito MT, Gutierrez-Baraja R, Reiter RJ, and Recio JM. 1996 Effect of calcium on melatonin secretion in chick pineal gland I, *Neurosci. Lett.* 217, 161-164.

Paetzel M, Dalbey RE and Strynadka NCJ. 1998 Crystal structure of a bacterial signal peptidase in complex with a β-lactam inhibitor. *Nature* 396, 186-190.

Pan Z, Radding W, Zhou T, Hunter E, Mountz J, and McDonald JM. 1996 Role of calmodulin in HIV-potentiated Fas-mediated apoptosis. *Am. J. Pathol.* 149, 903-910.

Patel S, and Austen BM. 1996 Substitution of fifty four homologue (Ffh) in Escherichia coli with the mammalian 54-kDa protein of signal-recognition particle. *Eur. J. Biochem.* 238, 760-768.

Patrick SM, and Turchi JJ. 1998 Human replication protein A preferentially binds cispaltin-damaged DNA in Vitro. *Biochemistry* 37, 8808-8815.

Pattanaik A, Bachowski G, Laib J, Lemkuil D, Shaw CF, Petering DH, Hitchcock A, and Saryan L. 1992 Properties of the reaction of cis-dichlorodiammineplatinum(II) with metallothionein. *J. Biol. Chem.* 267, 16121-16128.

Peitsch MC. 1995 Protein modelling by email. *Bio/Techology* 13, 658-660.

Peitsch MC. 1996 ProMod and Swiss-Model: internet-based tools for automated comparative protein modelling. *Biochem. Soc. Trans.* 24, 274-279.

Permyakov EA. 1993 Luminescent Spectroscopy of Proteins, CRC Press, Boca Raton.

Persechini A, Jarrett HW, Kosk-Kosicka D, Krinks G and Lee HG. 1993

Activation of enzymes by calmodulins containing intramolecular cross-links. *Biochim. Biophys. Acta* 1163, 309-314.

Persechini A, McMillan K, and Leakey P. 1994 Activation of myosin light chain kinase and nitric oxide synthase activities by calmodulin fragments. *J. Biol. Chem.* 269, 16148-16154.

Persechini A, Gansz KJ and Paresi RJ. 1996 A role in enzyme activation for the N-terminal leader sequence in calmodulin. *J. Biol. Chem.* 271,19279-19282.

Phillips GJ, and Silhavy TJ. 1992 The E. coli ffh gene is necessary for viability and efficient protein export. *Nature* 359, 744-746.

Pinto AL, and Lippard SJ. 1985 Binding of antitumor drug cis-diammine-dichloroplatinum (cisplatin) to DNA. *Biochim. Biophys. Acta* 780, 167-180.

Popovic M, Sarngadharan MG, Read E, and Gallo RC. 1984 Detection, isolation, and continuous production of cytopathic retroviruses (HTLV-III) from patients with AIDS and pre-AIDS. *Science* 224, 497-500.

Poritz MA, Bernstein HD, Strub K, Zopf D, Wilhelm H, and Walter P. 1990 An E. coli ribonucleoprotein containing 4.5S RNA resembles mammalian signal recognition particle. *Science* 250, 1111-1117.

Potapova O, Haghighi A, Bost F, Liu C, Birrer MJ, Gjerset R, and Mercola D. 1997 The Jun Kinase/Stress-activated Protein Kinase pathway functions to regulate DNA repair and inhibition of the pathway sensitizes tumor cells to cisplatin. *J. Biol. Chem.* 272, 14041-14044.

Powers T, and Walter P. 1997 Co-translational protein targeting catalyzed by the Escherichia coli signal recognition particle and its receptor. *EMBO J.* 16, 4880-4886.

Prati E, Gorla R, Malacarne F, Airo P, Brugnoni D, Gargiulo F, Tebaldi A, Castelli F, Carosi G, and Cattaneo R. 1997 Study of spontaneous apoptosis in HIV+ patients: correlation with clinical progression and T cell loss. *AIDS Res. Hum. Retroviruses* 13, 1501-1508.

Putkey JA, Quo T, VanBerkum MFA and Means AR. 1988 Functional significance of the central helix in calmodulin. *J. Bio. Chem.* 263, 11242-11249.

Quiocho, F. A., Johnson, K. A., Meador, W. E., and Beckingham, K. 1997 Abstract presented at the Tenth International Symposium on Calcium-Binding Proteins and Calcium Function in Health and Disease, Lund, Sweden, pp. 27.

Ranajit P, Gallo RC, and Sarngadharan MG. 1988 Processing of the structural proteins of human immunodeficiency virus type I in the presence of monoensin and cerulenin. *Proc. Natl. Acad. Sci. USA* 85, 9283-9286.

Rao ST, Satyshur KA, Greaser ML, Sundaralingham M. 1996 *Acta Cryst.* D52, 916-922.

Rapiejko PJ, and Gilmore R. 1994 Signal sequence recognition and targeting of ribosomes to the endoplasmic reticulum by the signal recognition particle do not require GTP. *Mol. Biol. Cell* 5, 887-897.

Rapoport TA. 1992 Transport of proteins across the endoplasmic reticulum membrane. *Science* 258, 931-936.

Rapoport TA, Jungnicket B, and Kutay U. 1996 Protein transport across the eukaryotic endiplasmic reticulum and bacterial inner membranes. *Annu. Rev. Biochem.* 65, 271-303.

Reedijk J. 1992 The relevance of hydrogen bonding in the mechanism of action of platinum antitumor compounds. *Inorg. Chim. Acta* 198-200, 873-881.

Reedijk J. 1996 Improved understanding in platinum antitumor chemistry. *Chem. Commun.* 1996, 801-806.

Reixhus JW and Martin DS, Jr. 1961 cis-Dichlorodiammineplatinum(II). Acid hydrolysis and isotopic exchange of the chloride ligands. *J. Am. Chem. Soc.* 83, 2457-2462.

Rhoads AR and Friedberg F. 1997 Sequence motifs for calmodulin recognition. *FASEB J.* 11, 331-340.

Ribes V, Römisch K, Giner A, Dobberstein B, and Tollervey D. 1990 E. coli 4.5S RNA is part of a ribonucleoprotein particle that has properties related to signal recognition particle. *Cell* 63, 591-600.

Rodriguez-Cabello JC, Agapito MT, Garcia-Herrero I, and Recio JM. 1989 Effects of EGTA and calmodulin, neutral thiol protease and protein kinase C inhibitors on loss of chicken pineal serotonin N-acetyltransferase activity, *J. Comp. Physiol B* 159, 583-588.

Römisch K, Webb J, Lingelbach K, Gausepohl, and Dobberstein B. 1990 The 54-kD protein of signal recognition particle contains a methionine-rich RNA binding domain. *J. Cell Biol.* 111, 1793-1802.

Rosenberg B. 1985 Fundamental studies of cisplatin. *Cancer* 55, 2303-2316.

Sambrook J, Fritsch EF and Maniatis T. 1989 Molecular Cloning, A Laboratory Manual. Cold Spring Harbor Press.

Samuelsson T, Olsson M, Wikström PM, and Johansson BR. 1995 The GTPase activity of the Escherichia coli Ffh protein is improtant for normal growth. *Biochim. Biophys. Acta* 1267, 83-91.

Sánchez-Perez I, Murguía JR, and Perona R. 1998 Cisplatin induces a persistent activation of JNK that is related to cell death. *Oncogene* 16, 533-540.

Sanders SL and Schekman R. 1992 Polypeptide trnaslocation across the endoplasmic reticulum membrane. *J. Biol. Chem.* 267, 13791-13794.

Sandler AB. 1998 Etoposide plus ifosfamide plus cisplatin in the treatment of small cell lung cancer. *Semin. Oncol.* 25, 38-41.

Sanyal G, Richard LM, Carraway III KL, and Puett D. 1988 Binding of amphiphilic peptides to a carboxy-terminal tryptic fragment of calmodulin. *Biochemistry* 27, 6229-6236.

Saponja JA, and Vogel HJ 1996 Metal-ion binding properties of the

transferrins: a vanadium-51 NMR study. *J. Inorg. Biochem.* 62, 253-270.

Scaloni, A., Miraglia, P., Orru, S., Amodeo, P., Motta, A., Marino, G. and Pucci, P. 1998 Topology of the calmodulin-melittin complex. *J. Mol. Biol* 277, 945-958.

Seeholzer SH, Cohn M, Putkey JA, Means AR, and Crespi HL. 1986 NMR studies of a complex of deuterated calmodulin with melittin. *Proc. Natl. Acad. Sci. USA* 83, 3634-3638.

Seeholzer SH, Cohn M, Wand AJ, Crespi HL, Putkey JA, and Means AR 1987 in Calcium-Binding Proteins in Health and Disease (Norman, A. W., Vanaman, T. C., and Means, A. R., eds.), pp. 360-371, Academic Press, San Diego.

Shi D, Hambley TW, and Freeman HC. 1999 Three new platinum(II)-dipeptide complexes. *J. Inorg. Biochem.* 73, 173-186.

Shoemaker MO, Lau W, Shattuck RL, Kwiatkowski AP, Matrisian PE, Guerra-Santos L, Wilson E, Lukas TJ, Van Eldik LJ, and Watterson DM. 1990 Use of DNA sequence and mutant analyses and antisense oligodeoxynucleotides to examine the molecular basis of nonmuscle myosin light chain kinase autoinhibition, calmodulin recognition, and activity. *J. Cell Biol.* 111, 1107-1125.

Siegel V, and Walter P. 1985 Elongation arrest is not a prerequisite for secretory protein translocation caross the microsomal membrane. *J. Cell Biol.* 100, 1913-1921.

Siegel V, and Walter P. 1988 Each of the activities of signal recognition particle (SRP) is contained within a distinct domain: analysis of biochemical mutants fo SRP. *Cell* 52, 39-49.

Silberstein D. 1994 Serotonin (5-HT) and migraine. *Headache* 34, 408-417.

Simons TJ. 1993 Lead-calcium interactions in cellular lead toxicity. *Neuro Toxicol* 14, 77-86.

Skelton NJ, Kordel J, Akke M, Forsén S and Chazin WJ. 1994 Signal transduction versus buffering activity in Ca^{2+}-binding proteins. *Nature Struct. Biol.* 1, 239-245.

Sklenár V, Bax A. 1987 Spin-echo water suppression for the generation of pure-phase two-dimensional NMR spectra. *J Magn Reson* 74, 469-479.

Smith RJ. 1995 Calcium and bacteria. *Adv. Microb. Physiol.* 37, 83-103.

Sodroski J, Goh WC, Rosen C, Campbell K, and Haseltine WA. 1986 Role of the HTLV-III/LAV envelope in syncytium formation and cytopathicity. *Nature*, 322, 470-474.

Speelmans G, Staffhorst RWHM, Versluis K, Reedijk J, and de Kruijff B. 1997 Cisplatin complexes with phosphatidylserine in membranes. *Biochemistry* 36, 10545-10550.

Spera S, Ikura M and Bax A. 1991 Measurement of the exchange rates of rapidly exchanging amide protons: application to the study of calmodulin and its complex with a myosin light chain kinase fragment. *J. Biomol. NMR* 1,

155-165.

Srinivas SK, Srinivas RV, Anantharamaiah GM, Segrest JP, and Compans RW. 1992 Membrane interactions of synthetic peptides corresponding to amphipathic helical segments of the human immunodeficiency virus type-1 envelope glycoprotein. *J. Biol. Chem.* 267, 7121-7127.

Srinivas SK, Srinivas RV, Anantharamaiah GM, Compans RW, and Segrest JP. 1993 Cytosolic domain of the human immunodeficiency virus envelop glycoprotein binds to calmodulin and inhibits calmodulin-regulated proteins. *J. Biol. Chem.* 268, 22895-22899.

Stein BS, Gowda SD, Lifson JD, Penhallow RC, Bensch KG, and Engleman EG. 1987 pH-independent HIV entry into CD4-positive T cells via virus envelope fusion to the plasma membrane. *Cell* 49, 659-668.

Steiner RF, Marshall L, and Needleman D. 1986 The interaction of melittin with troponin C. Arch. Biochem. Biophys. 246, 286-300.

Summers, M. F. 1988 Coord. Chem. Rev. 86, 43-134.

Swain AL, Kretsinger RH, Amma EL. 1989 Restrained least squares refinement of native (calcium) and cadmium-substituted carp parvalbumin using X-ray crystallographic data at 1.6-Å resolution. *J Biol Chem* 264, 16620-16628.

Szebenyi DM, Moffat K. 1986 The refined structure of vitamin D-dependent calcium-binding protein from bovine intestine. Molecular details, ion binding, and implications for the structure of other calcium-binding proteins. *J Biol*

Chem 261, 8761-8777.

Tencza SB, Miller MA, Islam K, Mietzner TA, and Montelaro RC. 1995 Effect of amino acid substitutions on calmodulin binding and cytolytic properties of the LLP-1 peptide segment of human immunodeficiency virus type 1 transmembrane protein. *J. Virol.* 69, 5199-5202.

Tencza SB, Mietzner TA, and Montelaro RC. 1997 Calmodulin-binding function of LLP segments from the HIV type 1 transmembrane protein is conserved among natural sequence variants. *AIDS Res. Hum. Retroviruses* 13, 263-269.

Thulin E, Anderson A, Drakenberg T, Forsén S, Vogel HJ 1984 Metal ion and drug binding to proteolytic fragments of calmodulin: proteolytic, cadmium-113, and proton nuclear magnetic resonance studies. *Biochemistry* 23, 1862-1870.

Timmer-Bosscha H, Mulder NH, and Vries EGE. 1992 Modulation of cis-diamminedichloroplatinum(II) resistance: a review. *Br. J. Cancer* 66, 227-238.

Trewhella J. 1992 The solution structures of calmodulin and its complexes with synthetic peptides based on target enzyme binding domains. *Cell Calcium* 13, 377-390.

Trewhella J, and Krueger JK. 2000 Small-angle solution scattering reveals information on comformational dynamics in calcium-binding proteins and in their interactions with regulatory targets. In Calcium binding proteins protocols. Ed. H. J. Vogel, Meth. Mol. Biol. (in press).

Trump CW and Berezesky IK. 1995 Ca^{2+}-mediated cell injury and cell-death. *FASEB J.* 9, 219-228.

Tsai MD, Drakenberg T, Thulin E, Forsén S. 1987 Is the binding of magnesium(II) to calmodulin significant? An investigation by magnesium-25 nuclear magnetic resonance. *Biochemistry* 26, 3635-3643.

VanBerkum MFA, George SE and Means AR. 1990 Calmodulin activation of target enzymes, consequences of deletions in the central helix. *J. Bio. Chem.* 265, 3750-3756.

Veenstra, T.D., Tomlinson, A.J., Benson L., Kumar, R. and Naylor, S. 1998 Low temperature aqueous electrospray ionization mass spectrometry of noncovalent complexes. *J. Am. Soc. Mass. Spectrom.* 9, 580-584.

Veronese FD, DeVico AL, Copeland TD, Oroszlan S, Gallo RC, and Sarangadharan MG. 1985 Characterization of gp41 as the transmembrane protein coded by the HTLV-III/LAV envelope gene. *Science* 229, 1402-1405.

Virk SS, Kirk CJ, Shears SB. 1985 Ca^{2+} transport and Ca^{2+}-dependent ATP hydrolysis by Golgi vesicles from lactating rat mammary glands. *Biochem. J.* 226, 741-748.

Vogel HJ. 1983 Structure of hen phosvitin: A 31P NMR, 1H NMR, and laser photochemically induced dynamic nuclear polarization 1H NMR study. *Biochemistry* 22:668-674.

Vogel HJ. 1994 Calmodulin: a versatile calcium mediator protein. *Biochem. Cell Biol.* 72, 357-376.

Vogel HJ and Forsén S. 1987 NMR studies of calcium-binding proteins. In: Berliner LJ, Reuben J, eds. Biological Magnetic Resonance, vol 7, 245-307, Plenum Press, New York.

Vogel HJ and Zhang M. 1995 Protein engineering and NMR studies of calmodulin. *Mol. Cell. Biochem.* 149/150, 3-15.

Vogel HJ, Lindahl L, and Thulin E. 1983 Calcium-dependent hydrophobic interaction chromatography of calmodulin, troponin C, and their proteolytic fragments. ***FEBS Lett.*** **157**, 241-246.

Vogel HJ. Huque, M.E. and Hiraoki, T. 1990 Characterization of the surface of calmodulin by NMR. *Adv Second Messenger Phosphoprotein Res.* 24:254-259.

Vogel HJ, Drakenberg T, Forsén S, O'Neil JD, and Hofmann T. 1985 Structural differences in the two calcium binding sites of the porcine intestinal calcium binding protein: a multinuclear NMR study. *Biochemistry* 24, 3870-3876.

Voisin P, Van Camp G, Pontoire C, and Collin JP. 1993 Protaglandins stimulate serotonin acetylation in chick pineal cells: involvement of cyclic AMP-dependent and calcium/calmodulin dependent mechanisms, *J. Neurochem.* 60, 666-670.

Von Heijne G. 1985 Signal sequence, the limitation of variation. *J. Mol. Biol.* 184, 99-105.

Walsh MP. 1994 Calmodulin and the regulation of smooth muscle contration.

Mol. Cell. Biochem. 135, 21-41.

Walter P, and Blobel G. 1983 Disassembly and reocnstitution of the signal recognition particle. *Cell* 34, 525-533.

Walter P, and Johnson AE. 1994 Signal sequence recognition and protein targeting to the endoplasmic reticulum membrane. *Annu. Rev. Cell. Biol.* 10, 87-119.

Walter P and Lingappa VR. 1986 Mechanism of protein translocation across the endoplasmis reticulum membrane. *Annu. Rev. Cell Biol.* 2: 499-516.

Walter P, Gilmore R, and Blobel G. 1984 Protein translocation across the endoplasmic reticulum. *Cell* 38, 5-8.

Waltersson Y, Linse S, Brodin P, and Grundström T. 1993 Mutational effects on the cooperativity of Ca2+ binding in calmodulin. *Biochemistry* 32, 7866-7871.

Wang CA, Aquaron RR, Leavis PC, Gergely J. 1982 Metal-binding properties of calmodulin. *Eur J Biochem* 124, 7-12.

Wang S, Trumble WR, Liao H, Wesson CR, Dunker AK and Kang C. 1998 Crystal structure of calsequestrin from rabbit skeletal muscle sarcoplasmic reticulum. *Nature Struct. Biol.* 5, 476-483.

Wei S and Stader J. 1994 Two distinct regions of the LamB signal sequences function in different steps in export. *J. Biol. Chem.* 269, 1648-1653.

Wei X, Gosh SK, Taylor ME, Johnson VA, Emini EA, Deutsch P, Lifson JD, Bonhoeffer S, Nowak MA, Hahn BH, Saag MS, and Shaw GS. 1995 Viral dynamics oin human immunodefiency virus type 1 infection. *Nature* 373, 117-122.

Weissenhorn W, Dessen A, Harrison SC, Skehel JJ, and Wiley DC 1997 Atomic structure of the ectodomain from HIV-1 gp41. *Nature* 387, 426-430.

Weljie, A. M., and Vogel, H. J. 2000 *Protein Eng.* (in press).

Willey RL, Bonifacino JS, Potts BJ, Martin MA, and Klausner RD. Biosynthesis, cleavage, and degradation of the human immunodeficiency virus type I envelope glycoprotein gp160. *Proc. Natl. Acad. Sci. USA* 85, 9580-9584.

Williams RJP. 1992 Calcium fluxes in cells: new view on their significance. *Cell Calcium* 13, 273-275.

Williams RJP. 1996 Calcium binding proteins in normal and transformed cells. *Cell Calcium* 20, 87-93.

Williams RJP. 1997 The natural selection of the chemical elements. Cell. *Mol. Life Sci.* 53, 816-829.

Williams RJP. 1998a Calcium: outside/inside homeostasis and signaling. Biochim. Biochem. Acta 1448, 153-165.

Williams RJP 1998b Calcium in health and disease. *Cell Calcium* 24, 233-237.

Winder G., Wuthrich K. 1993 A simple experimental scheme using pulsed field gradients for coherence-pathway rejection and solvent suppression in phase-sensitive heteronuclear correlation spectra, *J. Magn. Reson.* 102, 239-241.

Wingren AG, Björkdahl O, Labuda T, Björk L, Andersson U, Gullberg U, Hedlund G, Sjögren H, Kalland T, Widegren B, and Dohlsten M. 1996 Fusion of a signal sequence to the interleukin-1b gene directs the protein from cytoplamis accumulation to extracellular release. *Cell. Immuno.* 169, 226-237.

Wray V, Kinder R, Federau T, Henklein P, Bechinger B, and Schubert U. 1999 Solution structure and orientation of the transmembrane anchor domain of the HIV-1-encoded virus protein U by high-resolution and solid-state NMR spectroscopy. *Biochemistry* 38, 5272-5282.

Wyatt R, and Sodroski J. 1999 The HIV-1 envelope glycoproteins: fusogens, antigens, and immunogens. *Science* 280, 1884-1888.

Yang D, van Boom SSGE, Reedjik J, van Boom J, Farrell N, and Wang AHJ. 1995 A novel DNA structure induced by the anticancer cisplatinum compound crosslinked to a GpC site in DNA. *Nature Struct. Biol.* 2, 577-586.

Yoshino H, Izumi Y, Sakai K, Takezawa H, Matsuura I, Maekawa H, and Yazawa M. 1996 Solution X-ray scattering data show structural differences between yeast and vertebrate calmodulin: implications for structure/function. *Biochemistry* 35, 2388-2393.

Yost CS, Hedgepeth J and Lingappa VR. 1983 A stop transfer sequence

confers predictable transmembrane orientation to a previously secreted protein in cell-free systems. *Cell* 34, 759-766.

Yuan T. 1998 Protein Engineering and Nuclear Magnetic Resonance Studies of Calmodulin. Ph. D. dissertation, the University of Calgary.

Yuan, T., and Vogel, H. J. 1998 Calcium-calmodulin-induced dimerization of the carboxyl-terminal domain from petunia glutamate decarboxylase. A novel calmodulin-peptide interaction motif. *J. Biol. Chem.* 273, 30328-30335.

Yuan T, Mietzner TA, Montelaro RC, and Vogel HJ 1995 Characterization of the calmodulin binding domain of SIV transmembrane glycoprotein by NMR and CD spectroscopy. *Biochemistry* 34,10690-10696

Yuan T, Weljie A, Vogel HJ. 1998 Tryptophan fluorescence quenching by methionine and selenomethionine residues of calmodulin: orientation of peptide and protein binding. *Biochemistry* 37, 3187-3195.

Yuan, T., Ouyang, H. and Vogel., H.J. 1999a Surface exposure of the methionine side chains of calmodulin in solution. A nitroxide spin label and two-dimensional NMR study. *J. Biol. Chem.* 274, 8411-8420.

Yuan, T., Walsh, M. P., Sutherland, C., Fabian, H., and Vogel, H. J. 1999b Calcium-dependent and -independent interactions of the calmodulin-binding domain of cyclic nucleotide phosphodiesterase with calmodulin. *Biochemistry* 38,1446-1455.

Yuan T, Ouyang H, Huque MDE, Siivari K, and Vogel HJ 2000 Cadmium-113, proton NMR and spectroscopic studies of calmodulin-melittin interactions: an

half molecule appoach reveals two opposite binding orientations. *Biochim. Biophys. Acta* (submitted).

Zamble DB, and Lippard SJ. 1995 Cisplatin and DNA repair in cancer chemotherapy. *Trends Biochem. Sci.* 20, 435-439.

Zhang B, and Tang W. 1994 Kinetics of the reaction of platinum(II) complexes with metallothionein. *J. Inorg. Biochem.* 56, 143-153.

Zhang B, Sun W, and Tang W 1997 Determination of the association constant of platinum(II) to metallothionein. *J. Inorg. Biochem.* 65, 295-298.

Zhang M. 1993 Nuclear Magnetic Resonance and Protein Engeneering Studies of Calmodulin. Ph. D. dissertation, the University of Calgary.

Zhang, M., and Vogel, H. J. 1993 Determination of the side chain pKa values of the lysine residues in calmodulin. *J. Biol. Chem.* 268, 22420-22428.

Zhang M. and Vogel HJ. 1994 Two-dimensional NMR studies of selenomethionyl calmodulin. *J. Mol. Biol.* 239, 545-554.

Zhang, M., and Yuan, T. 1998 Molecular mechanisms of calmodulin's functional versatility. Biochem. *Cell Biol.* 76, 313-323.

Zhang M, Yuan T, and Vogel HJ. 1993 A peptide analog of the calmodulin-binding domain of myosin light chain kinase adopts an alpha-helical structure in aqueous trifluoroethanol. *Protein Sci.* 2, 1931-1937.

Zhang M, Fabian H, Mantsch HH, and Vogel HJ. 1994a Isotope-edited

Fourier transform infrared spectroscopy studies of calmodulin's interaction with its target peptides. *Biochemistry* 33:10883-10888.

Zhang M, Li M, Wang J, and Vogel HJ. 1994b The effect of Met→Leu mutations on clamodulin's ability to activate cyclic nucleotide phosphodiesterase. *J. Biol. Chem.* 269, 15546-15552.

Zhang M, Tanaka T and Ikura M. 1995a Calcium-induced conformational transition revealed by the solution structure of apo calmodulin. *Nature Struct. Biol.* 2, 758-767.

Zhang M, Yuan T, Aramini JM, and Vogel HJ. 1995b Interaction of calmodulin with its binding domain of rat cerebellar nitric oxide synthase. A multinuclear NMR study. *J. Biol. Chem.* 270, 20901-20907.

Zheng N, and Gierasch LM. 1997 Domain interactions in E. coli SRP: stabilization of M domain by RNA is required for effective signal sequence modulation of NG domain. *Mol Cell.* 1, 79-87.

Zhang YJ, Fadeel B, Hodara V, and Fenyo EM. 1997 Induciton of apotosis by primary HIV-1 isolates correlates with productive infection in peripheral blood mononuclear cell. *AIDS* 11, 1219-1225.

Zlatanova J, Yaneva J, and Leuba SH. 1998 Proteins that specifically recognize cisplatin-damaged DNA: a clue to anticancer activity of cisplatin. *FASEB J.* 12, 791-799.

Zopf D, Bernstein H, and Walter P. 1993 GTPase domain of the 54-kD subunit of the mammalian signal recognition particle is required for protein

translocation but not for signal sequences binding. *J. Cell Biol.* 120, 1113-1121.